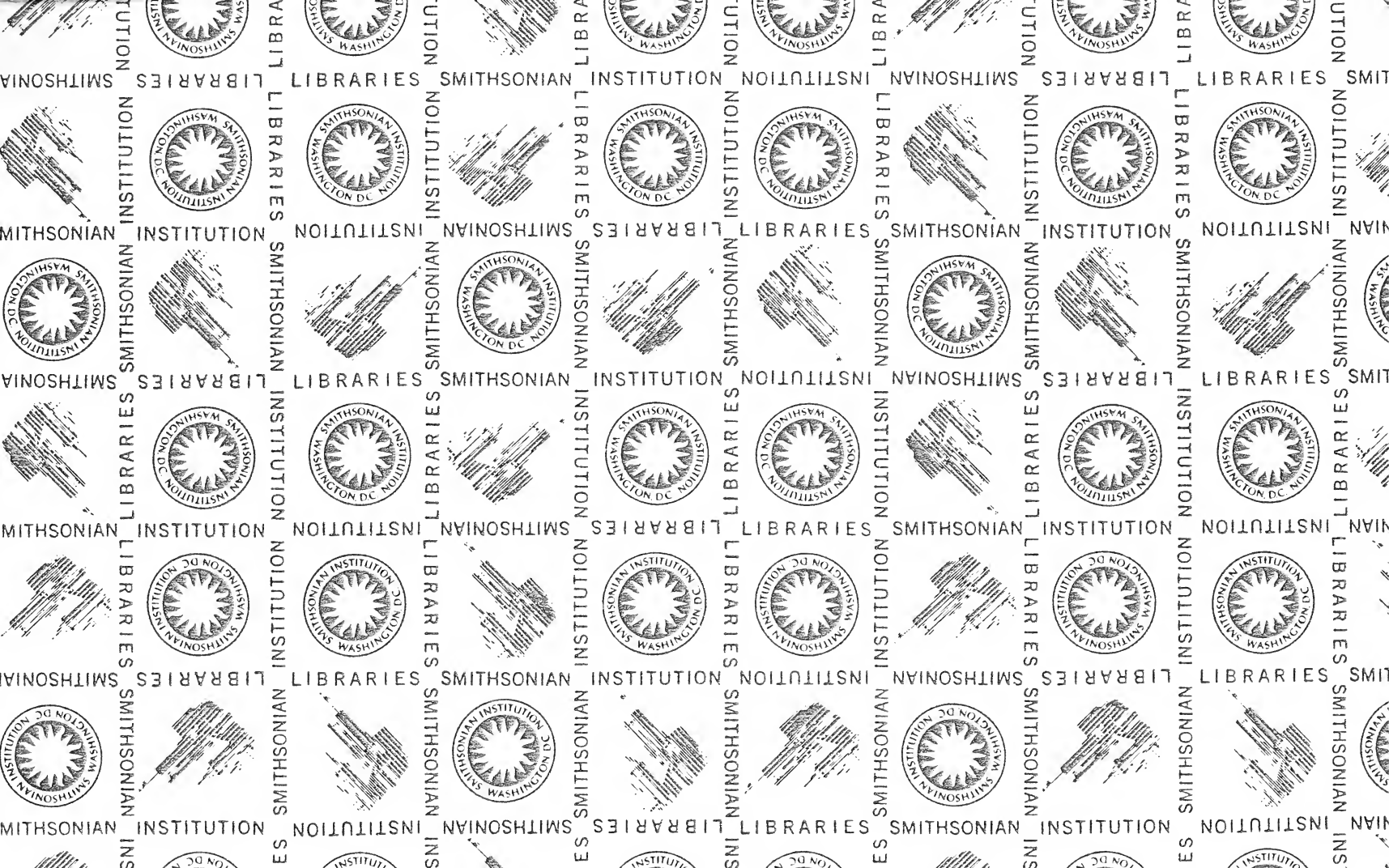
SMITHSONIAN INSTITUTION LIBRARIES

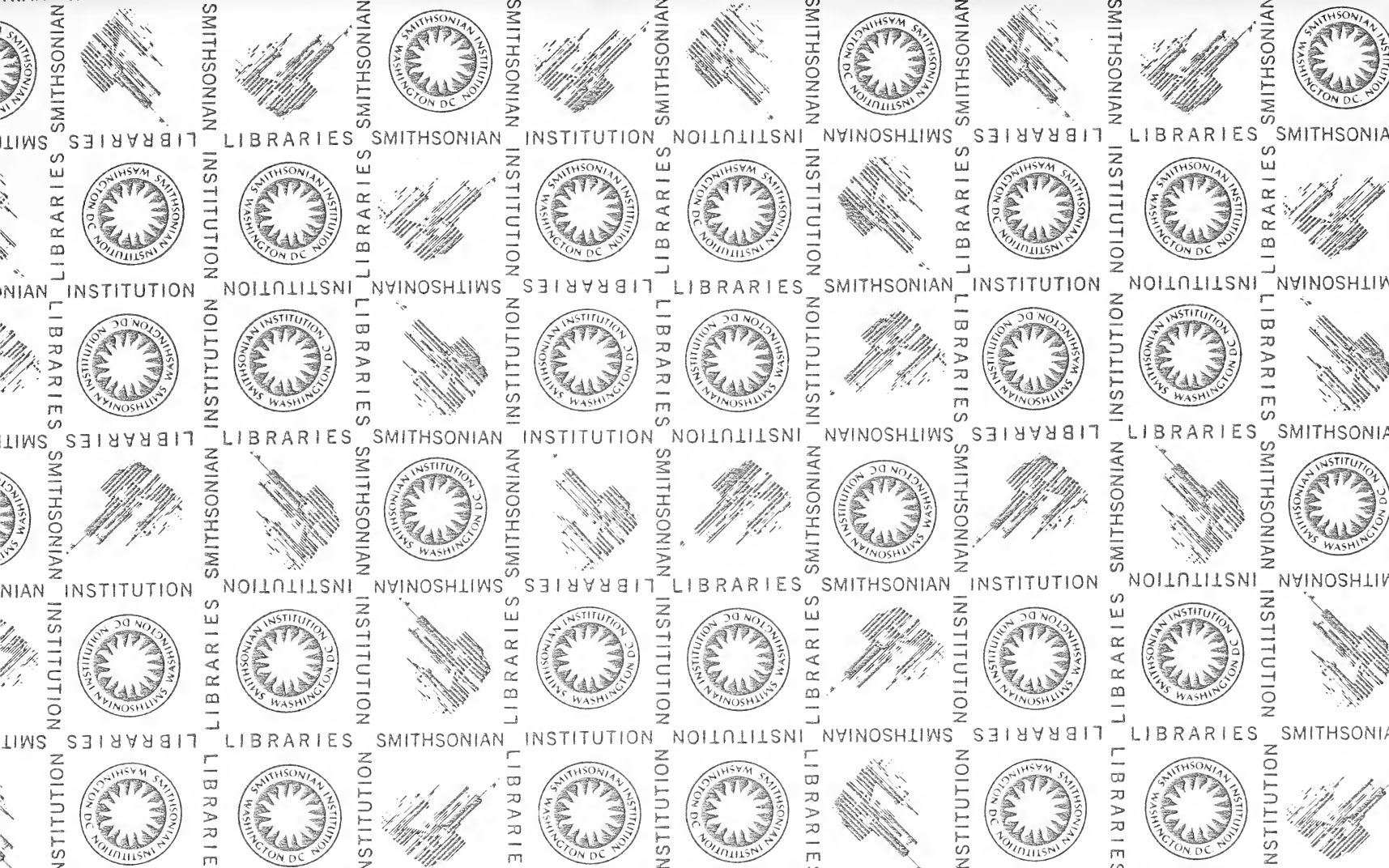
SMITHSONIAN INSTITUTION LIBRARIES

THE TEXAS JOURNAL OF SCIENCE

Volume XXXV

1983

Published by

THE TEXAS ACADEMY OF SCIENCE

THE TEXAS JOURNAL OF SCIENCE

Volume XXXV, No. 1 March 1983

CONTENTS

THE TEXAS JOURNAL OF SCIENCE

Volume XXXV, No. 2 July 1983

CONTENTS

THE TEXAS JOURNAL OF SCIENCE

Volume XXXV, No. 3 September 1983

CONTENTS

THE TEXAS JOURNAL OF SCIENCE

Volume XXXV, No. 4 January 1984

CONTENTS

Volume XXXV, Number 1 March 1983

THE TEXAS JOURNAL OF SCIENCE

PUBLISHED QUARTERLY BY
THE TEXAS ACADEMY OF SCIENCE

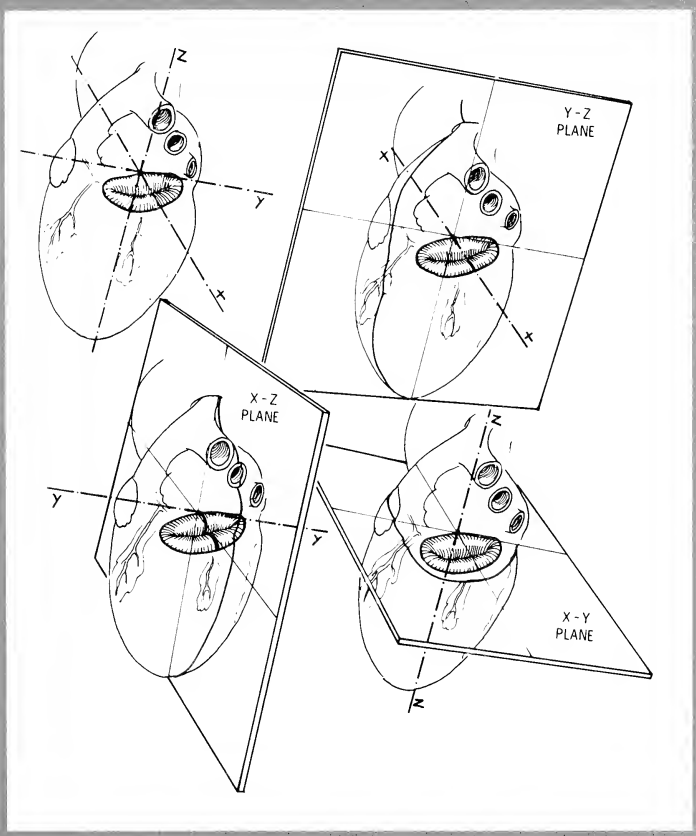

AFFILIATED ORGANIZATIONS
Texas Section, American Association of Physics Teachers
Texas Section, Mathematical Association of America
Texas Section, National Association of Geology Teachers

GENERAL INFORMATION

MEMBERSHIP. Any person or group engaged in scientific work or interested in the promotion of science is eligible for membership in The Texas Academy of Science. Dues for members are $20.00 annually; student members, $12.00 annually; sustaining members, at least $30.00 in addition to annual dues; life members, at least $400.00 in one payment; patrons, at least $500.00 in one payment; corporate members, $250.00 annually; corporate life members, $2000.00 in one payment. Library subscription rate is $45.00 annually. Payments should be sent to the Secretary-Treasurer, Box 2176, Huntsville, TX 77341.

The *Journal* is a quarterly publication of The Texas Academy of Science and is sent to all members and subscribers. Inquiries regarding back issues should be sent to Dr. Fred S. Hendricks, Dept. Wildlife & Fisheries Sciences, Texas A&M University, College Station, TX 77843.

Manuscripts submitted for publication in the *Journal* should be sent to Dr. W. H. Neill, Dept. Wildlife & Fisheries Sci., Texas A&M Univ., College Station, TX 77843.

The Texas Journal of Science (USPS 616740) is published quarterly at Huntsville, Texas U.S.A. (Second class postage paid at Post Office, Huntsville, TX 77341, and at additional mailing office at Lubbock, TX 79401.) Please send form 3579 and returned copies to Texas Tech Press, Box 4240, Lubbock, TX 79409.)

THE TEXAS JOURNAL OF SCIENCE

Volume XXXV, No. 1 March 1983

CONTENTS

NOTE: Authors with funds for page contributions are expected to make such payments. The contribution of $35.00 per page is encouraged to defray printing costs, and authors of articles exceeding ten printed pages are expected to make *some* contribution to the publication fund. However, payment of printing costs is not a condition for publication in The Texas Journal of Science, and NO AUTHOR, WHO WOULD OTHERWISE SUBMIT A MANUSCRIPT, SHOULD HESITATE TO DO SO BECAUSE OF LACK OF SUCH FUNDS. Members without funds may apply to the Texas Academy of Science for a grant to cover some or all costs of publication. This becomes effective January 23, 1982.

INSTRUCTIONS TO AUTHORS

Papers intended for publication in *The Texas Journal of Science* are to be submitted to Dr. William H. Neill, Dept. Wildlife & Fisheries Sciences, Texas A&M University, College Station, TX 77843.

The manuscript is not to have been published elsewhere. Triplicate typewritten copies (the original and 2 reproduced copies) *must* be submitted. Typing of both text and references should be *double-spaced* with 2-3 cm margins on *standard* 8½ X 11-inch typing paper. The title of the article should be followed by the name and business or institutional address of the author(s). *Be sure to include zip code* with the address. If the paper has been presented at a meeting, a footnote giving the name of the society, date, and occasion should be included but should not be numbered. Include a brief ABSTRACT at the beginning of the text (abstracting services pick this up directly) followed by an INTRODUCTION (understandable to any scientist) and then whatever paragraph headings are desired. The usual editorial customs, as exemplified in the most recent issue of the *Journal*, are to be followed as closely as possible.

In the text, cite all references by author and date *in chronological order*, i.e., Jones (1971); Jones (1971, 1972); (Jones 1971); (Jones 1971, 1972); Jones and Smith (1971); (Jones and Smith 1971); (Jones 1971; Smith 1972; Beacon 1973). If there are more than 2 authors, use: Jones et al. (1971); (Jones et al. 1971). References are then to be assembled, arranged ALPHABETICALLY, and placed at the end of the article under the heading LITERATURE CITED. For a PERIODICAL ARTICLE use: Jones, A. P., and R. J. Wilson. 1971. Effects of chlorinated hydrocarbons. J. Comp. Chem. 37:116-123. For a PAPER PRESENTED at a symposium, etc., use the form: Jones, A. P. 1971. Effects of chlorinated hydrocarbons. WMO Symposium on Organic Chemistry, New York, N.Y. For a PRINTED PAPER use: Jones, A. P. 1971. Effects of chlorinated hydrocarbons. Univ. of Tex., Dallas. *or* Jones, A. P. 1971. Effects of chlorinated hydrocarbons. Univ. of Tex. Paper No. 14, 46 p. A MASTERS OR Ph.D. THESIS should appear as: Jones, A. P. 1971. Effects of chlorinated hydrocarbons. M.S. Thesis, Tex. A&M Univ., College Station. For a BOOK, NO EDITORS, use: Jones, A. P. 1971. Effects of chlorinated hydrocarbons. Academic Press, New York, N.Y., 439 p. For a CHAPTER IN A BOOK WITH EDITORS: Jones, A. P. 1971. Structure of chlorinated hydrocarbons, p. 13-39. *In* A. P. Jones, B. R. Smith, Jr. and T. S. Gibbs (Eds.), Effects of chlorinated hydrocarbons. Academic Press, New York, N.Y. For a BOOK WITH EDITORS: Jones, A. P. 1971. Effects of chlorinated hydrocarbons. J. Doe (Ed.). Academic Press, New York, N.Y., p. 3-12. For an IN PRESS PERIODICAL reference, use: Jones, A. P. In Press. Effects of chlorinated hydrocarbons. J. Org. Chem. For an IN PRESS BOOK reference, use: Jones,

A. P. In Press. Effects of chlorinated hydrocarbons. Academic Press, New York, N.Y. References *must* include article title and page numbers.

References such as unpublished data or personal communications should not be listed in the LITERATURE CITED section. However, within the text they should be presented as: (unpubl. data from C. J. Jones, Dept. Zoology, Univ. Texas, Austin) *or* (pers. comm. from R. C. Smith, P.O. Box 133, Mexia, TX).

All tables are to be typed with a carbon ribbon, free of error, without handwritten notations, and ready for photographic reproduction. Tables should be placed on separate sheets with a marginal notation on the manuscript to indicate preferred locations. Tables must have a text reference, i.e., Table 2 shows...*or* (Table 2).

Figures are to be *original inked drawings* or *glossy photographs no larger* than 6½ X 4½ inches and mounted on standard 8½ X 11-inch paper. Legends for figures are to be typed separately. Figures must have a text reference, i.e., Figure 3 illustrates...*or* (Fig. 3).

All photographs, line drawings, and tables are to be provided with self-explanatory titles or legends. Each illustration should be marked on the back with the name of the principle author, the figure number, and the title of the manuscript of which it is a part.

Authors will receive galley proofs plus the original typescript along with information concerning reprints and page charges. Proofs must be corrected (using ink) and returned to the Editor within 3 days. Payment (check or purchase voucher) for page charges (or the publication grant request) must accompany the return of the corrected proofs or a delay in the printing of the manuscript could occur. Reprint orders should be returned directly to Texas Tech Press, Box 4240, Lubbock, TX 79409

NOTICE: IF YOUR ADDRESS OR TELEPHONE NUMBER CHANGES, NOTIFY US IMMEDIATELY SO WE CAN SEND YOUR GALLEY PROOFS TO YOU WITHOUT LOSS OR DELAY.

MODELING SYSTOLIC MITRAL VALVE MOTION: A TOOL FOR CLARIFYING MITRAL VALVE PROLAPSE[1]

by JON F. HUNTER,[ab] DAVID P. SEATON,[c]
WILLIAM M. LIVELY,[c] GERALD E. MILLER,[b]
and DAVID L. STONER[b]

[a]*Department of Veterinary Physiology and Pharmacology,*
[b]*Bioengineering Program, and*
[c]*Computing Science Division*
Texas A&M University
College Station, TX 77843

ABSTRACT

A dynamic model of the human heart's mitral valve motion during systole is presented. This model includes a description of the geometrical interrelationships between components of the mitral apparatus, namely mitral valve leaflets, annulus, chordae tendineae, papillary muscles, and left ventricle. The biomechanical properties of the mitral valve leaflets and chordae tendineae and the contractile nature of the annulus, papillary muscles and left ventricle are considered. Mitral valve profile/position is described for selected properties of model components.

INTRODUCTION

Mitral valve prolapse (also referred to as floppy or billowing mitral valve, systolic-click/late-systolic-murmur syndrome, Barlow's or Reid-Barlow's syndrome, or idiopathic mitral valve prolapse) has been described as the most common cardiac valve disorder (Jeresaty 1979). The exact prevalence of mitral valve prolapse is unknown, but results of various surveys indicate that approximately 4% of the general population may be affected (Brown et al. 1975; Procacci et al. 1976; Jeresaty 1979). Numerous articles describing this syndrome have been published during the past fifteen years and recent advances in ultrasound instrumentation have greatly aided in its detection. However, considerable controversy still remains regarding the etiology, criteria for diagnosis, and significance of mitral valve prolapse.

Normal function of the mitral apparatus depends upon the coordinated interaction of mitral valve leaflets, annulus, chordae tendineae, papillary muscles, the left ventricle, and the left atrium (Devereux et al. 1976). Mitral valve prolapse has been associated with alterations in all of these components except the left atrium. This model is a computer simulation of the anatomical and physiological interrelationships of

[1]This investigation was supported under United States Air Force Contract F33615-78-D-0629.

those components of the mitral apparatus which have been implicated as contributing to prolapse. It is based on published anatomical and physiological data and is limited, as are other models of the mitral valve, by the assumption of quasi-static forces in the system (Burch and DePasquale 1965; Burch and Giles 1972; Ghista and Rao 1972; Clark and Sutera 1973).

Large excursions of the mitral valve occur during five phases of the cardiac cycle—(1) rapid ventricular filling, (2) slow ventricular filling, (3) atrial systole, (4) isovolumetric systole (aortic valve closed), and (5) ventricular ejection (aortic valve open) (Karas and Elkins 1970). Valve motion during diastole is particularly complex. It is influenced by pressure differences across the mitral valve, geometry of the mitral opening and surrounding structures, transient vortices adjacent to the valve, and possibly active contraction of the muscle fibers in the leaflets (Zaky et al. 1969; Priola et al. 1970; Bellhouse 1972a, b; Hwang 1977). Diastolic valve motion has been excluded from this model due to the lack of quantitative information on the effects of pressure, flow, and active contraction during diastole.

The effects of flow through the mitral valve opening can be neglected during systole provided regurgitation is not occurring. This simplifies the mathematical description of valve motion and since the intent of this model is to provide a better understanding of mitral valve prolapse, a systolic event, it seems logical to concentrate on this phase of the cardiac cycle.

A computer program has been developed that accepts clinically obtained data, data based on published reports, and/or modeling assumptions and predicts mitral valve position/profile during systole. This approach was taken so that model verification and possibly diagnostic screening could easily be achieved without major alteration of the program. Thus, input parameters were selected so that clinical measurements could be obtained using non-invasive instrumentation—electrocardiography, apexcardiography, carotid pulse pressures, indirect blood pressure, and cardiac imaging techniques (cineangiography or real-time ultrasound).

DESCRIPTION OF THE MODEL

Coordinate System

Understanding the geometry of the mitral apparatus is essential for appreciating the interrelationships that exist between the various components of this model. An orthogonal coordinate system was devised to simplify the three dimensional description of the anatomy and dynamic motion associated with the various cardiac structures. This coordinate system is formed by the intersection of three planes (Fig. 1): (1) an x-y

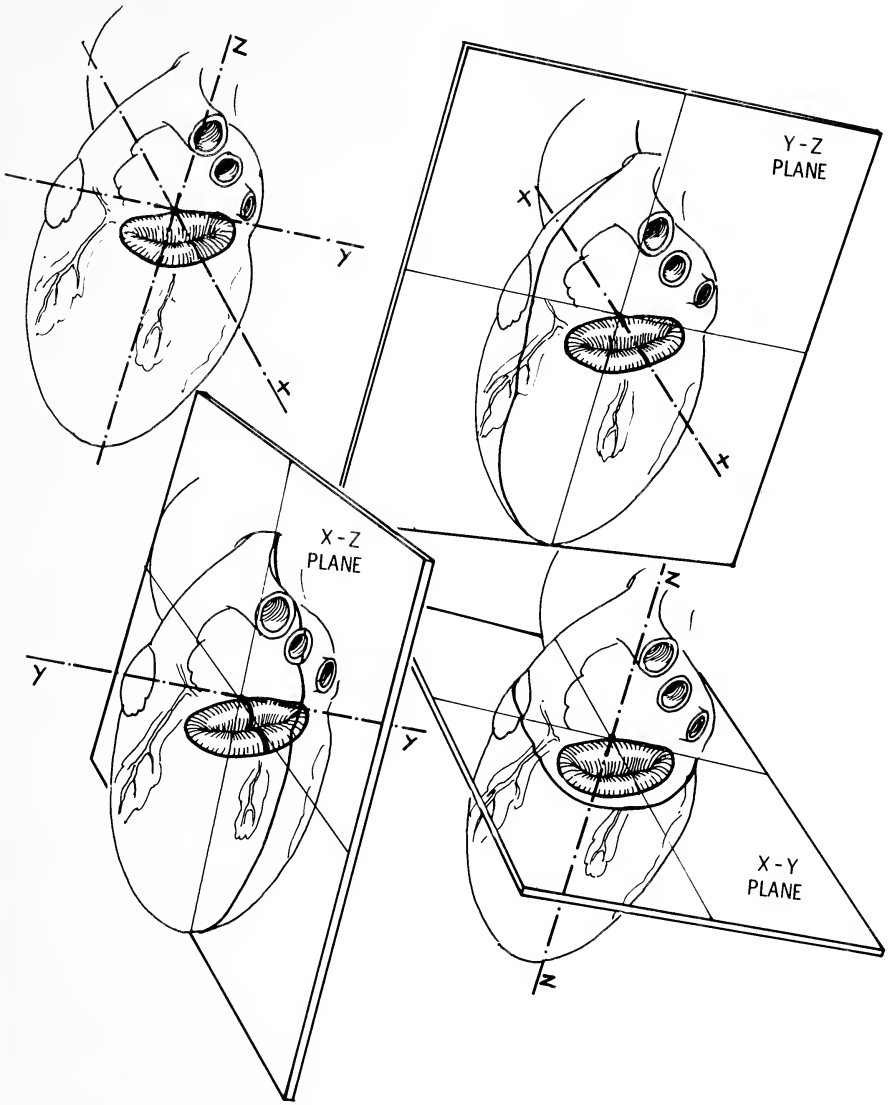

FIGURE 1. Coordinate system for the mitral apparatus. The origin is located at the center of attachment of the anterior leaflet to the annulus.

plane that contains the mitral valve annulus and remains perpendicular to the long axis of the ventricle throughout the cardiac cycle (Tsakiris et al. 1971), (2) an x-z plane that passes perpendicular to a line of coaptation and through the middle portions of the anterior and posterior mitral valve leaflets, and (3) a y-z plane passing through the anterior leaflet-annulus attachment.

Pressure and Timing Considerations

Systole has been classically defined as the period of ventricular contraction beginning with the rise of the left ventricular pressure and ending at the time of the incisural notch of the aortic pressure pulse (Wiggers 1921). For purposes of this simulation, ventricular systole is considered to be the interval between the Q-wave of the electrocardiogram and the incisural notch. To assist in properly sequencing the various active contractions and pressure related events that are described in this model, systole is subdivided into three time periods—(1) electromechanical delay time (EDT), (2) isovolumetric contraction time (IVCT), and (3) ejection time (ET). The duration of these various phases of systole is influenced by a number of factors, including stroke volume, aortic pressure, heart rate, and end diastolic volume (Wiggers 1921; Braunwald et al. 1958; Wallace et al. 1963).

Electromechanical delay time (EDT) is the interval between electrical stimulation and mechanical contraction of the myocardium. It probably represents the delay associated with the excitation-contraction coupling of individual muscle fibers (Spodick and Kumar 1968a). This phase of ventricular systole begins with the onset of the Q-wave of the ECG; however, the exact time of termination of this phase is poorly defined. Some researchers consider the mitral component of the first heart sound as defining the end of EDT (Frank and Kinlaw 1962). Other investigators believe that the kinetocardiograph provides an accurate indication of the termination of EDT (Harrison et al. 1964). Spodick and Kumar (1968a) report that the endpoint of EDT more appropriately corresponds to a distinctive portion of the apexcardiogram, the apexcardiogram upstroke (ACGU). They have shown that ACGU coincides with the onset of intramural myocardial tension and therefore appears to be the best indicator of the initiation of ventricular contraction.

Model assumptions:

1. During the period corresponding to the electromechanical delay time (EDT), the only component of the mitral apparatus that is actively contracting is the annulus (Tsakiris et al. 1971).
2. The mitral valves are in equilibrium and the leaflets are coapted during EDT. (This assumption is contradictory to published reports that valve closure does not occur until ventricular pressure rises, approximately 20 msec following the end of the EDT phase (Kostis et al. 1969; Fabian et al. 1972); however, this assumption is defensible based upon the fact that valve motion is negligible immediately following closure and therefore previous movements will have minimal influence on subsequent valve positions (Upton et al. 1976).)

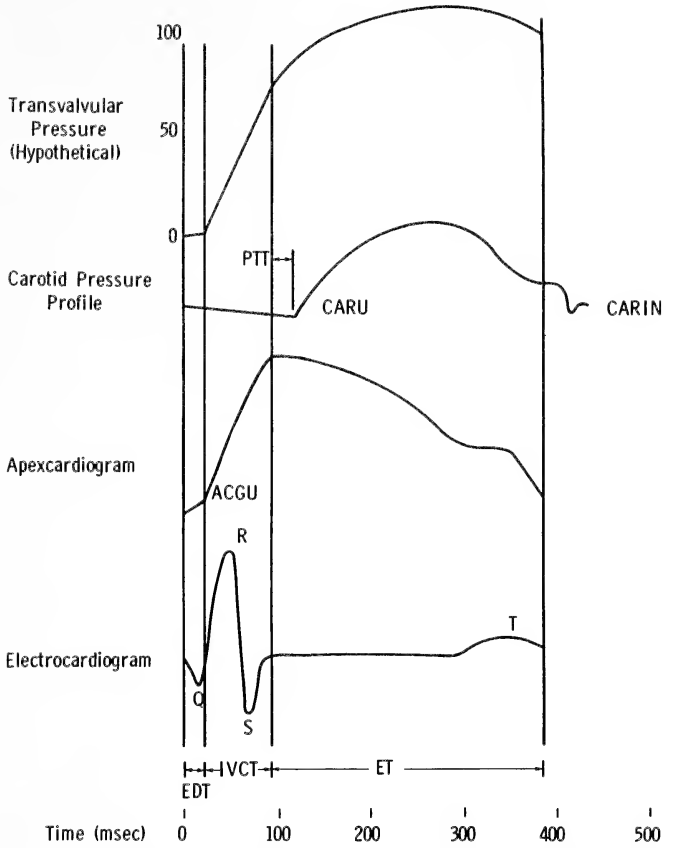

FIGURE 2. Diagrammatic representation of pressure and timing events during systole—electromechanical delay (EDT), isovolumetric contraction time (IVCT), ejection time (ET), apexcardiogram upstroke (ACGU), pulse transmission delay (PTT), carotid pulse upstroke (CARU), and carotid pulse incisura (CARIN).

Input data (Fig. 2):

Hypothetical—Electromechanical delay time (EDT) equals 22 msec (Spodick and Kumar 1968a).

Clinical—Electromechanical delay time (EDT) as determined by measuring the interval between the onset of the Q-wave and the upstroke of the apexcardiogram (EDT = QWAVE−ACGU).

Isovolumetric contraction time (IVCT) is the period of the caardiac cycle extending from the end of EDT to the opening of the aortic valve. IVCT changes from beat to beat and has been shown to be affected by heart rate, contractile state of the myocardium, ventricular end-diastolic volume, aortic diastolic pressure, and stroke volume (Wallace et al. 1963; Harrison et al. 1964; Kumar and Spodick 1970; Fabian et al. 1972; Hirschfeld et al. 1976). For purposes of this model the onset of this

phase is associated with the upstroke of the apexcardiogram (ACGU). The three most commonly used indicators for the end of IVCT are (1) the carotid pulse upstroke (CARU), (2) the carotid pulse upstroke corrected for pulse transmission delay (CARUC), and (3) the E point of the apexcardiogram (Spodick and Kumar 1968b; Kumar and Spodick 1970; Oreshkov 1972; Fabian et al. 1972). For purposes of this model, the carotid pulse upstroke corrected for pulse transmission delay is the most accurate timing index. Pulse transmission delay (PTT) may be determined by simultaneously recording carotid pulse profile and phonocardiograms; the time between the aortic component of the second heart sound and the nadir of the carotid incisura provides an accurate estimate of PTT. The average PTT for the right carotid artery is approximately 23 msec (Fabian et al. 1972).

Model assumptions:

1. Left ventricular wall and papillary muscle contractions begin with the onset of IVCT (Spodick and Kumar 1968b; Hirakawa et al. 1977).
2. Transvalvular pressure increases linearly during this phase of the cardiac cycle.

Input data (Fig. 2):

Hypothetical—Isovolumetric contraction time (IVCT) equals 71 msec (Kumar and Spodick 1970). Transvalvular pressure (TP) at the end of IVCT equals 80 mm Hg.

Clinical—Isovolumetric contraction time (IVCT) as determined from apexcardiogram and carotic pulse recordings corrected for pulse transmission delay (IVCT = ACGU−CARUC). Transvalvular pressure (TP) at the time of aortic valve opening may be estimated using standard indirect sphygmomanometric techniques to determine peripheral diastolic pressures (Krausman 1975).

Ejection time (ET) is defined as the period between the onset of the aortic pressure rise and the incisural notch. This can be clinically measured from the beginning of the carotid pulse upstroke (CARU) to the nadir of the carotid pulse incisura (CARIN) (Fabian et al. 1972). Close agreement exists between ET measured in this manner and direct measurements obtained within the aorta (Weissler et al. 1961; Van de Werf et al. 1975). Kumar and Spodick (1970) and Fabian et al. (1972) have experimentally derived equations relating heart rate to ET; however, other parameters that affect ET, namely stroke volume, aortic pressure, and myocardial contractility, have not been mathematically characterized.

During ejection the carotid pulse profile is closely related to the aortic pressure waveform (Robinson 1963) and thus may serve as an approximation of transvalvular pressure profile.

Model assumptions:

1. Annulus, left ventricular wall, and papillary muscle contractions continue throughout this phase of systole.

Input data (Fig. 2):

Hypothetical—Ejection time (ET) equals 292 msec (Kumar and Spodick 1970). Transvalvular pressure (mm Hg) is expressed by the following equation:

$$TP = 80 + 40 \cdot \sin(K \cdot ETT) \quad (1)$$

where ETT (msec) is the time measured from the start of the ejection phase and K is a constant (0.009) selected so that peak transvalvular pressure occurs at approximately 175 msec.

Clinical—Ejection time (ET) as determined by carotid pulse recordings (ET = CARU−CARIN) (Fabian et al. 1972; Van de Werf et al. 1975) or by echocardiography (Hirschfeld et al. 1975). Transvalvular pressure throughout the ejection phase may be estimated from carotid pulse recordings and peripheral systolic and diastolic blood pressure determinations using sphygmomanometric techniques (Krausman 1975).

Mitral Valve Leaflets

The mitral valve has been described by Chiechi et al. (1956) as a continuous veil of tissue attached around the entire circumference of the mitral orifice. The valve consists of fibrous, elastic, and muscular elements covered by an endocardial coat. The muscular elements are concentrated in the basal portion of the valve and appear to be anatomically and possibly functionally continuous with the left atrium (Fenoglio et al. 1972; Wit et al. 1973). Collagen fibers extend from the annulus through the leaflet to form chordae tendineae and thus form a continuous fibrous tissue from the annulus to the papillary muscles (Fenoglio et al. 1972).

The free edge of the veil of tissue is interrupted by indentations which divide the valvular tissue into two major leaflets (Fig. 3). The anterior leaflet (also referred to as the aortic, septal, greater, or anteromedial leaflet) has been described as semicircular or triangular in shape (Fig. 4) (Chiechi et al. 1956; Ranganathan et al. 1976). The posterior leaflet is rectangular in shape (Fig. 4). Indentations along the free edge of the posterior leaflet give it a scalloped appearance. In 92% of the normal human hearts studied by Ranganathan et al. (1976), the posterior leaflet was triscalloped with a large middle scallop.

Along the free edge of both leaflets is a zone of tissue that appears roughened (Fig. 4). This opaque portion of the mitral valve receives the insertion of chordae tendineae on its ventricular surface. This rough

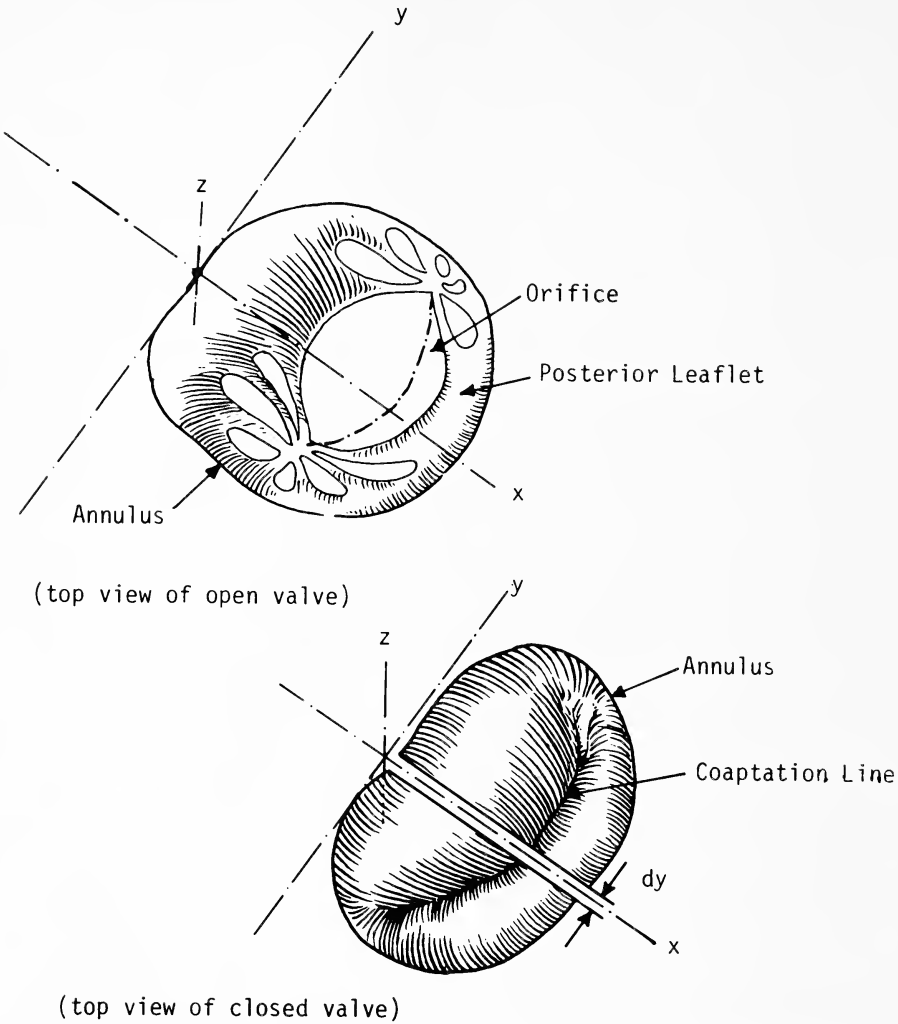

FIGURE 3. Anatomy of the mitral valve. Infinitesimal strip of leaflet extending along the x-axis represents the mitral valve position and profile (modified from Davila and Palmer 1962).

zone has been described as an area of coaptation for leaflet apposition (Carpentier et al. 1976; Ranganathan et al. 1976). The ratio of rough zone to smooth leaflet tissue in the anterior leaflet is 0.6 and for the posterior leaflet 1.4 (Ranganathan et al. 1976). Based on these ratios and anatomical data for leaflet heights (Table 1), the leaflets would contact each other along a strip approximately 0.8 cm wide at the center of the leaflets. However, this is not compatible with measurements of annulus dimensions since the portions of the leaflets that are not opposed would not physically reach from the anterior to the posterior

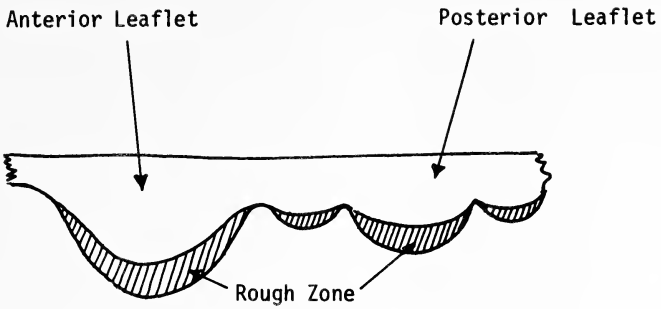

FIGURE 4. Schematic representation of mitral valve leaflets illustrating the shape of the leaflets and extent of the rough zone (modified from Ranganathan et al. 1970).

The mechanical properties of mitral valve leaflets have been studied by several investigators (Clark and Butterworth 1971; Ghista and Rao 1972; Clark 1973). There is an initial stretching of the leaflet at very low (pre-transition) stresses (Fig. 5A). With additional stress, the modulus of elasticity changes abruptly at the transition stress (Fig. 5B) to a larger post-transition modulus of elasticity characteristic of a stiffer material (Fig. 5C). Typical values for pre- and post-transition moduli, transition stress, and transition strain are listed in Table 2. The strain at transition is approximately 15% of the original unstretched leaflet height. From this curve and values for the elastic moduli, it is apparent edge of the annulus. The extent of coaptation probably varies from a single line to a plane of coaptation depending upon the degree of annulus narrowing, leaflet dimensions, and positions of the leaflets relative to the annulus.

TABLE 1. Selected anatomical data for mitral valve leaflets (from autopsy of normal human subjects).

Parameter	Average Value	Number Subjects	Sex	Reference
Anterior Leaflet Height	23 mm	50	?	Carpentier et al. 1976
Anterior Leaflet Height	24 mm	26	M	Ranganathan et al. 1970
Anterior Leaflet Height	22 mm	24	F	Ranganathan et al. 1970
Anterior Leaflet Height	24 mm	60	M	Chiechi et al. 1956
Anterior Leaflet Height	22 mm	45	F	Chiechi et al. 1956
Anterior Leaflet Height	23 mm	25	M	Rusted et al. 1952
Anterior Leaflet Height	21 mm	25	F	Rusted et al. 1952
Posterior Leaflet Height	14 mm	50	?	Carpentier et al. 1976
Posterior Leaflet Height	14 mm	26	M	Ranganathan et al. 1970
Posterior Leaflet Height	12 mm	24	F	Ranganathan et al. 1970
Posterior Leaflet Height	14 mm	60	M	Chiechi et al. 1956
Posterior Leaflet Height	12 mm	45	F	Chiechi et al. 1956
Posterior Leaflet Height	13 mm	25	M	Rusted et al. 1952
Posterior Leaflet Height	12 mm	25	F	Rusted et al. 1952

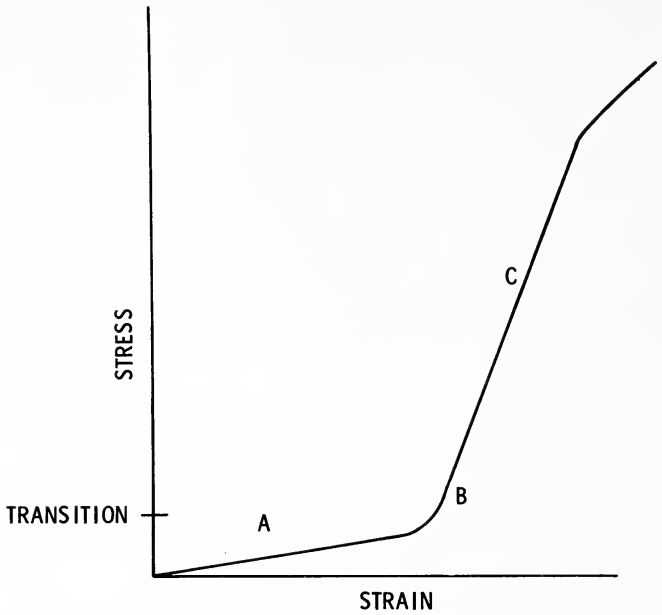

FIGURE 5. Typical stress-strain characteristics of mitral valve leaflets. Pre-transition (A), transition (B), and post-transition (C) properties.

that most of the total leaflet stretch is associated with the relative elastic properties of the leaflet prior to reaching transition.

Based on studies of Ghista and Rao (1972) and Miller et al. (1981), transition for the leaflets is reached at low transvalvular pressure (between 2 and 13 mm Hg). Lack of apparent leaflet stretch in angiographic and ultrasound imaging studies support the conclusion of Rushmer et al. (1956) and Miller et al. (1981) that the valve leaflets and chordae tendineae are normally under tension throughout the cardiac cycle and that this tension is sufficient to cause the leaflets to operate in the post-transitional region at all times.

Model assumptions:

1. The presystolic leaflet heights, which represent pre-stressed dimensions, are anterior leaflet height (AMVIL) = 2.4 cm, and posterior leaflet height (PMVIL) = 1.4 cm.

TABLE 2. Biomechanical properties of mitral valve leaflets ex situ.

Pre-Transition Modulus dyne/cm^2	Post-Transition Modulus dyne/cm^2	Transition Stress dyne/cm^2	Transition Strain %	Reference
$1 \cdot 10^5$	$5 \cdot 10^7$	$3 \cdot 10^4$		Ghista and Rao 1972
$1.1 \cdot 10^5$	$2.9 \cdot 10^7$	$3.4 \cdot 10^4$	14.3	Clark 1973
$2.8 \cdot 10^5$	$8.3 \cdot 10^7$	$3.8 \cdot 10^4$	15.0	Clark and Butterworth 1971

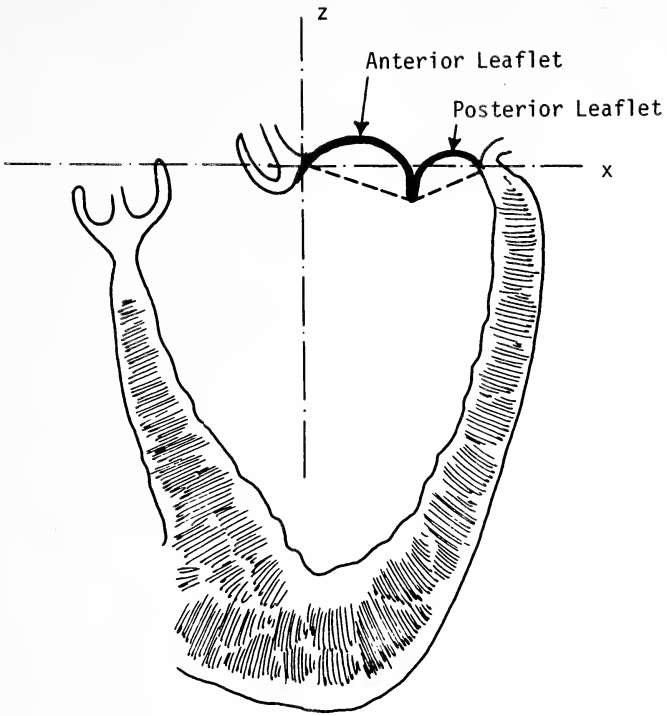

FIGURE 6. Elliptically shaped leaflets. Major axes drawn between annulus attachment and leaflet free edges.

2. The leaflets are uniform, thin membranes which are only capable of supporting internal stress in tension (Clark and Sutera 1973).
3. An infinitesimal strip of leaflet selected from the middle portion of each leaflet will represent the position and profile of the mitral leaflets and that this leaflet strip can only move in the x-z plane (Clark and Sutera 1973) (Fig. 3).
4. The leaflet assumes an elliptical shape which has as its major axis an imaginary line joining the free edge of the leaflet to the point of attachment of the leaflet to the annulus (Fig. 6).
5. The extent of coaptation is determined by the natural intersection of elliptical segments drawn to represent the anterior and posterior leaflets (Fig. 7).
6. The forces exerted by the chordae tendineae on the free edges of the leaflets can be represented as a distributed tension along the entire free edges (Clark and Sutera 1973).
7. The attachments between the annulus and the leaflets and between the chordae tendineae and the leaflets can be regarded as ideal hinges which offer no resistance to rotation (Clark and Sutera 1973).

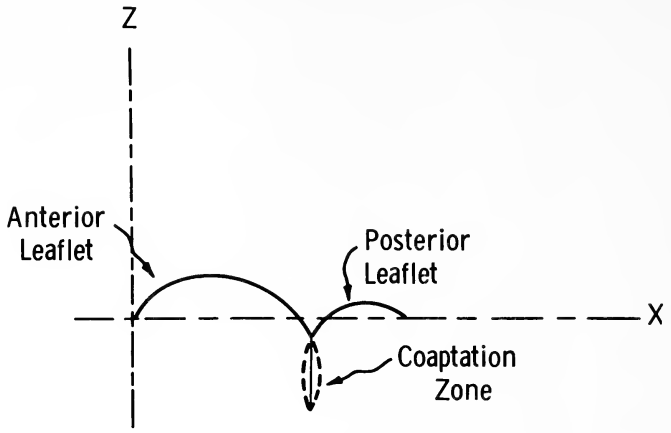

FIGURE 7. Zone of leaflet coaptation as determined by the natural intersection of elliptically shaped leaflets.

8. The inertial forces are neglected throughout the analysis and the mechanical forces generated by transvalvular pressure are treated in a quasi-static manner.
9. The mitral valve leaflets are pre-stressed and can be characterized by their post-transition modulus (MVE = $5 \cdot 10^7$ dyne/cm^2) (Ghista and Rao 1972).
10. The tension or stress in the leaflet (MVT) can be calculated by the following equation (Miller et al. 1981):

$$\text{MVT} = \frac{666 \cdot \text{TP} \cdot \text{ANL}}{\text{HL}} \tag{2}$$

where MVT is leaflet tension (dyne/cm^2), TP is transvalvular pressure (mm Hg), ANL is annulus diameter measured along x-axis (cm), and HL is leaflet thickness (assumed to be 0.05 cm).

11. The strain of the leaflets (MVSTR) is:

$$\text{MVSTR} = \frac{\text{MVT}}{\text{MVE}}. \tag{3}$$

12. The height of each leaflet is:

$$\text{AMVL} = \text{AMVIL} \cdot (1 + \text{MVSTR}), \tag{4}$$

where AMVL is the anterior mitral valve leaflet height (cm), and AMVIL is the anterior mitral valve leaflet height initially (assumed to be 2.4 cm). A similar expression applies for calculating the height of the posterior mitral valve:

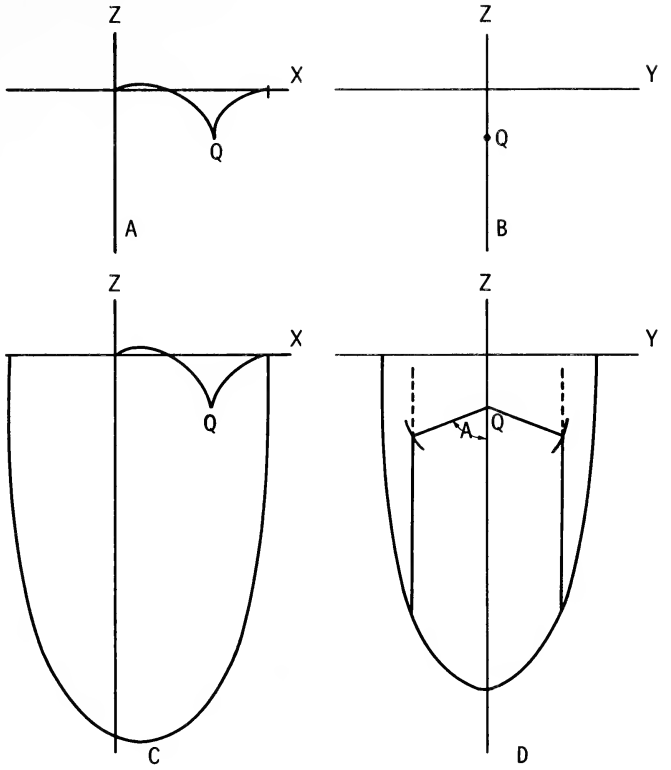

FIGURE 8. Diagrammatic representation of the initial geometry of the mitral apparatus. Point Q is located at the leaflet free edges. A is the angle between the chordae tendineae and a line parallel to the z-axis.

$$\text{PMVL} = \text{PMVIL} \cdot (1 + \text{MVSTR}). \tag{5}$$

Input data:

Hypothetical—The initial position (Figs. 8A and B) of the leaflet free edges (Q) is QX = 2.0, QY = 0.0, and QZ = −0.9.

Clinical—The initial position of the leaflets may be determined using real-time, two-dimensional ultrasound imaging techniques; however, translation of axes from a transducer-centered coordinate system to that used in this model must be performed to insure appropriateness of the data.

Mitral Valve Annulus

The annulus consists of dense collagenous tissue with scattered thin elastic fibers and serves as a framework for attachment of the mitral valve leaflets (Davila and Palmer 1962). Viewed from above with the atria removed (Fig. 9), the annulus consists of (1) a fibrous trigone situated between the anterior leaflet and the aortic and tricuspid valves,

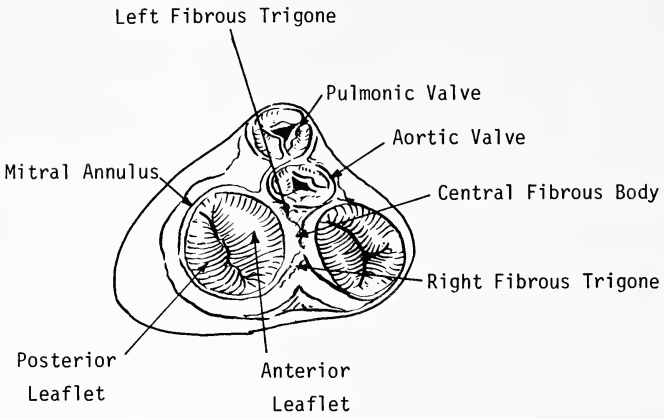

FIGURE 9. Anatomy of the mitral valve annulus (modified from Silverman and Hurst 1968).

and (2) a rather poorly defined band of fibroelastic tissue which forms the attachment site for the posterior leaflet (Silverman and Hurst 1968).

Besides serving as a base for leaflet attachment, the annulus may be involved in insuring competence of the mitral valve (Perloff 1976). Tsakiris et al. (1971) have demonstrated, using anesthetized dogs, that the annulus undergoes active contraction. After reaching a maximum size in late diastole, the area of the annulus decreases by 19 to 34% during atrial and ventricular systole. One-half to two-thirds of this decrease in area apparently occurs during atrial contraction. This narrowing of the annulus is eccentric: The portion of the annulus forming the attachment for the posterior leaflet moves toward a relatively fixed site of anterior leaflet attachment, the fibrous trigone. The degree of

TABLE 3. Selected anatomical data for mitral annulus (from autopsy of normal human subjects).

Parameter	Average Value	Number of Subjects	Sex	Reference
Circumference	9 cm	24	11M, 13F	Bulkley and Roberts 1975
Circumference	11.6 cm	60	?	Carpentier et al. 1976
Circumference	9 cm	26	M	Ranganathan et al. 1970
Circumference	7.5 cm	24	F	Ranganathan et al. 1970
Circumference	10.0 cm	60	M	Chiechi et al. 1956
Circumference	9.0 cm	45	F	Chiechi et al. 1956
Circumference	9.9 cm	25	M	Rusted et al. 1952
Circumference	8.5 cm	25	F	Rusted et al. 1952
Intercommissural Diameter	2.5 cm	25	M	Rusted et al. 1952
Intercommissural Diameter	2.1 cm	25	F	Rusted et al. 1952
Area of Annulus	7.93 cm^2	8	M	Chiechi et al. 1956
Area of Annulus	6.42 cm^2	8	F	Chiechi et al. 1956

narrowing of the annulus is a function of several factors, including duration of the P-R interval, duration of the ventricular systole, ventricular volume during diastole, and degree of emptying during systole. Table 3 is a compilation of published reports regarding dimensions of the human mitral valve annulus.

Model assumptions:

1. The annulus remains at right angles to the long axis of the ventricle during systole (Tsakiris et al. 1971).
2. The annulus does not rotate relative to the ventricle during systole (Tsakiris et al. 1971).
3. The orthogonal coordinate system used in this simulation is centered at the annular attachment of the mid-point of the anterior leaflet (Fig. 1).
4. The annulus narrows at a constant rate throughout systole.

Input data:

Hypothetical—Annulus diameter (ANEDL) at the start of systole = 2.90 cm. Annulus diameter (ANESL) at the end of ventricular ejection = 2.73 cm. (These dimensions are based on assuming a circular annulus with a maximal diastolic circumference = 10 cm, a total reduction in annulus area of 26.5% which corresponds to a decrease in diameter of 14.3%, and contraction during atrial systole accounting for 63% of the total narrowing.)

Clinical—Annulus measurements, obtained using cineangiography or ultrasound imaging, may be substituted for hypothetical data.

Chordae Tendineae

Chordae tendineae radiate from the tips of both papillary muscles to attach to the ventricular border of the mitral valve leaflets (Fig. 10). Chordae arising from the anterolateral papillary muscle connect to the anterolateral commissure and the adjoining halves of the anterior and posterior leaflets. Similarly, chordae arising from the posteromedial papillary muscle pass to the respective commissure and portions of the leaflets (Davila and Palmer 1962; Silverman and Hurst 1968).

Ranganathan et al. (1976) have categorized chordae tendineae on the basis of their size and location of attachment to the mitral valve. Chordae attaching to the anterior leaflet are classified as either (1) rough-zone chordae which branch before inserting on or near the free edge of the leaflet, or (2) strut chordae which are relatively large chordae and insert directly on the edge of the leaflet near its mid-portion. Posterior leaflet chordae are either (1) rough-zone chordae, (2) cleft chordae which attach between leaflet scallops, or (3) basal chordae which attach near the annulus and may arise directly from the wall of the left ventricle. An average of 25 primary chordae tendineae is associated with the

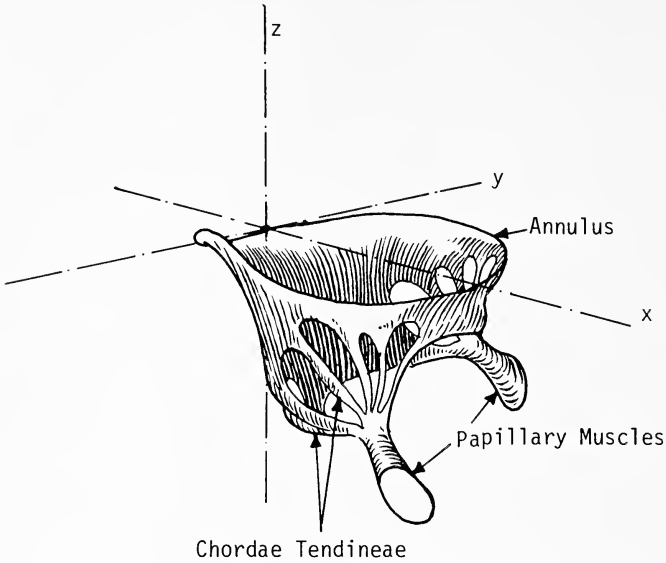

FIGURE 10. Anatomy of the chordae tendineae (modified from Davila and Palmer 1962).

mitral valve; 9 attach to the anterior leaflet (7 rough-zone and 2 strut types), 14 attach to the posterior leaflet (10 rough-zone, 2 cleft, and 2 basal), and 2 attach to the commissures separating the anterior and posterior leaflets (Lam et al. 1970; Ranganathan et al. 1976). The lengths of chordae attaching to the leaflets are summarized in Table 4.

Chordae tendineae are composed of three layers—(1) an outer layer of endocardial cells, (2) an intermediate layer of loosely meshed collagen and elastic fibers, and (3) an inner core of dense collagen (Fenoglio et al. 1972; Lim and Boughner 1977). The mechanical properties of chordae are similar to those of the mitral valve leaflets, in that these structures exhibit a non-linear stress-strain characteristic (Fig. 11) (Lim and Boughner 1975). Salisbury et al. (1963) measured tension along chordae tendineae throughout the cardiac cycle and reported that (1) presystolic chordae tendineae tension can be as high as 12 g; (2) during the isovolumetric contraction phase, tension in the chordae tendineae rises simultaneously with left ventricular pressure; and (3) during ejection, tension either drops or levels off and does not appear to be directly related to left ventricular pressure.

Model Assumptions:

1. Chordae tendineae insert on the free edges of the mitral valve leaflets.
2. Chordae tendineae are freely hinged at the sites of attachment to the leaflets and papillary muscles.

TABLE 4. Selected anatomical data for chordae tendineae (from autopsy of normal human subjects).

Parameter	Average Value	Number of Subjects	Sex	Reference
Chordae Tendineae Length Anterolateral P.M. to Anterior Leaflet	1.5 cm	50	?	Carpentier et al. 1976
Chordae Tendineae Length Posteromedial P.M. to Anterior Leaflet	1.7 cm	50	?	Carpentier et al. 1976
Chordae Tendineae Length Anterior Leaflet	1.75 cm	50	27M, 23F	Lam et al. 1970
Chordae Tendineae Length Posterior Leaflet	1.4 cm	50	?	Carpentier et al. 1976
Posterior Leaflet	1.4 cm	50	27M, 23F	Lam et al. 1970

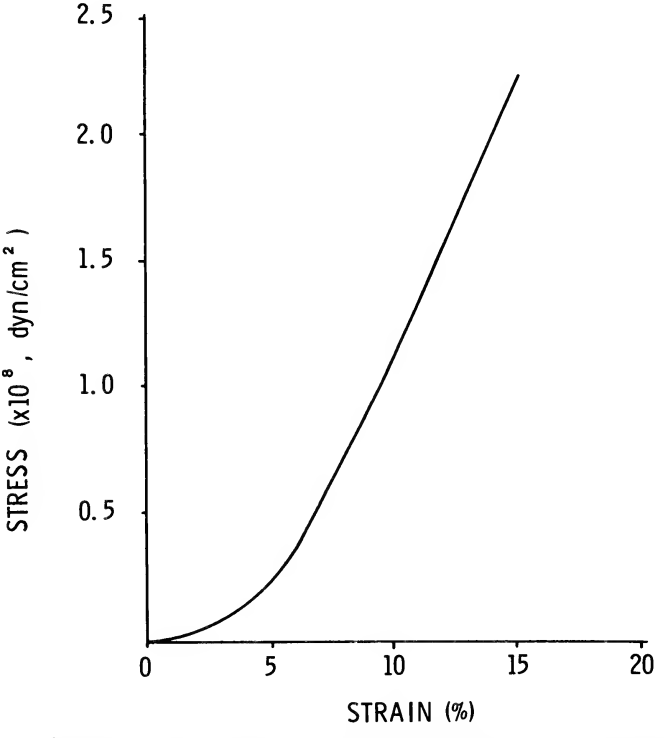

FIGURE 11. Biomechanical properties of the chordae tendineae. Cross-sectional area = 0.004 - 0.006 cm^2; strain-rate = 12.7 cm/min (from Lim and Boughner 1975).

3. Chordae tendineae operate in a pre-stressed condition at the start of systole (Salisbury et al. 1963) and thus may be characterized by their post-transition elastic modulus throughout systole (CTE = $2 \cdot 10^9$ dyne/cm^2) (Lim and Boughner 1975).
4. Chordae tendineae lengths reported in Table 4 represent pre-stressed measurements. The initial length for all chordae (CTIL) equals 1.5 cm.
5. Chordae tendineae tension (CTT) is a function of two parameters—transvalvular pressure (TP) and ventricular geometry. The chordae exert tension on the free edges of the leaflets to restrain their atrial-ward movement. Ventricular geometry influences the angle that the chordae make with respect to the z-axis and thus the tension within the chordae counteracting atrial-ward movement of the leaflets (Fig. 8D). Based on a study by Salisbury et al. (1963) and considerations for ventricular geometry, an empirical formula relating CTT to TP has been derived:

$$CTT = 650 \cdot \frac{TP}{COSA \cdot CTA} \tag{6}$$

where CTT is chordae tendineae tension (dyne/cm^2), TP is transvalvular pressure (mm Hg), COSA is the cosine of angle A, and CTA is the area of an average chordae tendineae (assumed to be .004 cm^2).
6. Chordae tendineae strain (CTSTR) may be calculated as follows:

$$CTSTR = \frac{CTT}{CTE}; \tag{7}$$

and the length of the chordae tendineae may be expressed by the following equation:

$$CTL = CTIL\ (1 + CTSTR) \tag{8}$$

where CTL is the chordae length (cm), and CTIL is the initial chordae length (assumed to be 1.5 cm).

Papillary Muscles

The two groups of papillary muscles, the anterolateral and posteromedial, are located immediately below the respective commissures of the leaflets. The antereolateral papillary muscle usually has a single muscle belly and is continuous with the ventricle along the anterolateral free wall; the posteromedial papillary muscle typically consists of two or three distinct muscle bellies and is located at the junction of the

posterior free wall and the ventricular septum (Rusted et al. 1952; Chiechi et al. 1956; Estes et al. 1966; Silverman and Hurst 1968; Roberts and Cohen 1972). Papillary muscles may also be classified on the basis of their morphology as follows: (1) Completely tethered, the papillary muscle is fully adherent to the ventricular myocardium; (2) Free and fingerlike, with one-third or more of the papillary muscle protruding freely into the ventricular cavity; and (3) Mixed or intermediate, with considerable trabecular attachments and tethering between the papillary muscle and ventricular wall (Ranganathan and Burch 1969).

The papillary muscles normally arise from the left ventricular wall at the apical and middle thirds (Silverman and Hurst 1968; Perloff 1976). They are oriented parallel to the left ventricular wall to which they are attached. The attachment usually extends almost the full length of the muscle and consists of crossing muscle bundles and threadlike bands (Estes et al. 1966; Silverman and Hurst 1968).

There is considerable disagreement among investigators regarding the timing and extent of papillary muscle contraction. Cronin et al. (1969) indicate that ventricular wall contraction precedes papillary muscle contraction. According to Semafuko and Bowie (1975), the anterolateral papillary muscle lengthens during isovolumetric contraction and the early ejection phase of the cardiac cycle. This study suggests that papillary muscle shortening may occur only when the force of muscle contraction exceeds the forces that tend to elongate the papillary muscle, i.e. chordae tendineae tension resisting atrial-ward leaflet excursion. Other investigators report that the papillary muscles shorten throughout systole (Burch and DePasquale 1965; Hirakawa et al. 1977). The total shortening, measured in dogs, varies in published data from 10% to 22.8% of the total length (Grimm et al. 1975; Hirakawa et al. 1977; Huntsman et al. 1977).

Model assumptions:

1. The papillary muscles are symmetrically oriented relative to the x-z plane and attach to the ventricular wall at points two-thirds of the distance from the annulus to the apex (Fig. 8D).
2. The papillary muscles are tethered along their entire lengths to the ventricular wall and maintain a longitudinal orientation, parallel to the x-axis, throughout systole.
3. The presystolic lengths of the papillary muscles are determined from geometric considerations following specifications of the presystolic position of the mitral valve, chordae tendineae lengths, and left ventricular dimensions.
4. A total contraction of 16.4% of the presystolic papillary muscle length occurs linearly with respect to time during the isovolumetric contraction and ejection phases of systole.

TABLE 5. Selected anatomical data for the left ventricle (normal human subjects).

Parameter	Average Value	Number of Subjects	Sex	Method[a]	Reference
Annulus to Apex Length at End-Diastole (AAEDL)	7.0 cm	24	11M, 13F	A	Bulkley and Roberts 1975
AAEDL	7.3 cm	25	M	A	Rusted et al. 1952
AAEDL	6.7 cm	25	F	A	Rusted et al. 1952
Minor Axis Length at End-Diastole (MAEDL)	5.0 cm	10	?	E	Fortuin et al. 1972
MAEDL	4.40 cm	20	11M, 9F	E	McDonald et al. 1972
MAEDL	5.18 cm	37	M	E	Gerstenblith et al. 1977
Minor Axis Length at End-Systole (MAESL)	3.8 cm	10	?	E	Fortuin et al. 1972
MAESL	2.83 cm	20	11M,9F	E	McDonald et al. 1972
MAESL	3.44 cm	37	M	E	Gerstenblith et al. 1977

[a]A = autopsy; E = echocardiography

Left Ventricle

Cardiac performance traditionally has been defined according to hemodynamic determinants and only recently have attemps been made to correlate these with muscle function and geometric considerations (Liedtke et al. 1972). The left ventricle has a particularly important role in the anatomy and physiology of the mitral apparatus. Ventricular shape and contraction patterns influence value motion directly through changes in transvalular pressure and indirectly through alternations in geometric relationships between the papillary muscles and the valve leaflets.

Major dimensional changes of the left ventricle are associated with the ejection phase of systole. During ejection, there is marked contraction of the left ventricle which results in continuous repositioning of the papillary muscles relative to the leaflets/annulus. Altered left ventricular shape will affect the overall operation of the mitral apparatus due to the complex geometric interrelationships among components of the mitral apparatus.

Table 5 summarizes published data regarding ventricular dimensions. Table 6 lists results of various studies that have attemped to measure the extent of ventricular contraction.

Model assumptions:

1. The left ventricle is a truncated ellipsoid of revolution (Koushanpour and Collings 1966; Hutchins et al. 1978) that both shortens and contracts symmetrically about its major axis throughout the ejection phase of systole (McDonald 1970).

TABLE 6. Selected physiological data for the left ventricle.

Parameter	Average Value	Subjects	Number of Subjects	Sex	Method[a]	Reference
Annulus to Apex % Shortening	6.9-8.1%	Canine	5	?	S	Hirakawa et al. 1977
Annulus to Apex % Shortening	8%	Canine	5	?	C	Liedtke et al. 1972
Annulus to Apex % Shorteing	4.6%	Canine	13	?	A	Ross et al. 1967
Minor Axis Length % Shortening	25%	Human	?	?	R	Daughters et al. 1977
Minor Axis Length % Shortening	35.5%	Human	20	11M 9F	E	McDonald et al. 1972
Minor Axis Length % Shortening	61%	Canine	5	?	C	Liedtke et al. 1972
Minor Axis Length % Shortening	26%	Canine	13	?	A	Ross et al. 1967
Minor Axis Length % Shortening	34%	Human	37	M	E	Gerstenblith et al. 1977
Minor Axis Length % Shortening	24%[b]	Human	10	?	E	Fortuin et al. 1972

[a]A = autopsy (special fixation); C = cineangiocardiography; E = echocardiography; R = radiopaque markers; S = sonomicrometry.
[b]Computed from anatomical data.

2. The contractions along the major and minor axes are linear functions of time (i.e. constant rate of contraction) (Bishop et al. 1969; Hinds et al. 1969; Bishop and Horwitz 1970).

Input data:

Hypothetical—Mitral annulus to apex dimensions (AAL) are end-diastole (AAEDL) = 7.30 cm, and end-systole (AAESL) = 6.75 cm—resulting in an overall 7.5% shortening. Minor axis dimensions (MAL) are end-diastole (MAEDL) = 4.86 cm, and end-systole (MAESL) = 3.34 cm—resulting in an overall 31% shortening. Extent of truncation (TRUNC): The annulus is located at 60% of the total eliptical major axis; major axis end-diastole = 12.17 cm, and major axis end-systole = 11.25 cm.

Clinical—Actual dimensional measurements of annulus-to-apex and minor axis may be obtained using cineangiography or ultrasound imaging and degree of truncation estimated from these measurements.

MODEL OPERATION

Mitral value motion is predicted by a computer program that describes the dynamic alterations in the various components of the mitral

TABLE 7. Input values for the model.

Abbreviation	Parameter	Assumed Value
EDT	Electromechanical Delay Time	22 msec
IVCT	Isovolumetric Contraction Time	71 msec
ET	Ejection Time	292 msec
TP	Transvalvular Pressure	(Refer to Fig. 2)
AMVIL	Anterior Leaflet Height (Initial)	2.4 cm
PMVIL	Posterior Leaflet Height (Initial)	1.4 cm
MVE	Mitral Valve Leaflet Elastic Modulus	$5 \cdot 10^7$ dyne/cm^2
QX	X—Coordinate of Leaflet Free Edge (Initial)	2.0 cm
QY	Y—Coordinate of Leaflet Free Edge (Initial)	0.0 cm
QZ	Z—Coordinate of Leaflet Free Edge (Initial)	−0.9 cm
ANEDL	Annulus Diameter at End-Diastole	2.70 cm
ANESL	Annulus Diameter at End-Systole	2.56 cm
CTIL	Chordae Tendineae Length (Initial)	1.5 cm
CTE	Chordae Tendineae Elastic Modulus	$2 \cdot 10^9$ dyne/cm^2
PMPER	Papillary Muscles-Percent Shortening	16.4%
AAEDL	Annulus to Apex—End-Diastolic Length	7.3 cm
AAESL	Annulus to Apex—End-Systolic Length	6.75 cm
MAEDL	Minor Axis—End-Diastolic Length	4.86 cm
MAESL	Minor Axis—End-Systolic Length	3.34 cm
TRUNC	Truncation—Percent (annulus to apex/major axis length)	60%
GAPIL	Distance Between the Point of Annular Attachment of the Posterior Leaflet and the Ventricular Wall (Initial)	0.0 cm
INCRT	Time Increment to Step Through Program	10 msec

apparatus. Following input of clinically obtained and/or hypothetical data (Table 7), the computer program initializes the geometry of the model using the coordinate system previously described (Fig. 1). The anterior portion of the annulus is located at x=0, y=0, and z=0 (Fig. 8A). The leaflets are represented by elliptical segments in the x-z plane, extending from the annulus to the point of coaptation (Q) at the leaflet free edges (Fig. 8A). In a y-z plane (x=Qx), the leaflets are represented as single point, Q (Fig. 8B). As previously described, a truncated ellipse is used to model the left ventricle. Its major axis is parallel to the z-axis and located within the x-z plane; the minor axis is parallel to the x-y plane and separated from this plane by a distance specified by the extent of truncation (Fig. 8C). The ellipse representing the ventricle is assumed to pass through the posterior portion of the annulus (x= ANEDL, y=0, z=0), but can be positioned anywhere along the x-axis by specifying a separation between the annulus and ventricle wall (GAPIL) as an input condition. The papillary muscles are represented as straight lines oriented parallel to the z-axis in a y-z plane (x=Qx), and attaching to the ventricular wall at a point two-thrids the distance from annulus to apex. The lengths of the papillary muscles are determined by geometric considerations—specifically, the intersection of

lines representing chordae tendineae with vertical lines projecting from the papillary muscle attachment sites toward the annulus (Fig. 8D). The computer program is designed so that this initial geometry can be easily altered to describe a wide range of clinical or hypothetical configurations of the mitral apparatus.

The model is "set in motion" by performing a series of subroutines that describe the dynamic alterations in the various components of the mitral apparatus. These alterations include (1) contractility of the annulus, papillary muscles, and the left ventricle (linear functions of time); (2) mechanical deformation of the mitral value leaflets (linearly related to transvalvular pressure); and, (3) lengthening of the chordae tendinease (a function of transvalvular pressure and ventricular geometry).

Calculations are performed to describe the geometry of the mitral apparatus at specific time intervals (INCRT) throughout systole. Subroutines are executed in the following sequence: (1) annulus contraction; (2) ventricular contraction (determines the x,y, and z coordinates of the sites for attachment of papillary muscles); (3) papillary muscle contraction (specifies the z coordinate of the papillary muscles-chordae tendineae junctions); (4) chordae tendineae length, Eq. (8) (determines point Q); and , (5) mitral value leaflet heights, Eqs. (4) and (5).
Note: During the electromechanical delay (EDT) phase of systole, only the annulus contraction subroutine is utilized; during the isovolumetric contraction (IVCT) phase, all subroutines except ventricular contraction are performed.

The output of the program is a time-series description of the mitral value components throughout systole. The following numerical output is listed at time intervals (INCRT) specified in the input data set: (1) anterior and posterior coordinates of the annular ring, (2) annulus to apex distance, (3) ventricular minor axis length, (4) papillary muscle length, (5) chordae tendineae length, (6) coordinates of point Q, (7) anterior and posterior leaflet heights, (8) major and minor axes for leaflet ellipses, and (9) maximum leaflet deflection in the z-direction for each leaflet.

RESULTS

Normal Model

The output of this model, using the hypothetical input data indicated in Table 7, is summarized in Fig. 12. Point Q moves slightly downward (0.02 cm) from its initial position during the isovolumetric contraction phase and then moves upward approximately 0.1 cm during the ejection phase. The anterior leaflet elongates approximately 0.05 cm and the posterior leaflet elongates approximately 0.02 cm. The

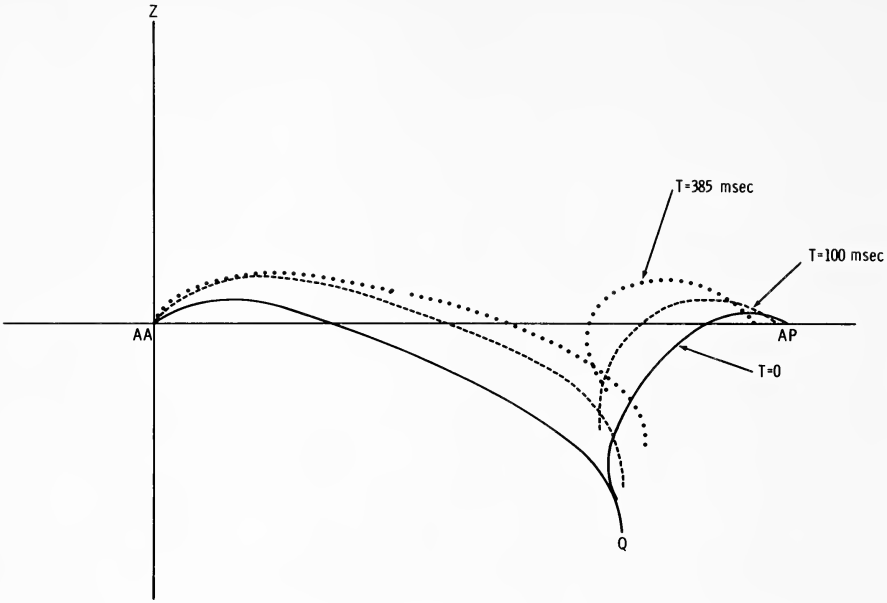

FIGURE 12. Mitral valve position/profile at selected times during systole. Input data as specified in Table 7. AA is the anterior portion of the annulus, AP is the posterior portion of the annulus, and point Q is located at the leaflet free edges.

maximum leaflet deflection in the z-direction is less than 0.1 cm above the plane of the annulus. Fig. 12 illustrates, in a graphical way, the motion of the leaflets and demonstrates the relatively small displacements throughout systole.

Sensitivity Analysis

Perturbation of the model may be performed by altering any of the input parameters. In terms of mitral valve prolapse, the model is insensitive to changes in the annulus diameter, chordae tendineae length, time of onset of papillary muscle contraction, time of onset of ventricular contraction, ventricular minor axis dimension, and annulus to apex distance. The model is moderately sensitive to changes in the percent of papillary muscle contraction and changes in the papillary muscle attachment point. The model is extremely sensitive to change in leaflet and chordae tendineae properties.

Three selected perturbations are illustrated in Figs. 13-15. Increasing the elasticity of the leaflets (MVE = $5{\cdot}10^6$ dyne/cm^2, $\simeq 1/10$ the stiffness of normal valvular tissue) produces a rapid ballooning of the anterior leaflet (Fig. 13). Increasing the elasticity of the chordae tendineae (CTE = $1 \cdot 10^8$ dyne/cm^2, $\simeq 1/20$ the stiffness of normal chordae tendineae) results in an early prolapse of both leaflets (Fig. 14). Eliminating

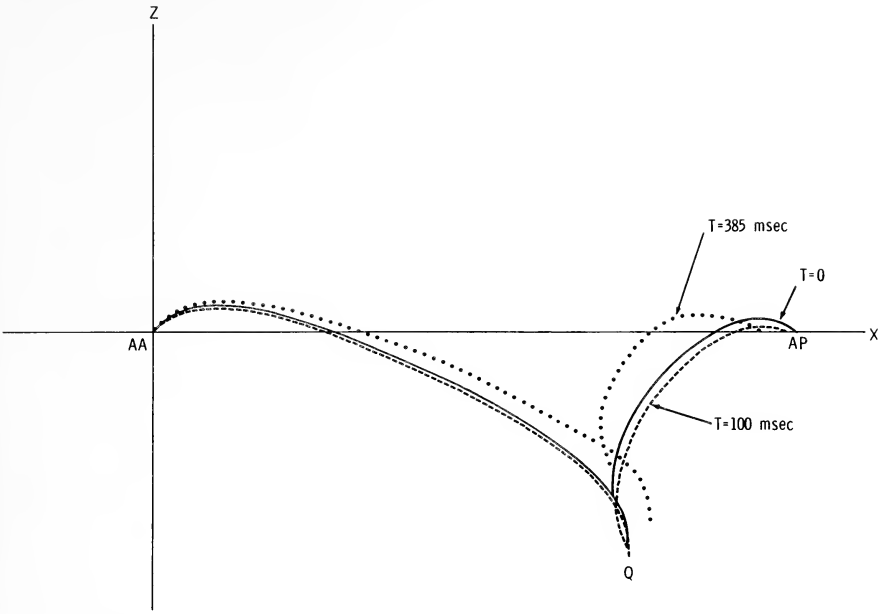

FIGURE 13. Mitral valve position/profile at selected times during systole. Input data as specified in Table 7, except the leaflets have increased elasticity (MVE = $5 \cdot 10^6$ dyne/cm^2). AA is the anterior portion of the annulus, AP is the posterior portion of the annulus, and point Q is located at the leaflet free edges.

papillary muscle contraction produces a late prolapse, which is most noticeable in the posterior leaflet (Fig. 15).

DISCUSSION

Biological models are, by necessity, limited in scope and subjective in nature (Yates 1978). They represent an attempt to mathematically express anatomical, physiological, and/or pathological concepts that quite often, are not fully defined. Despite these inherent limitations in biological models, they are extremely useful tools for (1) identifying the essential components of a system, (2) quantifying information about a subject, (3) exposing contradictions or incompleteness in data sets, (4) examining major implications regarding a system, and (5) determining the effects of selected perturbations upon the performance of a system (Yates 1978).

This model will hopefully provide a better overall understanding of the functioning of the mitral value and associated structures in relation to prolapse. The model has established that the basic components that must be included in any model of the mitral valve prolapse are mitral value leaflets, annulus, chordae tendineae, papillary muscles, and the left ventricle. Alteration in the physical dimensions, mechanical prop-

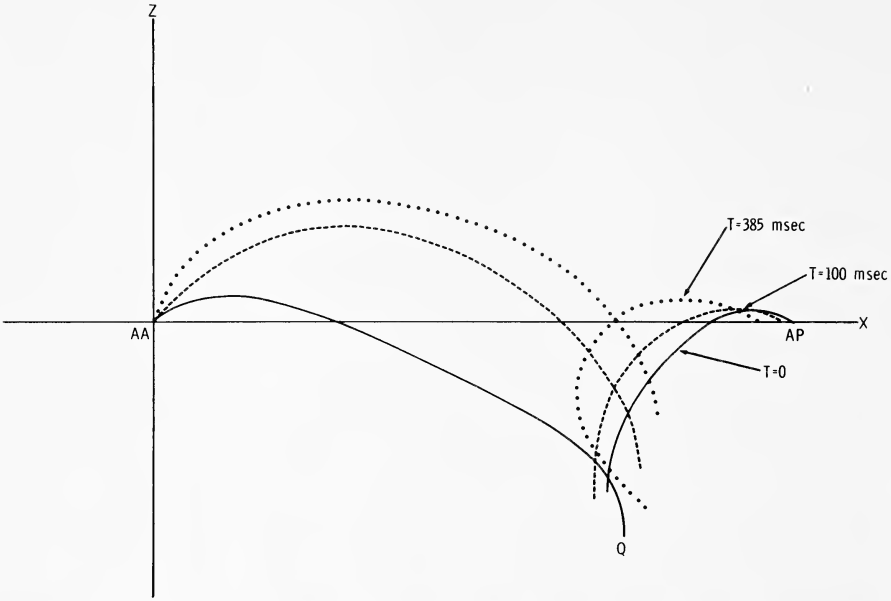

FIGURE 14. Mitral valve position/profile at selected times during systole. Input data as specified in Table 7, except the chordae tendineae have increased elasticity (CTE = $1 \cdot 10^8$ dyne/cm^2). AA is the anteior portion of the annulus, AP is the posterior portion of the annulus, and Q is located at the leaflet free edges.

erties, or contractile properties of these elements can markedly influence the performance of the mitral value itself.

Construction of this model represents a compilation of published anatomical and physiological information regarding the mitral apparatus. Review of the literature indicates that an adequate, quantitiative description of dynamic cardiac anatomy and physiology does not exist. Published data regarding the mitral apparatus are fragmentary and occasionally contradictory. Unfortunately, this rather tenuous data base has been used to support various hypotheses for mitral valve prolapse.

The primary abnormalities producing mitral valve prolapse still elude description. Prolapse has been associated with (1) myxomatous degeneration of the valve leaflets (Read et al. 1965; Pomerance 1969; Kern and Tucker 1972; Marshall and Shappell 1974; Silver 1976), (2) anomalous arrangement of chordae tendineae (Edward 1971; Silver 1976), (2) anomalous arrangement of chordae tendineae (Edwards 1971; Silver 1976), (3) coronary artery disease (Aranda et al. 1976), (4) left ventricular asynergies (Pisano et al. 1977), (5) annulus dilatation (Bulkley and Roberts 1975), (6) papillary muscle dysfunction (Nutter et al. 1975; Cobbs and King 1977), and (7) postural changes in left ventricular geometry (Fontana et al. 1975). Results of this modeling effort support the belief of Barlow et al. (1968), who claim that there is obviously more than one etiology for mitral valve prolapse.

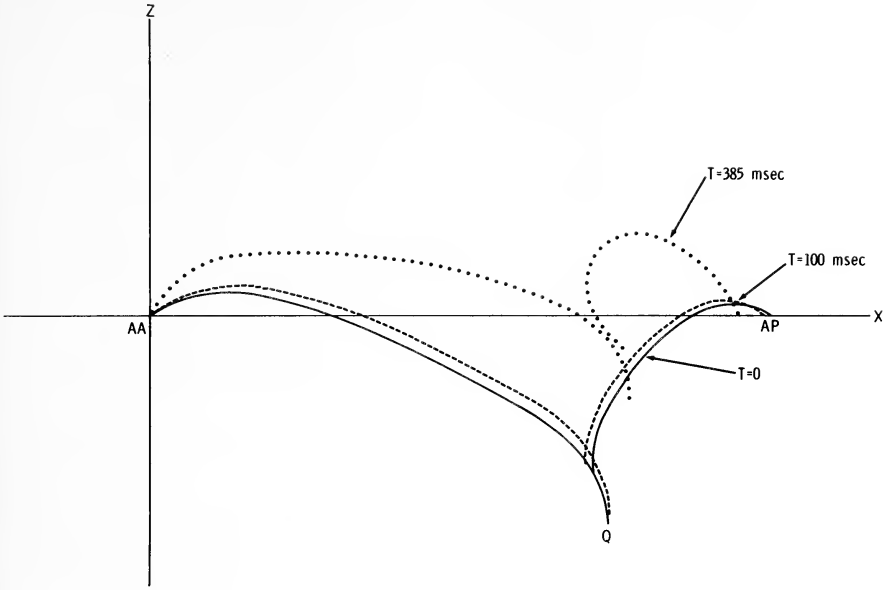

FIGURE 15. Mitral valve position/profile at selected times during systole. Input data as specified in Table 7, except the papillary muscles are non-contractile (PMPER = 0%). AA is the anterior position of the annulus, AP is the posterior portion of the annulus, and point Q is located at the leaflet free edges.

Perhaps the greatest value of this model is in predicting mitral valve profile/position under various conditions. Perturbation studies indicate that prolapse can either result from or be accentuated by (1) reducing the degree of annulus contraction (annular calcification), (2) increasing the elasticity of the leaflets (myxomatous degeneration), (3) increasing the elasticity of the chordae tendineae, (4) decreasing the contractility of the papillary muscles (coronary artery disease), (5) decreasing end-systolic ventricular volume, and (6) increasing preload /afterload. Particularly dramatic changes occur with alterations in either leaflet properties, chordae tendineae properties, or papillary muscle contractility.

One exciting potential application of this model is its use as a clinical tool in determining the underlying pathological alteration(s) contributing to a particular pattern of mitral valve prolapse. Mitral valve profiles obtained in patients using either biplane cineagiography or ultrasound imaging could be compared to profiles based on selected model perturbations and therby establish relationships between mitral valve profiles and specific pathological conditions. It is apparent in Figures 13-15 that a particular perturbation may result in a distinctive time sequence of mitral profiles. This potentially provides the cardiologist with an extremely valuable diagnostic and prognostic tool.

Final conclusions regarding the possible value of this model await validation studies to determine the accuracy of simulation in predicting mitral valve performance in the normal subject and in those persons exhibiting mitral valve prolapse.

LITERATURE CITED

Aranda, J. M., B. Befeler, N. El-Sherif, A. Castellanos, and R. Lazzara. 1976. Mitral valve prolapse. Recent concepts and observations. Am. J. Med. 60:997-1004.

Barlow, J.B., C.K. Bosman, W.A. Pocock, and P. Marchand. 1968. Late systolic murmurs and non-ejection (mid-late) systolic clicks. An analysis of 90 patients. Br. Heart J. 30:203-218.

Bellhouse, B.J. 1972a. The fluid mechanics of aortic and mitral valves, p. 72P-73P. *In* M.M. Black (Ed.), Developments in Biomedical Engineering. Crane Russak, New York, N.Y.

Bellhouse, B.J. 1972b. Fluid mechanics of a model mitral valve and left ventricle. Cardiovasc. Res. 6:199-210.

Bishop, V.S., and L.D. Hortwitz. 1970. Left ventricular transverse internal diameter: value in studying left ventricular function. Am. Heart J. 80:507-514.

Bishop, V.S., L.D. Horwitz, H.L. Stone, H.F. Stegall, and E.J. Engelken. 1969. Diameter and cardiac function in conscious dogs. J. Appl. Physiol. 27:619-623.

Braunwald, E., S.J. Sarnoff, and W.N. Stainsby. 1958. Determinants of duration and mean rate of ventricular ejection. Circ. Res. 6:319-325.

Brown, O.R., F.E. Kloster, and H. DeMots. 1975. Incidence of mitral value prolapse in the asymptomatic normal. Circulation (abstract) 52 (Suppl II):77.

Bulkley, B.H., and W.C. Roberts. 1975. Dilatation of the mitral anulus. A rare cause of mitral regurgitation. Am. J. Med. 59:457-463.

Burch, G.E., and N.P. DePasquale. 1965. Time course of tension in papillary muscles of heart. Theoretical considerations. JAMA 192:701-704.

Burch, G.E., and T.D. Giles. 1972. Angle of traction of the papillary muscle in normal and dilated hearts: A theoretical analysis of its importance in mitral valve dynamics. Am. Heart J. 84:141-144.

Carpentier, A., J. Guerinon, A. Deloche, J.B. Fabiani, and J. Relland. 1976. Pathology of the mitral value, p. 65-77. *In* D. Kalmanson (Ed.), The Mitral Valve. A Pluridisciplinary Approach. Publishing Sciences Group, Inc., Acton, Mass.

Chiechi, M.A., W.M. Lees, and R. Thompson. 1956. Functional anatomy of the normal mitral valve. J. Thorac. Surg. 32:378-398.

Clark, R.E., 1973. Stress-strain characteristics of fresh and frozen human aortic and mitral leaflets and chordae tendineae. Implications for clinical use. J. Thorac. Cardiovasc. Surg. 66:202-208.

Clark, R.E., and G.A.M. Butterworth. 1971. Characterization of the mechanics of human aortic and mitral valve leaflets. Surg. Forum 22:134-136.

Clark, R.E., and S.P. Sutera. 1973. Methods of design of leaflet valvular prostheses. I. Stresses in the mitral valve leaflets in health and disease. J. Throac. Cardiovasc. Surg. 65:890-896.

Cobbs, B.W., Jr., and S.B. King. 1977. Ventricular buckling: A factor in the abnormal ventriculogram and peculiar hemodynamics associated with mitral valve prolapse. Am. Heart J. 93:741-758.

Cronin, Ṙ., J.A. Armour, and W.C. Randall. 1969. Function of the in-situ papillary muscle in the canine left ventricle. Circ. Res. 25:67-75.

Daughters, G.T., II, N.B. Ingels, Jr., E.B. Stinson, E.L. Alderman, and C.W. Mead. 1977. Computation of left ventricular dynamics from surgically implanted markers, p.97-

103. *In* J.I. Martin (Ed.), Proceedings of the San Diego Biomedical Symposium. Academic Press, New York, N.Y.

Davila, J.C., and T.E. Palmer. 1962. The mitral valve. Anatomy and pathology for the surgeon. Arch. Surg. 84:38-62.

Devereux, R.B., J.K. Perloff, N. Reichek, and M.E. Josephson. 1976. Mitral valve prolapse. Circulation 54:3-14.

Edwards, J.E. 1971. Mitral insufficiency resulting from "overshooting" of leaflets. Circulation 43:606-612.

Estes, E.H., Jr., F.M. Dalton, M.L. Entman, H.B. Dixon, and D.B. Hackel. 1966. The anatomy and blood supply of the papillary muscles of the left ventricle. Am. Heart J. 71:356-362.

Fabian, J., E.J. Esptein, and N. Coulshed. 1972. Duration of phases of left ventricular systole using indirect methods. I: Normal subjects. Br. Heart J. 34:874-881.

Fenoglio, J.J., Jr., T.D. Pham, A.L. Wit, A.L. Bassett, and B.M. Wagner. 1972. Canine mitral complex. Ultrastructure and electromechanical properties. Circ. Res. 31:417-430.

Fontana, M.E., C.F. Wooley, R.F. Leighton, and R.P. Lewis, 1975. Postural changes in left ventricular and mitral valvular dynamics in the systolic click-late systolic murmur syndrome. Circulation 51:165-173.

Fortuin, N.J., W.P. Hood, Jr., and E. Craige. 1972. Evaluation of left ventricular function by echocardiography. Circulation 46:26-35.

Frank, M.N., and W.B. Kinlaw. 1962. Indirect measurement of isovolumetric contraction time and tension period in normal subjects. Am. J. Cardiol. 10:800-806.

Gerstenblith, G., J. Frederiksen, F.C.P. Yin, N.J. Fortuin, E.G. Lakatta, and M.L. Weisfeldt. 1977. Echocardiographic assessment of a normal adult aging population. Circulation 56:273-278.

Ghista, D.N., and A.P. Rao. 1972. Structural mechanics of the mitral valve: stresses sustained by the valve; non-traumatic determination of the stiffness of the *in vivo* valve. J. Biomech. 5:295-307.

Grimm, A.F., B.L. Lendrum, and H. Lin. 1975. Papillary muscle shortening in the intact dog. A cineradiographic study of tranquilized dogs in the upright position. Circ. Res. 36:49-57.

Harrison, T.R., K. Dixon, R.O. Russell, P.S. Bidwai, and H.N. Coleman. 1964. The relation of age to the duration of contraction, ejection, and relaxation of the normal human heart. Am. Heart. J. 67:189-199.

Hinds, J.E., E.W. Hawthorne, C.B. Mullins, and J.H. Mitchell. 1969. Instantaneous changes in the left ventricular lengths occurring in dogs during the cardiac cycle. Fed. Proc. 28:1351-1357.

Hirakawa, S., S. Sasayama, H. Tomoike, B. Crozatier, D. Franklin, D. McKown, and J. Ross, Jr. 1977. In situ measurement of papillary muscle dynamics in the dog left ventricle. Am. J. Physiol. 233:H384-H391.

Hirschfeld, S., R. Meyer, J. Korfhagen, S. Kaplan, and J. Leibman. 1976. The isovolumic contraction time of the left ventricle. An echographic study. Circulation 54:751-756.

Hirschfeld, S., R. Meyer, D.C. Schwartz, J. Korfhagen, and S. Kaplan. 1975. Measurement of right and left ventricular systolic time intervals by echocardiography. Circulation 51:304-309.

Huntsman, L.L., S.R. Day, and D.K. Stewart. 1977. Nonuniform contraction in the isolated cat papillary muscle. Am. J. Physiol. 233:H613-H616.

Hutchins, G.M., B.H. Bulkley, G.W. Moore, M.A. Piasio, and F.T. Lohr. 1978. Shape of the human cardiac ventricles. Am. J. Cardiol. 41:646-654.

Hwang, N.H.C. 1977. Flow dynamics of nautral valves in the left heart, p. 825-850. *In* N.H.C. Hwang and N.A. Normann (Eds.), Cardiovascular Flow Dynamics and Measurements. University Park Press, Baltimore, MD.

Jeresaty, R.M. 1979. Mitral Valve Prolapse. Raven Press, New York, N.Y., p. 4-7.

Karas, S., Jr., and R.C. Elkins. 1970. Mechanisms of function of the mitral valve leaflets, chordae tendineae and left ventricular papillary muscles in dogs. Circ. Res. 26:689-696.

Kern, W.H., and B.L. Tucker. 1972. Myxoid changes in cardiac valves: Pathologic, clinical, and ultrastructural studies. Am. Heart J. 82:294-301.

Kostis, J.B., D. Fleischmann, and S. Bellet. 1969. Use of the ultrasonic doppler method for timing of valvular movement. Application in the differential diagnosis of extra heart sounds. Circulation 40:197-207.

Koushanpour, E., and W.D. Collins. 1966. Validation and dynamic applications of an ellipsoid model of the left ventricle. J. Appl. Physiol. 21:1655-1661.

Krausman, D.T. 1975. Methods and procedures for monitoring and recording blood pressure. Am. Psychol. 30:285-294.

Kumar, S., and D.H. Spodick. 1970. Study of the mechanical events of the left ventricle by atraumatic techniques: Compariston of methods of measurement and their significance. Am. Heart J. 80:401-413.

Lam, J.H.C., N. Ranganathan, E.D. Wigle, and M.D. Silver. 1970. Morphology of human mitral valve. I. Chordae tendineae: A new classification. Circulation 41:449-458.

Lieotke, A.J., A. Pasternac, E.H. Sonneblick, and R. Gorlin. 1972. Change in canine ventricular dimensions with acute changes in preload and afterload. Am. J. Physiol. 223:820-827.

Lim, K.O., and D.R. Boughner. 1975. Mechanical properties of human mitral valve chordae tendineae: Variation with size and strain rate. Can. J. Physiol. Pharmacol. 53:330-339.

Lim, K.O., and and D.R. Boughner. 1977. Scanning electron microscopical study of human mitral value chordae tendineae. Arch. Pathol. Lab. Med. 101:236-238.

Marshall, C.E., and S.D. Shappell. 1974. Sudden death and the ballooning posterior leaflet syndrome. Detailed anatomic and histochemical investigation. Arch. Pathol. 98:134-138.

McDonald, I.G. 1970. The shape and movements of the human left ventricle during systole. A study by cineangiography and by cineradiography of epicardial markers. Am. J. Cardiol. 26:221-230.

McDonald, I.G., H. Feigenbaum, and S. Chang. 1972. Anlysis of left ventricular wall motion by reflected ultrasound. Application to assessment of myocardial function. Circulation 46:14-25.

Miller, G.E., J.F. Hunter, and W.M. Lively. 1981. A note on mitral value mechanics: A prestressed leaflet concept. J. Biomech. 14:373-375.

Nutter, D.O., C. Wickliffe, C.A. Gilbert, C. Moody, and S.B. King. 1975. The pathophysiology of idiopathic mitral valve prolapse. Circulation 52:297-305.

Oreshkov, V.I. 1972. Isovolumic contraction time and isovolumic contraction time index in mitral stenosis. Br. Heart J. 34:533-536.

Perloff, J.K. 1976. Anatomic-physiologic properties of the mitral apparatus, p. 33-40. *In* D. Kalmanson (Ed.), The Mitral Valve. A Pluridisciplinary Approach. Publishing Sciences Group, Inc., Acton, Mass.

Pisano, D., S.D. Cha, A.S. Gooch, V. Maranhao, and H. Goldberg. 1977. Mean velocity of circumferential fiber shortening in prolapsed mitral leaflet syndrome. Circulation 56:853-855.

Pomerance, A. 1969. Ballooning deformity (mucoid degeneration) of atrioventricular valves. Br. Heart J. 31:343-351.

Priola, D.V., C. Fellows, J. Moorehouse, and R. Sanchez. 1970. Mechanical activity of canine mitral valve in situ. Am. J. Physiol. 219:1647-1651.

Procacci, P.M., S.V. Savran, S.L. Schreiter, and A.L. Bryson. 1976. Prevalence of clinical mitral-value prolapse in 1169 young women. N. Engl. J. Med. 294:1086-1088.

Ranganathan, N. and G.E. Burch. 1969. Gross morphology and arterial supply of the papillary muscles of the left ventricle of man. Am. Heart J. 77:506-516.

Ranganathan, N., J.H.C. Lam, E.D. Wigle, and M.D. Silver. 1970. Morphology of the human mitral valve. II. The valve leaflets. Circulation 41:459-467.

Ranganathan, N., M.D. Silver, and E.D. Wigle. 1976. Recent advances in the knowledge of the anatomy of the mitral valve, p. 3-13. *In* D. Kalmanson (Ed.), The Mitral Valve. A Pluridisciplinary Approach. Publishing Sciences Group Inc., Acton, Mass.

Read, R.C., A.P. Thal, and V.E. Wendt. 1965. Symptomatic valvular myxomatous transformation (the floppy valve syndrome). A possible forme fruste of the Marfan syndrome. Circulation 32:897-910.

Roberts, W.C., and L.S. Cohen. 1972. Left ventricular papillary muscles. Description of the normal and a survey of conditions causing them to be abnormal. Circulation 46:138-154.

Robinson, B. 1963. The carotid pulse. II: Relation of external recordings to carotid, aortic, and brachial pulses. Br. Heart J. 25:61-68.

Ross, J., Jr., E.H. Sonnenblick, J.W. Covell, G.A. Kaiser, and D. Spiro. 1967. The architecture of the heart in systole and diastole. Technique of rapid fixation and analysis of left ventricular geometry. Circ. Res. 21:409-421.

Rushmer, R.F., B.L. Finlayson, and A.A. Nash. 1956. Movements of the mitral valve. Circ. Res. 4:337-342.

Rusted, I.E., C.H. Scheifley, and J.E. Edwards. 1952. Studies of the mitral valve. I. Anatomic features of the normal mitral valve and associated structures. Circulation 6:825-831.

Salisbury, P.F., C.E. Cross, and P.A. Rieben. 1963. Chorda tendinea tension. Am. J. Physiol. 205:385-392.

Semafuko, W.E.B., and W.C. Bowie. 1975. Papillary muscle dynamics: In situ function and responses of the papillary muscle. Am. J. Physiol. 228:1800-1807.

Silver, M.D. 1976. Recent advances in the knowledge of pathology of natural and artificial valves, p. 51-63. *In* D. Kalmanson (Ed.), The Mitral Valve. A Puridisciplinary Approach. Publishing sciences Group, Inc., Acton, Mass.

Silverman, M.E., and J.W. Hurst. 1968. The mitral complex. Interaction of the anatomy, physiology, and pathology of the mital annulus, mitral valve leaflets, chordae tendineae, and papillary muscles. Am. Heart. J. 76:399-418.

Spodick, D.H., and S. Kumar. 1968a. Electromechanical lag of the left ventricle. Cardiovasc. Res. 4:338-340.

Spodick, D.H., and S. Kumar. 1968b. Isovolumetric contraction period of the left ventricle. Results in a normal series and comparison of methods of calculation by atraumatic techniques. Am. Heart J. 76:498-503.

Tsakiris, A.G., G. von Bernuth, G.C. Rastelli, M.J. Bourgeois, J.L. Titus, and E.H. Wood. 1971. Size and motion of the mitral value annulus in anesthetized intact dogs. J. Appl. Physiol. 30:611-618.

Upton, M.T., D.G. Gibson, and D.J. Brown. 1976. Instantaneous mitral valve leaflet velocity and its relation to left ventricular wall movement in normal subjects. Br. Heart J. 38:51-58.

Van de Werf, F., J. Piessens, H. Kesteloot, and H. DeGeest. 1975. A comparison of systolic time intervals derived from the central aortic pressure and from the external carotid pulse tracing. Circulation 51:310-316.

Wallace, A.G., J.H. Mitchell, N.S. Skinner, and S.J. Sarnoff. 1963. Duration of the phases of left ventricular systole. Circ. Res. 12:611-619.

Weissler, A.M., R.G. Peeler, and W.H. Roehll, Jr. 1961. Relationships between left ventricular ejection time, stroke volume, and heart rate in normal individuals and patients with cardiovascular disease. Am. Heart J. 62:367-378.

Wiggers, C.J. 1921. Studies on the consecutive phases of the cardiac cycle. I. The duration of the consecutive phases of the cardiac cycle. I. The duration of the consecutive phases of the cardiac cycle and the criteria for their precise determination. Am. J. Physiol. 56:415-438.

Wit, A.L., J.J. Fenoglio, Jr., B.M. Wagner, and A.L. Bassett. 1973. Electrophysiological properties of cardiac muscle in the anterior mitral valve leaflet and the adjacent atrium in the dog. Circ. Res. 32:731-745.

Yates, F.E. 1978. Good manners in good modeling: Mathematical models and computer simulations of physiological systems. Am. J. Physiol. 3:R159-R160.

Zaky, A., E. Steinmetz, and H. Feigenbaum. 1969. Role of atrium in closure of mitral valve in man. Am. J. Physiol. 217:1652-1659.

THIN LAYER CHROMATOGRAPHY OF NITROGEN HETEROCYCLES ON A MODIFIED SILICA GEL SUPPORT

by W. E. RUDZINSKI

Department of Chemistry
Southwest Texas State University
San Marcos, TX 78666

ABSTRACT

Square planar dialkylphosphorodithioate complexes of nickel have been sorbed onto a silica gel surface, and the extent of adduct formation with nitrogen heterocyclic bases has been evaluated and explained in terms of steric hindrance between the nickel complex and associating base.

INTRODUCTION

The neutral square planar dialkylphosphorodithioate complexes of nickel have a tendency to form tetragonal adducts in the presence of Lewis bases (Coucouvanis 1979). If the Lewis base is a heterocyclic nitrogen compound, the structure of the heterocycle plays a dominant role in the extent of adduct formation (Rudzinski 1977). In order to study the coordination chemistry of bis(0,0'-dimethylphosphorodithioate) nickel (II), Ni $(DMPDT)_2$, the nickel complexes are sorbed onto a silica gel plate forming a surface available for adduct formation. Nitrogen heterocyclic bases then are spotted on the plate and their affinity for the surface evaluated. Bulky or sterically-hindered bases are not expected to have a high retentivity on the surface. If the dialkylphosphorodithioate ligand had large alkoxy groups bonded to the phosphorus, then these also will affect the extent of adduct formation.

MATERIALS AND METHODS

Bis(0,0'-dimethylphosphorodithioate) nickel (II) was synthesized as described elsewhere (Rudzinski et al. 1977). Bis(0,0'-diethylphosphorodithioate) nickel (II) was synthesized in the same manner as above by using ethanol instead of methanol.

The chelate was dissovlved in reagent grade benzene, and the solution was sprayed on a thin layer silica gel plate (Eastman Chromagram Sheet 6061) using a dichlorofluoromethane aerosol. Three coats were sufficient to cover the silica gel plate. The plates then were allowed to air dry for ten minutes.

Table 1. Thin layer chromatography results.

Heterocycle	# of Samples	R_f	Standard Deviation
	$Ni(DEPDT)_2$ with 1-propanol as the solvent		
isoquinoline	9	.83	2×10^{-2}
quinoline	3	.76	2×10^{-2}
8-aminoquinoline	3	.75	3×10^{-2}
6-methoxyquinoline	3	.77	5×10^{-2}
	$Ni(DMPDT)_2$ with 2-propanol as the solvent		
aridine	4	.68	6.2×10^{-2}
isoquinoline	4	.33	1.7×10^{-2}
	$Ni(DMPDT)_2$ with 1-propanol as the solvent		
isoquinoline	10	.04	1.2×10^{-2}
pridine	7	0	0
1,10-phenanthroline	2	.005	
quinoline	12	.74	7.1×10^{-2}
2-methoxyquinoline	3	.65	9.1×10^{-2}

The nitrogen heterocycles used for the study were the following: (1) pyridine (Mallinckrodt), (2) quinoline (Aldrich Chemical Co.), (3) isoquinoline (J. T. Baker Chemical Co.), (4) 2-methoxy quinoline (Aldrich Chemical Co.), (5) 6-methoxyquinoline (K and K Laboratories), (6) 8-aminoquinoline (G. Frederick Smith Chemical Co.), (7) acridine (Aldrich Chemical Co.), (8) phenazine (Aldrich Chemical Co.), and (9) 1,10-phenanthroline (J. T. Baker Chemical Co.). Isoquinoline, quinoline, and pyridine were redistilled. The remaining compounds were used as received from the manufacturer.

The developing solvents (ethanol, 1-propanol, 2-propanol) were redistilled. Liquid samples were spotted at one end of the plate and then developed by an ascending technique in a closed container saturated with developer vapor. The plate then was dried and the R_f values measured. No reagent was needed for the detection of the components since they were self-indicating. Solids were dissolved in the minimum amount of developing solvent, and then spotted and developed as above.

RESULTS AND DISCUSSION

The results of the thin layer chromatography are summarized in Table 1. The R_f values obtained with $Ni(DEPDT)_2$ as the stationary phase and 1-propanol as the mobile phase indicate that there is little variation in the R_f value with a variation in heterocycle. This is ascribed to the steric hindrance provided by the ethoxy group bonded to the phosphorus atom. In this case, the alkyl group of the phosphorodithioate is the primary regulator in adduct formation. The silica gel support does not seem to influence significantly the retention of the

heterocycles (all $R_f > 0.75$). When Ni (DMPDT)$_2$ is the stationary phase and 1-propanol is the solvent, the nature of the heterocyclic base is a primary regulator in adduct formation. As an example, quinoline has an R_f value of 0.74 while isoquinoline essentially does not move (R_f = 0.04). This is attributed to the fact that quinoline is sterically hindered in aligning itself for proper coordination:

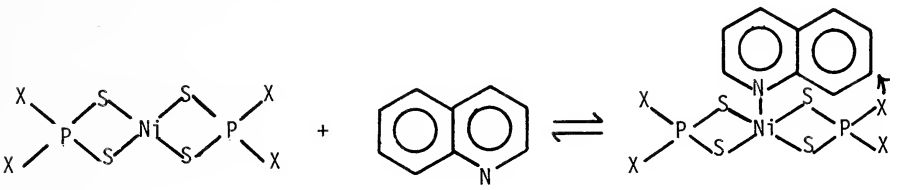

X = -OCH_3, - OCH_2CH_3

Isoquinoline on the other hand can coordinate with a minimum of steric interaction:

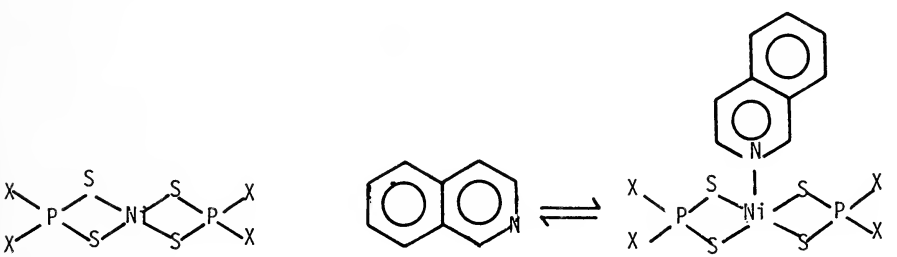

X = -OCH_3, - OCH_2CH_3

The adducts of pyridine (Ooi and Fernando 1967), and 1,10-phenanthroline (Shetty and Fernando 1970) with dialkylphosphorodithioate nickel (II) are known to exist and have been characterized by single crystal X-ray structure determinations, and the low R_f values support the interpretation of adduct formation.

Finally, there appears to be a correlation between the solvent and the extent of adduct formation. The longer the carbon chain in the alkyl group of the developing solvent the stronger the adduct formed between the nigrogen heterocycle and Ni(DMPDT)$_2$. In analyzing the comparative R_f values of quinoline and isoquinoline in ethanol, 2-propanol, and 1-propanol, quinoline retains essentially the same R_f value, while

that of isoquinoline decreases (R_f = 0.59 in ethanol, R_f = 0.33 in 2-propanol, R_f = 0.04 in 1-propanol). This decrease in R_f with developing solvent correlates well with the solvent strength of the alcohols (Snyder and Kirdland 1979).

LITERATURE CITED

Coucouvanis, D. 1979. The chemistry of the dithioacid and 1,1-dithiolate complexes, 1968-1977, p. 301-469. *In* S. J. Lippard (Ed.), Progress in Inorganic Chemistry, v. 26. John Wiley and Sons, New York, NY.

Ooi, S., and Fernando, Q. 1967. The crystal and molecular structure of the adduct of bis(0,0'-diethyldithiophosphato) nickel (II) with pyridine. Inorg. Chem. 6:1558-1562.

Rudzinski, W.E. 1977. Stability of transition metal complexes of 0,0'-dialkyldithiophosphates and their adducts. Ph.D. Dissertion, University of Arizona, Tucson, AZ.

Rudzinski, W.E., Behnke, G.T., and Fernando, Q. 1977. A normal coordinate analysis of bis(0,0'-dialkyldithiophosphate) nickel (II) complexes. Inorg. Chem. 16:1206-1210.

Shetty, P.S., and Fernando, Q. 1970. Structures of five and six-coordinated mixed-ligand chelates of nickel (II) containing sulfur and nitrogen donor atoms. J. Am. Chem. Soc. 92:3964-3969.

Snyder, L. R., and Kirkland, J. J. 1979. Introduction to Modern Liquid Chromatography, 2 Ed. John Wiley and Sons, Inc., New York, NY., 246-268.

SOME STRUCTURAL ASPECTS OF A WESTERN CROSS TIMBERS FOREST IN NORTH CENTRAL TEXAS[1]

by GLENN C. KROH *and* JAMES NISBET

Department of Biology
Texas Christian University
Fort Worth, TX 76129

ABSTRACT

Structural aspects of a north-central Texas tract of the cross timbers forest were determined. The one-hectare study area was located within the Fort Worth, Texas, Nature Center and Refuge. Specifically, average basal area, frequency distribution of height and size classes, diversity, importance values and taxonomic composition of the forest were determined. Mean basal area by species indicated post oak (*Quercus stellata*) is dominant (80%), followed by blackjack oak (*Quercus marilandica*) (9%). Mean basal area for all tree species combined was 24.6 m^2/ha, indicating that the forest is mature. Tree diversity, calculated by the Shannon-Weiner method, is 1.03.

INTRODUCTION

The cross timbers, as described by Dyksterhuis (1948), occurs from the Arkansas River in Oklahoma to approximately 150 miles south of the Red River. At the Red River, the forest splits into two bands, the western cross timbers and eastern cross timbers. Rice and Penfound (1955) evaluated different methods of sampling upland oak forests based on the cross timbers of Oklahoma, and later (Rice and Penfound 1959) did a descriptive study of the area. Risser and Rice (1971a) used an ordination technique to determine upland tree species associations of the Oklahoma cross timbers and then (Risser and Rice 1971b) compared diversity indices with the mixed mesophytic and oak hickory forest in the southern Appalachian region. The oak upland forest was significantly less diverse than those in the eastern United States. The objectives of the present study were to determine structural parameters of a north Texas post-oak forest and contrast some aspects of this community with similar oak forest communities in Oklahoma.

STUDY AREA

The study area is located in the western cross timbers community at the Fort Worth, Texas, Nature Center and Refuge. Principal trees in the undisturbed forest are *Quercus stellata* (post oak), *Quercus marilandica* (blackjack oak), *Celtis laevigata* (hackberry) and *Ulmus crassi-*

[1]Funded by Texas Christian University Research Foundation Grant #B7986. Presented at the 1978 Texas Academy of Science Meeting At Texas Tech University, Lubbock, TX.

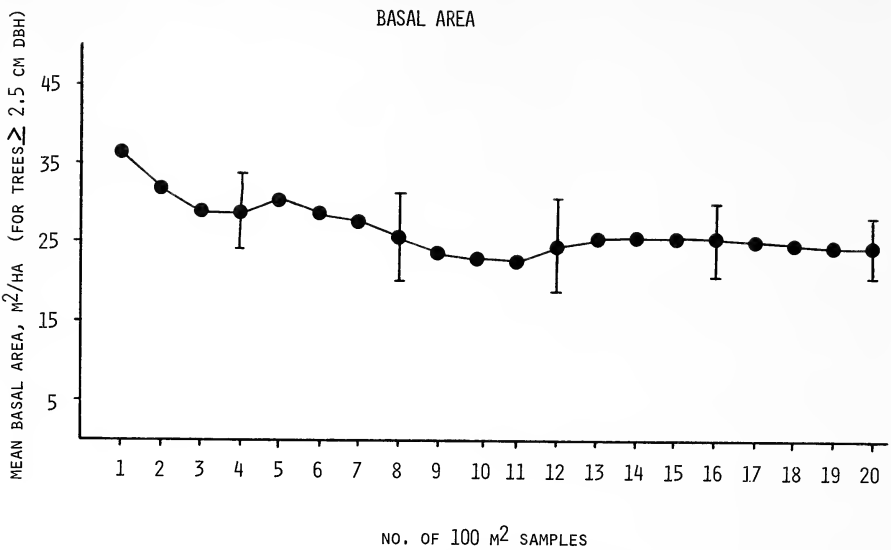

FIGURE 1. Performance curve. Only trees greater than 2.5 cm in diameter were considered. Vertical bars represent ± two standard errors.

folia (cedar elm). The climate is humid subtropical with hot summers. It is also continential, characterized by a wide range in annual temperature extremes. Precipitation averages about 81 cm annually, but varies considerably from year to year, ranging from less than 51 to more than 127 cm. Greatest amount of rain occurs during April and May. The soil is a yellow-brown podsolic derived from Cretaceous strata. The study area was selected within the forest on the basis of accessibility and general representativeness of the stand.

TABLE 1. Density, dominance, frequency, and importance of woody species with DBH of 2.5 cm or greater.[a]

Species	Relative Density %	Relative Dominance %	Relative Frequency %	Importance Value[b]
Post Oak	54	80.0	82.0	216.0
Blackjack Oak	24	9.0	13.0	46.0
Hackberry	14	7.0	4.0	25.0
Cedar Elm	5	3.0	1.0	9.0
Red Mulberry	3	0.4	0.06	3.46
TOTAL	100	99.4	100.06	299.46

[a]Woody species with DBH less than 2.5 cm were *Acer negundo, Bumelia lanuginosa, Cornus drummondii, Crataegus sp., Forestiera acuminata, Fraxinus pennsylvanica, Gleditsia triacanthos, Ilex decidua, Viburnum rufidulum.*

[b]Importance value is the sum of relative density, relative dominance and relative frequency.

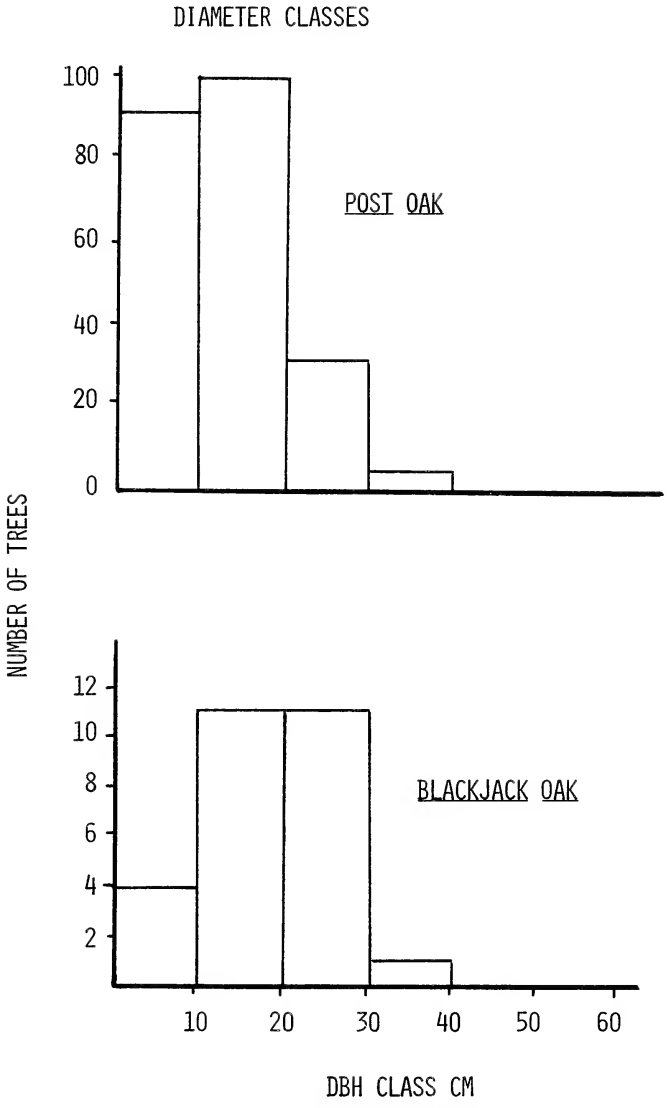

FIGURE 2. Frequency distribution of post oak and blackjack oak by diameter at breast height (DBH).

MATERIALS AND METHODS

A 1-ha area was measured and ten 100-m transects, 10 m apart, were established with permanent numbered stakes placed at 25-m intervals. Sampling sites were randomly selected with the aid of a random numbers table. A circular sample of 100 m^2 was taken at each site. The number of sites sampled was determined with a performance curve

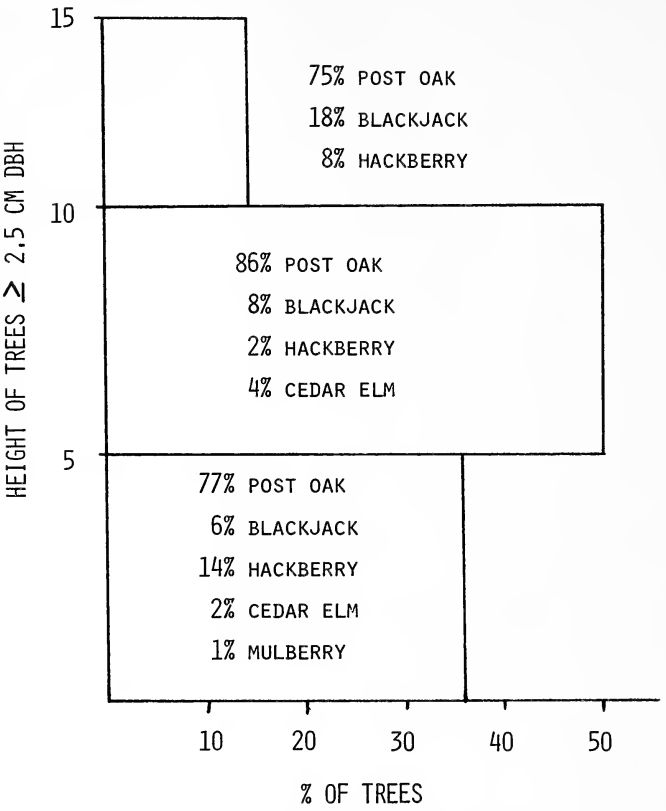

FIGURE 3. Frequency distribution of trees by height. Only trees with DBH greater than 2.5 cm were considered.

(Greig-Smith 1957), with total basal area used as the criterion (Fig. 1). Twenty sites were sampled.

Only trees with diameters at breast height (DBH) greater than 2.5 cm were measured. Heights were determined using a Haga altimeter. Total basal area, basal area per species, density, frequency, tree diversity using the Shannon-Weiner index ($H' = -\sum p_i \log_2 p_i$; Cox 1980), size and height class frequencies were determined.

RESULTS AND DISCUSSION

A total of 14 species of trees was noted at the study site (Table 1). The four dominant trees were post oak, blackjack oak, hackberry, and cedar elm. Post oak had the greatest importance value (Cox 1980), followed by blackjack oak, hackberry, cedar elm and red mulberry (*Morus rubra*). Importance values have been used as a measure of niche size (Whittaker 1970) and may indicate the proportion of site resources used by each species (Kroh and Stephenson 1980).

Post oak and blackjack oak together account for approximately 70% of the total basal area in the upland forests of Oklahoma (Rice and Penfound 1959). In our forest, 80% of the basal area was comprised by post oak and 9% by blackjack oak. Rice and Penfound (1959) indicated that upland forest stands rarely exceed a total basal area of 25 m^2/ha. The oak stand in which Johnson and Risser (1974) measured biomass and net primary production had a basal area of 18 m^2/ha. With a mean basal area of 24.6 m^2/ha (Fig. 1), the forest we studied seems certain to be an old-growth forest and is quite possibly a climax community. The Shannon-Weiner index was 1.03, a value similar to that (0.94) found by Risser and Rice (1971a) in Oklahoma upland forest areas.

Frequency distributions of size classes (Fig. 2) show that blackjack oak may be declining in the study area; its replacement rate seems to be less than one. Post oak, however, appears to be maintaining its population. There may be a dynamic equilibrium between post oak and blackjack oak as a function of the availiability of moisture and nutrients. Johnson and Risser (1974) showed that post oak required a higher level of moisture and nutrients than blackjack oak. Replacement rates may decrease in post oak populations during years of drought, releasing blackjack oak seedlings from competition.

Height-class frequency distributions show that about 50% of the trees sampled were between 5 and 10 m tall, with only 14% taller than 10 m (Fig. 3). Red mulberry was restricted to the lower understory; cedar elm was not greater than 10 m tall; and post oak, blackjack oak, and hackberry were found in all three layers.

LITERATURE CITED

Cox, G. 1980. Laboratory Manual of General Ecology. 4th ed. W. C. Brown Co., Dubuque, Iowa.

Dyksterhuis, E. J. 1948. The vegetation of the western cross timbers. Ecol. Monogr. 18:325-376.

Greig-Smith, P. 1957. Quantitative Plant Ecology. Butterworths, London.

Johnson, F. L., and P. G. Risser. 1974. Biomass, annual net primary production, and dynamics of six mineral elements in a post oak-blackjack oak forest. Ecology 55:1246-1258.

Kroh, G. C., and S. N. Stephenson. 1980. Effects of diversity and pattern on relative yields of four Michigan first-year fallow-field plant species. Oecologia 45:366-371.

Rice, E.L., and W.T. Penfound. 1955. An evaluation of the variable-radius and paired-tree methods in the blackjack-post oak forest. Ecology 36:315-320.

Rice, E. L., and W. T. Penfound. 1959. The upland forests of Oklahoma. Ecology 40:593-608.

Risser, P. G., and E. L. Rice. 1971a. Diversity in tree species in Oklahoma upland forest. Ecology 52:876-880.

Risser, P. G., and E. L. Rice. 1971b. Phytosociological analysis of Oklahoma upland forest species. Ecology 52:940-945.

Whittaker, R. H. 1970. Communities and Ecosystems. Macmillan, London.

HEAVY METAL POLLUTION IN EL PASO DURING SELECTED TIME PERIODS

by HOWARD G. APPLEGATE

Center for Inter-American and Border Studies
University of Texas at El Paso
El Paso, TX 79968

and KEITH REDETZKE

Department of Biology
University of Texas at El Paso
El Paso, TX 79968

ABSTRACT

Ambient concentrations of lead, zinc, cadmium and arsenic were measured in El Paso, Texas. Data collected before, during and after strike periods at a local copper smelter were compared. Lowest values were obtained during the strike period. This suggests the smelter was a source of a portion of the heavy metals.

INTRODUCTION

A previous article in this journal detailed the use of a scanning electron microscope and ion-probe to identify sources of particulates in ambient air (Gray et al. 1980). By means of morphology and chemical composition, individual particles were related to processing steps at a local smelter. This equipment is not available to all investigators interested in identifying point sources of particulates. Another way to identify these sources is to monitor the atmosphere when the suspected source is and is not in operation. This is difficult to do if the plant operates 24-hours a day, seven days a week. In such a case, one way to gather data is when the plant is on strike.

METHODS

Suspended particulates were collected by the El Paso City-County Air Polllution Control Unit using hi-vol samplers according to Environmental Protection Agency-approved methodology (40 CFR 50.1, 1978). The samples were analyzed by atomic absorption spectroscopy for lead, zinc, cadmium and arsenic (Hubert et al. 1980). Sampling sites were shown in a previous publication (Hubert et al 1981a).

RESULTS AND DISCUSSION

Data are presented in Table 1. Pre-and post-strike data were collected for the same length of time as the duration of the strike. Exceptional operating conditions can be expected when a plant is preparing to shut down prior to a strike and again when the plant is starting up production subsequent to the strike. Accordingly, data for the last week prior to the shut down and the first week of the start up are shown separately. Each time period thus has five sets of data: normal pre-strike emissions, shutting-down emissions, strike emissions, starting-up emissions and normal post-strike emissions.

These data were analyzed statistically using a t-test. A one-tailed test was used with a probability value of 0.05, since lowered ambient levels were expected during the strike period. Each metal was tested separately, pairing strike levels versus normal levels by site and year. Normal operating levels were calculated as the average of pre- and post-strike emissions. Ambient levels of lead, cadmium, and arsenic were significantly reduced ($P = 0.05$) during the strike periods, and the reduction in zinc levels was nearly significant ($P = 0.1$).

These results indicate that the smelter is a significant source of lead, cadmium and arsenic. Zinc showed consistent declines during strike periods, but the relationship is less certain and may involve other sources.

Only for cadmium and arsenic were zero amounts recorded during strikes. This probably reflects the low concentrations of these two compounds during normal pre- and post-strike conditions. Usually, they are found in concentrations of less than one microgram per cubic meter of air. Several times during the abnormal conditions associated with shutting down and starting up, concentrations of cadmium and arsenic were found to be greater than one microgram per cubic meter of air.

The relatively high concentrations of lead and zinc in ambient air even during the longest strike (5 months) are probably due to blowing residual dust. Also, ores are stockpiled in the open. Particulates blown from these stocks could be deposited on hi-vol filters and thus detected in atomic-absorption spectroscopic analysis. Cadmium and arsenic were not present in the ores in high enough concentrations to be detected on a routine basis during strikes.

Abnormal ambient concentrations of the metal can be expected in the process of shutting down and staring up an industry. A comparison was made between the values found the week prior to and the week following the strike with their respective "normal" values. A greater perecentage of abnormally high ambient concentrations was found prior to the strike than following the strike—i.e., 58 percent vs 37 percent in 1974; 75 percent vs 17 percent in 1977; 31 precent vs zero percent in

TABLE 1. Ambient concentrations of heavy metals in the atmosphere of El Paso, Texas, before, during, and after smelter strikes. All values are micrograms per cubic meter of air. ND indicates no data.

	Site 1				Site 2				Site 3				Site 4			
	Pb	Zn	Cd	As	Pb	Zn	Cd	As	Pb	Zn	Cd	As	Pb	Zn	Cd	As
1974																
14 Jun-6 Jul[a]	0.65	0.12	0.07	0.01	14.66	10.52	0.74	0.96	0.89	0.18	0.04	0.03	0.55	0.13	0.02	0.01
7 Jul-13 Jul[b]	ND	ND	ND	ND	19.24	10.53	1.17	1.74	0.65	0.25	0.00	0.01	0.45	0.25	0.00	0.01
14 Jul-19 Aug[c]	0.96	0.10	0.00	0.00	1.28	0.72	0.05	0.08	0.08	0.11	0.00	0.00	0.48	0.11	0.00	0.00
20 Aug-27 Aug[d]	0.51	0.42	0.00	0.02	7.07	3.22	0.43	0.73	0.26	0.04	0.00	0.03	0.24	0.23	0.08	0.02
28 Aug-14 Sep[e]	1.07	0.23	0.00	0.07	13.82	9.23	0.52	1.48	0.82	0.24	0.00	0.03	0.50	0.13	0.00	0.03
1977																
17 Apr-23 Jun[a]	0.98	0.34	0.01	0.23	6.64	3.23	0.24	0.42	1.00	0.52	0.02	0.10	0.36	0.13	0.00	0.04
24 Jun-30 Jun[b]	1.33	0.49	0.03	0.13	4.43	5.40	0.99	1.82	1.04	0.58	0.03	0.11	0.30	0.28	0.01	0.03
1 Jul-6 Sep[c]	0.70	0.07	0.00	0.00	1.69	0.70	0.06	0.09	0.50	0.10	0.00	0.01	0.21	0.04	0.01	0.00
7 Sep-13 Sep[d]	0.43	0.19	0.00	0.00	10.09	4.15	0.24	0.15	ND	ND	ND	ND	0.10	0.06	0.00	0.00
14 Sep-14 Nov[e]	1.71	0.50	0.02	0.10	5.78	2.01	0.25	0.32	1.69	0.53	0.04	0.09	0.94	0.23	0.01	0.04
1980																
15 Feb-22 Jun[a]	1.73	0.96	0.08	0.13	3.00	1.92	0.18	0.25	1.70	0.90	0.08	0.11	0.47	0.50	0.04	0.07
23 Jun-30 Jun[b]	0.27	0.46	0.00	0.00	14.23	7.57	1.03	3.08	0.87	0.56	0.00	0.02	0.33	0.43	0.00	0.07
1 Jul-19 Nov[c]	0.83	0.49	0.00	0.00	1.52	1.65	0.02	0.26	1.39	0.42	0.00	0.00	0.57	0.39	0.00	0.00
20 Nov-27 Nov[d]	ND	ND	ND	ND	0.87	0.38	0.00	0.00	0.87	0.38	0.00	0.00	0.49	0.42	0.00	0.00
28 Nov-15 Apr[e]	1.98	1.10	0.05	0.15	7.16	4.69	0.56	0.88	3.51	1.16	0.07	0.20	1.22	0.68	0.02	0.10

[a]normal pre-strike
[b]abnormal pre-strike
[c]strike
[d]abnormal post-strike
[e]normal post-strike

1980. This suggests the process of shutting down is inherently more dirty than the processes involved in starting up.

Thermal inversions start in the fall, peak during the winter and are least during the summer in El Paso. These affect the quantities of heavy metals measured in the area (Hubert et al. 1981a, b). Comparisons cannot be made among the three data sets for 1974, 1977 and 1980 since they cover different time spans and different inversion conditions.

Meteorological conditions at the smelter are not known. Official meteorological data from the El Paso International Airport were compared with data from the Cd. Juarez Airport and two continuous air monitoring stations. Wind speeds and directions at the four stations could not be correlated. None of the stations was near the smelter.

LITERATURE CITED

40 CFR 50.1. 1978. Code of Federal Regulations: "Protection of the Environment." Parts 50-59.

Gray, R. W., H. G. Applegate and W. R. Roser. 1980. Analysis of particulates by scanning electron microscopy and ion probe. Texas J. Sci. 32 (3): 259-264.

Hubert, J. S., R. M. Candelaria and H. G. Applegate. 1980. Determination of lead, zinc, cadmium and arsenic in environmental samples. Atomic Spectroscopy, 1 (4):90-93.

Hubert, J. S., R. M. Candelaria, B. F. Rosenblum and H. G. Applegate. 1981a. A survey of ambient air levels of lead in El Paso, Texas, from 1972-1979. Air Pollution Control Association Jour. 31(3):259-261.

Hubert, J. S., R. M. Candelaria, B. F. Rosenblum, R. Munoz and H. G. Applegate. 1981b. A survey of ambient air levels of arsenic and cadmium in El Paso, Texas, from 1972-1979. Air Pollution Control Association Jour. 31(3):262-263.

THE COMMERCIAL PRODUCTION OF MUDMINNOWS (*FUNDULUS GRANDIS*) FOR LIVE BAIT: A PRELIMINARY ECONOMIC ANALYSIS

by BENITA P. WAAS *and* KIRK STRAWN

Department of Wildlife and Fisheries Sciences
Texas A&M University
College Station, TX 77843

and MICHAEL JOHNS *and* WADE GRIFFIN

Department of Agricultural Economics
Texas A&M University
College Station, TX 77843

ABSTRACT

The economic feasibiltiy of operating a commercial mudminnow farm was determined using the Generalized Budget Simulation Model for Aquaculture developed at Texas A&M University. A 10-yr planning horizon was used for the study. Initial investment costs, annual budgets and cash flows were estimated to determine cost, returns and profit. Economic profit, break-even analysis and net present value were used to evaluate the economic feasibility. Based on a grow-out stocking density of 400,000/ha, 85% projected survival, 2 crops per year and achieved production at 80% of capacity, the 24-ha facility showed an economic profit of $41,160 for the 6th year of operation. The break-even price of $0.40/dozen was $0.25 less than the market price of $0.65. The break-even production of 278,705 dozen/yr is 174,629 dozen less than the assumed annual production of 453,334 dozen.

INTRODUCTION

In recent years there has been an increased interest not only in developing biological and technological aspects of aquaculture systems but also in looking into their economic relationships. Economic, investiment and feasibility studies have been undertaken for a number of aquacultural systems including catfish (Griffin and Lacewell 1978; Ekstrom 1979), penaeid shrimp (Anderson and Tabb 1970; Williams 1973; Aquacop 1975; Adams et al. 1979; Johns et al. 1981a, b), freshwater prawn (Gibson and Wang 1977; Shang and Fujimura 1977; Roberts and Baur 1978) pompano (Cuevas 1978) and oysters (Im et al. 1976; Lipschultz and Krantz 1978, 1980). Although commercial baitfish farming has proved to be a rapidly growing, high-profit business, very few economic studies on baitfish production have been documented in scientific literture (Shang and Iversen 1971; Herrick and Baldwin 1975).

The Texas Journal of Science, Vol. XXXV, No. 1, March 1983

Fundulus grandis (Cyprinodontidae), regionally called "bullminnow", "chub", "mudfish" or "mudminnow", is in popular demand as live bait for sport fishes such as southern flounder, spotted seatrout and red drum along the coastal Gulf of Mexico and South Atlantic states. Local suppliers of mudminnows rely exclusively on catches from the wild. Fish are either seined from tidal marshes or trapped using minnow traps baited with cracked crabs. Since these methods are not reliable, supply is irregular and has continued to fall short of demand since 1970. As a result, there is much interest in raising this fish as a commercial enterprise.

Initial research efforts on the culture of mudminnows were conducted at Claude Peteet Mariculture Center in Alabama. Studies focused on the maintenance, spawning and harvesting techniques of broodstock and young, and rearing of juveniles to bait size utilizing commercial feeds (Tatum and Helton 1977; Tatum et al. 1979). McIlwain (1977) reared mudminnows in a closed system and concluded that it would not be a commercially feasible venture because of the high cost of rearing systems. Our studies at Houston Lighting & Power Company's Cedar Bayou Generating Station research facility east of Baytown, Texas, have shown positive technological feasibility for mudminnow farming along the Texas Gulf coast (Waas 1982). However, commercial baitfish production is a highly specialized industry due to the nature of transportation and sales facilities needed, the restricted areas in which production can occur economically, and the seasonal nature of the market. Thus, it is important not only to know the biological and technological aspects of production but also to be able to establish and demonstrate the economic feasibility of such an operation before prospective investors commit substantial resources to production.

METHODS AND DATA

The economic feasibility of a mudminnow hatchery/grow-out operation was examined using the Generalized Budget Simulation Model for Aquaculture developed at the Department of Agricultural Economics, Texas A&M University (Griffin et al. 1980). The model is designed to produce itemized fixed and variable costs, annual and monthly budgetary outputs, cash flows, break-even quantities and prices for a specified aquaculture system. These values are then presented to reveal production and net revenue for a venture.

The proposed 24-ha (60 acre) facility would consist of a system of 40 0.2-ha spawning/hatching ponds and 10 1.0-ha grow-out ponds covering a total area of 18 hectares. The facility design (Fig. 1) is based on data relative to growth and reproductive biology of mudminnows

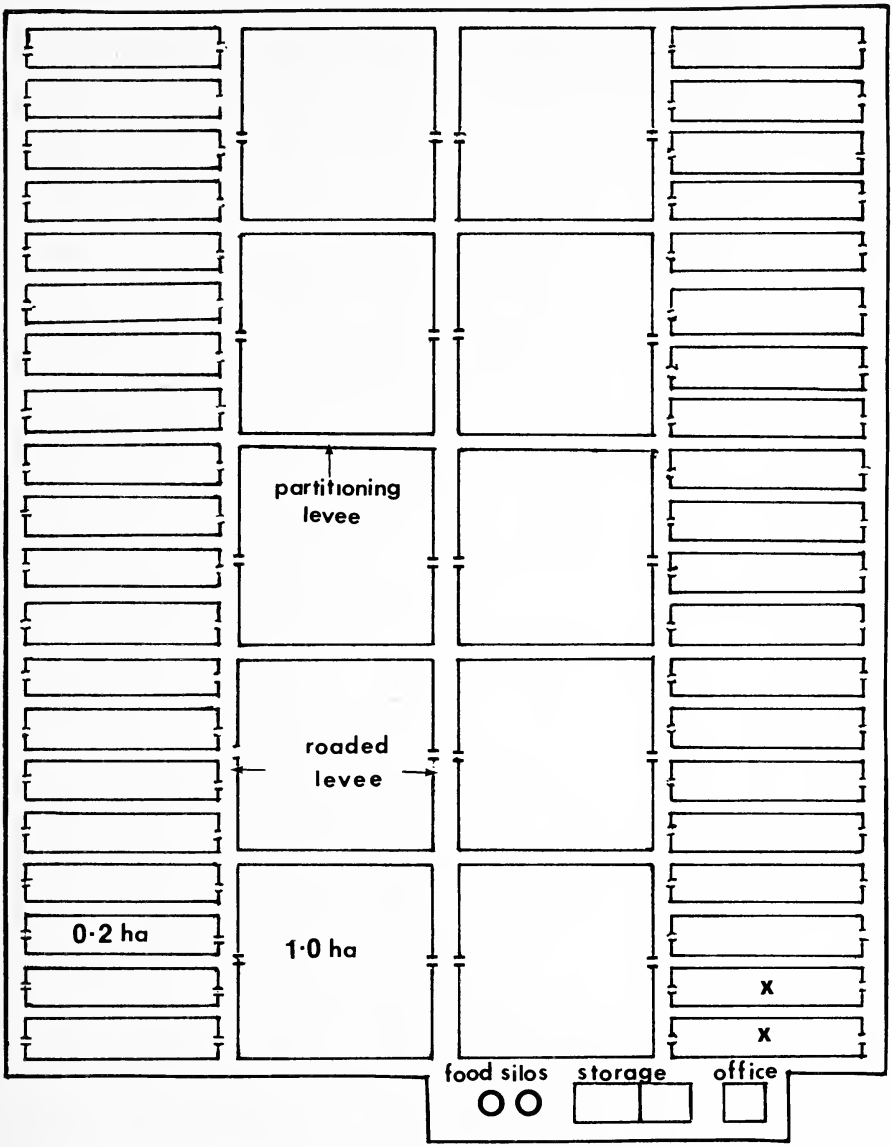

FIGURE 1. Design of the proposed 3-phase pond production facility (spawning/hatching/grow-out) for mudminnow farming. Ponds marked X are equipped with wooden piers.

obtained from studies at Cedar Bayou as well as from previous work in Alabama (Tatum et al. 1979; Trimble et al. unpubl. data). Several biological parameters, discussed below, are assumed to be of importance for optimal production of mudminnows.

Climatic Conditions

The designed facility can be adapted for production anywhere along the Texas Gulf coast where a sufficient water supply is available and outdoor temperatures are suitable for continued spawning (approximately 22-28°C) from March to October (Fivizzani 1977; Waas 1982).

Production of Fry

During the spawning season 20 0.2-ha ponds would function as spawning ponds while the other 20 would function as hatching ponds. Eggs laid on spawing mats will be hatched in the latter and the fry grown to an average size of 0.5 g (28-30 mm). Stocked at 65,000 brood fish/ha, production for each spawning pond is assumed to be 400,000 fry (at 75% survival from egg to fry) during the spawning season (late February to October). Fry produced from late February to May and May to August would be raised as crops I and II, respectively. Fry resulting from spawning activities after August would be overwintered and used for broodstock the following year. The recommended size for spawning/hatching ponds is 0.2 ha as it would be necessary to keep them small to facilitate efficient egg collection and fry harvest. Two of the 0.2 ha ponds would be equipped with wooden piers and would serve as holding facilities for fish during harvest (Fig. 1). Fish would be held in large net cages and sold to bait dealers at the facility.

Grow-out Ponds

The 10 1.0-ha grow-out ponds would be stocked at a density of 400,000 fish/ha. Fry would be graded prior to stocking to ensure size uniformity. Although this stocking density has not been tested, work in Alabama has demonstrated that fish stocked at 370,000/ha grew only a little slower than those stocked at 250,000/ha (Trimble et al. 1981). Current studies show sufficient growth rates can be maintained at stocking densities as high as 500,000/ha (P. Perschbacher, pers. comm.). A grow-out season of 55-65 days and 85% survival is based on Cedar Bayou and Alabama data (Tatum et al. 1979).

Food and Feeding

Fish would be fed commercial minnow feed (33% protein; particle size 0.5 mm) at the rate of 3% of body weight/day for brood fish. Food comsumption values for grow-out fish were based on an average food conversion ratio of 2.0. Average weight of brood fish and of fish sold is considered to be 7 and 3 g, respectively.

RESULTS OF ECONOMIC ANALYSIS

The analysis first calculates capital investment for the designed facility followed by yearly gross revenue and operating costs. It also pro-

TABLE 1. Estimate of capital cost for year 6 in the 10-year planning horizon of the mudminnow hatchery/grow-out operation, 1982.

1.	*Land* (60 acres @ $2,000/acre)	$120,000
2.	*Pond Construction*	
	a. Levees: excavation, caliche, grass seed	$101,768
	b. Pipes, Drains, Water Supply System	28,646
	Subtotal	$130,414
3.	*Buildings*	
	a. Storage and Shop (1,800 sq. ft.)	$36,000
	b. Office Building (750 sq. ft.)	15,000
	c. Architecture and Engineering Fee	13,457
	Subtotal	$64,457
4.	*Machinery and Equipment*	
	a. Pumps	$1,100
	b. Stand Pipe Screen, Filter Bags	755
	c. Transport Tank and Agitators	1,060
	d. Feed Blower/Trailer	3,610
	e. Feed Silos (2)	8,000
	f. Spawning Mats (2,400 @ $5.00 per mat)	12,000
	g. Minnow Graders, Holding Baskets, Seines etc.	2,146
	h. Refrigerator	950
	i. Miscellaneous Lab Equipment (microscope, scale, refractometer, etc.)	4,031
	j. Shop Tools	1,290
	k. Office Equipment	1,518
	Subtotal	$36,460
5.	*Vehicles*	
	a. Tractor	$8,762
	b. Pick-up	10,000
	Subtotal	$18,762
6.	*Broodstock Establishment* (21,666 doz. @ $0.85/doz.)	$18,417
	TOTAL CAPITAL COSTS	$388,510

vides a detailed annual budget for the sixth year of operation. All input and output prices are assumed to remain constant over the planning horizon. Break-even analysis, economic profit and net present value are then examined to evaluate the feasibility of the facility. Revenue and cost are in 1982 dollars.

Capital Investment

Included in this category are funds initially committed to the project (Table 1). All equipment and construction prices were obtained during the spring of 1982 and are representative of the upper Texas coastal area. A 10-yr planning horizon is used for the facility. The total capital cost (CC) of the facility is $388,510. Pond construction and land value are the two major expenses, accounting for 33.6 and 30.9% of the total investment. Building cost constitutes 16.6% of CC; buildings consist of

Table 2. Schedule of activities for a 2-crop mudminnow farming enterprise.

	Spawning Phase	Hatching to Juveniles	Grow-out Phase	Harvest	Total Grow-out Days
Crop I	Feb. 15-Apr. 30	Feb. 22-May 25	June 1-Aug. 5	Aug. 5-Aug. 20	65
Crop II	May 1-July 30	May 8-Aug. 20	Sept. 1-Nov. 5	Nov. 5-Nov. 20	65
	Aug. 1-Oct. 10	Fry resulting from this spawning activity would be raised, wintered and used for broodstock the following year.			

a storage facility for spawning mats and equipment and an office. Cost of machinery and equipment is 9.4%. The useful life of all facilities is estimated at 10 years, and salvage value of buildings and pond facility are estimated by the straight-line depreciation method. Adult broodstock would be initially purchased from trappers for 85 ¢ per dozen, which amounts to only 4.7% of CC.

Annual Production and Revenue

A suggested schedule of activities for the 2-crop operation is presented in Table 2. This operation is based on a production rate of 80% of the total capacity of the facility, allowing for problems such as occasional outbreaks of disease, equipment failures, adverse weather conditions, bird predation, or other production problems. Also, based on the stocking density of 400,000/ha and projected survival of 85%, a total of 453,333 dozen mudminnows would be produced on an 8-9 month production schedule (crop I in August; crop II in November). At $0.65 per dozen of baitfish, sales would generate an annual revenue of $294,667 (Table 3).

Operating Costs

Estimated annual operating costs (OC) (Table 4) are considered in two categories, variable costs (VC) and fixed costs (FC). Feed is the

Table 3. Summarized annual budget for year 6 in 10-year planning horizon for baitfish hatchery/grow-out operation.

Gross revenue from baitfish production	$294,667.00
Total variable cost (VC)	$ 31,795.00
Total fixed cost (FC)	$149,363.00
Total cost (FC + VC)	$181,158.00
Net revenue	$113,509.00
Income tax	$ 52,214.00
Net after-tax revenue	$ 61,295.00
Required return to equity capital	$ 20,135.00
Economic profit	$ 41,160.00
Break-even price	$ .40
Break-even quantity	278,705 dozen
Total capital investment	$388,510.00
Net present value based on 25% initial investment in capital costs	$341,866.00

TABLE 4. Estimated annual opeating costs for year 6 in the 10-year planning horizon of the mudminnow hatchery/grow-out opeation, 1982.

Variable Costs	
1. Feed (52.6 metric tons)	$12,185
2. Fuel	$ 2,134
3. Part-time labor	$ 9,240
4. Utilities	
a. Electricity	$ 4,898
b. Telephone	$ 600
c. Water	$ 400
5. Repair and Maintenance	
a. Equipment	$ 232
b. Machinery	$ 663
6. Payroll taxes	$ 1,443
Total Variable Costs	$31,795
Fixed Costs	
1. Salary—full time personnel	$60,000
2. Interest	$32,999
3. Depreciation	$42,016
4. Taxes	$ 6,126
5. Insurance	$ 8,222
Total of Fixed Costs	$149,363
TOTAL OPERATION COSTS	$181,158

major VC item, representing 38.3%. Feed costs are calculated at $0.232/kg. Part-time labor is 29.1% of VC. This labor would be utilized during harvest of fry for stocking and adults for marketing. Salaries of full-time personnel (manager and 6 laborers) represent 40.2% of FC. Depreciation is 28.1% of FC. Interest calculated at 21% per year is the third highest FC item (22.1%). Total annual operating cost of the facility is $181,158.

The annual budget for year 6 of the planning horizon is given in Table 3. Net revenue above total OC is $113,509. Income tax calculated on a corporate basis is $52,214, resulting in a net after-tax return of $61,295.

Break-even Analysis

Break-even analysis is useful in studying the relationship between FC, VC, and profit. Break-even price (BEP) and break-even production (BEQ) are considered in the analysis (Table 3). BEP of $0.40 represents the lease price required for the yield to equal OC for year 6 of operation assuming the projected yearly production rate of 453,334 dozen baitfish. This is $0.25 less than the market price of $0.65/doz. BEQ of 278,705 dozen at the current unit price of $0.65 indicates the lowest level of production needed to prevent losses. This BEQ is 61% of the production capacity assumed in the analysis.

Economic Profit

Economic profit helps to evaluate the investment potential of the baitfish operation as opposed to an alternative investment. This is done by estimating returns the owner can expect for his equity capital from the alternative investment. Equity capital is taken as 25% down payment of the total investment of the facility. The alternative investment in this study is taken as corporate bonds which have a return rate of 15.73% per year, with an added 5% per year as adjustment for risk and uncertainty associated with the baitfish operation. That is, mudminnow farming, being a new venture, can be considered a high risk in comparison to corporate bonds. Changes in demand for baitfish, depletion of sportfish stocks, discovery of additional or alternative bait sources are some additional factors that contribute to the risk. The required return to equity capital (Table 3) is $20,135 and economic profit is $41,160. Positive value of economic profit implies that investment of equity capital in the baitfish operation results in higher returns than the next best alternative.

Net Present Value

By taking into account the time value of expenditures and earnings, the net present value (NPV) method allows one to make a realistic comparison of future returns with initial expenditures. This is done by discounting the expected future returns by an appropriate discount rate over the planning horizon of the project. Discount rate used for the analysis is 19.75%. A NPV value greater than zero means the investment is economically profitable. In the present analysis NPV was estimated considering the owner's investment as 25% of the capital investment and remaining 75% financed at 17% interest rate for the life of the investment. A net present value of $341,866 (Table 3) indicates the investor would receive a rate of return greater than 21.7%.

CONCLUSION

Based on the assumptions incorporated into the framework of the model, a commercial mudminnow operation of the assumed design, located along the Texas coast would be economically profitable. Some of the assumptions that have major impact on its feasibility are fry production levels, stocking densities in grow-out ponds, timing of the production cycle to take advantage of peak periods, and a ready market. As previously mentioned, biological assumptions are based on experimental data and work is presently being carried out to further optimize stocking densities and increase fry production. Use of a higher ratio of females in spawning ponds has been shown to increase fry production (Waas unpubl. data). Timing of crop harvest with peak demand periods may be the key element in success of the operation, as demand for mudminnows is seasonal. Along the Texas coast demand is low during

the first 6 months of the year. It increases steadily from late July to a November peak during the flounder season. Even if all possible steps are taken to market the crop during high-demand periods, oversupply or shortages of baitfish are not always forseeable. Climatic conditions that curtail fishing can cause a temporary decline in sales of bait.

Since mudminnows have not been raised commercially, a thorough market survey is necessary before large-scale production is undertaken. Prospective producers should visit fish camps and other bait selling areas and determine the scope of the market. Although there will be initial competition from the wild catch, bait dealers have clearly shown a preference for pond raised mudminnows because of their higher quality, uniform size, and most of all, because of the assurance of a reliable and adequate supply during high-demand periods. Supply of fish for bio-assay work and the sale of fingerlings as food for predatory aquarium fish are additional marketing channels that should be explored.

Economies of size were not investigated in this study. It would be useful to determine the facility size that captures most of the available economies, as it aids in the reduction of fixed costs per unit of output. Since production of mudminnows for bait is a relatively new venture it would be wise initially to start with a smaller-sized production facility. Possibly 4-6 hectares (10-15 acres) in a one-man or family operation would help minimize investment per unit.

ACKNOWLEDGEMENTS

This research was funded by the Houston Lighting & Power Company through the Department of Wildlife and fisheries Sciences and Texas Agricultural Experiment Station Project 6462-3790. We thank Ron Biever, Mark Byford, Mark Hardin, Pete Perschbacher, Celeste Rees and Dr. Larry Wiesepape for their help in data collection. The economic analysis was supported through a research project sponsored (in part) by the Texas A&M University Sea Grant College Program, supported by the National Oceanic and Atmospheric Administration's Office of Sea Grant, Department of Commerce, under grant number NA81AA-D-00092.

This paper represents contribution number TA-18031 of the Texas Agricultural Experiment Station.

LITERATURE CITED

Adams, C. M., W. L. Griffin, J. P. Nichols, and R. W. Brick. 1979. Bioengineering-economic-model for shrimp mariculture systems, 1979. TAMU-SG-80-203, Texas A&M University, College Station, TX.

Anderson, L. G., and D. C. Tabb. 1970. Some economic aspects of pink shrimp farming. Gulf Carr. Fish Ins. 23:113-124.

Aquacop. 1975. Maturation and spawning in captivity of penaeid shrimp *Penaeus merguiensis* de Man, *Penaeus japonicus* Bate, *Penaeus aztecus* Ives, *Metapenaeus ensis* de Hann, and *Penaeus semisulcatus* de Hann. Proc. World Mar. Soc. 6:123-132.

Cuevas, H. Jr. 1978. Economic feasibility study of Florida pompano (*Trachinotus carolinus*) and rainbow trout (*Salmo gairdneri*) production in brackish water ponds. M.S. Thesis, Auburn Univ., Auburn, AL.

Ekstrom, J. P. 1979. A computerized budget simulator for use in catfish farming. M.S. Thesis, Texas A&M University, College Station, TX.

Fivizzani, A. J., Jr. 1977. Environmental and hormonal regulation of seasonal conditions of the Gulf killifish (*Fundulus grandis*). Ph.D. Dissertation, Louisiana State University, Baton Rouge, LA.

Gibson, R. T., and J. Wang. 1977. An alternative prawn production system design in Hawaii. UNIHI-Sea Grant TR-77-05. HAES J. Ser. paper no. 2142.

Griffin, W. L., and R. D. Lacewell. 1978. Estimated cost of producting catfish in Texas, 1977-1978. Proc. 1978 Fish Farm. Conf., Ann. Conv. Fish Farmers TX. p. 35-61.

Griffin, W. L., C. M. Adams, and L. A. Jensen. 1980. A generalized simulation model for aquaculture. Texas A&M University, Sea Grant Programs. Sea Grant 04-8-Mol-133.

Herrick, S. F., and W. J. Baldwin. 1975. The commercial production of top minnows—A preliminary economic analysis. Sea Grant Advisory Report. Unviersity of Hawaii. UNIHI-SG-AR-75-02. HIMB Contirb. no. 464.

Im, K. H., R. H. Johnson, and R. D. Langmo. 1976. The economics of hatchery production of Pacific oyster seed—a research report. Proc. Nat. Shellfish Assoc. 66:81-94.

Johns, M., W. Griffin, A. Lawrence, and D. Hutchins. 1981a. Budget analysis of shrimp maturation facility. J. World Mar. Soc. 12:104-109.

Johns, M., W. Griffin, A. Lawrence, D. Hutchins, and J. Fox. 1981b. Budget analysis of shrimp hatchery facilities. J. World Mar. Soc. 12(2). In press.

Lipschultz, F., and G. E. Krantz. 1978. An analysis of oyster hatchery production of cultched and cultchless oysters utilizing linear programming techniques. Proc. Nat. Shellfish. Assoc. 68:5-10.

Lipschultz, F., and G. E. Krantz. 1980. Production optimization and economic analysis of an oyster (*Crassostrea virginica*) hatchery in the Chesapeake Bay, Maryland, USA. Proc. World Mar. Soc. 11:580-591.

McIlwain, T. D. 1977. Bait fish rearing. Project GR-76-005, Mississippi Mar. Res. Council., Long Beach, MS.

Roberts, K. J., and L. C. Bauer. 1978. Costs and returns for *Macrobrachium* grow-out in South Carolina, USA. Aquaculture 15:383-390.

Shang, Y. C., and T. Fujimura. 1977. Production economics of fresh water prawn (*Macrobrachium rosenbergii*) farming in Hawaii. Aquaculture 11:99-110.

Shang, Y. C., and R. T. B. Iversen. 1971. The production of threadfin shad as live bait for Hawaii's skipjack tuna fishery: an economic feasibility study. Economic Research Center, Univ. of Hawaii, Honolulu, HI.

Tatum, W. M., and R. F. Helton, Jr. 1977. Preliminary results of experiments on the feasibility of producing bullminnows (*Fundulus grandis*) for the live bait industry. Proc. World Mar. Soc. 8:49-54.

Tatum, W. M., W. C. Trimble, and R. F. Helton, Jr. 1979. Production of Gulf killfish in brackish water ponds. Proc. An. Conf. Southeast. Assoc. Fish. Wildlife Agencies 32:502-508.

Trimble, W. C., W. M. Tatum, and S. A. Styron. 1981. Pond studies on Gulf killifish (*Fundulus grandis*) mariculture. J. World Mar. Soc. 12(2). In press.

Waas, P. B. 1982. Development and evaluation of a culture system suitable for the production of Gulf killifish (*Fundulus grandis* Baird and Girard) for live bait in the thermal effluent of a power plant. Ph.D. Dissertation, Texas A&M University, College Station, TX.

Williams, R. J. 1973. Economic feasibility of commercial shrimp farming in Texas. M. S. Thesis, Texas A&M Unviersity, College Station, TX.

EFFECTS OF A HIGH POTASSIUM DIET AND PROSTAGLANDIN ON INDUCED GASTRIC ULCERATION IN RATS[1]

by MARSHALL J. MANN *and* DAVID P. SHEPHERD

Department of Biology
Southeastern Louisiana University
P.O. Box 791
Hammond, LA 70402

ABSTRACT

Forty (40) Sprague-Dawley rats were placed on a high potassium (K), low sodium diet for 23 days while another 40 received standard rat chow. All animals received an IP injection of 20mg/kg indomethacin to induce gastric ulcers. Twenty (20) animals from each of the above groups received a 0.15mg/kg oral dose of prostaglandin (PGE_2).. The high K diet alone reduced the number and severity of indomethacin-induced gastric ulcers and it enhanced the anti-ulcer effect of PGE_2.

INTRODUCTION

Prostaglandin E_2 (PGE_2) has been shown to have a cytoprotective effect upon the gastric mucosa of rats exposed to various ulcer-inducing compounds, including the drug indomethacin (Lippman 1974; Robert 1976). Shepherd et al. (1973) reported that 65% of rats they fed a special diet high in potassium survived exposure to 1000R whole-body gamma irradiation. This amount of radiation typically results in the death of all animals, and the primary cause of death is damage to the gastrointestinal tract (Quastler 1956; Casarett 1968). Therefore, a high-potassium diet may protect the gastrointestinal tract from radiation damage.

The purpose of this study was to evaluate potassium as a potential protecting agent for the gastric mucosa of rats given the ulcer-inducing compound indomethacin. The approach was to use a high-potassium diet and standard laboratory chow to form two experimental groups. Half of each experimental group was given oral doses of PGE_2. All animals were injected with indomethacin.

MATERIALS AND METHODS

Eighty (80) Sprague-Dawley rats, mixed sexes and weighing 100-125 g each, were divided into equal groups (A and B). Group A was placed

[1]Paper presented at 84th Annual Meeting of the Texas Academy of Science, Austin, TX, March 1981.

on a standard laboratory chow (Purina Rat Chow), while Group B as given a special diet high in potassium (0.73%) and low in sodium (0.019%) (ICN Life Science Group, Cleveland, Ohio). This is half the sodium and four times more potassium than the minimum requirements of these ions. Other data related to consumption of the high-potassium diet—including food intake, duration of the diet, weight gain and serum Na and K levels—have been previously reported (Shepherd et al. 1973). Animals of Group B were maintained on the diet for 23 days. All animals received distilled water ad libitum.

After 23 days, Groups A and B were subdivided into groups of twenty animals each (A1, A2, B1, B2). All animals were fasted 24 h with distilled water ad libitum. Then, groups A2 and B2 were given Prostaglandin E_2 (PGE_2) (Sigma Chemical Company, St. Louis, Mo.) orally at a dose of 0.15mg/kg (Main and Whittle 1975). PGE_2 was combined with absolute ethanol (0.1ml/mg) and added to 1% methyl cellulose and mixed five minutes with a magnetic stirrer. Oral administration of PGE_2 was accomplished via a 76-mm intubation needle. Immediately following oral PGE_2, all animals were injected (IP) with 20mg/kg indomethacin (Djahanguiri 1969). Preparation of the indomethacin followed the method of Main and Whittle (1975). Five hours later (Lippman 1974) all animals were etherized; the stomach was removed and opened along the greater curvature. The stomach was inverted on the index finger, washed under tap water and examined by an observer to whom the treatment was not known. The necrohemmorrhagic areas were counted, and graded on a severity scale of one to three (1 = less than 1mm; 2 = 1-2mm; 3 = greater than 3mm) (Main and Whittle 1975).

RESULTS

The effects of a high potassium diet and synthetic prostaglandin (PGE_2) on the incidence of indomethacin-induced acute gastric ulcers are indicated in Table 1. The most striking datum in Table 1 is the 80% reduction in the number of animals experiencing ulcers in the experimental group B2. These animals were on the high potassium diet and received oral PGE_2 before indomethacin injection. The 80% reduction is by comparison with group B1. Group A2 which was on standard lab chow also received oral PGE_2 but only had a 30% reduction in incidence of ulcers, compared with A1.

The difference in incidence of ulcers between groups A1 and B1 was not significant, but there was a significant difference in the total number of ulcers (Table 2). The data from Table 2 demonstrates that diet was significantly involved in reducing the total number of indomethacin-induced ulcers. Group B1, on the high-potassium diet,

TABLE 1. Effect of high-potassium diet and PGE_2 on incidence of gastric ulcers in rats.

Group[a]	Diet	Dose of PGE_2	# of Animals with Ulcers per group (20)	% Incidence	% Reduction[b]
A1	Lab Chow		18/20	90%	
A2	Lab Chow	0.15mg/kg	12/20	60%	30%
B1	High K^+		20/20	100%	
B2	High K^+	0.15mg/kg	4/20	20%	80%[c]

[a]All groups received 20mg/kg indoemthacin.
[b]Reduction is based on comparison of A2 to A1 and B2 to B1.
[c]Significant at 0.005 probability level.

had 184 ulcers as compared to 328 ulcers for the lab-chow Group A1. Those animals that were on the high-potassium diet and given PGE_2 (Group B2) had only 5 ulcers as compared to those animals on lab chow and receiving PGE_2 (Group A2), which had 73 ulcers.

Both prostaglandin treatment and the high potassium diet, when used alone, reduced the total number of ulcers; however, when used together, not only was the total number of ulcers reduced but also the severity was reduced (Table 3). Because ulcers of severity 3 had areas ranging from $(2mm)^2$ to approximately total glandular surface, it is very significant that all the ulcers in Group B2 were less than 1mm. Of the four B2 animals with ulcers, three had only one (#1 severity) and the fourth had two (#1 severity). The sole difference between this group (B2) and Group A2 was the high potassium diet. Therefore, the synergism of PGE_2 and a high potassium diet resulted in a smaller surface area of the stomach having necrohemmorrhagic lesions.

DISCUSSION

The fact that potassium is an essential requirement for protein synthesis and growth is well established (Eagle 1955; Lubin 1964, 1967; Ledbetter and Lubin 1977). When cells are damaged by irradiation, potassium moves out of the cells (Ting and Zirkle 1940; Harrison et al. 1958; Portela et al. 1963); but when animals are provided with optimal availability of potassium in the diet, they are somewhat protected from

TABLE 2. Effect of high-potassium diet and PGE_2 on the number of gastric ulcers in rats.

Group[a]	Diet	Dose of PGE_2	Total # Ulcers	Average # Per Rat
A1	Lab Chow		328	16.4
A2	Lab Chow	0.15mg/kg	73	3.6
B1	High K^+		184	9.2
Bw	High K^+	0.15mg/kg	5	0.25

[a]All groups received 20mg/kg indoemthacin.

TABLE 3. Effect of high-potassium diet and PGE_2 on the severity of gastric ulcers in rats.

Group[a]	Diet	Dose of PGE_2	Number of Ulcers with Severity = 1	2	3
A1	Lab Chow		267	48	13
A2	Lab Chow	0.15mg/kg	57	12	4
B1	High K^+		158	20	6
			(85.8%)	(10.8%)	(3.2%)
B2	High K^+	0.15mg/kg	5	0	0
			(100%)		

[a]All groups received 20mg/kg indoemthacin.

the radiation as shown by a reduction in the number of deaths (Shepherd et al 1973). Therefore, the primary objective of the present investigation was to determine whether optimal availability of potassium would protect gastrointestinal cells from a potentially damaging agent, indomethacin.

The results show that rats placed on a diet high in potassium and low in sodium enjoyed some degree of protection: the total number of experimental ulcers was reduced by almost half. But when oral administration of prostaglandin (PGE_2) accompanied the special diet, the effects were synergistic. PGE_2 treatment alone resulted in a 30% reduction in animals with ulcers. When PGE_2 was combined with the high potassium diet, there was an 80% reduction in animals with ulcers.

Most evidence suggests that the initial action of some damaging agents on the gastric mucosa is the inhibition of active ion transport (Kuo et al. 1974; Sernka et al. 1974; Kuo and Shanbour 1976a,b). Specifically, studies have shown that indomethacin inhibits active transport of sodium (Chaudhury and Jacobson 1978) while prostaglandin stimulates active transport of sodium (Bowen et al. 1975), and these results have been used to postulate a mechanism of PGE_2 cytoprotection (Chaudhury and Jacobson 1978). There are no significant data concerning potassium in relation to this phenomenon.

There is some evidence to suggest that there may exist a separate transfer mechanism resonsible for accumulating intracellular potassium and that this mechanism is not directly coupled to active sodium transport (Delong and Civan 1978). This could provide the basis for potassium acting as an independent protecting agent against the number and severity of indomethacin-induced ulcers. This could also explain why potassium acts synergistically with, or independent of, PGE_2 in protecting the mucosa against indomethacin.

Consistent with potassium being involved in cellular protection is the hypothesis that intracellular potassium controls the rate of macromolecular synthesis. The latter hypothesis is based on the observation that when cells are induced to leak potassium, there is a parallel

depression in the rate of protein and DNA synthesis. When the potassium level in the medium around the cells is increased, near normal levels of cellular K can be sustained and macromolecular synthesis continues (Ledbetter and Lubin 1977). This implies the possibility that a high-potassium medium may provide the cell with a means of "recovery" from various damaging agents. The specific role of dietary potassium in the apparent protection of the gastric mucosa against damaging agents such as indomethacin and radiation needs further investigation.

LITERATURE CITED

Bowen, J. C., Y-J. Kuo, W. Pawlik, D. Williams, L. L. Shanbour, E. D. Jacobson. 1975. Electrophysiological effects of burimamide and 16, 16-dimethyl prostaglandin E^2 on the canine gastric mucosa. Gastroenterology 68: 1480-1484.

Casarett, A. P. 1978. Radiation Biology. Prentice-Hall, Englewood Cliffs, NJ.

Chaudhury, T. K., and E. D. Jacobson. 1978. Prostaglandin cytoprotection of gastric mucosa. Gastroenterology 74:59-64.

DeLong, J. and M.M. Civan. 1978. Dissociation of cellular K^+ accumulation from net Na^+ transport by toad urinary bladder. J. Membr. Biol. 42:19-31.

Djahanguiri, B. 1969. The production of acute gastric ulceration by indomethacin in the rat. Scand. J. Gastroent. 4:265-268.

Eagle, H. 1955. Nutrition needs of mammalian cells in tissue culture. Science 122:501-502.

Harrison, A. P., A. K. Bruce, and G. E. Stapleton. 1958. Influence of X-irradiation on potassium retentivity by *Escherichia coli*. Proc. Soc. Exp. Biol. Med. 98:740-746.

Kuo, Y-J., L. L. Shanbour, and T. J. Sernka. 1974. Effect of ethanol on permeability and ion transport in the isolated dog stomach. Am. J. Dig. Dis. 19:818-819.

Kuo, Y-J., and L. L. Shanbour. 1976a. Mechanism of action of aspirin on canine gastric mucosa. Am. J. Physiol. 230:762-768.

Kuo, Y-J., and L. L. Shanbour. 1976b. Inhibition of ion transport by bile salts in canine gastric mucosa. Am. J. Physiol. 231:1433-1436.

Leadbetter, M. L. S., and M. Lubin. 1977. Control of protein synthesis in human fibroblasts in intracellular potassium. Exp. Cell Res. 105:223-227.

Lippman, W. 1974. Inhibition of indomethancin induced gastric ulceration in the rat by perorally administered synthetic and natural prostaglandin analogues. Prostaglandins 7:1010-1023.

Lubin, M. 1964. Intracellular potassium and control of protein synthesis. Fed. Proc. 23:994-999.

Lubin, M. 1967. Intracellular potassium and macromolecular synthesis in mammalian cells. Nature (Lond.) 213:451-458.

Main, I. H. M., and B. J. R. Whittle. 1975. Investigation of the vasodialator and antisecretory role of prostaglandins in the rat gastric mucosa by use of non-steroidal anti-inflammatory drugs. Br. J. Pharmac. 53:217-226.

Portela, A., J. C. Perez, P. Stewart, M. Hines, and V. Reddy. 1963. Radiation damage in muscle cell membranes and regulation of cell metabolism. Exp. Cell Res. 29:527-531.

Quastler, H. 1956. The nature of intestinal radiation death. Radiat. Res. 4:303-307.

Robert, A. 1976. Antisecretory, antiulcer, cytoprotective and diarrheogenic properties of prostglandins. Advances in Prostaglandin and Thromboxane Research 2:507-516.

Sernka, T. J., C. W. Gilleland, and L. L. Shanbour. 1974. Effect of ethanol on active transport in the dog stomach. Am. J. Physiol. 226:397-399.

Shepherd, D. P., S. O. Brown, G. M. Krise, and H. R. Crookshank. 1973. Dietary protection against ionizing radiation. Radiat. Res. 56:282-289.

Ting, T. P., and R. C. Zirkle. 1940. The kinetics of the diffusion of salts into and out of X-irradiated erythrocytes. J. Cell Comp. Physiol. 16:197-201.

BIOLOGICAL FORM REPRESENTATION BY TECHNIQUES DEVELOPED FOR AIRFOILS[1]

by W. M. HEFFINGTON

Department of Mechanical Engineering
Texas A&M University
College Station, TX 77843

and K. L. EAVES

Department of Biochemistry
Texas A&M University
College Station, TX 77843

ABSTRACT

Representation of biological forms that are approximately teardrop-shaped is possible by use of systems developed for describing airfoils. Such approaches include the Joukowski transformation (a conformal transformation which changes a circle in one complex plane into a teardrop shape in another complex plane) and the empirical NACA four-digit system. Both techniques require little data to represent the original object, unlike anthropological and biological methods which use large numbers of linear measurements and descriptive terms to describe shapes. Length, thickness and curvature angle are the only data required to represent a teardrop shape using the Joukowski transformation, and four digits and the length are all that are required when using the NACA four-digit system. In this work, both the Joukowski tranformation and the NACA four-digit system are applied to incisors of olive baboons (*Papio cynocephalus anubis*), and the resulting shapes are compared to outlines of the original teeth. Shapes symmetrical about a central axis and unsymmetrical shapes are treated. Other transformations are discussed, and the use of microcomputers for obtaining outline drawings from photographs of biological specimens is described. Possible uses and applications of these techniques are discussed.

INTRODUCTION

Biological forms such as teeth are presently described in anthropological and biological literature by photographs, drawings, or a series of linear measurements such as labial and lingual height and breadth, anterior-posterior crown length, and breadth of each molar cusp (Ashton and Zuckerman 1950). Descriptive terms used include biscuspid, sectorial, molariform, D-Y-5 cusp pattern, and bunodont-cusped (Zeisz and Nuckolls 1949; Krogman 1969). Problems with popular tooth-description methods are due in part to the quantity of data required to accurately describe a tooth.

[1]Presented at the Eighty-fourth Annual Meeting of the Texas Academy of Science, Austin, Texas, March, 1981.

Acquisition of a completely faithful quantitative representation of a biological form would require storage and manipulation of a infinite number of data points. Even to reproduce a two-dimensional outline of a tooth as viewed from a particular aspect (buccal or distal, for instance) would require an infinite number of data points for complete fidelity. In order to avoid this complexity, resort is made to approximate systems in which the forms are represented by a finite number of points, and the features near the points are obtained by interpolation or extrapolation. As many as seventy points may be used to represent an object as simple as a tooth (Ashton and Zuckerman 1950). Another way of circumventing this difficulty is to provide a likeness of the original specimen such as a physical model, x-ray film, or a photograph (Zeisz and Nuckolls 1949).

Lacking sufficient quantitative data from which an outline shape may be obtained, sources report only selected data deemed to be important. Often little data is required to represent individual shapes. Simply giving the length and thickness of the buccal aspect of an olive baboon's (*Papio cynocephalus anubis*) lateral incisor may be sufficient data for an anthropologist to construct a suitable representation for the task at hand.

Since subsonic airfoils and some teardrop-shaped biological forms have similar outlines, systems developed by aerodynamicists for describing these airfoil shapes should apply to teardrop-shaped teeth. Two such systems, the Joukowski conformal transformation and the NACA[2] four-digit series, are used here to describe incisors from an olive baboon.

Transformations of biological shapes into related biological shapes often have been accomplished by reliance upon empirical formulations of the type used by Thompson (1917). Later works, such as those by Bookstein (1977) and Rosen (1978), have attempted more mathematically-based transformations; or, as Bookstein (1977) observed, they have used methods less geometrically precise than those of Thompson but more arithmetically tractable. The present effort belongs to the latter category.

Aerodynamicists have long known of conformal transformations using complex variables which transform simple circles into teardrop-shaped forms similar to the shapes of symmetrical and unsymmetrical subsonic airfoils. Many older text books—including those by Piercy (1937), von Karman and Burgers (1943), von Mises (1945), Pope (1951), and Rauscher (1953)—deal with this subject. These tranformations are perhaps less valuable to aerodynamicists for the shapes they transform

[2]NACA is an acronym for National Advisory Committee for Aeronautics, which has been replaced by NASA (National Aeronautics and Space Administration).

than for the characteristics of the related fluid-flow fields about the cylinders and airfoils. Advantages of applying shape transformations of this type to those biological shapes which may be transformed from circles include, for example, representation of relatively complicated shapes at different stages of growth by circles that differ progressively in radii and center coordinates. The amount of data required to describe a shape can be reduced to the Cartesian coordinates of the center and the radius of the circle.

Ad hoc methods for describing airfoils also were developed during the first half of this century. One such simple method is the NACA four-digit series, which can also be applied to teardrop-shaped biological forms.

Microcomputers, coupled with digitizer boards, provide a precise and quick method of obtaining the digital coordinates necessary for plotting and drawing the outline shape of physical specimens. In this study, coordinates were taken (digitized) from specimen photographs selected to provide data for the construction of the circles and whose shapes were used subsequently for comparison with the transformed circles.

MATERIALS AND METHODS

As an example of these techniques we apply the Joukowski transformation to circles for which size and location were determined from measurements of the length, thickness, and curvature of the two different teeth pictured in Plate 1. We also calculated the NACA 4-digit series that best describes these teeth. Both specimens are isolated lateral incisors from adult olive baboons. A line drawn equidistant from the upper and lower portions of the profile of tooth (A) shown in Plate 1 would be approximately straight (curvature approximately zero). Biological forms lacking curvature are referred to as symmetrical. The other tooth shown in Plate 1 has significant curvature of a line equidistant between the upper and lower portions of its profile, and provides data for the unsymmetrical example to be discussed.

In Plate 1 the boundaries of the teeth were visually aligned in an object plane and photographed at an object distance of about 116 mm with a 55 mm lens-equipped camera. The aspects forming the boundaries of the forms were estimated to be within 3 mm of the object plane (plane of focus) which leads to a maximum error in relative distance between points on the boundaries of the teeth shown in Plate 1 of less than 3%. Error of this type resulting from photographic technique decreases linearly with increasing object distance. The photographs were printed at a magnification of approximately four times actual tooth size. During early phases of this study, coordinates of points on

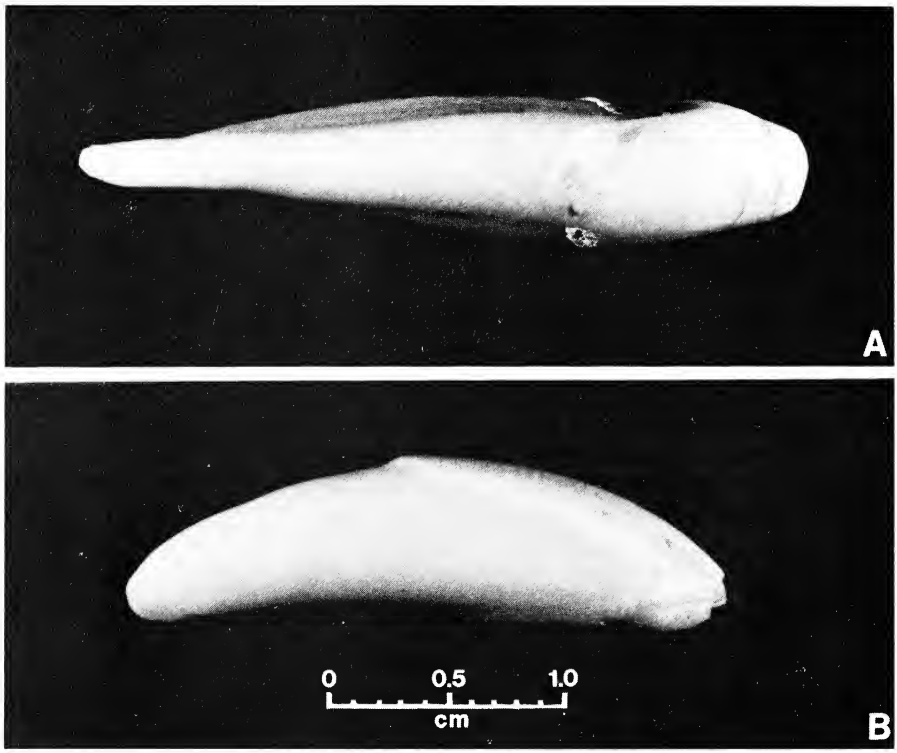

PLATE 1. Photographs of lateral incisors showing (A) symmetrical tooth (buccal aspect), and (b) unsymmetrical tooth (distal aspect).

the boundaries of the teeth were digitized using a TALOS model 611 digitizer board with an advertised accuracy of less than ± 0.13 mm for coordinate location. The digitizer board was interfaced with a Hewlett-Packard System 9815A desk-top microcomputer which provided a digital display of the coordinate values. As many as seventy locations were digitized per tooth, and the overall accuracy of any location digitized was estimated to be less than 3% of the length of the tooth, with most of the possible error due to the photographic phase. The coordinates were then plotted on graph paper and connected by curved segments in order to obtain outline drawings of the teeth. In an alternative method, the outline drawings were traced from the photographs. All measurements were made directly on the resulting drawings and are about four times greater than corresponding measurements made on the actual teeth due to the photographic magnification factor.

Many microcomputer systems have the capability to provide the drawings directly, either by plotting and connecting the digitized points or by printing closely spaced dots.

THE JOUKOWSKI TRANSFORMATION

A simple transformation that transforms certain circles in the z-plane to teardrop shapes in the w-plane is the Joukowski transformation[3] (Pope 1951),

$$w = z + \frac{b^2}{z} \tag{1}$$

where z and w can both be expressed in complex notation as $z = x + iy$ and $w = u + iv$, and b is a real constant. Not all circles in the z-plane are transformed into teardrop shapes; for instance, a circle of radius b centered at the origin of the z-plane will be transformed into a straight line between the points (−2b,0) and (2b,0), in the w-plane. A problem in working with some conformal transformations is the lack of general analytical solutions that give information such as the resulting length and thickness. For the Joukowski transformation an approximate analytical solution exists, valid when the thickness T is approximately small compared to the length L, and it yields for the symmetrical transformation (Pope 1951)

$$x_c \cong T/3\sqrt{3} \tag{2}$$

and

$$b \cong L/4 \tag{3}$$

where x_c is the x-coordinate of the center of the circle and −b is the intersection of the circle and the negative real axis. The y-coordinate of the center of the circle for the symmetrical transformation is, of course, equal to zero, and the circle radius is equal to the sum of x_c and b.

Figure 1 is a profile drawing of the symmetrical tooth from Plate 1. The measurements required to obtain the thickness and length for use in Eqs. (2) and (3) are indicated in relation to the outline drawing of the specimen. Substituting the thickness T = 24.5 mm and the length L = 122 mm into Eqs. (2) and (3), respectively, yields $x_c \cong 4.7$ mm and $b \cong 31$ mm. The circle in the z-plane resulting from these values has radius 36 mm and is shown in Fig. 1. The w-plane containing the Joukowski profile (transformed circle) according to Eq. (1) is superimposed on the z-plane in Fig. 1 also, and shows the teardrop shaped transformation compared to the outline drawing of the actual tooth.

[3]The Joukowski transformation is sometimes referred to as the Kutta-Joukowski transformation, after Kutta and Joukowski who worked independently in Germany and Russia, respectively, and who both advanced the transformation about 1910.

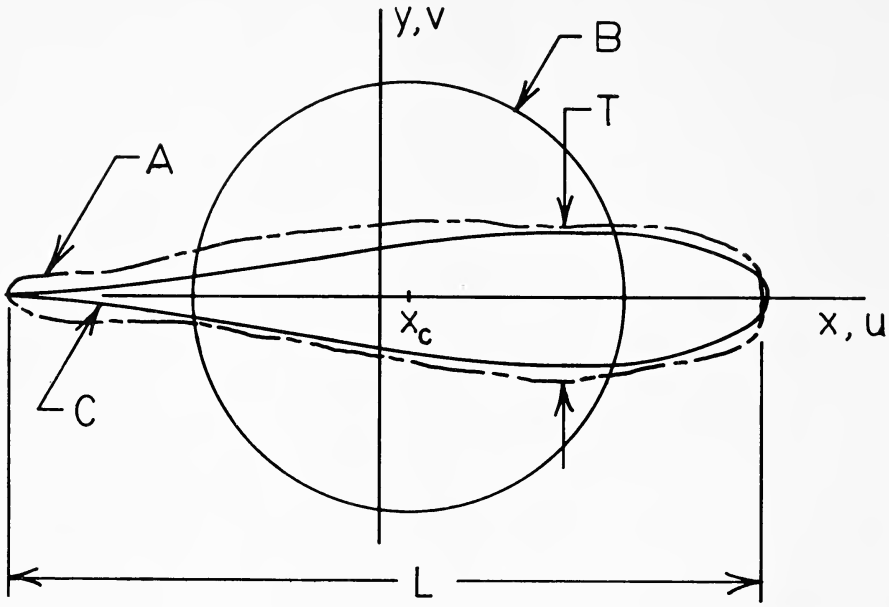

FIGURE 1. Diagram of (A) the outline of the symmetrical tooth in Plate 1 showing the thickness T = 24.5 mm and the length L = 122 mm, (B) the circle in the z-plane, and (C) the Joukowski profile in the w-plane.

The Joukowski profile is about 2% longer and about 10% thinner than the actual tooth due to the approximations involved in obtaining the analytical solutions for thickness and length.

For the unsymmetrical transformation (Piercy 1937) x_c and b are given by Eqs. (2) and (3), and the y-coordinate of the center of the circle is given approximately by

$$y_c \cong (b + x_c)\beta \tag{4}$$

where β is a curvature parameter which must be appropriately small in order to obtain Eq. (4). For the unsymmetrical Joukowski transformation, β is equal to one-half the acute angle formed by the cusp and the x-axis. For the unsymmetrical tooth shown in Plate 1 and drawn in Fig. 2, $\beta \cong 14$ degrees was estimated to be one-half the angle formed between an imaginary curvature line and the x-axis when the tooth was graphically extended to form a point at the narrow end, approximately the shape of mature teeth from certain specimens (Taylor 1978). For the curved tooth shown in Fig. 2, application of Eqs. (2) - (4) to a thickness of 25 mm, an extended length of 113 mm, and $\beta = 14$ degrees yields $x_c \cong 4.8$ mm, $b \cong 28$ mm, and $y_c \cong 7.9$ mm. The resulting circle (shown in Fig. 2) has a radius (equal to the distance from the center to $-b$) of 34 mm. The w-plane with the transformation of the z-plane circle in

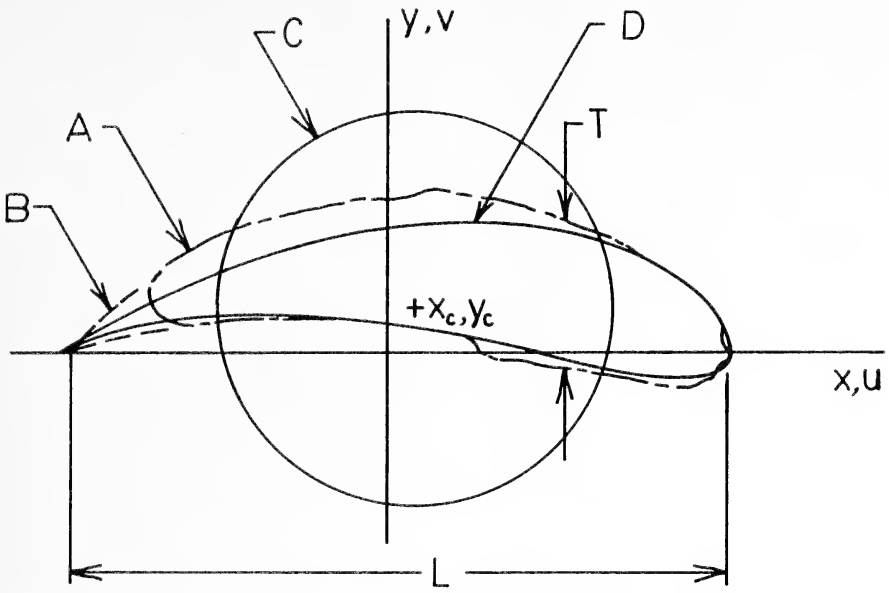

FIGURE 2. Diagram of the (A) outline of unsymmetrical tooth shown in Plate 1 showing the thickness T = 25 mm, (B) the graphically extended root to yield an overall length L = 113 mm, (C) the circle in the z-plane, and (D) the Joukowski profile in the w-plane.

Fig. 2 shows the Joukowski profile for comparison, which in this case is about 2% longer and 10% thinner than the tooth from which it was derived.

Both Joukowski profiles in Figs. 1 and 2 end in cusps at the narrow ends of the teeth. The cusps are a result of the singular point $-b$ lying on the circumference of each circle. Equation (1) is also not conformal at $+b$, but this point causes no problem because it lies within both circles. For reasons having to do with the air flow about the shape, aerodynamicists have usually required the desired circles to pass through one singularity and enclose the other (Pope 1951). In working with shapes alone these requirements are not necessary. If the radius of each circle is increased slightly so that the point $-b$ is enclosed, both singularities are enclosed, and transformation is possible in a manner that is everywhere conformal. The cusps in Figs. 1 and 2 then could be replaced by rounded shapes more suitable for biological forms.

In obtaining the approximate Eqs. (1) - (4), $x_c/_b$ and β have been assumed to be small (Piercy 1937; Pope 1951). Requiring $x_c/_b$ to be small in equivalent to requiring the thickness T to be small compared to the length L, because dividing Eq. (2) by Eq. (3) yields $x^c/^b \cong 0.77T/L$. Additional results of the approximate method used here to solve Eq. (1) are that the maximum thickness of the Joukowski profile

occurs at about one-fourth the length, near the rounded end, and that the line of curvature is the arc of a circle (Pope 1951). These results obviously should influence the choice of biological shapes to which the Joukowski transformation may be applied.

OTHER CONFORMAL TRANSFORMATIONS

The Joukowski transformation described by Eq. (1) is a special case of the general transformation (known as the von Mises transformation)

$$w = z + \frac{c_1}{z} + \frac{c_2}{z^2} + \ldots + \frac{c_n}{z^n} \tag{5}$$

where the c_n are constants (von Mises 1945). For the Joukowski transformation, $c_1 = b^2$ and the remainder of the constants are zero. Increasing the number of terms used in a transformation results in better representation and greater analytical difficulty. Application of Eq. (5) is discussed in von Karman and Burgers (1943), von Mises (1945) and Rauscher (1953).

Another simple transformation of interest is the Karman-Trefftz transformation (Von Karman and Burgers 1943)

$$\frac{w - mb}{w + mb} = \left(\frac{z - b}{z + b}\right)^m \tag{6}$$

where $m = 2 - (k/\pi)$ and k is the tail angle. This transformation is similar to the Joukowski transformation, but rather than yielding a cusp, produces a finite angle, k (for k greater than zero), at the transformation of the point where the circle passes through the singularity in Figures 1 and 2. For $k = 0$, the Joukowski transformation [Eq. (1)] is obtained from Eq. (6), and for k not equal to zero, Eq. (6) can be shown to correspond to an infinite series (von Karman and Burgers 1943).

NACA FOUR-DIGIT SERIES

This method of characterizing airfoils has corresponding designations used in reference to teeth. The *chord* of an airfoil finds its corollary in the *length* of a tooth, and the *camber* of an airfoil is designated *curvature* (Fig. 3) when applied to a tooth (von Mises 1945). The chord and the length are generally the largest physical measurements that can be made on an airfoil profile and a tooth, respectively.

The mean camber line may be defined as a curved line generated by the locus of centers of the line segments drawn across the airfoil section perpendicular to the chord. The mean curvature line of a tooth is used here in a similar fashion. Other definitions of camber are possible, and

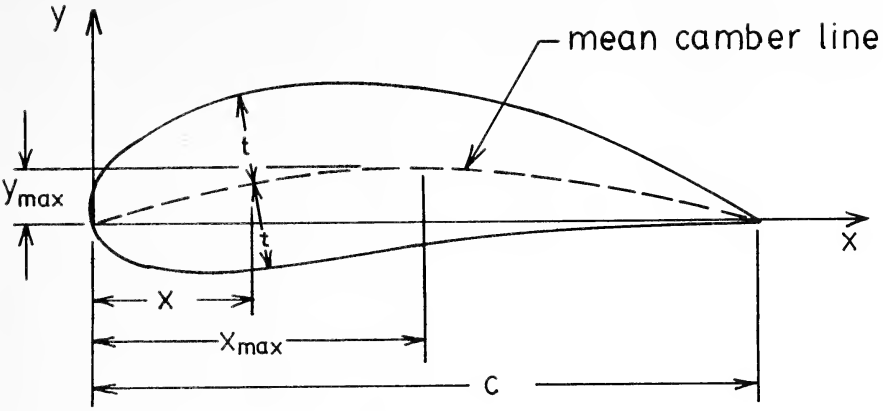

FIGURE 3. Drawing of a cambered airfoil in an orthogonal x-y coordinate system showing the ordinate of maximum camber, y_{max}; the abcissa of maximum camber, x_{max}; the chord, c; mean camber line; and thickness t at location x given by the thickness function (Eq.11). Note that the thickness is measured normal to the mean camber line. For a tooth the chord would be designated length and the mean camber line as mean curvature line. Thickness is defined the same for both airfoil and tooth.

usually are approximately equivalent (von Mises 1945). The maximum thickness may be defined in various ways (von Mises 1945). Here we define it as the length of a line segment, locally perpendicular to the mean camber line across the airfoil section or tooth, in accordance with the NACA definition (Jacobs et al. 1933). Generally, the length or chord is oriented parallel to an axis in an orthogonal coordinate system when constructing a graphic representation.

The NACA four-digit specification (Jacobs et al. 1933; Jacobs and Pinkerton 1935; Jacobs et al. 1937) for an airfoil shape contains four digits and is often specified as NACA ABCD where the A, B, C, and D are digits. The first two digits determine the form of the mean camber line (graphically indicated in Fig. 3). The first digit indicates the ordinate y_{max} (see Fig. 3) of the maximum camber in percent of chord (and thus its utility in this form is limited to airfoils of maximum camber less than 10% of the chord length). For a NACA ABCD airfoil, the digit $A = 10\ y_{max}/c$, where c is the chord. Applied to a tooth,

$$A = 100\ y_{max}/L \tag{7}$$

where L is the tooth length. The second digit, B, is the abcissa of the location x_{max} of maximum camber in tenths of the chord length, or $B = 10\ x_{max}/c$. For a tooth,

$$B = 10\ x_{max}/L. \tag{8}$$

For a symmetrical airfoil (one having a straight camber line) the A and B are identically zero, e.g., NACA 00CD.

The last two digits CD give the relative thickness of the airfoil in percent of chord, CD = 100 T/c, where T is the maximum airfoil thickness measured normal to the mean camber line (see Fig. 3). Notice two digits are used to represent the thickness. For a tooth,

$$CD = 100\ T/L, \tag{9}$$

and T here is the maximum tooth thickness measured normal to the curvature line. From the information given in the first two digits of the profile, obviously the x- and y- coordinates of the maximum camber location for unsymmetrical teeth can be derived from Eqs. (7) and (8); e.g., $y_{max} = AL/100$ and $x_{max} = BL/10$. The mean camber line then can be constructed from the following equations of parabolic arcs (von Mises 1945):

$$y = \frac{y_{max}}{(x_{max})^2}(2x_{max} - x)x \quad \text{for } 0 \leq x \leq x_{max} \tag{10a}$$

and

$$y = \frac{y_{max}}{(L - x_{max})^2}(L - x)(L - x - 2x_{max}) \tag{10b}$$

for $x_{max} \leq x \leq c$. Once the camber line is known, the thickness function t, given by

$$t = \pm T\left[1.4845\sqrt{\frac{x}{L}} - 0.6300\frac{x}{L} - 1.7580\left(\frac{x}{L}\right)^2 + 1.4215\left(\frac{x}{L}\right)^3 - 0.5075\left(\frac{x}{L}\right)^4\right], \tag{11}$$

can be used to determine the actual profile. At the abcissa x on the mean camber line, t is measured above and below (along a line normal to) the mean camber line to determine points on the profile (Fig. 3).

The length and thickness of the distal aspect of a curved tooth have been measured as L = 25.4 mm and T = 7 mm. The location of the y-coordinate of the maximum curvature was calculated to be $y_{max} = 2.3$ mm from measurements indicated in Fig. 4, according to

$$y_{max} = (y_1 + y_2)/2. \tag{12}$$

Values of y_1 and y_2 and the value $x_{max} = 12.8$ mm were estimated directly from the tooth profile in the manner described in Fig. 4.

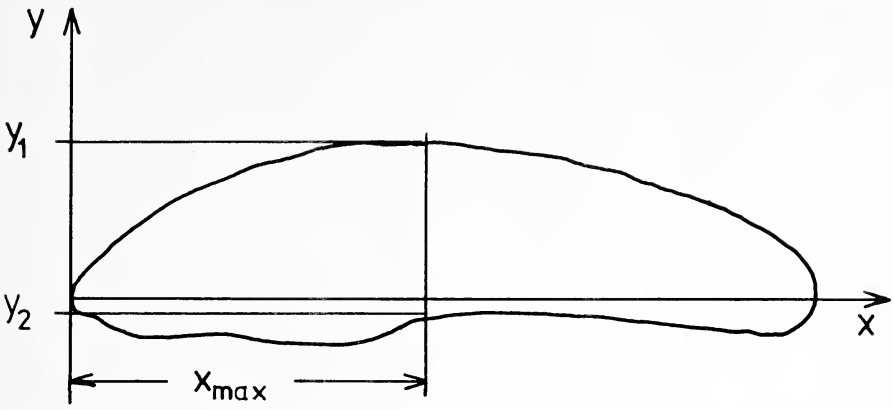

FIGURE 4. Diagram of measurements to be made in order to estimate x_{max} and y_{max}. The measurements may be made on the actual specimen, or a photograph or other likeness.

Application of Eqs. (7)-(9) resulted in a designation of NACA 9528. Once the profile designation and the length were available, a representation of the tooth could be constructed by applying Eqs. (7) and (8) to determine x_{max} and y_{max} (had they not been known already, as in this case) and Eq. (9) to determine T. From Eq. (10) the mean camber line was drawn (Fig. 5), and from Eq. (11) the upper and lower portions of the profile were determined (Fig. 5).

The NACA 9528 shape fit the profile of the 25.4 mm long tooth reasonably well (Fig. 5). However, this airfoil profile resulted in a fairly sharp[4] end at the root of the tooth. An arbitrary length extension of 10% (thickness still 7mm) improved fit near the root (Fig. 6). This length extension gave, by Eq. (7), a two digit A value of 11 and the complete profile could be written NACA $\underline{11}525$.[5] The tooth and profile are compared in Fig. 6. Estimated values of y_{max} and x_{max} were 3.2 mm and 14 mm respectively, for the lengthened profile.

The thickness function for airfoils (Eq. 11) was developed from a polynomial relation with five adjustable constants (Jacobs et al. 1933), which were chosen to yield desirable airfoil characteristics (such as nose shape, location of maximum thickness, and trailing-edge angle). At this time representational similarities between shapes of airfoils and teeth may be regarded as fortuitous and the method *ad hoc*. The method of development of the airfoil representation does suggest that perhaps an even better fit to teardrop-shaped biological forms may be obtained by

[4]The airfoil thickness function (Eq. 11) yields 0.10105T at the trailing edge (narrow end) rather than zero as might be expected.

[5]A bar is here introduced under the first two digits to show that they represent one item (ordinate of maximum camber, y_{max}). In particular, this designation should not be confused with the NACA five-digit series.

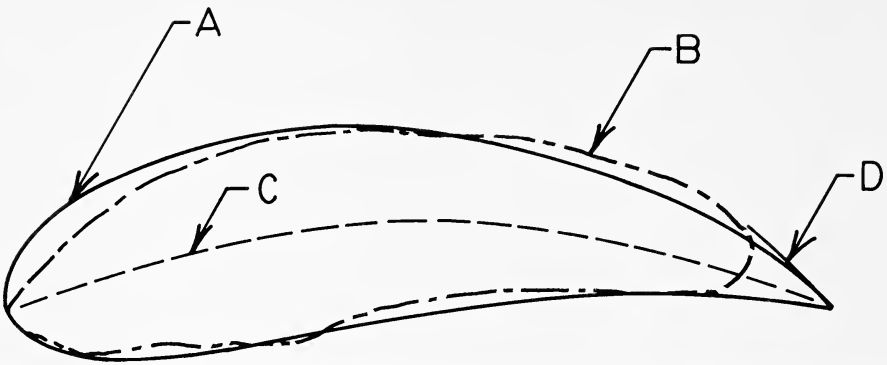

FIGURE 5. Schematic of (A) NACA 9528 profile, (B) tracing of the photograph of a tooth, and (C) mean curvature line.

further adjustment to an appropriate thickness function such as that used by Jacobs et al. (1933) to fit data taken from average biological forms rather than desirable airfoil characteristics.

CONCLUSIONS

The Joukowski transformation shown in Eq. (1) yields a reasonable fit to the shapes of the selected unicuspid teeth. Collection, storage, and manipulation of length, thickness, and curvature angle are all that are required to relate the teeth to the simple geometric shape of a circle from which teardrop shapes similar to the original profiles can be generated. Alternatively, the data representing a given shape may be stored and manipulated as the center coordinates (x_c, y_c) and the radius (or the parameter b) for a circle. Different circles may be used to represent different stages of growth or species. Both distal and buccal aspects of appropriate teeth may be represented.

The approximate solution to the Joukowski transformation is valid only for small values of the parameters x_c/b and β. Significant errors (about 10% for the thicknesses in Figs. 1 and 2) in the thickness and length of the Joukowski profiles were introduced here by using specimens with only marginally small values of x_c/b and β. However, the results are appropriate as an example of the technique. The error introduced by using relatively large values of x_c/b and β rapidly decreases as the sizes of these parameters become smaller.

The alignment of the outlines of the actual teeth for comparison with the derived profiles is somewhat arbitrary, and the graphical extension of the length of the tooth in Fig. 2 in order to measure the curvature parameter β is also arbitrary. Other alignments and changes (one is not restricted to length extensions alone) are possible; however, they should be biologically defensible in some manner. In this case the

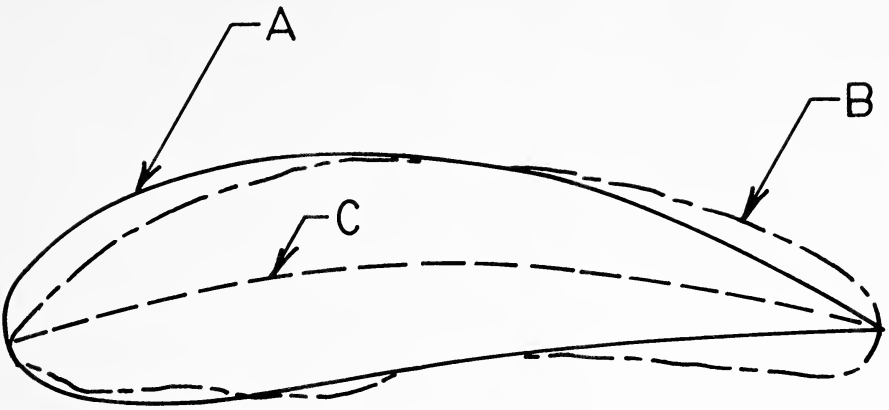

FIGURE 6. Schematics of (A) NACA 11525 profile, (B) tracing of the photograph of a tooth, (C) mean curvature line, and (D) graphical length extension (the bottom portion of the graphical extension coincides with the NACA 11525 profile).

sharper point added to Fig. 2 is somewhat characteristic of certain mature specimens (Taylor 1978). A similar extension would have improved the transformed profile in Fig. 1. The fit of the NACA four-digit profiles in Figs. 5 and 6 to the selected tooth seems to be very good. The profile in each case results from application of Eq. (7) -(11) to the data stored in the digits of the profiles and the length (the extended length in Fig. 6). Storage and manipulation of the profile designated and the length are obviously easier than storage of photographs, models, or several coordinate points to be used in plotting the tooth, and are compatible with modern computational techniques involving electronic computers.

Obvious improvements can be made in the system to improve accuracy and versatility, such as allowing A to be two digits as shown here. A further improvement of the NACA four-digit system useful in aeronautics was the NACA five-digit system, which allowed for improved aerodynamic performance. In this system the mean camber line is either an arc of a cubic parabola and a straight line, or portions of two cubic parabolas (von Mises 1945) and might find applicability to a teardrop shaped biological form with an S-shaped curvature line. Original documents dealing with the NACA five-digit series are studies by Jacobs and Pinkerton (1935) and Jacobs et al. (1937).

This paper deals only with permanent unicuspid teeth. However, premolars and molars may be described as a collection of fused teardrop shapes which can each be described as either a transformed circle or by a NACA 4-digit profile (Taylor 1978). Also human tooth buds develop from a spherical form to the final shape through a series of shapes which may be approximated by transformed circles (Langman 1975). It also might be possible to calculate the NACA series for an

entire developmental sequence of teeth and show how tooth shape changes through time. Also, fossil teeth can be characterized by a NACA four-digit number which could be used as part of the published description of each find. This would enable other investigators to reconstruct outlines of the teeth.

Other biological shapes could also be described by the Joukowski transformation and by NACA 4-digit series. Potentially describable objects include leaves, fish, and wings—any teardrop-shaped object of small thickness-to-length ratio (small x_c/b), small curvature approximating that of a circular arc, and possessing maximum thickness at about 25% of the length, near the rounded end. A possible use for the simpler description of teardrop-shaped biological forms is in taxonomy. Brief descriptions generated by the method discussed here may be easier to deal with than those given in standard taxonomic keys.

The Joukowski transformation and the NACA 4-digit series are two parsimonious descriptive methods that can adequately represent certain teardrop biological shapes such as teeth.

ACKNOWLEDGEMENTS

The authors wish to thank Dr. Ordean J. Oyen for supplying the specimens and for helpful discussions about the manuscript. We are also grateful to Dr. Robert S. Rice and Dr. John T. Demel for helpful comments, and to Mr. John Purcell for photographic work.

LITERATURE CITED

Ashton, E. H., and S. Zuckerman. 1950. Some quantitative dental characteristics of the chimpanzee, gorilla, and orangutan. Phil. Trans. Roy. Soc. (London), Series B. 234:471-484.

Bookstein, F. L. 1977. The study of shape transformation after D'Arcy Thompson. Math. Biosci. 34:177-219.

Jacobs, E. N., and R. M. Pinkerton. 1935. Tests in the variable-density wind tunnel of related airfoils having the maximum camber unusually far forward, p. 521-529. *In* NACA Technical Report 537, 21st Annual Report. Government Printing Office, Washington.

Jacobs, E. N., R. M. Pinkerton, and H. Greenberg. 1937. Tests of related forward camber airfoils in the variable-density wind tunnel, p. 697-731. *In* NACA Technical Report 610, 23rd Annual Reprot. Government Printing Office, Washington.

Jacobs, E. N., K. E. Ward, and R. M. Pinkerton. 1933. The characteristics of 78 related airfoil sections from tests in the variable density wind tunnel, p. 299-354. *In* NACA Technical Report 460, 19th Annual Report. Government Printing Office, Washington.

Von Karman, Th., and J. M. Burgers. 1943. General aerodynamic theory: perfect fluids, p. 1-367. *In* W. F. Durnat (Ed.), Aerodynamic Theory. Verlag Julius Springer, Berlin.

Krogman, W. M. 1969. Growth changes in skull, face, jaws, and teeth of the chimpanzee, p. 104-164. *In* The Chimpanzee, vol. 1. Karger Press, Basel, Switzerland.

Langman, J. 1975. Medical Embryology, 3rd ed. The Williams and Wilkins Co., Baltimore, MD.
Von Mises, R. 1945. Theory of Flight. McGraw Hill, New York, NY.
Piercy, N. A. V. 1937. Aerodynamics. D. van Nostrand, New York, NY.
Pope, A. 1951. Basic Wing and Airfoil Theory. McGraw Hill, New York, NY.
Rauscher, M. 1953. Introduction to Aeronautical Dynamics. John Wiley, New York, NY.
Rosen, R. 1978. Dynamical similarity and the theory of bilogical transfomations. Bull. Math. Biol. 40:549-579.
Taylor, R. M. S. 1978. Variation in Morphology of Teeth: Anthropologic and Forensic Aspects. Charles C. Thomas, Springfield, IL.
Thompson, D. W. 1917. On Growth and Form. Cambridge Unviersity Press, Cambridge, MA.
Zeisz, R. C., and J. Nuckolls. 1949. Dental Anatomy. C. V. Mosby. St. Louis, MO.

CIRCULATING CORTICOSTEROID AND LEUCOCYTE DYNAMICS IN CHANNEL CATFISH DURING NET CONFINEMENT

by J. R. TOMASSO[1], BILL A. SIMCO, *and* KENNETH B. DAVIS

Department of Biology
Memphis State University
Memphis, TN 38152

ABSTRACT

Channel catfish (*Ictalurus punctatus*) were stressed by close confinement in a net for periods up to 24 h. Plasma corticosteroid concentrations increased from 0.8 ± 0.3 μg/100 ml (mean ± S.E.) to a peak of 5.7 ± 0.6 μg/100 ml after 6 h, then declined by 24 h. Leucocrit decreased during the first 6 h, owing to a decline in lymphocyte numbers, then increased by 12 h. Hematocrit did not vary significantly during the 24-h period.

INTRODUCTION

Increases in circulating corticosteroid concentrations have been demonstrated in many species of fishes in response to a variety of stressors (Strange et al. 1977; Leach and Taylor 1980; Tomasso et al. 1981). Corticosteroids (cortisol, cortisone, corticosterone) are released from the interrenal tissue (Wedemeyer 1970). A detrimental effect of increased corticosteroid release is immunosuppression (Grant 1967). One immunosuppressive effect identified in fishes is the corticosteroid-mediated decrease in circulating leucocytes (Weinreb 1958; Pickford et al. 1971; McLeay 1973). This study was conducted to determine the effect of stress-induced elevation of circulating corticosteroids on abundance and types of circulating leucocytes in the channel catfish (*Ictalurus punctatus*).

MATERIALS AND METHODS

Channel catfish were obtained from the Southeastern Fish Cultural Laboratory (Marion, Alabama) and maintained in large indoor recirculating systems (20-22 C) for at least 2 months prior to use. Fish were fed a commercial diet equivalent to approximately 1% of their body wieght per day. Feeding was suspended 48 hours prior to experiments.

Blood was obtained from the caudal peduncle by the use of a heparinized syringe after the fish were anesthetized in a 0.02% solution of

[1]Present address: Department of Biology, Southwest Texas State University, San Marcos, TX 78666.

MS-222. A portion of the blood was then immediately transferred to hematocrit tubes and centrifuged for 5 minutes at 13,000 x *g*. The remaining blood was also centrifuged and the plasma frozen until used for corticosteroid analysis.

Total blood volume and total packed cell volume in the hematocrit tubes were measured with dial calipers (± 0.01 mm) and packed white cells were measured using an ocular micrometer. The hematocrit and leucocrit (McLeay and Gordon 1977) were then determined by dividing the total packed cell volume and packed white cell volume, respectively, by the total blood volume. All measurements were taken within one hour of sampling. Total plasma corticosteriod concentrations were determined by competitive protein binding (Murphy 1967), as modified by Fagerlund (1970) using chicken serum as a transcortin source.

To determine the effect of net confinement on leucocrit and plasma corticosteroid levels, 10 fish (9-15 cm standard length) were netted from the holding system and immediately bled. Thirty more fish were then captured and confined in a dip net suspended in the tank in a way that allowed the fish to be underwater but severely crowded. Some of the confined fish were then bled after 6, 12, and 24 hours of confinement. The initial sampling (time 0) and the sampling after 6 hours of confinement were repeated three times and, the replicate data from each bleeding time being similar, were pooled for further analysis. In all cases, each fish was sampled only once.

To determine changes, if any, in types of circulating leucocytes during the confinement, three fish (30-40 cm standard length) were captured and immediately bled. Each was fin clipped for further identification, and confined in a net suspended in the holding tank as previously described. After 6 and 12 hours each fish was bled again. Following each bleeding, blood smears were made, stained, and relative numbers of cell types determined.

One-way analysis of variance followed by Duncan's multiple range test was used to compare changes in leucocrits, hematocrits, and corticosteroids during the course of the experiment. A probability level of $\leq$ 0.05 was considered significant.

RESULTS AND DISCUSSION

Plasma corticosteroid concentrations increased from baseline levels (0.8 ± 0.3 μg/100 ml, mean ± S.E.) to a peak of 5.7 ± 0.6 μg/100 ml after 6 hours of confinement (Fig. 1). A slight decrease in plasma corticosteroid levels was apparent after 24 hours although the animals were still confined. This decrease, while fish are sill confined, has been observed in channel catfish elsewhere (Davis and Parker, unpublished data) and in chinook salmon (Strange and Schreck 1978) and may

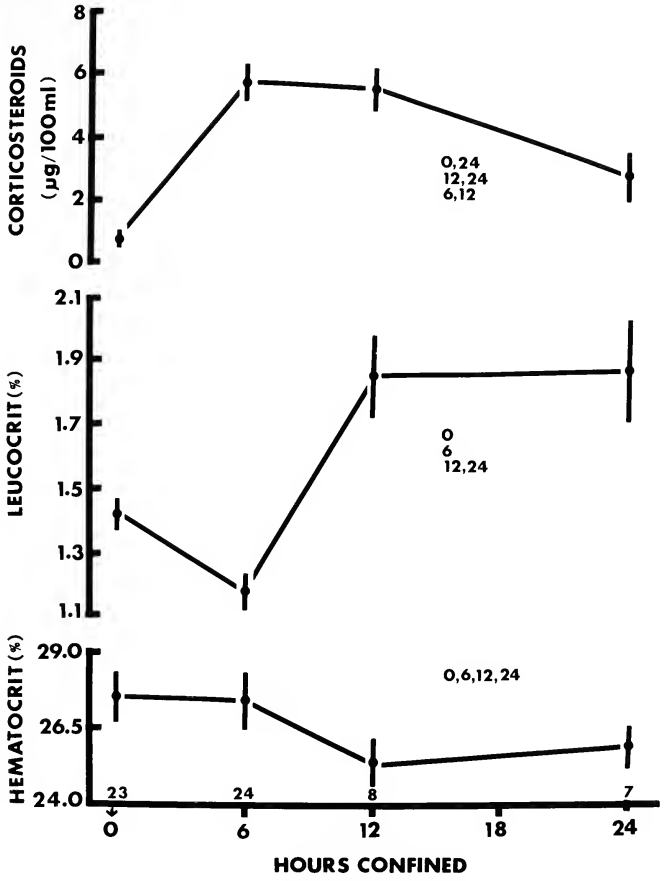

FIGURE 1. Leucocrit, hematocrit and plasma corticosteroid dynamics in channel catfish confined in a net for up to 24 hours. Dots with vertical lines represent mean ± S.E. Numbers of fish measured are given directly above the x-axis. Sampling periods with statistically similar means share a common line.

represent the beginning of adaptation to the stressor (Selye 1950). Boehlke et al. (1966) reported higher resting corticosteroid concentrations in channel catfish (about 10 µg/100 ml) than reported here and elsewhere (Strange 1980). It has been suggested that this discrepancy may be due to the use of fluorimetric assay by Boehlke and his coworkers in contrast to the competitive protein binding assay (Strange 1980).

Leucocrits decreased significantly from baseline levels (1.42 ±0.05) during the first 6 hours of confinement, but by 12 hours of confinement leucocrits were significantly higher than baseline levels (Fig. 1). An increase in the leucocrit of eels during social stress was explained by changes in the ratio of lymphocytes to granulocytes (Peters et al.

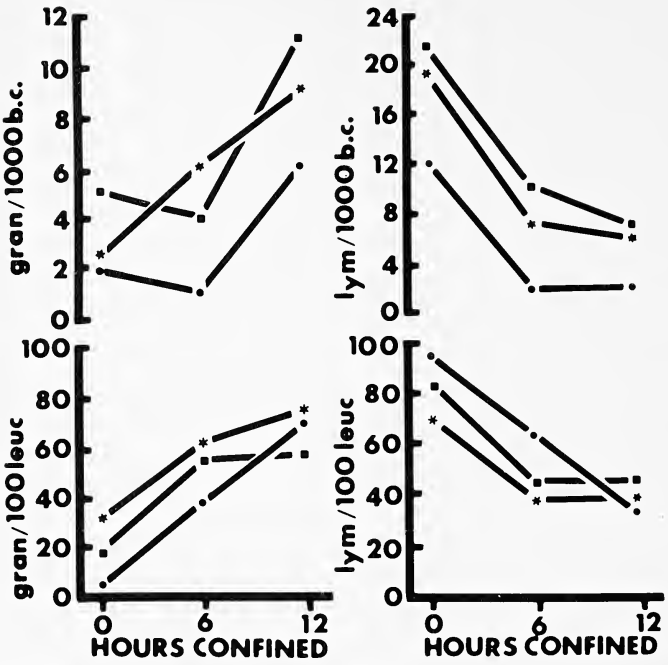

FIGURE 2. Circulating leucocyte dynamics in three channel catfish serially sampled during 12 hours of net confinement. Each individual fish is represented by an asterisk, dot or square (gran = granulocytes, lym = lymphocytes, leu = leucocytes, b. c. = total blood cells).

1980). While the total white cell count of the eel decreased due to a decreased number of circulating lymphocytes, the number of granulocytes actually increased. The increase in number of the larger granulocytes was apparently more than enough, in terms of volume, to offset the decrease in the small lymphocytes, resulting in an increased leucocrit. Similar decreases in lymphocyte counts and increases in granulocyte counts have been described in largemouth bass (Esch and Hazen 1980) and coho salmon (McLeay 1973). However, it should be noted that while granulocyte counts increased in response to stress, numbers of circulating granulocytes are not corticosteriod mediated (Dougherty and White 1944).

The decrease in leucocrit observed after 6 hours of confinement in a net may be attributed to different temporal responses of lymphocytes and granulocytes to stress. Figure 2 shows the relationship of circulating lymphocytes and granulocytes to confinement time. In all three fish examined, lymphocytes/100 cells had decreased after 6 hours of confinement. Granulocytes/1000 cells increased, but not substantially, until after 12 hours of confinement. The decreased leucocrit after 6 hours of confinement corresponds to the time when lymphocyte counts

are decreased and granulocyte counts are unchanged. Fin clipping and serial bleeding placed additional stress on these animals. However, the increase in numbers of circulating granulocytes would indicate that measured changes in numbers of leucocytes are due to actual changes in leucocyte number and not to serial removal of blood. The absence of a stress effect on hematocrit indicates that changes in leucocyte number were due solely to changes in absolute leucocyte number and not changes in the red to white cell ratio.

ACKNOWLEDGEMENTS

We thank B. Tabatabai for technical advice and assistance. Fish were supplied by the Southeastern Fish Cultural Laboratory, Marion, Alabama. Master-Mix Fish Grower No. 971 was provided by Central Soya Company, Fort Wayne, Indiana.

LITERATURE CITED

Boehlke, K. W., R. L. Church, O. W. Tiemeier and B. E. Eleftheriou. 1966. Diurnal rhythm in plasma glucocorticoid levels in channel catfish (*Ictalurus punctatus*). Gen. Comp. Endocrinol. 7:18-21.

Dougherty, T. F. and A. White. 1944. Influence of hormones on lymphoid tissue structure and function. The role of pituitary adrenotrophic hormone in the regulation of the lymphocytes and other cellular elements of the blood. Endocrinology 35:1-14.

Esch, G. W., and T. C. Hazen. 1980. Stress and body condition in a population of largemouth bass: implications for red-sore disease. Trans. Amer. Fish. Soc. 109:532-536.

Fagerlund, U. H. M. 1970. Determining cortisol and cortisone simultaneously in salmonid plasma by competive protein binding. J. Fish. Res. Bd. Can. 27:596-601.

Grant, N. 1967. Metabolic effects of adrenal glucocorticoid hormones, p 269-292. *In* A. B. Eisenstein (ed.), The Adrenal Cortex. Little, Brown and Company, Boston, MA.

Leach, G. J., and M. H. Taylor. 1980. The role of cortisol in stress-induced metabolic changes in *Fundulus heteroclitus*. Gen. Comp. Encocrinol. 42:219-227.

McLeay, D. J. 1973. Effects of ACTH on the pituitary-interrenal axis and abundance of white blood cell types in juvenile coho salmon, *Oncorhynchus kisutch*. Gen. Comp. Endocrinol. 21:431-440.

McLeay, D. J. and M. R. Gordon. 1977. Leucocrit: a simple hematological technique for measuring acute stress in salmonid fish, including stressful concentrations of pulp-mill effluent. J. Fish. Res. Bd. Can. 34:2164-2175.

Murphy, B. E. P. 1967. Some studies of the protein binding of steroids and their application to the routine micro and ultramicro measurements of various steroids in body fluids by competitive protein binding radioassay. J. Clin. Endocrinol. 27:973-990.

Peters, G., H. Delventhal and H. Klinger. 1980. Physiological and morphological effects of social stress in the eel (*Anguilla anguilla* L.). Arch. Fischwiss. 30:157-180.

Pickford, G. E., A. K. Srivastava, A. M. Slicher and P. K. T. Pang. 1971. The stress response in the abundance of circulating leucocytes in the killifish, *Fundulus heteroclitus*. III. The role of the adrenal cortex and a concluding discussion of the leucocyte-stress syndrome. J. Exp. Zool. 177:109-118.

Selye, H. 1950. Stress and the general adaptation syndrome. Brit. Med. J. 1:1383-1392.

Strange, R. J. 1980. Acclimation temperature influences cortisol and glucose concentrations in stressed channel catfish. Trans. Amer. Fish. Soc. 109:298-303.

Strange, R. J. and C. B. Schreck. 1978. Anesthetic and handling stress on survival and cortisol concentration in yearling chinook salmon (*Oncorhynchus tshawytscha*). J. Fish. Res. Bd. Can. 35:345-349.

Strange, R. J., C. B. Schreck and J. T. Golden. 1977. Corticoid stress responses to handling and temperature in salmonids. Trans. Amer. Fish. Soc. 106:213-218.

Tomasso, J. R., K. B. Davis and B. A. Simco. 1981. Plasma corticosteroid dynamics in channel catfish (*Ictalurus punctatus*) exposed to ammonia and nitrite. Can. J. Fish. Aquat. Sci. 38:1106-1112.

Wedemeyer, G. 1970. The role of stress in the disease resistance of fishes, p. 30-35. *In* S. F. Snieszko (ed.), A Symposium on Diseases of Fishes and Shellfishes. The American Fisheries Society, Washington, D. C.

Weinreb, E. L. 1958. Studies on the histology and histopathology of the rainbow trout, *Salmo gairdneri irideus*. I. Hematology: under normal and experimental conditions of inflammations. Zoologica 43:145-153.

COMPARATIVE DIGESTIVE EFFICIENCY OF WHITE-TAILED AND SIKA DEER

by CHRISTOPHER WHEATON[1]
and ROBERT D. BROWN

Caesar Kleberg Wildlife Research Institute
Texas A&I University
Kingsville, TX 78363

ABSTRACT

The digestive efficiencies of white-tailed and sika deer were compared on a standard pelleted diet. Four deer of each species were housed in individual digestion crates for 14 days. Digestion coefficients for dry matter, crude protein, crude fiber, ether extract, nitrogen free extract, and digestible energy were determined, and total digestible nutrients calculated. There was no significant difference ($P > .05$) between the two species in any of the parameters. The greater survivability of sika deer over white-tailed deer on marginal lands is due to factors other than their abilities to better utilize a standard feed.

INTRODUCTION

The hunting of exotic game on private ranches is a popular sport in Texas. One of these exotic animals, the sika deer (*Cervus nippon*), is particularly hardy. The most recent Texas census counted 6,217 sika deer enclosed in game ranches in 49 counties, for an overall increase of 104% over the previous census 6 years earlier (Harmel 1980). Neither census included free ranging animals which may have escaped from game ranches.

State biologists are concerned that sika deer and other exotic animals escaping from game ranches may proliferate and compete with native deer. In 1971, 6 sika deer and 6 white-tailed deer (*Odocoileus virginianus*) were introduced into a 39 ha pasture at the Kerr Wildlife Management Area in order to evaluate competition between the species. The sika population increased steadily to a total of 62 animals in 9 years while the white-tailed population increased slightly, then completed died out, largely due to starvation (Armstrong and Harmel 1981). Sika deer apparently compete directly with the white-tails for browse and forbs. The sika, however, seems to have a greater ability to shift its diet to grasses when stressed by drought or overgrazing (Butts 1979).

The greater survivability of sika deer may have been related to more opportunistic feeding patterns or to species differences in forage digestion and nutrient retention. Preliminary to a study of the relationships

[1]Present address: Texas Parks & Wildlife Department, 1904 Sixth Ave., Canyon, TX 79015.

between forage utilization and survivability, this experiment was conducted to determine if sika deer and white-tailed deer differ in their ability to digest a high-quality formulated ration.

METHODS

Research was conducted at the Texas A&I University Wildlife Research Facility, near Kingsville, Texas. Four white-tailed fawns and 4 sika fawns were captured in the South Texas area during the spring and summer of 1978. The deer were bottle fed on goat's milk, with various pelleted and green feeds offered as available to facilitate weaning. Fawns were weaned at approximately 4 months of age and were subsequently fed a custom mixed pelleted ration for an additional 4 months prior to the digestibility studies. The ration averaged 21.2% crude protein and 15.9% crude fiber. Its major ingredients were dried brewer's grains, alfalfa meal, and ground corn. The ration was formulated to provide adequate or superior levels of all nutritents required for the growth and development of young white-tailed deer (French et al. 1955; French et al. 1956; McEwen et al. 1957; Ullrey et al. 1967; Smith et al. 1975).

The comparative digestibility of the ration by the 2 species of deer was determined by digestion trials designed according to procedures outlined by Ullrey et al. (1975), Mothershead et al. (1972), and Smith et al. (1975). The metabolism crates used in the experiment were similar to those designed by Cowan et al. (1969) as modified by Ullrey (pers. comm.). Animals were habituated to the crates for 7 days. A 7 day fecal collection period followed, during which each animal was fed at 90% of its adjustment period *ad libitum* consumption. The intakes of all 8 animals during the digestion trails were similar.

Total fecal collections for each animal were made every 24-28 hours and frozen until the trial was complete. Upon completion of the trial, collections from each animal were thoroughly mixed, and duplicate sub-samples were removed, labeled, and frozen until laboratory analysis. Feed and fecal samples were dried at 40C and ground in a Wiley mill with a 1 mm screen and analyzed in duplicate via proximate analysis (AOAC 1980) and bomb calorimetry (Parr Instrument Co. 1975). Duplicate analyses of all duplicate subsamples were averaged. Digestion coefficients for dry matter (DM), crude protein (CP), crude fiber (CF), ether extract (EE) and nitrogen free extract (NFE) were determined and total digestible nutrients (TDN) calculated. Gross energy (GE) for each feed and fecal sample was determined, and the digestible energy (DE) was calculated. The mean % digestibility of the components of the ration were compared by t-test (Steel and Torrie 1960).

TABLE 1. Digestibility of a pelleted ration by 4 sika and 4 white-tailed deer.[a]

	Percent Digestibility													
	Dry Matter	SD	Crude Protein	SD	Crude Fiber	SD	Ether Extract	SD	Nitrogen Free Extract	SD	Total Digestible Nutrients (%)	SD	Digestible Energy (Kcal/g)	SD
White-tailed	57.0	2.6	68.86	5.02	30.38	3.0	72.15	9.71	71.55	2.72	55.20	2.19	2.618	0.252
Sika	54.7	10.0	66.95	6.33	35.21	15.2	77.37	5.76	64.55	11.6	57.56	8.54	2.578	0.326

[a]Custom mixed pellet (21.2% C.P.) by P&M Products, San Antonio.

RESULTS

The digestibility of the DM and its components, CP, CF, EE and NFE, were not significantly different ($P>.05$) between the 2 species of deer (Table 1). The total digestible nutrients (TND) and the DE were also not significantly different ($P>.05$) between the 2 species. The relatively large standard deviations of the sika digestibility results were due to low values of one animal. Recalculation of the means exluding this animal still resulted in no significant differences between the groups of deer. One must be cautious in interpreting these results due to the relatively small number of animals involved and the relative high quality of the ration offered. Nevertheless, it is concluded that the greater survivability of the sika deer over white-tailed deer on limited rangeland is not due to superior digestive efficiency.

While the ability of the sika deer to digest natural browse and forbs better than the white-tailed deer cannot yet be ruled out, the sika's superiority may be due to its more opportunistic feeding patterns, natural aggression (A.B. Bubenik, pers. comm.) or some other factor.

LITERATURE CITED

AOAC. 1980. Official Methods of Analysis, 12th ed. Assn. Official Analytical Chemists, Washington, D. C.

Armstrong, W. E. and D. E. Harmel. 1981. Exotic mammals competing with the natives. Texas Parks and Wildl. Magazine. February. p. 6-7.

Butts, G. L. 1979. The status of exotic big game in Texas. Rangelands 1:152-153.

Cowan, R. L., W. E. Hartsook, J. B. Whelan, T. A. Long, and R. S. Wetzel. 1969. A cage for metabolism and radioisotope studies with deer. J. Wildl. Manage. 33:204-208.

French, C. E., L. C. McEwen, N. D. Magruder, R. H. Ingram, and R. W. Swift. 1955. Nutritional requirements of white-tailed deer for growth and antler development. Pa. Agric. Exp. Stn. Bull., (600) 8 p.

French, C. E., L. C. McEwen, N. D. Magruder, R. H. Ingram, and R. W. Swift. 1956. Nutrient requirements for growth and antler development in the white-tailed deer. J. Wildl. Manage. 20:221-232.

Harmel, D. E. 1980. Statewide census of exotic big game animals. Job Peroformance Report (21) 33 p.

McEwen, L. C., E. E. French, N. D. Magruder, R. W. Swift, and R. H. Ingram. 1957. Nutrient requirements of the white-tailed deer. Trans. North Am. Wildl. Nat. Resour. Conf. 22:119-130.

Mothershead, C. L., R. L. Cowan, and A. L. Amman. 1972. Variations in determinations of digestive capacity of the white-tailed deer. J. Wildl. Manage. 36:1052-1060.

Parr Instument Co. 1975. Instructions for the 1241 and 1242 adiabatic calorimeters. Parr Manual No. 153. Parr Insturment Co., Moline, Illinois.

Smith, S. H., J. B. Holter, H. H. Hayes, and H. Silver. 1975. Protein requirement of white-tailed deer fawns. J. Wildl. Manage. 39:582-589.

Steel, R. G. D. and J. H. Torrie. 1960. Principles and Procedures of Statistics. McGraw-Hill, N. Y. 481 p.

Ullrey, D. E., W. G. Youatt, H. E. Johnson, L. D. Fay, and B. L. Bradley. 1967. Protein requirement of white-tailed deer fawns. J. Wild. Manage. 31:679-685.

Ullrey, D. E., W. G. Youatt, H. E. Johnson, L. D. Fay, R. L. Covert, and W. T. Magee. 1975. Consumption of artificial browse supplements by penned white-tailed deer. J. Wildl. Manage. 39:699-704.

SUMMER DIET OF FINFISH FROM NEARSHORE HABITATS OF WEST BAY, TEXAS

by STEVE K. ALEXANDER

Department of Marine Biology
Texas A&M University at Galveston
Galveston, TX 77553

INTRODUCTION

The finfish community of the Galveston Bay stystem of Texas has been characterized in studies by Reid (1955), Chin (1961) and Parker (1965). However, little information is available on the diet and trophic position of individual species in this estuarine system. Diener et al. (1974) examined the stomach contents of finfish collected by otter trawl from Clear Lake, a small bay on the northwestern edge of the Galveston Bay system. Although 40 species were examined, shallow water (nearshore) species were not adequately represented. The present study examined the diet and trophic position of predominant finfish from nearshore habitats of West Bay, a bay on the southwestern edge of the Galveston Bay system.

MATERIALS AND METHODS

During June and July 1981, shorelines of West Bay were sampled biweekly with a 7-m long bag seine (3-mm mesh bag). The net was pulled parallel to the *Spartina alterniflora* dominated shorelines at water depths of 0.3 to 1.0 m. A cast net (10-mm mesh) was also used to catch larger, more motile shoreline species. A representative number of predominant species was transferred from the net to a plastic bag and stored on ice for transport to the laboratory. Fish were frozen until analysis, which usually occurred within several weeks of collection. The stomach was removed from specimens and opened lengthwise. The contents were placed in a petri dish and identified with the aid of a stereomicroscope.

RESULTS AND DISCUSSION

The most abundant finfish in these catches were juveniles of *Cyprinodon variegatus* (sheepshead minnow), *Fundulus grandis* (gulf killifish), *Menidia peninsulae* (tidewater silverside), *Lagodon rhomboides* (pinfish), *Leiostomus xanthurus* (spot) and *Mugil cephalus* (striped

The Texas Journal of Science, Vol. XXXV, No. 1, March 1983

TABLE 1. Percentage of stomachs containing various food items. Based only on those stomachs which contained food.

	Cyprinodon variegatus	*Fundulus grandis*	*Menidia peninsulae*	*Lagodon rhomboides*	*Leiostomus xanthurus*	*Mugil cephalus*
Stomachs examined which contained food	114	73	50	102	75	37
Total length range (mm)	25-46	35-96	50-72	54-96	42-96	69-199
Food Items						
Sand	96	4	0	31	100	100
Vascular Plant	89	57	16	59	40	100
Microalgae	99	27	100	95	100	97
Meiobenthos[a]	7	20	6	84	100	19
Macrobenthos[b]	0	14	26	17	11	0
Invertebrate larvae[c]	0	0	94	0	0	0
Calanoid copepods	0	0	30	0	0	0
Small fish/crustaceans	0	99	10	9	0	0
Insects	0	3	16	2	0	0

[a]Harpacticoid copepods, nematodes, ostracods, foraminifera, and mysids.
[b]Polychaetes and small molluscs.
[c]Predominantly crab zoea.

mullet). The diet of these six species based on stomach analysis is presented in Table 1.

Cyprinodon variegatus and *Mugil cephalus* were bottom feeding herbivores in West Bay; their diet consisted almost exclusively of sand, vascular plant material and microalgae. Similar results were obtained by Odum (1970) for *M. cephalus* in a Georgia salt marsh and by Odum and Heald (1972) for *C. variegatus* in a Florida mangrove estuary.

Small fish and crustaceans were frequent in the diet of *Fundulus grandis*. This species also consumed with less regularity vascular plant material, microalgae and small benthic animals. Odum and Heald (1975) classified *F. grandis* as a low level carnivore in a Florida mangrove estuary.

Menidia peninsulae appears to have the most varied feeding habit of the six species examined. Analysis of stomach contents indicates both a planktonic diet of invertebrate larvae and copepods and a benthic diet principally of microalgae. Two feeding niches for this species, therefore, are suggested: 1) a low level carnivore in the water column, and 2) a herbivore on the bottom. Odum and Heald (1972) likewise reported that *M. peninsulae* occupies several niches in a Florida mangrove estuary, feeding in the water column during the day and near the bottom at night.

Lagodon rhomboides and *Leiostomus xanthurus* were bottom feeders with an omnivorous diet typically of sand, vascular plant material, microalgae and meiobenthos. Specimens of these species from Clear Lake, Texas, consumed small benthic animals, organic detritus and

sand (Diener et al. 1974). A review of available literature led Parker (1971) to conclude that *L. xanthurus* is a non-selective feeder whose diet reflects the availability of bottom food.

LITERATURE CITED

Chin, E. 1961. A trawl study of an estuarine nursery area in Galveston Bay, with particular reference to penaeid shrimp. Ph. D. Dissertation, University of Washington, Seattle. 123 p.

Diener, R. A., A. Inglis, and G. B. Adams. 1974. Stomach contents of fishes from Clear Lake and tributary waters, a Texas estuarine area. Contrib. Mar. Sci. 18:7-17.

Odum, W. E. 1970. Utilization of the direct grazing and plant detritus food chains by the striped mullet *Mugil cephalus*, p. 222-240. *In* J. Steele (ed.), Marine Food Chains. University of California Press, Berkeley.

Odum, W. E., and E. J. Heald. 1972. Trophic analysis of an estuarine mangrove community. Bull. Mar. Sci. 22:671-738.

Odum, W. E., and E. J. Heald. 1975. The detritus-based food web of an estuarine mangrove community, p. 265-286. *In* L. Cronin (ed.), Estuarine Research, Volume 1. Academic Press, New York.

Parker, J. C. 1965. An annotated checklist of the fishes of the Galveston Bay System, Texas. Publ. Inst. Mar. Sci. 10:201-220.

Parker, J. C. 1971. The biology of the spot, *Leiostomus xanthurus* Lacepede, and Atlantic croaker, *Micropogon undulatus* (Linnaeus), in two Gulf of Mexico nursery areas. Texas A&M University Sea Grant Publ. No. TAMU-SG-71-210.

Reid, G. K., Jr. 1955. A summer study of the biology and ecology of East Bay, Texas. Part I. Introduction, description of area, methods, some aspects of the fish community, and invertebrate fauna. Texas J. Sci. 7:316-343.

OFFICERS

President:	Bernard T. Young, Angelo State University
President-Elect:	Michael Carlo, Angelo State University
Vice-President:	William J. Clark, Texas A&M University
Immediate Past President:	Elray S. Nixon, Stephen F. Austin State University
Secretary-Treasurer:	Everett D. Wilson, Sam Houston State University
Editor:	William H. Neill, Texas A&M University
AAAS Council Representative:	Arthur E. Hughes, Sam Houston State University

DIRECTORS

1981	Richard L. Noble, Texas A&M University
	Bob F. Perkins, University of Texas, Arlington
1982	Billy J. Franklin, Texas A&I University
	Ethel W. McLemore, Dallas
1983	D. Lane Hartsock, Austin
	Katherine Mays, Bay City

SECTIONS

I—*Mathematical Sciences*: Philip S. Morey, Jr., Texas A&I University
II—*Physical Sciences*: R. Charles Ivey, La Jet Corporation, Abilene
III—*Earth Sciences*: S. Christopher Caran, University of Texas, Austin
IV—*Biological Sciences*: Frank W. Judd, Pan American University
V—*Social Sciences*: Rollo K. Newsom, Southwest Texas State University
VI—*Environmental Sciences*: D. Lane Hartsock, Texas Air Control Board
VII—*Chemistry*: John T. Moore, Stephen F. Austin State University
VIII—*Science Education*: Rebecca Sparks, San Marcos
IX—*Computer Sciences*: Charles N. Adams, North Texas State University
X—*Aquatic Sciences*: G. Dan McClung, SK Engineering, San Angelo

Collegiate Academy Counselors: Shirley Handler, East Texas Baptist College
Helen Oujesky, University of Texas, San Antonio
Junior Academy Counselors: Ruth Spear, San Marcos
Peggy Carnahan, San Antonio

COVER PHOTO

Coordinate System of the Heart
for a Mitral Valve Model

by Hunter, Seaton, Lively,
Miller and Stoner, pp. 5-36

2nd CLASS POSTAGE
PAID AT HUNTSVILLE
TEXAS 77341
AND AT ADDITIONAL
MAILING OFFICE
AT LUBBOCK
TEXAS 79401

Volume XXXV, Number 2 July 1983

THE TEXAS JOURNAL OF SCIENCE

PUBLISHED QUARTERLY BY
THE TEXAS ACADEMY OF SCIENCE

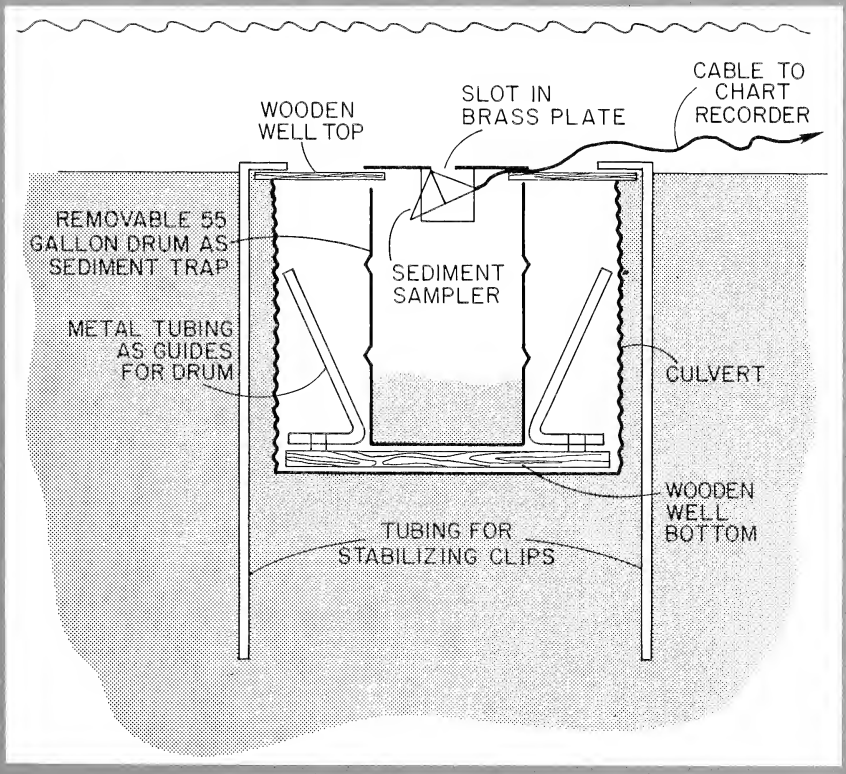

AFFILIATED ORGANIZATIONS
Texas Section, American Association of Physics Teachers
Texas Section, Mathematical Association of America
Texas Section, National Association of Geology Teachers

GENERAL INFORMATION

MEMBERSHIP. Any person or group engaged in scientific work or interested in the promotion of science is eligible for membership in The Texas Academy of Science. Dues for members are $20.00 annually; student members, $12.00 annually; sustaining members, at least $30.00 in addition to annual dues; life members, at least $400.00 in one payment; patrons, at least $500.00 in one payment; corporate members, $250.00 annually; corporate life members, $2000.00 in one payment. Library subscription rate is $45.00 annually. Payments should be sent to the Secretary-Treasurer, Box 2175, Huntsville, TX 77341.

The *Journal* is a quarterly publication of The Texas Academy of Science and is sent to all members and subscribers. Inquiries regarding back issues should be sent to Dr. Fred S. Hendricks, Dept. Wildlife & Fisheries Sciences, Texas A&M University, College Station, TX 77843.

Manuscripts submitted for publication in the *Journal* should be sent to Dr. W. H. Neill, Dept. Wildlife & Fisheries Sci., Texas A&M Univ., College Station, TX 77843.

The Texas Journal of Science (USPS 616740) is published quarterly at Huntsville, Texas U.S.A. Second class postage paid at Post Office, Huntsville, TX 77341, and at additional mailing office at Lubbock, TX 79401. Please send form 3579 and returned copies to Texas Tech Press, Box 4240, Lubbock, TX 79409.

THE TEXAS JOURNAL OF SCIENCE

Volume XXXV, No. 2 July 1983

CONTENTS

NOTE: Authors with funds for page contributions are expected to make such payments. The contribution of $35.00 per page is encouraged to defray printing costs, and authors of articles exceeding ten printed pages are expected to make *some* contribution to the publication fund. However, payment of printing costs is not a condition for publication in The Texas Journal of Science, and NO AUTHOR, WHO WOULD OTHERWISE SUBMIT A MANUSCRIPT, SHOULD HESITATE TO DO SO BECAUSE OF LACK OF SUCH FUNDS. Members without funds may apply to the Texas Academy of Science for a grant to cover some or all costs of publication. This becomes effective January 23, 1982.

INSTRUCTIONS TO AUTHORS

Papers intended for publication in *The Texas Journal of Science* are to be submitted to Dr. William H. Neill, Dept. Wildlife & Fisheries Sciences, Texas A&M University, College Station, TX 77843.

The manuscript is not to have been published elsewhere. Triplicate typewritten copies (the original and 2 reproduced copies) *must* be submitted. Typing of both text and references should be *double-spaced* with 2-3 cm margins on *standard* 8½ X 11-inch typing paper. The title of the article should be followed by the name and business or institutional address of the author(s). *Be sure to include zip code* with the address. If the paper has been presented at a meeting, a footnote giving the name of the society, date, and occasion should be included but should not be numbered. Include a brief ABSTRACT at the beginning of the text (abstracting services pick this up directly) followed by an INTRODUCTION (understandable to any scientist) and then whatever paragraph headings are desired. The usual editorial customs, as exemplified in the most recent issue of the *Journal*, are to be followed as closely as possible.

In the text, cite all references by author and date *in chronological order*, i.e., Jones (1971); Jones (1971, 1972); (Jones 1971); (Jones 1971, 1972); Jones and Smith (1971); (Jones and Smith 1971); (Jones 1971; Smith 1972; Beacon 1973). If there are more than 2 authors, use: Jones et al. (1971); (Jones et al. 1971). References are then to be assembled, arranged ALPHABETICALLY, and placed at the end of the article under the heading LITERATURE CITED. For a PERIODICAL ARTICLE use: Jones, A. P., and R. J. Wilson. 1971. Effects of chlorinated hydrocarbons. J. Comp. Chem. 37:116-123. For a PAPER PRESENTED at a symposium, etc., use the form: Jones, A. P. 1971. Effects of chlorinated hydrocarbons. WMO Symposium on Organic Chemistry, New York, N.Y. For a PRINTED PAPER use: Jones, A. P. 1971. Effects of chlorinated hydrocarbons. Univ. of Tex., Dallas. *or* Jones, A. P. 1971. Effects of chlorinated hydrocarbons. Univ. of Tex. Paper No. 14, 46 p. A MASTERS OR Ph.D. THESIS should appear as: Jones, A. P. 1971. Effects of chlorinated hydrocarbons. M.S. Thesis, Tex. A&M Univ., College Station. For a BOOK, NO EDITORS, use: Jones, A. P. 1971. Effects of chlorinated hydrocarbons. Academic Press, New York, N.Y., 439 p. For a CHAPTER IN A BOOK WITH EDITORS: Jones, A. P. 1971. Structure of chlorinated hydrocarbons, p. 13-39. *In* A. P. Jones, B. R. Smith, Jr. and T. S. Gibbs (Eds.), Effects of chlorinated hydrocarbons. Academic Press, New York, N.Y. For a BOOK WITH EDITORS: Jones, A. P. 1971. Effects of chlorinated hydrocarbons. J. Doe (Ed.). Academic Press, New York, N.Y., p. 3-12. For an IN PRESS PERIODICAL reference, use: Jones, A. P. In Press. Effects of chlorinated hydrocarbons. J. Org. Chem. For an IN PRESS BOOK reference, use: Jones,

A. P. In Press. Effects of chlorinated hydrocarbons. Academic Press, New York, N.Y. References *must* include article title and page numbers.

References such as unpublished data or personal communications should not be listed in the LITERATURE CITED section. However, within the text they should be presented as: (unpubl. data from C. J. Jones, Dept. Zoology, Univ. Texas, Austin) *or* (pers. comm. from R. C. Smith, P.O. Box 133, Mexia, TX).

All tables are to be typed with a carbon ribbon, free of error, without handwritten notations, and ready for photographic reproduction. Tables should be placed on separate sheets with a marginal notation on the manuscript to indicate preferred locations. Tables must have a text reference, i.e., Table 2 shows...*or* (Table 2).

Figures are to be *original inked drawings* or *glossy photographs no larger* than 6½ X 4½ inches and mounted on standard 8½ X 11-inch paper. Legends for figures are to be typed separately. Figures must have a text reference, i.e., Figure 3 illustrates...*or* (Fig. 3).

All photographs, line drawings, and tables are to be provided with self-explanatory titles or legends. Each illustration should be marked on the back with the name of the principle author, the figure number, and the title of the manuscript of which it is a part.

Authors will receive galley proofs plus the original typescript along with information concerning reprints and page charges. Proofs must be corrected (using ink) and returned to the Editor within 3 days. Payment (check or purchase voucher) for page charges (or the publication grant request) must accompany the return of the corrected proofs or a delay in the printing of the manuscript could occur. Reprint orders should be returned directly to Texas Tech Press, Box 4240, Lubbock, TX 79409

NOTICE: IF YOUR ADDRESS OR TELEPHONE NUMBER CHANGES, NOTIFY US IMMEDIATELY SO WE CAN SEND YOUR GALLEY PROOFS TO YOU WITHOUT LOSS OR DELAY.

OBSERVATION OF EPISODIC SEDIMENTATION IN A TIDAL INLET (SABINE PASS, TEXAS AND LOUISIANA)

by GEORGE H. WARD, JR.

Espey, Huston & Associates, Inc.
P.O. Box 519
Austin, TX 78767

ABSTRACT

Time variation in sedimentation was monitored with a recording tipping-bucket sampler in Sabine Pass, the inlet connecting Sabine Lake (on the Texas-Louisiana boundary) and the Gulf of Mexico. Observed sedimentation was episodic, characterized by events widely spaced in time. There was no apparent relation to astronomical tide, even at maximum declination. Rather, sedimentation seemed to be dictated by hydrometeorological factors. The most intense sedimentation episode of the study period (October and November 1978) was associated with the most energetic frontal passage.

INTRODUCTION

For purposes of assessing gross sedimentation in a coastal or marine zone, the most common method of routine measurement is the construction of a sediment trap which yields a long-term rate of sediment accumulation. However, sediment transport is not a constant process, but highly time variable and probably episodic, being dictated by such transient factors as tidal phase, wave climate, and the hydrometeorological regime. In order to examine the detailed time behavior of sedimentation within a coastal inlet, field measurements were performed employing a recording "bedload" sampler within a trap.

The site of this study was the upper segment of Sabine Pass, the inlet connecting Sabine Lake with the Gulf of Mexico (Fig. 1). Sabine Lake is a broad, shallow embayment on the Texas-Louisiana coast which communicates with the Gulf only through the narrow inlet of Sabine Pass. Like most of the Gulf bays, the principal hydrographic controls on Sabine Lake are tides, meteorological events, freshwater inflows and salinity-induced density currents (Ward 1980a). Because of its large surface-area-to-volume ratio and the extended overwater fetch, Sabine Lake is highly responsive to meteorological forcing. The most dramatic routine meteorological effect is denivillation, the tilting of the water surface by imposed windstress. As the Gulf of Mexico exhibits a smiliar response to wind, relatively large head gradients can develop from bay to Gulf, entailing significant flows in Sabine Pass. The occurrence of

The Texas Journal of Science, Vol. XXXV, No. 2, July 1983

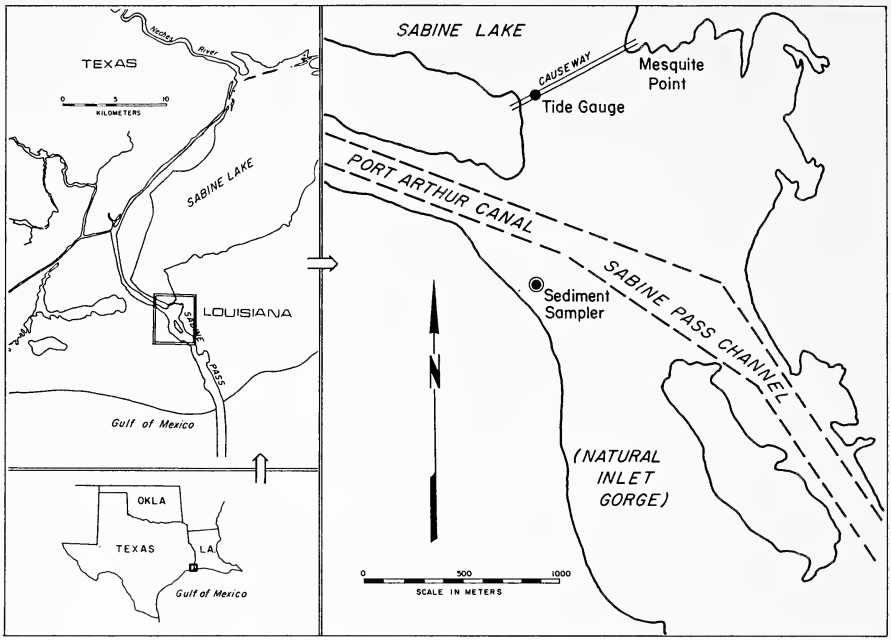

FIGURE 1. Study area: Upper Sabine Pass.

wind setup and setdown (elevation and depression of bay levels owing to wind stress) is usually precipitated, not so much by strong wind *per se*, as by a change in wind, notably that accompanying a frontal passage (Ward 1980b).

The study site, Upper Sabine Pass, is a hydrodynamically complex region of the inlet, a zone of confluence and difluence of flow, where the natural tidal gorge intersects the present dredged Sabine Pass Channel. Hydrographic studies have indicated that all of the channels and passes offering access to Upper Sabine Pass participate in the circulation in this reach of the inlet, namely the Port Arthur Canal to the northwest, the natural tidal pass to Sabine Lake to the northeast, the Sabine Pass Channel to the south, and the old natural tidal channel to the southwest (Fig. 1). Under pure tidal conditions, significant flow is carried in all of these channels with a somewhat greater proportion in the Sabine Pass Channel and in the tidal access to Sabine Lake at the causeway (Ward and Johnston 1977). In contrast, most of the frontal efflux, associated with the response of the system to a frontal passage, is confined to the natural tidal channel rather than the dredged channel (Ward and Chambers 1978).

A study of historical aerial photographs has revealed the frequent occurrence of a narrow band of extremely turbid water adjacent to the west shore of Upper Sabine Pass. The source of the sediment is

unknown, although the source may be erosion of the south bank of the Port Arthur canal, which has exhibited marked shoreline retreat in recent years. The scale of the phenomenon is difficult to estimate, though the width of the turbid band from aerial photographs ranges up to two hundred meters.

MEASUREMENTS

The sediment sampling station was established in the Upper Sabine Pass area in 1-m water depths approximately 60 m from shore (Fig. 1). The sediment trap construction consisted of an evacuated circular pit containing a removable drum. The pit well was stabilized by a 1.1-m diameter steel culvert, jetted into the bed so that its top was flush with bed level, and the contents evacuated by hydraulic pump. The depth of this well (i.e., length of the culvert) was 1.2 m. The well was fitted with a bottom of waterproofed plywood to ensure the integrity of the well. Within this well was placed a 0.21 cu m (55-gallon) drum which served as the actual sediment trap. Appurtenances to the drum were designed for its easy removal and replacement. Finally, the well was capped by a waterproof plywood top, in whose center was bolted a brass plate containing a slot aperture below which was mounted the sediment sampler. The general construction and installation of the sediment well and trap are shown in Figure 2. The operation of the trap consists of deploying the drum and replacing the top to the well. After an appropriate period of time (two to four weeks in the present study) the top to the well is pulled, and the drum capped, winched out of the well, and transported back to the laboratory where the contents are weighed and analyzed.

Clearly, the only aperture to the sediment trap is the slot in the brass plate mounted in the top of the well. From a practical point of view, the slot must be sufficiently large to ensure a valid measurement, yet not be so large as to tax the capacity of the trap. An additional factor is the efficiency of the slot, in that the slot must be made wide enough to intercept the saltating particles. Slot efficiency has been discussed by Poreh et al. (1970). Because the largest grain size expected in any significant proportion in this area was that of coarse sand (1-2 mm diameter), the slot width was sized to 5 cm, which would entail 100% efficiency in these grain-size ranges. (Though one might expect this slot dimension to represent 100% efficiency for smaller diameters as well, once grain sizes decrease below those of fine sands and into the silts, particle transport becomes quasi-suspended, so that the slot efficiency in fact decreases.) A slot length of 20 cm was used in the present study to present an adequate aspect ratio to the flow. At installation the long dimension of the slot was oriented normal to the shorelines on the pre-

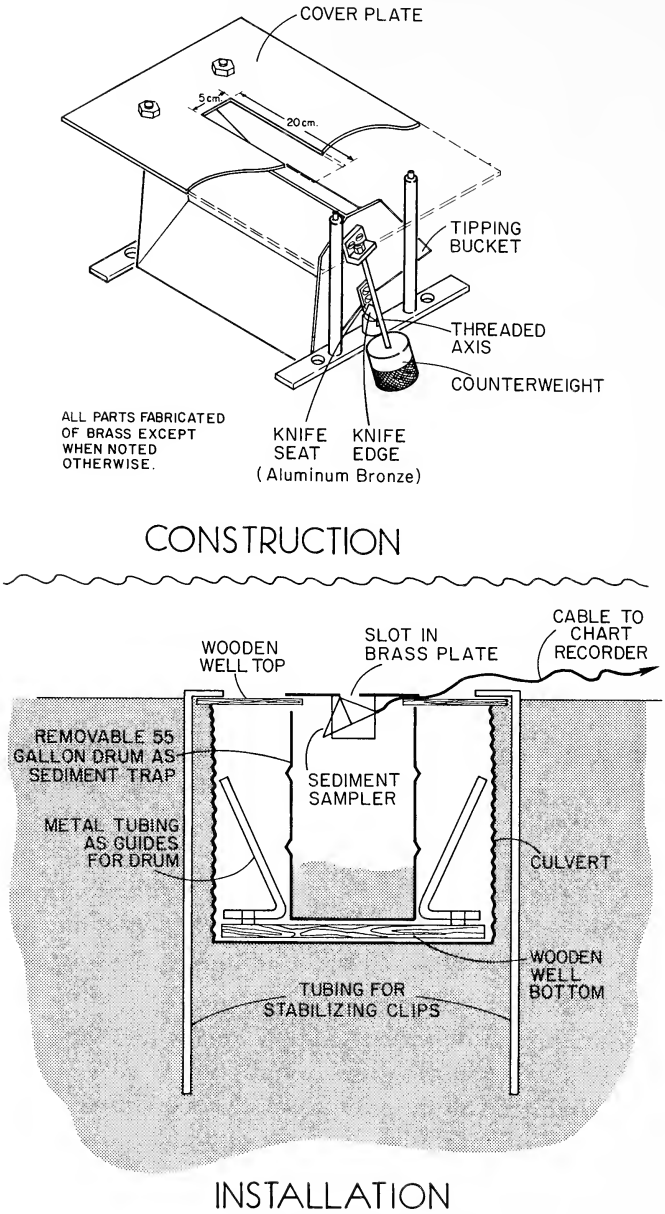

FIGURE 2. Construction of recording sediment sampler and installation in trap.

sumption that sediment transport would be directed primarily parallel to the shore.

The continuous sediment sampling device was adapted from the traditional tipping bucket that has been used for many years for the monitoring of rainfall or snowfall rates in meteorology. The particular

tipping-bucket design utilized in this study was modeled after that of Racotch and Sagi (1977; see also Amin 1978), although modified somewhat for present purposes. The basic sampler design is shown in Figure 2. The sampler was constructed primarily of brass parts for resistance to corrosion in the saline environment. The sampler has two stable configurations, exposing one side or the other of the median plate to sediment falling through the slot. Once sufficient material has accumulated, this side is overbalanced, the bucket tips on the knife edges to the other side, and the collected sediment falls into the trap. Depending upon the attitude of the sample bucket, a magnetic reed switch is either engaged or disengaged, closing a circuit when engaged. An event recorder, i.e., a two-state chart recorder, continuously records the status of the reed switch, a change corresponding to a trip of the bucket. The counterbalance was set to trip under water at 300 grams of material. Cables were run to shore where the battery-powered event recorder was housed in a weatherproof locked steel case hidden from view in the heavy vegetation. Grain-size analysis of the intercepted material showed a high proportion of silts and clays. In much of the data there was a discrepancy between the recording sampler deposition rates and the accumulation in the trap, the latter being larger. Since about half the entrapped sediment was disaggregated clays, we speculate that clays short-circuit the bucket through low-intensity turbulence.

RESULTS AND DISCUSSION

The scheduled period of operation was the two months of October and November 1978. These two months were chosen on the basis of climatology, in order to provide a range of hydrometeorological conditions from pure tidal to energetic frontal passages. Upper Sabine Pass proved to be a very hostile environment for the operation of this sampler system, and various mishaps prevented continuous data collection in this period: the periods 1-3 October, 7-17 October and 22-30 November were lost. The intent of encountering a range of hydrometeorological conditions was somewhat frustrated by the vagaries of 1978 weather. Early in the October-November period, the area came under the domination of a pressure ridge, which eliminated or ameliorated frontal passages and produced largely light winds and clear conditions. The tide record of the Mesquite Point gauge (Fig. 1) shows an almost undistorted astronomical tide for the entire October-November period, a remarkable occurrence for this season of year. The most intense cold front of the period (in terms of wind shift and speed) passed the area late 16 November; because the north winds coincided with the falling tide, a total water-level depression of 0.64 m occurred, still a rather modest response (cf. Ward 1980b).

The data from the recording sampler provide some insight into the time behavior of the nearshore sediment transport. Contrary to our expectations, there appeared to be no correlation between sediment transport and phase or amplitude of the tide (at least to the 300-gram resolution dictated by the counterbalance weight of the sampler), even at maximum lunar declination. The main sedimentation was of an event-type character, widely isolated in time. For example, during the period 10-21 November, some half-dozen sediment-accumulation events were recorded in which the sampler indicated a series of trips of the bucket within a few hours. During the intervening times, no trips were recorded. The most significant of these, 17 and 19 November, appear to be associated with strong winds from the northerly quadrant produced by the frontal passage of 16 November and reinforced by a frontal passage on 20 November. (Indeed, during 17-20 November there occurred the highest sustained northerly winds of the study period.)

The time relation between the frontal passage and the 17 November sedimentation event is displayed in detail in Figure 3. The reasons for the 26-hour lag between frontal passage and sediment response are not known. Sabine Lake will become fetch-limiting for a 15-knot north wind after about 2-3 hours. Further, propagation speed of shoaling waves within Sabine Lake is 7-8 knots. Thus maximum wave activity impingent upon the shore, due to the orientation of the body of Sabine Lake with frontal (northerly) winds, should be established within a few hours. Therefore, wave development cannot account for the delay. (There is also the possibility that a portion of the sediment deposition measured in this study originated in the erosion of the shoreface along the project area itself, though this cannot have been the source of all the sediment load since historical aerial photography establishes the reality of the nearshore plume.)

The sedimentation event may be associated with transport of materials out of the system due to north-wind setdown, in which case the lag may arise from the response of the system and the travel time from the origin of the sediment. It is my hypothesis that most of this sediment originates in the erosion of the south bank of the Port Arthur Canal upstream from the study area, and is transported into the area along the south shore. If this is the case, then the lag would be the result of the time of travel from the eroding banks plus the time required for the increased current (due to frontal setdown) to erode —perhaps undercut—the channel sides.

Finally, the reader is cautioned that the findings reported here are based on data collected at a single station within a very complex system. In Sabine Pass, flow is influenced by channel bathymetry and shifts its axes with ebb and flood (Ward and Johnston 1977). Thus, the single station probably was biased towards one or the other conditions. A

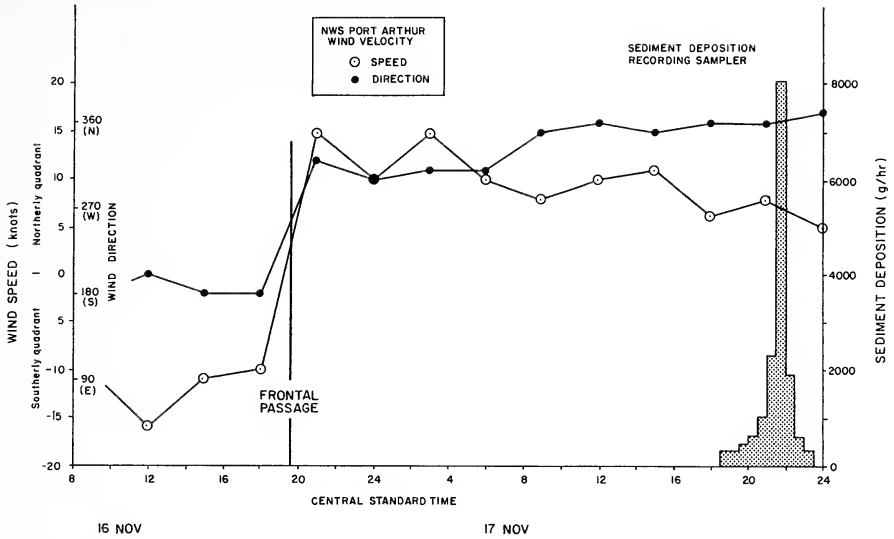

FIGURE 3. Time variation of wind velocity (left axis) and sedimentation rate (right axis) during frontal passage of 16 November 1978.

quantitative estimate of total sediment-mass transport due to an event like the frontal passage on 16 November would require several sediment traps deployed throughout the system, and attendant current measurements.

ACKNOWLEDGMENTS

The sediment sampler was installed on land of the State of Texas. I am grateful to the General Land Office for granting us access to state property for this purpose. Tide data were graciously provided by the Houston Office of U.S. Geological Survey, from their Mesquite Point gauge. Phillip Winsborough and Lowell Eck were responsible for the fabrication and installation of the equipment. This study was supported in part by Mobil Research and Development.

LITERATURE CITED

Amin, M. L. 1978. Bedload sampler for streams with sandy bed (discussion). Proceedings, American Society of Civil Engineers 104 (HY5):805-806.

Poreh, M., A. Sagui, and I. Seginer. 1970. Sediment sampling efficiency of slots. Proceedings, American Society of Civil Engineers 96 (HY10):2065-2078.

Racotch, A., and R. Sagi. 1977. Bedload sampler for streams with sandy bed. Proceedings, American Society of Civil Engineers 103 (HY8):923-928.

Ward, G. H. 1980a. Hydrography and circulation processes of Gulf estuaries, p. 183-215. *In* P. Hamilton and K. MacDonald (Eds.), Estuarine and wetland processes. Plenum Publishing Corp., New York.

Ward, G. H. 1980b. Frontal-induced hydrographic responses of the Texas bays, p. 304-307. *In* Second conference on coastal meterology, preprint volume American Meteorological Society, Boston.

Ward, G. H., and C. L. Chambers. 1978. Meteorologically forced currents in Upper Sabine Pass, Texas. Document number 7869, Espey, Huston & Associates, Inc., Austin, TX. 131 p.

Ward, G. H., and W. A. Johnston. 1977. Hydrographic survey of Upper Sabine Pass, Texas. Document number 7730-R1, Espey, Huston & Associates, Inc., Austin, TX 114 p.

MIDWATER FISHES OF THE GULF OF MEXICO COLLECTED FROM THE R/V *ALAMINOS*, 1965-1973

by EDWARD O. MURDY, RICHARD E. MATHESON JR., JANICE D. FECHHELM, *and* MICHAEL J. McCOID

Department of Wildlife and Fisheries Sciences
Texas A&M University
College Station, TX 77843

ABSTRACT

Cruises of the R/V *Alaminos* during 1965-1973 involved the collection of fishes by midwater trawl from 38 locations in the Gulf of Mexico and the northwestern Caribbean. The 4,232 specimens comprised 32 families, 75 genera, and at least 116 species of meso- and bathypelagic fishes. Considering the collections as a whole, gonostomatids were the dominant group and *Cyclothone* the dominant genus. The families Gonostomatidae, Myctophidae, Sternoptychidae, and Melamphaidae accounted for 95% of the catch. Relative abundance of gonostomatids varied little with sampling depth (to 1,000 m); myctophids were relatively most abundant in samples from the upper 500 m; sternoptychids and melamphaids were relatively most abundant in samples extending to depths of 1,000 m.

INTRODUCTION

The Texas Cooperative Wildlife Collection (TCWC) recently acquired the fishes taken during cruises of the R/V *Alaminos* in the years 1965-1973. This paper deals with those juvenile and adult specimens collected in 35 midwater-trawl (MWT) samples from various locations in the Gulf of Mexico and 3 MWT samples from the northwestern Caribbean (Table 1 and Fig. 1).

All samples were taken with oblique tows of a 3.0 m (10-foot) Isaacs-Kidd midwater trawl (IKMT; Isaacs and Kidd 1953). Water depth, sampling depth, and start-stop times are provided for each sample in Table 1.

This represents the most comprehensive survey, to date, of the midwater fishes from the entire Gulf of Mexico. It complements and extends the work of Becker et al. (1975), who dealt primarily with midwater fishes from the Caribbean Sea and eastern Gulf of Mexico.

OVERVIEW

The 38 MWT samples consisted of 4,232 specimens (excluding epipelagic, benthic, and miscellaneous larval fishes) representing at least 116 species of meso- and bathypelagic fishes in 75 genera and 32 families. The following section provides a species-by-species account; here we

Table 1. Summary of collection data.

Sample	Date	Position		Sampling Depth Start-Stop (m)	Maximum Water Depth (m)	Time Start-Stop (CST)
		Lat. (N)	Long. (W)			
11	7 Mar 65	26°15′	95°00′	0-930	2322	1700-1800
104	4-5 Jul 65	23°15′	84°02′	0-2500	2622	1820-0035
107	6 Jul 65	20°35′	84°47′	0-1875	4529	0935-1720
120	14-15 Jul 65	24°58′	84°16′	0-1410	3285	2255-0310
123	16 Jul 65	27°17′	89°59′	0-980	2057	1545-1915
127	3 Jul 65	24°03′	83°07′	0-675	1028	1835-2110
129	7-8 Jul 65	19°58′	85°14′	0-2400	4721	2215-1130
132	9-10 Jul 65	20°53′	85°35′	0-2600	4474	2355-1005
133	12-13 Jul 65	23°43′	85°51′	0-2800	3574	2340-1220
140	2 Oct 65	26°17′	94°50′	0-1250	1625	1355-1650
143	3 Oct 65	24°11′	95°06′	0-2500	3605	1235-1745
153	27 Mar 66	25°33′	88°57′	150-350	3294	2255-2340
156	30 Mar 66	25°34′	86°28′	0-375	3252	1320-1440
166	4 Apr 66	28°45′	87°46′	0-1000	1870	1028-1230
169	3 Jul 66	23°03′	94°34′	0-100	3737	0731-0845
171	4-5 Jul 66	23°34′	93°30′	0-900	3658	2400-0300
175	8 Jul 66	24°01′	86°52′	0-300	1171	1730-1740
182	11 Jul 66	28°13′	87°17′	0-150	1470	1345-1520
184	11 Jul 66	28°13′	87°21′	250-500	2683	1627-1727
187	12 Jul 66	27°18′	88°51′	0-175	2200	1138-1230
189	12 Jul 66	27°18′	88°51′	500-950	2200	1330-1420
190	12 Jul 66	27°18′	88°51′	1000-0	2200	1420-1500
192	13 Jul 66	27°19′	88°53′	175-500	2141	2030-2250
198	22 Aug 69	21°27′	96°53′	700-750	1180	1340-1440
200	26-27 Aug 69	22°52′	96°18′	0-1500	2150	2335-0300
203	27 Aug 69	23°52′	95°35′	2300-0	3109	2135-0300
205	5 Oct 69	24°53′	90°45′	2500-1600	3569	1735-1930
206	5 Oct 69	24°53′	90°45′	1600-0	3569	1930-2025
209	6 Oct 69	24°36′	90°25′	3600-0	3687	1430-1620
210	7 Oct 69	24°33′	88°27′	0-600	1829	0910-1105
213	7 Oct 69	24°41′	88°11′	650-1100	1565	1550-1650
214	7 Oct 69	24°41′	88°11′	1100-0	1565	1650-1745
216	8 Oct 69	25°22′	86°36′	1000-1225	3248	1100-1200
219	8 Oct 69	25°25′	86°28′	750-0	3248	1405-1505
221	4 Jul 70	25°54′	90°58′	0-2500	3418	1705-2020
234	9 Jul 72	24°36′	96°19′	900-0	1290	1745-1815
239	2 Mar 73	26°45′	94°53′	0-480	641	1255-1742
247	3 Mar 73	26°02′	93°50′	0-800	?	1700-2120

present only a summary of our observations regarding species composition of the samples.

Considering the samples as a whole, gonostomatids were clearly the dominant group: 2,858 specimens (2,731 of them *Cyclothone* spp.), or 67.5% of the total number of fishes caught, were of this family. Next in relative abundance were the Myctophidae with 15.5% of the catch by

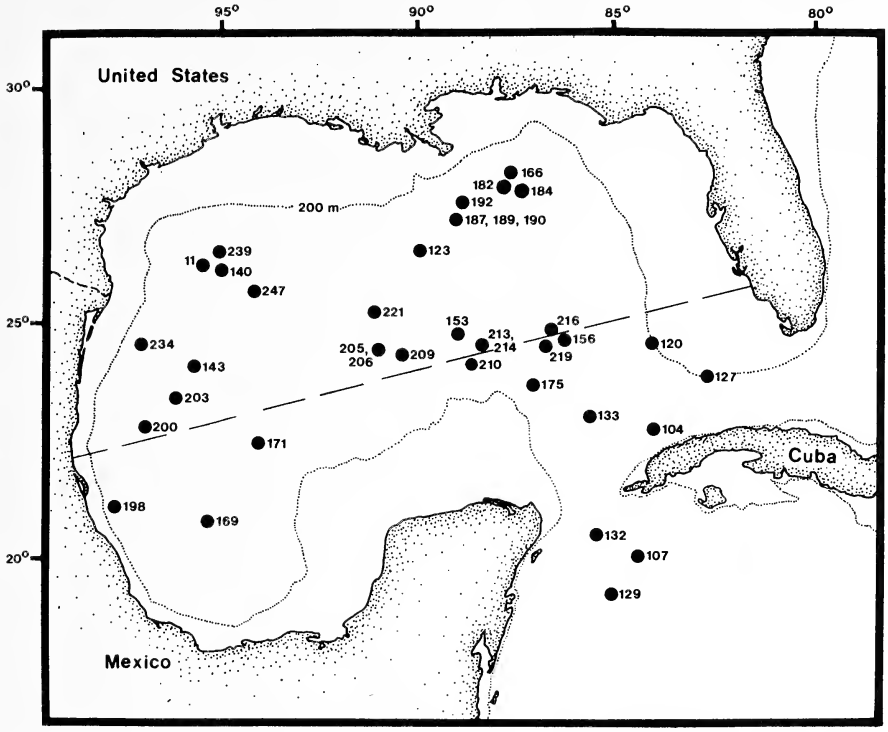

FIGURE 1. Map showing approximate location of each midwater trawl station. Dashed line indicates division of stations into more temperate (north of line) and more tropical (south of line) categories.

number; Sternoptychidae with 10.2%; and Melamphaidae with 1.8%. These four families represented 95% of the catch. Craddock and Mead (1970) found the same four families dominating the midwater ichthyofauna of the eastern Pacific.

The importance to the total fauna of relatively few forms was also evident at the species level. Nearly 65% of all fishes caught were *Cyclothone* spp. *Cyclothone* spp. were found in 71% of the tows, whereas *Valenciennellus tripunculatus* was collected in 52.6%. The three most abundant taxa—*Cyclothone* spp., *Sternoptyx pseudobscura* and *Lepidophanes guentheri*—comprised 71.3% of the total. The ten most abundant species formed over 83.6% of the fauna, while the 36 least abundant species contributed an almost negligible 0.9%.

The most speciose families were Myctophidae, with 45 species; Sternoptychidae, 10; Gonostomatidae, 8; Melamphaidae, 8; and Photichthyidae, 7.

The relative abundance of the dominant families varied with respect to depth. The percentage composition of each MWT collection is provided in Table 2 for the dominant families. (We follow Craddock and

TABLE 2. Percentage composition of collections by sampling depth. A, 0-500 m; B, 0-1000 m; C, 0-1000+ m. Totals exclude values for the genus *Cyclothone*, which is already accounted for in the values for Gonostomatids.

	Collection	Gonostomatids	*Cyclothone*	Myctophids	Sternoptychids	Melamphaids	Total
A.	153	2.2	2.2		91.1	2.2	95.6
	156	74.7	74.7	4.0	9.3		88.0
	169						
	175	41.4	35.7	49.3	2.9		93.6
	182						
	184	98.9	96.6	0.3	0.3	0.3	99.5
	187						
	192	11.1		22.2		22.2	55.6
	239	64.5	48.4	26.1	5.0		95.6
	$\bar{X}$	67.8	59.8	18.4	7.5	0.4	94.2
B.	11	50.0	50.0		12.5		62.5
	123	48.3	47.6	30.3	15.6	2.2	96.4
	127	18.9	16.9	66.0	5.7		90.6
	166	61.4	61.4	20.5	8.4	1.2	91.5
	171	91.8	91.2		2.1	2.7	96.6
	189	18.2	18.2		81.8		100.0
	190	70.4	69.8	8.8	16.9	1.3	97.4
	198	25.0		25.0			50.0
	210	77.3	77.3	12.4	6.6	0.8	97.1
	213	58.8	58.8	19.1	11.8	5.9	95.6
	214			31.8	68.2		100.0
	219	73.5	70.1	16.6	4.9	0.6	95.6
	234	69.9	68.5	10.9	1.4	6.8	89.0
	247	67.9	64.6	4.4	17.4	3.2	93.4
	$\bar{X}$	64.8	63.2	15.8	12.3	2.3	95.2
C.	104	83.8	83.4	9.2	4.4		97.4
	107	65.2	63.8	15.9	10.1	2.9	94.1
	120	52.9	50.0	12.9	22.9	2.9	91.6
	129	45.0	45.0	35.0	10.0		90.0
	132						
	133	8.3	8.3	75.0		8.3	91.7
	140			100			100.0
	143			37.5	50.0	12.5	100.0
	200	72.4	69.0	9.6	7.7	3.5	93.2
	203				100.0		100.0
	205	83.3	83.3		5.6		88.9
	206	5.3		10.5	31.6	21.1	68.5
	209	77.8	73.3	6.7	8.9	2.2	95.6
	216	95.3	95.3	1.9	0.9		98.1
	221	72.6	72.6	16.6	6.4	1.3	96.9
	$\bar{X}$	72.6	71.1	12.1	8.1	2.2	94.9

Mead (1970) in the organization of this table, while recognizing the limitations of data based on non-closing nets.) Gonostomatids were the dominant fishes in samples from depths less than 500 m (67.8%), from depths between the surface and 1,000 m (64.8%), and from depths extending to more than 1,000 m (72.6%). Myctophids reached their maximum abundance at depths less than 500 m (18.4%) and were much less abundant (12.1%) at depths between 0 and 1,000 m. Sternoptychids achieved their maximum relative abundance in the 0-1,000 m stratum (12.3%) but were also well represented in the 0-500 m stratum (7.5%) and 0-1,000+ m stratum (8.1%). Melamphaids were almost equally important from 0-1,000 m (2.3%) and 0-1,000+ m (2.2%), while their importance was least from 0-500 m (0.4%).

A straight line from Tampico, Mexico, to Miami, Florida (Fig. 1), approximately bisects the Gulf of Mexico based on the tropical-temperate inshore fish faunal boundary of Hoese and Moore (1977). The 24 collections taken north of this line represented 53 hours of fishing effort and contained 2,804 specimens comprising 87 species. The 14 hauls, amounting to 65.5 total fishing hours, south of the line yielded 1,428 specimens representing 80 species. Thus, the number of specimens taken per unit of fishing effort was more than twice as great north of the line than south. However, the number of species taken per hour north of the line was only 1.3 times greater than that south of the line.

Several individual samples were of particular interest. MWT 175 resulted in the collection of the only representatives of *Taracichthys longipinnis*, *Idiacanthus fasciola*, *Diaphus effulgens*, *D. anderseni*, and *D. termophilus*. MWT 219 was the only haul to yield representatives of Evermannellidae. The samples with the largest diversity were MWT 123 (39 spp.), MWT 200 (38 spp.), and MWT 247 (33 spp.).

As indicated by Backus et al. (1977) for myctophids, the midwater fish fauna of the Gulf of Mexico closely parallels that of the northwest Atlantic and Caribbean. The number of species appears substantial (116), and the number of specimens per fishing hour (935.7) in our collections is quite similar to that (40) obtained in the Gulf by Becker et al. (1975), but considerably less than that (82.8) reported by Craddock and Mead (1970) for the eastern Pacific.

SPECIES ACCOUNT

Each entry below gives the specific name, the IKMT collection(s) in which the species was taken, and the number of specimens followed, in parentheses, by the range of standard lengths. We have adopted the phylogenetic arrangement proposed by Nelson (1976), except in a few

cases where recent work has indicated otherwise; exceptions are noted and documented as they occur.

Species that comprised at least 1% of the total number of non-*Cyclothone* specimens are followed by numbers in brackets. Numbers in brackets are, respectively, (1) total number of specimens of that species; (2) percentage of the total number of specimens of all species; (3) percentage of the total number of non-*Cyclothone* specimens; (4) number of collections in which the species occurred; and (5) percentage of collections in which the species occurred.

All specimens are deposited in the TCWC, Texas A&M University, College Station, Texas.

ANGUILLIFORMES

Anguilloidei

Serrivomeridae

Serrivomer sp.

MWT 166:1 (480 mm); MWT 247:1(567 mm)

SALMONIFORMES

Argentinoidei

Argentinidae

Microstoma microstoma (Risso, 1810)

MWT 221:1 (39 mm)

This seems to be only the second specimen of *M. microstoma* recorded from the Gulf of Mexico (see Cohen 1964). One larval *Microstoma* sp. reported by Houde et al. (1979) from the eastern Gulf of Mexico should, however, be *M. microstoma* since this genus currently is considered monotypic (Cohen 1964).

Bathylagidae

Bathylagus c.f. *berycoides* (Borodin, 1929)

MWT 153:1(103 mm)

This seems to be only the second specimen of *B. berycoides* recorded from the Gulf of Mexico (see Cohen 1964).

Bathylagus longirostris Maul, 1948

MWT 123:2(27-28 mm); MWT 171:1(28 mm)

Alepocephalidae

Photostylus pycnopterus Beebe, 1933

MWT 171:1(70 mm); MWT 206:1(100 mm); MWT 247:2(16-37 mm)

Based on the records of Wisner (1976), our 100 mm specimen is the largest yet collected from the western Atlantic.

Searsiidae

Holtbyrnia sp.

MWT 200:1(65 mm)

Pellisolus facilis Parr, 1951

MWT 247:3(25-47 mm)

This rare searsiid is known from California to Peru in the eastern Pacific Ocean (Parr 1960; Bussing 1965; Anderson et al. 1979) and from one previous record (Becker et al. 1975) in the Gulf of Mexico.

STOMIIFORMES (=Salmoniformes (in part) of Nelson 1976, see Rosen 1973 and Steyskal 1980)

Gonostomatoidei (=Stomiatoidei (in part) of Nelson 1976, change made due to ranking and Weitzman 1974)

Gonostomatidae

Bonapartia pedaliota Goode and Bean, 1896

MWT 104:1(35 mm); MWT 175:2(41-53 mm); MWT 200:1(83 mm)

Grey (1964) lists the known maximum size as 72 mm S.L. Our 83 mm specimen represents a new size record.

Cyclothone spp. [2731, 64.5%, - , 27, 71.0%]

MWT 11:4(29-31 mm); MWT 104:191(8-50 mm); MWT 107:44(13-27 mm); MWT 120:35(23-47 mm); MWT 123:286(17-50 mm); MWT 127:9(20-50 mm); MWT 129:9(28-48 mm); MWT 133:1(31 mm); MWT 153:1(16 mm); MWT 156:56(14-40 mm); MWT 166:51(10-46 mm); MWT 171:299(17-50 mm); MWT 175:50(18-32 mm); MWT 184:283(14-43 mm); MWT 189:4(16-26 mm); MWT 190:111(13-48 mm); MWT 200:180(16-49 mm); MWT 205:15(23-48 mm); MWT 209:33(15-48 mm); MWT 210:187 (16-34 mm); MWT 213:40(18-46 mm); MWT 216:102(19-49 mm); MWT 219:128(15-47 mm); MWT 221:114(20-53 mm); MWT 234:50(12-46 mm); MWT 239:184(15-47 mm); MWT 247:264(15-51 mm)

Due to the poor condition of many of our specimens of *Cyclothone*, we decided to combine all specimens under *Cyclothone* spp. At least four species, *C. braueri*, *C. pseudopallida*, *C. pallida*, and *C. acclinidens*, occur in the Gulf of Mexico (Baird et al. 1975; Becker et al. 1975). Based on the distinguishing characters utilized by Kawaguchi (1971) and Bond and Tighe (1974), our collections contain at least the first three of these species.

Diplophus taenia Günther, 1873

MWT 171:1(102 mm); MWT 200:1(65 mm); MWT 239:1(66 mm)

Gonostoma atlanticum Norman, 1930

MWT 120:1(34 mm); MWT 123:3(25-45 mm); MWT 198:1(49 mm); MWT 200:1(34 mm); MWT 247:1(51 mm)

Gonostoma elongatum Günther, 1878 [97, 2.3%, 6.4%, 14, 36.8%]

MWT 107:1(90 mm); MWT 120:1(138 mm); MWT 127:1(122 mm); MWT 171:1(90 mm); MWT 175:5(89-165 mm); MWT 184:7(27-106 mm); MWT 190:1(114 mm); MWT 192:1(147 mm); MWT 200:4(24-176 mm); MWT 209:2(163-164 mm);

MWT 219:5(26-204 mm); MWT 234:1(34 mm); MWT 239:60(24-93 mm); MWT 247:7(34-76 mm)

Gonostoma spp.
MWT 123:1(24 mm); MWT 175:1(30 mm); MWT 200:2(34-34 mm); MWT 206:1(37 mm); MWT 247:6(damaged)

Margrethia obtusirostra Jespersen and Tåning, 1919
MWT 219:1(22 mm); MWT 239:1(19 mm)

Maurolicus muelleri (Gmelin, 1788)
MWT 182:1(18 mm); MWT 184:1(17 mm); MWT 247:1(14 mm)

Sternoptychidae

Argyropelecus aculeatus Valenciennes, 1849
MWT 120:1(60 mm); MWT 200:1(30 mm); MWT 206:1(10 mm); MWT 219:1(57 mm); MWT 247:1(14 mm)

Argyropelecus affinis Garman, 1899
MWT 175:2(12-14 mm); MWT 205:1(29 mm); MWT 239:2(13-15 mm)

Argyropelecus gigas Norman, 1930 [15, 0.4%, 1.0%, 4, 10.5%]
MWT 123:1(23 mm); MWT 210:9 (22-28 mm); MWT 214:1(22 mm); MWT 239:4(30-32 mm)

Argyropelecus hemigymnus Cocco, 1829
MWT 206:1(11 mm); MWT 210:1(15 mm); MWT 239:2(16-19 mm); MWT 247:1(22 mm)

Argyropelecus spp.
MWT 107:2(10-16 mm); MWT 123:3(7-9 mm); MWT 153:2(8-9 mm); MWT 200:2(11-24 mm); MWT 214:2(9 mm)

Polyipnus asteroides Schultz, 1938
MWT 171:1(31 mm); MWT 210:2(30-32 mm)

Sternoptyx diaphana Hermann, 1781 [72, 1.7%, 4.8%, 17, 44.7%]
MWT 11:1(22 mm); MWT 104:2(15-20 mm); MWT 107:4(10-25 mm); MWT 120:5(11-29 mm); MWT 123:9(11-32 mm); MWT 153:5(10-27 mm); MWT 156:2(17-21 mm); MWT 189:10(9-26 mm); MWT 190:3(17-19 mm); MWT 200:5(12-26 mm); MWT 203:1(13 mm); MWT 209:2(11-12 mm); MWT 213:2(11-16 mm); MWT 214:2(17-30 mm); MWT 221:4(10-25 mm); MWT 239:10(16-29 mm); MWT 247:5(17-42 mm)

Sternoptyx pseudobscura Baird, 1971 [147, 3.5%, 9.8%, 13, 34.2%]
MWT 104:3(23-36 mm); MWT 120:4(19-26 mm); MWT 123:18(11-44 mm); MWT 153:8(11-35 mm); MWT 190:24(6-46 mm); MWT 200:7(14-28 mm); MWT 206:2(15-30 mm); MWT 213:6(15-35 mm); MWT 214:4(27-33 mm); MWT 219:5(6-11 mm); MWT 221:3(8-23 mm); MWT 239:1(20 mm); MWT 247:62(9-45 mm)

Sternoptyx spp. [105, 2.5%, 6.9%, 12, 31.6%]
MWT 104:5(8-11 mm); MWT 120:4(7-10 mm); MWT 123:49(6-14 mm); MWT 143:4(damaged); MWT 153:18(6-11 mm); MWT

156:3(9-10 mm); MWT 166:1(7 mm); MWT 171:5(7-13 mm); MWT 189:8(7-9 mm); MWT 209:1(8 mm); MWT 214:6(7-10 mm); MWT 216:1(9 mm)

Valenciennellus tripunctulatus (Esmark, 1871)
[65, 1.5%, 4.3%, 20, 52.6%]
MWT 107:1(26 mm); MWT 120:2(21-24 mm); MWT 123:14(18-29 mm); MWT 127:3(21-28 mm); MWT 129:2(27-29 mm); MWT 153:8(16-30); MWT 156:2(23-24 mm); MWT 166:6(12-27 mm); MWT 171:1(22 mm); MWT 175:2(13-23 mm); MWT 184:1(17 mm); MWT 192:2(28-28 mm); MWT 200:5(22-30 mm); MWT 206:2(23-24 mm); MWT 209:1(26 mm); MWT 210:4(24-29 mm); MWT 219:3(23-27 mm); MWT 221:3(28-28); MWT 234:1(25 mm); MWT 247:2(24-27 mm)

Photichthyoidei (=Stomiatoidei (in part) of Nelson 1976, change made due to ranking and Weitzman 1974)

Photichthyidae (=Gonostomatidae (in part) of Nelson 1976, see Weitzman 1974)

Ichthyococcus ovatus (Cocco, 1838)
MWT 221:1(15 mm)

Pollichthys mauli (Poll, 1953)
MWT 104:1(26 mm); MWT 156:4(22-39 mm); MWT 171:1(39 mm); MWT 216:1(28 mm); MWT 234:1(15 mm)

Polymetme corythaeola (Alcock, 1898)
MWT 104:1(32 mm) *Vinciguerria attenuata* (Cocco, 1838) MWT 166:2(18-34 mm); MWT 184:3(13-16 mm); MWT 192:1(20 mm); MWT 247:3(15-37 mm)

Vinciguerria nimbaria (Jordan and Williams, 1895)
[16, 0.4%, 1.1%, 8, 21.1%]
MWT 104:1(24 mm); MWT 107:1(28 mm); MWT 123:3(15-18 mm); MWT 127:1(29 mm); MWT 156:1(25 mm); MWT 166:2(22-36 mm); MWT 184:1(16 mm); MWT 247:1(23 mm)

Vinciguerria poweriae (Cocco, 1838)
MWT 123:4(13-17 mm); MWT 156:1(14 mm); MWT 171:1(19 mm); MWT 200:4(19-26 mm); MWT 210:1(26 mm); MWT 221:2(19-21 mm); MWT 247:3(15-23 mm)

Vinciguerria spp.
MWT 200:4(16-20 mm)

Chauliodontidae

Chauliodus sloani Bloch and Schneider, 1801
MWT 171:1(26 mm); MWT 175:1(27 mm); MWT 184:3(58-104 mm); MWT 206:1(109 mm); MWT 210:6(22-35 mm); MWT 219:1(60 mm); MWT 239:1(102 mm)

Chauliodus spp.
MWT 132:1(140 mm); MWT 239:5(26-52 mm)

Astronesthidae

Astronesthes indicus Brauer, 1902
MWT 133:1(100 mm)

Astronesthes micropogon Goodyear and Gibbs, 1969
MWT 234:1(49 mm)

Astronesthes richardsoni Poey, 1853
MWT 239:1(41 mm)

The only previous record of *A. richardsoni* from the Gulf of Mexico seems to be that of Becker et al. (1975).

Astronesthes similis Parr, 1927
MWT 205:1(24 mm)

Melanostomiidae (=Melanostomiatidae of Nelson 1976, see Steyskal 1980)

Eustomias brevibarbatus Parr, 1927
MWT 175:1(77 mm); MWT 234:1(51 mm)

Eustomias spp.
MWT 123:2(72-75 mm); MWT 190:1(60 mm)

Flagellostomias boureei (Zugmayer, 1913)
MWT 171:1(164 mm)

We find no previous records of *F. boureei* from the Gulf of Mexico, but the record of *Flagellostomias* sp. from the Gulf by Bullis and Thompson (1965) probably refers to this species (see Morrow and Gibbs 1964.)

Leptostomias spp.
MWT 171:1(88 mm); MWT 175:1(67 mm)

Photonectes c.f. *braueri* (Zugmayer, 1913)
MWT 153:1(28 mm)

This species has not been reported previously in the Gulf of Mexico, but is known to occur in the Bahamas (Morrow and Gibbs 1964).

Photonectes margarita (Goode and Bean, 1895)
MWT 200:1(87 mm)

Malacosteidae

Aristostomias sp.
MWT 209:1(26 mm)

Malacosteus niger Ayres, 1848
MWT 200:1(36 mm); MWT 219:1(53 mm)

Photostomias guernei Collett, 1889
MWT 166:1(96 mm); MWT 171:1(109 mm); MWT 184:1(32 mm); MWT 234:2(93-96 mm); MWT 239:2(25-77 mm); MWT 247:1(damaged)

Idiacanthidae

Idiacanthus fasciola Peters, 1877
MWT 175:1(101 mm)

AULOPIFORMES (=Myctophiformes (in part) of Nelson 1976, see Rosen 1973)

Aulopoidei (no suborder designated by Nelson 1976, see Rosen 1973)

Scopelosauridae

Scopelosaurus lepidus (Krefft and Maul, 1955)

MWT 239:2(34-35 mm)

Alepisauroidei (no suborder designated by Nelson 1976, see Rosen 1973)

Paralepididae

Lestidiops affinis (Ege, 1930)

MWT 120:1(43 mm); MWT 123:3(30-44 mm); MWT 156:1(71 mm); MWT 169:4(38-55 mm); MWT 198:1(37 mm); MWT 200:1(59 mm)

Lestidium atlanticum Borodin, 1928

MWT 120:1(70 mm)

Paralepis c.f. *atlantica* Krøyer, 1891

MWT 200:1(27 mm)

Sudis atrox Rofen, 1963

MWT 198:1(17 mm)

Our identification of this specimen is based on the characters given by Shores (1969) for small specimens.

Omosudidae

Omosudis lowei Günther, 1887 [22, 0.5%, 1.5%, 11, 28.9%]

MWT 104:1(16 mm); MWT 120:2(18-28 mm); MWT 123:3(15-20 mm); MWT 171:2(15-17 mm); MWT 200:1(25 mm); MWT 205:1(26 mm); MWT 206:1(75 mm); MWT 209:1(33 mm); MWT 213:2(26-30 mm); MWT 234:1(16 mm); MWT 247:7(11-49 mm)

Alepisauridae

Alepisaurus spp.?

MWT 206:1(8 mm); MWT 221:1(10 mm)

Evermannellidae

Coccorella atrata (Alcock, 1893)

MWT 219:1(97 mm)

According to Rofen (1966), large specimens of *C. atrata* (>40 mm) are relatively rare in collections.

Odontostomops normalops (Parr, 1928)

MWT 219:1(47 mm)

Scopelarchidae

Scopelarchus analis (Brauer, 1902) MWT 127:1(42 mm); MWT 234:1(22 mm); MWT 239:1(31 mm);
MWT 247:1(24 mm)

Scopelarchus guentheri Alcock, 1896

MWT 175:1(41 mm); MWT 206:1(20 mm)

Myctophiformes

Myctophidae

Benthosema suboritale (Gilbert, 1913) [81, 1.9%, 5.4%, 11, 28.9%]
MWT 104:1(22 mm); MWT 123:19(14-29 mm); MWT 127:3(23-24 mm); MWT 175:3920-27 mm); MWT 190:1(26 mm); MWT 200:5(24-27 mm); MWT 210:11(12-27 mm); MWT 219:1(22 mm); MWT 221:8(16-29 mm); MWT 239:25(12-31 mm); MWT 247:4(11-30 mm)

Bolinichthys photothorax (Parr, 1928)
MWT 129:1(57 mm); MWT 175:2(17-22 mm); MWT 219:2(18-30 mm); MWT 234:1(21 mm); MWT 239:1(24 mm); MWT 247:1(33 mm)

Bolinichthys supralateralis (Parr, 1928)
MWT 200:1(21 m); 213:1(16 mm); MWT 221:1(13 mm); MWT 239:9(20-35 mm)

Bolinichthys spp.
MWT 123:1(56 mm); MWT 219:1(12 mm)

Centrobranchus nigroocellatus (Günther, 1873)
MWT 104:2(12-14 mm); MWT 175:1(17 mm); MWT 239:1(34 mm)

Ceratoscopelus warmingi (Lütken, 1892) [86, 2.0%, 5.7%, 11, 28.9%]
MWT 104:1(21 mm); MWT 107:3(22-36 mm); MWT 123:45(17-51 mm); MWT 127:5(24-33 mm); MWT 143:1(26 mm); MWT 175:9(20-38 mm); MWT 190:5(22-25 mm); MWT 200:6(21-36 mm); MWT 213:3(21-32 mm); MWT 221:7(17-22 mm); MWT 247:1(59 mm)

Diaphus c.f. *anderseni* Tåning, 1932
MWT 175:1(19 mm)

Nafpaktitis el al. (1977) consider *D. anderseni* uncommon in the North Atlantic and record only one specimen from the Gulf of Mexico. The identification of our specimen is somewhat questionable due to its damaged condition; however, it agrees with the description of *D. anderseni* in the placement and size of the luminous organs on the head.

Diaphus dumerili (Bleeker, 1856)
MWT 127:1(27 mm); MWT 210:1(61 mm); MWT 214:2(24-28 mm); MWT 247:1(54 mm)

Diaphus effulgens (Goode and Bean, 1896)
MWT 175:1(106 mm)

Diaphus fragilis Tåning, 1928
MWT 107:1(34 mm)

Diaphus garmani Gilbert, 1906
MWT 210:1(32 mm)

Diaphus lucidus (Goode and Bean, 1896)
MWT 123:1(70 mm); MWT 175:2(23-25 mm); MWT 239:1(83 mm)
Diaphus luetkeni (Brauer, 1904)
MWT 120:1(42 mm); MWT 123:1(39 mm); MWT 127:1(38 mm); MWT 143:1(18 mm); MWT 166:1(52 mm); MWT 200:1(40 mm); MWT 239:2(42-48 mm)
Diaphus mollis Tåning, 1928
MWT 175:1(48 mm); MWT 190:1(17 mm); MWT 200:1(51 mm); MWT 213:1(20 mm); MWT 247:2(47-51 mm)
Diaphus perspicillatus (Ogilby, 1898)
MWT 239:1(54 mm)
Diaphus problematicus Parr, 1928
MWT 107:2(33-54 mm); MWT 127:1(50 mm); MWT 175:1(48 mm); MWT 210:4(33-58 mm); MWT 219:4(23-39 mm); MWT 247:1(42 mm)
Diaphus rafinesqui (Cocco, 1838)
MWT 107:1(83 mm); MWT 184:1(78 mm); MWT 210:6(31-80 mm)
Diaphus splendidus (Brauer, 1904)
MWT 133:1(32 mm); MWT 175:1(61 mm)
Diaphus taaningi Norman, 1930
MWT 123:1(57 mm)
Diaphus termophilus Tåning, 1928
MWT 175:2(34-38 mm)
Diaphus spp.
MWT 120:1(63 mm); MWT 127:2(66-74 mm); MWT 129:2(29-35 mm); MWT 166:1(14 mm); MWT 219:1(61 mm); MWT 239:1(20 mm)
Diogenichthys atlanticus (Tåning, 1928) [127, 0.6%, 1.8%, 8, 21.1%]
MWT 104:2(12-14 mm); MWT 120:1(12 mm); MWT 123:9(11-21 mm); MWT 166:1(21 mm); MWT 190:1(12 mm); MWT 200:1(18 mm); MWT 239:10(16-22 mm); MWT 247:2(22-23 mm)
Gonichthys coccoi (Cocco, 1829) [15, 0.4%, 1.0%, 3, 7.9%]
MWT 123:9(18-22 mm); MWT 127:1(27 mm); MWT 210:5(20-26 mm)
Hygophum benoiti (Cocco, 1838) [64, 1.5%, 4.3%, 8, 21.1%]
MWT 104:9(9-12 mm); MWT 120:4(11-13 mm); MWT 123:36(10-23 mm); MWT 190:4(10-12 mm); MWT 192:1(12 mm); MWT 210:1(23 mm); MWT 214:2(20-22 mm); MWT 221:7(11-15 mm)

Hygophum hygomi (Lütken, 1892)
MWT 123:1(44 mm); MWT 156:1(14 mm); MWT 239:2(16-23 mm)

Hygophum macrochir (Günther, 1864)
MWT 123:1(38 mm); MWT 127:3(30-44 mm); MWT 206:1(13 mm)

Hygophum reinhardti (Lütken, 1892)
MWT 104:1(14 mm); MWT 107:1(14 mm); MWT 143:1(13 mm); MWT 200:1(14 mm)

Hygophum taaningi Bekker, 1965
MWT 123:2(20-32 mm); MWT 127:1(32 mm); MWT 156:2(12-14 mm) MWT 166:1(32 mm); MWT 200:2(23-27 mm); MWT 209:2(20-21 mm); MWT 214:1(14 mm)

According to Nafpaktitis el al. (1977), *H. taningi* and *H. macrochir* are easily confused. Based on photophore patterns, some of our specimens identified as *H. taaningi* could be *H. macrochir*; however, gill raker counts clearly separate the two species: 19-20 in *H. macrochir* vs. 17 in *H. taaningi.*

Lampedena luminosa (Garman, 1899)
MWT 140:1(47 mm); MWT 175:2(20-25 mm); MWT 219:2(37-43 mm); MWT 239:4(43-68 mm)

Lampedena sp.
MWT 219:1(14 mm)

Lampanyctus alatus Goode and Bean, 1896 [45, 1.1%, 3.0%, 14, 36.8%]
MWT 107:1(37 mm); MWT 120:1(34 mm); MWT 123:16(23-47 mm); MWT 127:2(44-45 mm); MWT 133:1(36 mm); MWT 166:4(43-46 mm); MWT 175:2(32-33 mm); MWT 200:1(41 mm); MWT 209:1(21 mm); MWT 214:1(27 mm); MWT 219:2(32-38 mm); MWT 221:1(30 mm); MWT 239:9(32-44 mm); MWT 247:3(37-43 mm)

Lampanyctus ater Tåning, 1928
MWT 234:1(86 mm)

Lampanyctus cuprarius Tåning, 1928
MWT 213:1(66 mm)

Lampanyctus nobilis Tåning, 1928
MWT 129:2(34-53 mm); MWT 166:1(36 mm); MWT 200:1(37 mm); MWT 234:2(32-50 mm)

Lampanyctus spp.
MWT 127:2(39-84 mm); MWT 133:1(110 mm); MWT 192:1(105 mm); MWT 216:2(77-99 mm); MWT 239:2(20-41 mm)

Lepidophanes guentheri (Goode and Bean, 1896) [140, 3.3%, 9.3%, 15, 39.5%]
MWT 104:2(16-17 mm); MWT 107:3(24-30 mm); MWT 120:1(19 mm); MWT 123:20(16-60 mm); MWT 127:13(26-53 mm); MWT 129:3(23-37 mm); MWT 133:6(33-48 mm); MWT 140:1(20 mm); MWT 166:4(20-57 mm); MWT 175:38(17-43 mm); MWT 200:1(25 mm); MWT 213:2(21-47); MWT 219:16(16-44 mm); MWT 239:27(30-51 mm); MWT 247:3(50-54 mm)

Lobianchia gemellari (Cocco, 1838)
MWT 166:1(41 mm); MWT 200:2(31-46 mm); MWT 206:1(47 mm); MWT 210:1(44 mm)

Lobianchia sp.
MWT 213:1(48 mm)

Myctophum affine (Lütken, 1892)
MWT 123:8(16-33 mm); MWT 239:4(17-52 mm)

Myctophum nitidulum Garman, 1899
MWT 104:2(15-71 mm); MWT 166:1(15 mm); MWT 200:1(34 mm)

Myctophum selenops Tåning, 1928
MWT 190:2(11-36 mm); MWT 200:1(47 mm)

Notolychnus valdiviae (Brauer, 1904)
MWT 104:1(19 mm); MWT 123:1(19 mm); MWT 166:3(15-21 mm); MWT 175:2(11-20 mm); MWT 198:1(19 mm); MWT 221:1(18 mm); MWT 234:4(16-20 mm)

Notoscopelus resplendens (Richardson, 1845) [17, 0.4%, 1.1%, 4, 10.5%]
MWT 123:11(36-56 mm); MWT 213:4(45-57 mm); MWT 214:1(56 mm); MWT 221:1(42 mm)

Symbolophorus rufinus Tåning, 1928)
MWT 123:1(16 mm); MWT 175:1(26 mm); MWT 239:1(44 mm)

Taaningichthys minimus (Tåning, 1928)
MWT 239:1(27 mm)

GADIFORMES

Gadoidei

Melanonidae

Melanonus zugmayeri Norman, 1930
MWT 123:1(105 mm); MWT 127:1(120 mm)

Bregmacerotidae

Bregmaceros atlanticus Goode and Bean, 1886
MWT 104:1(28 mm); MWT 107:1(42 mm); MWT 123:1(35 mm); MWT 127:2(27-32 mm); MWT 213:1(55 mm)

Bregmaceros macclellandi Thompson, 1840
MWT 190:2(37-39 mm); MWT 216:1(48 mm)

Bregmaceros spp.
MWT 129:1(18 mm); MWT 175:3(18-27 mm); MWT 190:1(21 mm); MWT 200:1(26 mm); MWT 219:1(20 mm); MWT 247:2(20-25 mm)

Based on Houde et al. (1979) and Belyanina (1980), there are at least three species of *Bregmaceros* in the Gulf of Mexico. Using Belyanina (1974), we were able to identify our larger specimens as either *B. atlanticus* or *B. macclellandi.* However, due to the difficulty in counting anal and dorsal fin rays in small specimens, we have designated such specimens as *Bregmaceros* spp.

LOPHIIFORMES
Ceratioidei
Melanocetidae
Melanocetus murrayi Günther, 1887
MWT 247:1(49 mm)
Melanocotus sp.
MWT 200:1(12 mm)
Ceratiidae
Cryptopsaras couesi Gill, 1883
MWT 171:1(8 mm); MWT 187:1(11 mm); MWT 234:1(11 mm)

BERYCIFORMES
Cetomimoidei
Cetomimidae
Ditropichthys storeri (Goode and Bean, 1895)
MWT 200:1(31 mm)

This represents the first definitive record of this cetomimid for the Gulf of Mexico (see Harry 1952.)

Stephanoberycoidei
Melamphaidae (=Melamphaeidae of Nelson 1976, see Steyskal 1980)
Melamphaes pumilis Ebeling, 1962
MWT 200:1(18 mm); MWT 206:1(20 mm); MWT 213:1(17 mm); MWT 234:5(21-25 mm)
Melamphaes simis Ebeling, 1962
MWT 123:2(13-15 mm); MWT 166:1927 mm); MWT 171:3(17-28 mm); MWT 184:1(27 mm); MWT 192:2(20-21 mm)
Melamphaes typhlops (Lowe, 1843) [17, 0.4%, 1.1%, 4, 10.5%]
MWT 123:7(22-29 mm); MWT 200:5(19-28 mm); MWT 210:2 (21-25 mm); MWT 247:3(22-24 mm)
Melamphaes spp.
MWT 107:2(24-25 mm); MWT 206:3(18-27 mm)
Poromitra crassiceps (Günther, 1878)
MWT 190:1(88 mm)
Poromitra megalops (Lütken, 1877)
MWT 247:2(44-50 mm)

Scopeloberyx opisthopterus (Parr, 1933) [26, 0.6%, 1.7%, 9, 23.7%]
MWT 120:1(27 mm); MWT 123:2(19-28 mm); MWT 133:1(27 mm); MWT 143:1(28 mm); MWT 171:6(22-27 mm); MWT 200:2(26-27 mm); MWT 213:3(18-23 mm); MWT 221:2(22-26 mm); MWT 247:8(18-26 mm)

Scopeloberyx robustus (Günther, 1887)
MWT 120:1(18 mm); MWT 123:2(17-21 mm); MWT 153:1(40 mm); MWT 190:1(85 mm); MWT 200:1(24 mm); MWT 209:1(52 mm); MWT 219:2(11-14 mm)

Trachichthyoidei (=Berycoidei (in part) of Nelson 1976, see Zehren 1979)

Anoplogastridae (=Anoplogasteridae of Nelson 1976, see Steyskal 1980)

Anoplogaster cornuta (Valenciennes, 1833)
MWT 192:1(84 mm); MWT 206:1(16 mm)

Diretmidae

Diretmus argenteus Johnson, 1863 ?
MWT 247:1(13 mm)

Trachichthyidae

Gephyroberyx darwini (Johnson, 1866) ?
MWT 187:2(5-9 mm)

PERCIFORMES

Percoidei

Bramidae

Brama caribbea Mead, 1972
MWT 120:1(12 mm)

Pterycombus brama Fries, 1837
MWT 104:1(10 mm); MWT 156:1(17 mm)

Taracichthys longipinnis (Lowe, 1843)
MWT 175:1(9 mm)

Trachinoidei (=Trachinoidea of Nelson 1976, change due to ranking)

Chiasmodontidae

Kali spp. ?
MWT 120:1(32 mm); MWT 123:1(29 mm)

Scombroidei

Gempylidae

Diplospinus c.f. *multistriatus* Maul, 1948
MWT 156:1(163 mm); MWT 219:1(138 mm)

Promethichthys c.f. *prometheus* (Cuvier, 1832)
MWT 11:3(11-18 mm); MWT 107:1(13 mm); MWT 123:1(12 mm); MWT 187:1(28 mm); MWT 200:1(41 mm); MWT 247:2(15-16 mm)

Trichiuridae

Lepidopus c.f. *caudatus* (Euphrasen, 1788)
MWT 239:2(90-102 mm)

ACKNOWLEDGEMENTS

We acknowledge W. E. Pequenat and J. H. Wormuth for their help in making these collections available to us. We thank Janet Gomon (USNM) for identifying the species of *Eustomias*. The 1978 and 1979 classes in Systematic Ichthyology, Texas A&M University, also aided in identification of specimens. The manuscript benefitted from the review given it by John D. McEachran.

LITERATURE CITED

Anderson, M. E., G. M. Caillet, and B. S. Antrium. 1979. Notes on some uncommon deep-sea fishes from the Monterey Bay area, California, U.S.A. Calif. Fish Game 65(4):256-264.

Backus, R. H., J. E. Craddock, R. L. Haedrich, and B. H. Robison. 1977. Atlantic mesopelagic zoogeography. *In* Fishes of the western North Atlantic, Mem. Sears Found. Mar. Res. 1(7):226-287.

Baird, R. C., N. P. Thompson, J. L. Hopkins, and W. R. Weiss. 1975. Chlorinated hydrocarbons in mesopelagic fishes of the eastern Gulf of Mexico. Bull. Mar. Sci. 25(4):473-481.

Becker, V. E., Y. N. Scherbachev, and V. M. Chuvasov. 1975. (Deep-sea pelagic fishes of the Caribbean Sea, Gulf of Mexico, and Puerto Rican Trench.) Trudy Inst. Okeanol. (100):289-336. (In Russian).

Belyanina, T. N. 1974. (Material on the development, systematics, and distribution of the fishes of the family Bregmacerotidae.) Trudy Inst. Okeanol. (96):143-188. (In Russian).

Belyanina, T. N. 1980. Codlets (Bregmacerotidae, Osteichthyes) of the Caribbean Sea and the Gulf of Mexico. J. Ichthyol. (Engl. trans.) 20(1):138-141.

Bond, G. W., Jr., and K. A. Tighe. 1974. A diagnostic character for rapid identificaiton of lightly pigmented species of the genus *Cyclothone* (Gonostomatidae) in the North Atlantic. Copeia 1974 (1):272-275.

Bullis, H. R., Jr., and J. R. Thompson. 1965. Collections by the exploratory fishing vessels *Oregon*, *Silver Bay*, *Combat*, and *Pelican* made during 1956-1960 in the southwestern North Atlantic. U.S. Fish and Wildlife Service, SSR-F510. 130 p.

Bussing, W. A. 1965. Studies of the midwater fishes of the Peru-Chile Trench. Biol. Antarct. Seas II. Anarct. Res. Ser. 5:185:227.

Cohen, D. M. 1964. Suborder Argentinoidea. *In* Fishes of the western North Atlantic. Mem. Sears Found. Mar. Res. 1(4):1-70.

Craddock, J. E., and G. W. Mead. 1970. Midwater fishes from the eastern South Pacific Ocean. Anton Bruun Rep. 3, Sci. Res. of S. E. Pac. Exped. 46 p.

Grey, M. 1964. Family Gonostomatidae. *In* Fishes of the western North Atlantic. Mem. Sears Found. Mar. Res. 1(4):77-238.

Harry, R. R. 1952. Deep sea fishes of the Bermuda Oceanographic Expeditions. Families Cetomimidae and Rondeletiidae. Zoologica (N.Y. Zool. Soc.) 37:55-72.

Hoese, H. D., and R. H. Moore. 1977. Fishes of the Gulf of Mexico: Texas, Louisiana and adjacent Waters. Texas A&M University Press, College Station, TX. 327 p.

Houde, E. D., J. C. Leak, C. E. Dowd, S. A. Berkeley, and W. J. Richards. 1979. Ichthyoplankton abundance and diversity in the eastern Gulf of Mexico. Report to the Bureau of Land Management, contract no. AA550-CT7-28. 546 p.

Isaacs, J. D., and L. W. Kidd. 1953. Isaacs-Kidd midwater trawl. Scripps Inst. Oceanogr., Ref. 53-3. 21 p.

Kawaguchi, K. 1971. Gonostomatid fishes of the western North Pacific. Japan. J. Ichthyol. 18:1-16.

Morrow, J. E., Jr., and R. H. Gibbs. 1964. Family Melanostomiatidae. *In* Fishes of the western North Atlantic. Mem. Sears Found. Mar. Res. 1(4):351-511.

Nafpaktitis, B. G., R. H. Backus, J. E. Craddock, R. L. Haedrich, B. H. Robison, and C. Karnella. 1977. Family Myctophidae. *In* Fishes of the western North Atlantic. Mem. Sears Found. Mar. Res. 1(7):13-258.

Nelson, J. S. 1976. Fishes of the world. John Wiley & Sons, Inc., N.Y. xvi + 416 p.

Parr, A. E. 1960. The fishes of the family Searsidae. Dana-Report No. 51. 108 p.

Rofen, R. R. 1966. Family Evermannellidae. *In* Fishes of the western North Atlantic. Mem. Sears Found. Mar. Res. 1(5):511-565.

Rosen, D. E. 1973. Interrelationships of higher euteleostean fishes, p. 397-513. *In* P. H. Greenwood, R. S. Miles, and C. Patterson (Eds.), Interrelationships of fishes. Academic Press, New York, N.Y.

Shores, D. L. 1969. Postlarval *Sudis* (Pisces: Paralepididae) in the Atlantic Ocean. Breviora (334):1-14.

Steyskal, G. C. 1980. The grammar of family-group names as exemplified by those of fishes. Proc. Biol. Soc. Wash. 93(1):168-177.

Weitzman, S. H. 1974. Osteology and evolutionary relationships of the Sternoptychidae, with a new classification of stomiatoid families. Bull. Am. Mus. Nat. Hist. 153:329-478.

Wisner, R. L. 1976. New data on the rare alepocephalid fish *Photostylus pycnopterus*. Bull. South. Calif. Acad. Sci. 75(2):153-158.

Zehren, S. J. 1979. The comparative osteology and phylogeny of the Beryciformes (Pisces: Teleostei). Evol. Monogr. 1:1-389.

IN VITRO ANALYSIS OF TRANSFER FACTOR ACTIVITY IN GUINEA PIG LEUKOCYTE EXTRACTS BY THE AGAROSE DROP ASSAY

by ANDREW PAQUET, JR.

Biology Department
Texas Christian University
Fort Worth, TX 76129

and GEORGE B. OLSON and C. G. DRUBE

Department of Microbiology
University of Arizona
Tucson, AZ 85721

ABSTRACT

The agarose drop migration inhibition test of Harrington and Stastny was used for *in vitro* assay of transfer factor (TF) activity in leukocyte extracts from guinea pigs sensitized to *Listeria monocytogenes*. These cell-free extracts were also assayed by passive transfer of delayed hypersensitivity-type skin reactions. Only the combination of TF plus specific *Listeria* antigens caused significant migration inhibition *in vitro*; neither substance alone was effective. However, TF preparations could be incubated simultaneously with normal peritoneal exudative cells plus *Listeria* antigens to produce migration inhibition in 18 hours. This procedure eliminates the need for incubation of cells with TF prior to antigen addition, thus saving considerable time over some previously used assays. Migration inhibition factor (MIF) was able to inhibit macrophage migration in the absence of antigen, whereas gamma globulin from sensitized animals had no effect on this *in vitro* assay. The most active TF preparations were in the molecular weight fractions between 500 and 10,000. Because this assay requires fewer cells and can be performed with much smaller volumes of leukocyte preparations than capillary tube assays, it together with the *Listeria*-sensitized guinea pig, comprises a good animal model for *in vivo* and *in vitro* studies of TF activity.

INTRODUCTION

Cellular immunity is important in combatting many microbial infections, in rejecting foreign tissue transplants, and in tumor suveillance. One of the active materials believed responsible for these expressions of cellular immunity has been termed "transfer factor" (Lawrence and Pappenheimer 1956). Transfer factor from human leukocyte extracts has been studied and characterized extensively (Lawrence 1971). Its use in the clinical treatment of immunodeficiency disease, infectious diseases, and cancers has been promising (Fudenberg el al. 1974). However, study of the exact mode of action of transfer factor has been ham-

pered by the lack of good *in vitro* assays (Petersen and Kirkpatrick 1979). Success in assaying transfer factor activity by *in vitro* lymphocyte transformation has been reported (Arala-Chaves et al. 1974; Ascher et al. 1974); yet, this technique has been criticized (Petersen and Kirkpatrick 1979) as inconsistent and not dependent on the antigen-specific sensitivities of the transfer factor donor. Other investigators (e.g. Salaman 1974) have used the capillary tube migration inhibition test successfully. Apparently, transfer factor has the ability to cause normal peritoneal exudative cells, cultured with mixtures of specific transfer factor and antigen, to respond to the specific antigen by producing migration inhibition factor (MIF). The disadvantage of the capillary tube assay is that large numbers of cells are required and some methods require 36-48 hours to complete. A positive correlation between skin-test results and the inhibition of human peripheral blood leukocyte migration *in vitro* from wells cut in agarose plates has also been reported (Wilson et al. 1979) but, again, large numbers of leukocytes are required.

Transfer factor from leukocyte extracts and from "incubation fluids" of other cells of the guinea pig has also been described (Burger and Jeter 1971). Additionally, Dunnick and Bach (1975, 1977) reported *in vitro* analysis of guinea pig transfer factor by capillary tube migration inhibition assay. Yet, they did not report any *in vivo* results, and their assay required more cells and a longer incubation time (38-60 h) than we describe in this study. Nevertheless, these studies indicate that guinea pig transfer factor has many characteristics in common with human transfer factor. The guinea pig thus offers an animal model to study both *in vivo* and *in vitro* activities of transfer factor.

The purpose of the present paper is two-fold: First, to report on the production and characterization, both *in vivo* and *in vitro*, of transfer factor activity in leukocyte extracts from guinea pigs sensitized to *Listeria monocytogenes*; and second, to report on the agarose drop migration inhibition test as an *in vitro* assay for transfer factor. The agarose drop assay of Harrington and Stastny (1973) is technically simple and requires only small amounts of media and cells; usually enough can be obtained from a single animal for several hundred wells. This eliminates the variability caused by using pools of cells from several animals.

MATERIALS AND METHODS

Animals and Antigen

Hartley guinea pigs of either sex were used. The animals were housed in individual cages and were given Purina guinea pig chow, fresh cabbage, and water supplemented with ascorbic acid (300 mg/liter).

Listeria monocytogenes was grown in tryptose phosphate broth (Difco) in a New Brunswick fermentor at 37 C for 48 h with constant stirring and aeration. The culture was killed by treatment with an equal volume of 2% Formalin for 24 h at room temperature, then centrifuged. The killed organisms then were washed seven times with 0.15 M saline, pH 7.2; suspended in distilled H_20; sonicated; lyophilized; and, stored at 4 C. Endotoxin content was determined to be less than 0.5 ng/ml via the *Limulus* assay (Sigma).

Sensitization and Skin Testing

Guinea pigs (500 g) were sensitized to the *Listeria* antigens by subcutaneous injection, into three sites in the back of the neck, of 1 mg of the antigen emulsified in Freund's incomplete adjuvant (1 ml volume).

Three weeks following sensitization, the guinea pigs were skin tested by intradermal injection of 10 ug of *Listeria* antigen (0.1 ml) at previously shaved (24 h prior) surfaces of the abdomen. Skin-test sites were observed immediately and at 6 and 24 h following the injection. Length and width of any erythematous induration were measured to the nearest millimeter and recorded. Passive transfer recipients were skin-tested 48 h after the intraperitoneal (IP) injection of the various leukocyte extracts or other factors and the skin reactions were observed at 0, 6, 24, 48 and 72 h.

Collection of Leukocytes and Serum from Actively Sensitized Animals

Two days prior to skin testing, 20 ml of sterile light mineral oil was injected IP into each donor guinea pig to induce peritoneal exudative cells. On the day after skin testing, the animals were sacrificed by cervical dislocation, exsanguinated and the peritoneal exudates were harvested by washing out the peritoneal cavity with approximately 200 ml of ice-cold Hanks' balanced salt solution (HBSS). Cervical and suprascapular lymph nodes and spleens were removed at the same time and teased apart into ice-cold HBSS. All cell populations were washed three times and certrifuged (400 $\times$ *g*, 10 min) in a refrigerated centrifuge. Cells were collected quickly and kept at 4 C until put into culture media. Serum was collected and fractionated by Geon Pevikon block electrophoresis to obtain the gamma globulin fraction according to the procedure of Fahey and McLaughlin (1963).

Preparation of Guinea Pig Transfer Factor (TF)

Transfer factor was prepared according to the procedure of Burger and Jeter (1971), from peritoneal exudates, lymph node cells, and spleen cells obtained from sensitized animals. In brief, 10^9 cells were incubated in 7.5 ml of HBSS for 4 h at 37 C in a water bath with intermittent shaking. The incubation fluid was centrifuged (800 $\times$ *g*)

for 10 minutes, then desalted and concentrated by ultrafiltration on an Amicon UM05 membrane and then lyophilized. The salt-free material retained by the UM05 membrane (Transfer Factor) was stored at −20 C or used immediately in passive transfer experiments. Control TF was prepared in the same manner, except with cell populations from non-sensitized animals.

Preparation of Guinea Pig Migration Inhibition Factor (MIF)

Peritoneal exudative cells from sensitized animals were cultured at a concentration of 2.5×10^{-7} cells/ml in TC 199 medium [penicillin (100 U/ml), streptomycin (100 ug/ml), and 0.01 M HEPES buffer and no serum] and 5 ug of *Listeria* antigen/ml for 24 h at 37 C in a humidified air incubator. The cells were removed by centrifugation ($800 \times g$, 10 min) and the supernatant fluid was desalted and concentrated by ultrafiltration on an Amicon UM05 membrane, lyophilized, and stored at −20 C. Control MIF was also prepared in the same manner, except with cells from non-sensitized animals.

Passive Transfer of Activity

Transfer factor, MIF and gamma globulin preparations were injected IP into normal, 300-g guinea pigs. The concentration of TF was equivalent to material obtained from 10^9 cells, and an average of 5 mg of MIF and gamma globulin was injected. Protein concentrations of MIF and gamma globulin were determined by the method of Lowry et al. (1951).

The activity of TF *in vitro* was assayed by using a slight modification of the agarose drop migration inhibition test of Harrington and Stastny (1973). The various TF, MIF, and gamma globulin preparations were assayed for their ability to inhibit the migration of normal guinea pig peritoneal exudative macrophages in the presence and absence of antigen. One-microliter agarose droplets containing 5×10^5 cells were dispensed in flat-bottom microtiter plates (Falcon, Microtest II) without precoating the wells with agarose. The droplets of cells were gelled by placing in the refrigerator for 5 minutes. The medium used for the cell suspension was TC-199 medium containing 15% normal guinea pig serum (heated 56 C, 30 min), streptomycin (100 ug/ml), penicillin (100 U/ml), 0.2% agarose, and 0.01 M HEPES buffer. Each well containing an agarose droplet of cells was then filled (0.3 ml) with TC-199 medium alone (without agarose) or TC-199 medium containing the various factors to be tested with or without *Listeria* antigen. The chambers were incubated at 37 C in humidified air for 18 to 24 h before the distances of cellular migration were determined. All materials were tested in quadruplicate. Inhibition was considered significant when the percent migration dropped below 80%. The range of variation observed

TABLE 1. Skin test reactions in non-sensitized and *Listeria* sensitized guinea pigs. Products represent length × width (both in mm) of erythematous induration following injection with 10 ug *Listeria* antigen.

Non-sensitized			Antigen-sensitized		
Animal	6 hr.	24 hr.	Animal	6 hr.	24 hr.
1	1 × 1[a]	1 × 1	1	4 × 6	5 × 8
2	1 × 1	2 × 2	2	1 × 1	20 × 21
3	1 × 1	1 × 1	3	1 × 1	11 × 11
4	1 × 1	1 × 1	4	1 × 1	11 × 12
5	1 × 1	2 × 2	5	2 × 2	13 × 15
6	1 × 1	1 × 1	6	1 × 1	11 × 12
7	1 × 1	2 × 2	7	1 × 1	11 × 12
8	1 × 1	1 × 1	8	2 × 2	10 × 10
9	1 × 1	1 × 1	9	1 × 1	11 × 12
10	1 × 1	2 × 2	10	1 × 1	8 × 9
			11	4 × 4	10 × 10
			12	1 × 1	12 × 12
			13	1 × 1	1 × 11
			14	2 × 2	5 × 7
			15	1 × 1	11 × 12
Average	1 × 1	1.4 × 1.4		1.6 × 1.6	10.6 × 11.6

[a]Animals with no visible skin reactions were scored as 1 × 1 in order to have a numerical average for comparison.

in data from this technique is quite small; typically, 95% confidence limits about the means of distances of migration amount to only $\bar{X} \pm 5\%$ (Paquet et al. 1975).

Molecular Weight Determinations

The molecular weight of the fractionated transfer-factor preparation was determined by using a thin layer gel filtration apparatus (Pharmacia) with superfine Sephadex G-75. The migration distances of the TF fractions were compared with those of known molecular weight standards.

RESULTS

Table 1 presents data from non-sensitized and *Listeria*-sensitized animals when skin tested with 10 ug of the *Listeria* antigen. Skin-test reactions in non-sensitized animals were negative at 6 and 24 h. Sensitized animals showed minimal reactions at 6 h and strong positive reactions 24 h after testing (avg. diameters of erythema and induration, 11 × 12 mm).

Histological evaluation of these positive reactions showed the classical responses of mononuclear cellular inflitration throughout the epidermis and dermis to the striated muscle layer. In some cases, large

deposits of cells were noted in the papillary layer of the dermis. Even animals with minimal skin reactions (5 × 5 mm) showed considerable mononuclear cell infiltration.

Passive transfer recipients were tested with the same concentration of antigen (10 ug) and only reactions involving 5 × 5 mm or greater erythema and induration were considered positive.

Since the agarose drop migration inhibition test was to be used to assay for transfer factor *in vitro* and as a direct migration inhibition test to detect *in vivo* sensitization of TF recipients, its credibility first had to be established by testing peritoneal exudative cells from non-sensitized, but skin-tested animals. Cells from ten such animals (those listed in Table 1) were tested. Average migration was 102 % that of controls. Hence, the skin testing of a non-sensitized animal did not appear to cause positive migration inhibition *in vitro* three days later. Apparently the amount of antigen in a skin test is not enough to sensitize an animal (i.e., not enough to convert a migration inhibition test from negative to positive). However, peritoneal exudative cells from sensitized donors when tested in the presence of antigen always showed inhibition of migration, with distances comparable to only 40-70 % of the control values.

Table 2 shows a summary of passive-transfer attempts and macrophage migration inhibition assays for different batches of transfer factor, migration inhibition factor, and serum gamma globulin. Sometimes we did not have enough material for both *in vivo* and *in vitro* assays. Generally when the transfer-factor preparations caused a positive passive transfer (11 positive/ 13 attempts, 84 %), the same preparation would cause a positive inhibition of macrophage migration (values in Table 3) in the presence of the *Listeria* antigen, and no inhibition in the absence of antigen. The MIF preparations, on the other hand, were able to inhibit macrophage migration in the absence of antigen. Serum gamma globulin as a control had no effect in either assay. Control or "mock" transfer factor and MIF preparations, prepared from normal cells by the same procedure used for sensitized cells, did not inhibit macrophage migration and did not cause passive transfer to recipients.

In further experiments, the recipients of two different TF (TF 1 and 3) and two different MIF (MIF 2 and 4) preparations were injected IP with sterile mineral oil on the day of skin testing (Table 2). Three days later, the peritoneal exudative cells were removed and assayed in a direct migration inhibition test to determine if the passive transfer of *Listeria* sensitivity could be detected by *in vitro* tests. Cells from the 4 recipients of TF-1 and the 2 recipients of TF-3 showed positive inhibition of macrophage migration in the presence of the *Listeria* antigen (34-38 %); yet, it should be noted that recipients of the TF-3 preparation

TABLE 2. Summary of *in vitro* and *in vivo* activity of leukocyte factors from *Listeria*-sensitized guinea pigs.

	Inhibition of Macrophage Migration *in vitro*[a]		Passive Transfer of Sensitivity *in vivo*	
Factor	Antigen absent	Antigen present	Skin Test Reactions	Recipient MMI[c]
TF 1	No	N.D.[d]	12,10,8,8(4^+/4)	Yes, 34%
TF 3	No	Yes	3,4(0^+/2)	Yes, 38%
TF 5	No	Yes		
TF 7	No	Yes		
TF 8	No	Yes		
TF 9	N.D.	N.D.	8(1^+/1)	
TF 10	No	Yes	8(1^+/1)	
TF 12	No	Yes	8(1^+/1)	
TF 14	No	Yes	5(1^+/1)	
TF (>10^4MW)[e]	No	Yes	8,8(2^+/2)	
TF (<10^4MW)[e]	No	Yes	8(1^+/1)	
MIF 2	Yes	N.D.	-[f],6,8,8($^+$/4)	Yes, 21%
MIF 4	Yes	N.D.	-,-(0^+/2)	No, 4%
MIF 6	Yes	Yes		
MIF 11	Yes	Yes		
MIF (>10^4MW)[e]	Yes	Yes		
MIF (<10^4MW)[e]	No	No		
gamma globulin	No	No	-,-,-,-(0^+/4)	

[a]Percent migration values of these factors are given in Table 3.

[b]Recipient skin test avg. diameter in mm (number positive/number tested).

[c]MMI = Macrophage migration inhibition of cells from passive transfer recipient, recorded as percent inhibition.

[d]N.D. denotes not done.

[e]Fractions with molecular weights greater than (>) or less than (<) 10,000.

[f]-denotes no visible reaction.

were negative by skin-test standards. As shown earlier (see Table 1), the injection of antigen for skin testing would not have been responsible for the positive macrophage migration inhibition responses. Cells from recipients of the MIF preparations gave variable results. Three of four animals treated with the MIF-2 preparation became skin-test positive and cells from these animals demonstrated borderline inhibition of macrophage migration in the presence of antigen (21 %). Animals treated with the MIF-4 preparation did not become skin-test positive, and the cells of these recipients were not inhibited from migrating in the presence of antigen.

Table 3 shows the average values from ten experiments for the migration of normal peritoneal exudative cells when cultured with the different TF preparations from Table 2. In the absence of antigen the crude TF had little effect on the migration of normal cells; however, in the presence of antigen and transfer factor simultaneously there was

TABLE 3. Percent migration of normal peritoneal exudative cells incubated *in vitro* with leukocyte extracts from *Listeria* sensitized guinea pigs.

Type of material	Concentration of material (ug/ml)	Concentration of *Listeria* antigen (ug/ml)	
		0	5
Crude TF extracts	800[a]	83	58
	400	91	72
	200	93	68
Fraction from TF	800	78	54
with MW greater	400	83	59
than 10,000[b]	200	93	68
Fraction from TF	125	75	57
with MW between	60	74	66
500 and 10,000[c]	30	80	66
Media alone	-	100	90

[a]Mean values from separate assays on nine different preparations.
[b]Material > 10,000 M.W. retained by Amicon P-10 membrane. Actual M.W. determined to be 20,000 by gel filtration.
[c]Material < 10,000 M.W. passing through P-10 membrane but retained by Amicon UM05 membrane.

significant reduction (values 54-72 %) compared to the cell controls. The responses appeared concentration-dependent, and the higher concentrations of TF alone seemed to cause slight inhibition (83 % migration).

One TF preparation (TF-13) was fractionated into components with M.W. greater than 10,000 and into components with M.W. between 500 and 10,000. Both fractions caused inhibition of migration of macrophages in the presence of antigen. The effect was more pronounced in the presence of the 500-10,000 M.W. fraction. Some non-antigen dependent inhibition was noted at the higher concentratins with the 500-10,000 M.W. material.

Table 4 shows the effect of MIF and serum gamma globulin on the migration of normal peritoneal exudative cells when tested in the same manner. Crude MIF was active in the absence of antigen and, when fractionated, the activity remained in the preparation having substances with M.W. greater than 10,000. Data shown in Tables 3 and 4 suggest that fractions with M.W. greater than 10,000 may have been contaminated with TF as both fractions showed an antigen-dependent inhibition of macrophages. Gamma globulin preparations had essentially no effect on the migration of normal peritoneal exudate cells in the presence or absence of antigen.

DISCUSSION

The sensitization of guinea pigs to *Listeria monocytogenes* offers an animal model for study of cellular immunity. Sensitization of animals

TABLE 4. Percent migration of normal peritoneal exudative cells incubated *in vitro* with MIF and gamma globulin.

Type of material	Concentration of material (ug/ml)	Concentration of *Listeria* antigen (ug/ml)	
		0	5
MIF	400[a]	58	56
Fraction from MIF	800	61	55
with MW greater	400	75	55
than 10,000[b]	200	96	66
Fraction from MIF	200	100	92
with MW between	100	105	94
500 and 10,000[c]			
Gamma globulin	400[d]	115	93
	200	107	103
	100	115	96
Media alone	-	100	90

[a]Mean values from separate assays on five different MIF preparations.
[b]Material > 10,000 M.W. retained by Amicon P-10 membrane.
[c]Material < 10,000 M.W. passing through P-10 membrane but retained by Amicon UM05 membrane.
[d]Mean values from separate assays on two different gamma globulin preparations.

was easily established as evidenced by skin-test results done 3 weeks later. The skin tests showed typical delayed-type responses, with mononuclear cell infiltration and visible erythematous induration reaching a peak after 48 hours.

Transfer factor was easily obtained from *Listeria*-sensitized guinea pigs, provided a conscientious effort was made to keep the cells cold and to do the processing quickly. Transfer factor preparations were effective in achieving passive transfer of sensitivity to recipient guinea pigs as measured by skin testing (11 positive/13 attempts, 84 % success). This success rate is comparable to that obtained with human dialyzable transfer factor (Spitler 1979). Ours, we believe, is the first report of passive transfer with cell-free extracts using a *Listeria* model.

Migration inhibition factor also was easily obtained by culturing *Listeria*-sensitive cells in the presence of the antigen. In one case, an MIF preparation (MIF-2) appeared to cause the passive transfer of antigen specificity to recipients. The positive transfer with MIF-2 may be due to the presence of antigen in the preparation, although the time interval of 48 h prior to skin testing of recipients is quite short for active sensitization to have developed. Sensitized human cells mixed with antigen may release TF into the supernatant (Lawrence 1971). This possibly could occure in the guinea pig system also.

The agarose drop migration inhibition test of Harrington and Stastny (1973) was easily adapted to assay the biological activity of transfer factor and to compare the activities of TF, MIF and gamma

globulin. The agarose drop assay has several advantages over the capillary tube method. It certainly requires fewer cells and less incubation time than the method of Dunnick and Bach (1975). The agarose drop assay should be a considerable aid in studying the mode of action of purified TF preparations that may be available only in limited amounts.

Ten different batches of TF were assayed by the agarose drop migration inhibition test. Transfer factor activity was detected routinely and appeared to correlate with results obtained by skin test. The TF preparation TF-3 was positive by the agarose drop assay, but negative by skin test standards (3-4 mm), although this diameter is double the average value of non-sensitized, skin-test controls (Table 1). Furthermore, the histology of these reactions showed mononuclear cell infiltration exceeding that of control sites. Hence, study of the biological activity of TF on the basis of skin testing alone would be quite limiting. It is therefore most appropriate to have other measurements such as the *in vitro* migration inhibition test.

Transfer factor preparations showed little effect on the migration of normal peritoneal exudative cells unless the specific antigen was present. Then, the migration was considerably reduced in a concentration-dependent way. This agrees with data obtained by the capillary tube method (Salaman 1974). However, both antigen-dependent and independent migration inhibition have been reported for human dialyzable leukocyte extracts (DLE). Wilson et al. (1979) report that with high amounts of DLE, a non-cytotoxic antigen-independent leukocyte migration inhibition occurs which may be accompanied by antigen-dependent specific migration inhibition, the latter activity denoting the presence of TF in DLE.

The apparent specificity of the TF preparation was studied in a few experiments where normal peritoneal exudative cells were cultured in the presence of *Listeria* TF and either *Listeria* antigens or *Candida albicans* antigens. These studies showed inhibition of macrophage migration only when the specific *Listeria* antigen was present.

The agarose drop assay with MIF and gamma globulin preparations showed distinctly different responses. The MIF, as expected, was capable of strong inhibition of macrophage migration in the absence of antigen. Upon fractionation, all the MIF activity remained in the fraction above 10,000 M.W., which agrees with the 35,000-65,000 M.W.-values reported for guinea pig MIF (Bennett and Bloom 1968; Remold, et al., 1972). This fractionated MIF preparation may also contain some TF activity, as some antigen dependent inhibition was occasionally noticed. Unlike the TF fractions, the smaller molecular weight fractions from MIF preparations were devoid of activity. Likewise, gamma

globulins had essentially no effect, evidencing the cellular nature of immunity to Listeria.

Until now, there has been concern regarding the lack of animal models with which to characterize TF. Our *Listeria* system would seem more than adequate, but regardless of the sensitizing antigen, the agarose drop migration inhibition test provides a simple micromethod for *in vitro* studies with transfer factor and other biological factors.

ACKNOWLEDGEMENTS

This research was supported in part by a grant from the TCU Research Foundation and a grant from Schering Corporation, Bloomfield, New Jersey.

LITERATURE CITED

Arala-Chaves, M., M. T. F. Ramos, R. Rosado, and P. Branco. 1974. Transfer factor in vitro. Int. Arch. Allergy 46:612-618.

Ascher, M. S., W. J. Schneider, F. T. Valentine, and H. S. Lawrence. 1974. In vitro properties of leukocyte dialysates containing transfer factor. Proc. Nat. Acad. Sci. USA 71:1178-1182.

Bennett, B., and B. R. Bloom. 1968. Reactions in vivo and in vitro produced by a soluble substance associated with delayed type hypersensitivity. Proc. Natl. Acad. Sci. USA 59:756-762.

Burger, D. R., and W. S. Jeter. 1971. Cell-free passive transfer of delayed hypersensitivity to chemical in guinea pigs. Infect. and Immunity. 4:575-580.

Dunnick, W., and F. H. Bach. 1975. Guinea pig transfer factor-like activity detected in vitro. Proc. Natl. Acad. Sci. USA 72:4573-4576.

Dunnick, W., and F. H. Bach. 1977. Specificity and structural analysis of a guinea pig transfer factor-like activity. J. Immunol. 118:1944-1950.

Fahey, J. L., and C. McLaughlin. 1963. Preparation of antisera specific for 6.6s γ-globulins, β_{2A}globulins, γ-macroglobulins, and for type I and II common γ-globulin determinants. J Immunol. 91:484-497.

Fundenberg, H. H., A. S. Levin, L. E. Spitler, J. Wybran, and V. Byers. 1974. The therapeutic uses of transfer factor. Hospital Practice, Jan:95-104.

Harrington, J. T., and P. Stastny. 1973. Macrophage migration from an agarose droplet: Development of a micromethod for assay of delayed hypersensitivity. J Immunol. 110:752-759.

Lawrence, H. S. 1971. Transfer factor and cellular immunity, p. 104-113. *In* R. A. Good and D. W. Fischer (Eds.), Immunobiology. Sinauer Associates, Inc., Stamford, Connecticut.

Lawrence, H. S., and A. M. Pappenheimer, Jr. 1956. Transfer of delayed hypersensitivity to diptheria toxin in man. J. Exp. Med. 104:321-336.

Lowry, D. H., H. J. Rosenbrough, and R. J. Randall. 1951. Protein measurement with the folin phenol reagent. J. Biol. Chem. 193:264-275.

Paquet, A., Jr., E. D. Rael, and G. B. Olson. 1975. Cellular immunity in *Listeria* sensitized young chickens: assayed by an agarose drop macrophage migration inhibition test. Microbios 14:175-182.

Petersen, E. A., and C. H. Kirkpatrick. 1979. Nature and analysis of transfer factor, p. 216-227. *In* H. Friedman (Ed.), Subcellular factors in immunity. Annals of the New York Academy of Sciences, vol. 332.

Remold, H. G., R. A. David, and J. R. David. 1972. Characterization of migration inhibition factor from lymphocytes stimulated with Concanavalin A. J. Immunol. 109:578-586.

Salaman, M. R. 1974. Studies on the transfer factor of delay hypersensitivity. Immunology 26:1069-1080.

Spitler, L. E. 1979. Transfer factor in immunodeficiency diseases, p. 228-235. *In* H. Friedman (Ed.), Subcellular factors in immunity. Annals of the New York Academy of Science, Vol. 332.

Wilson, G. B., H. H. Fundenberg, and G. V. Paddock. 1979. Detection of a "dialyzable transfer factor" in vitro: Structural and chemical characterization of the activity specific for tuberculin, p. 579-590. *In* H. Friedman (Ed.), Subcellular actors in immunity. Annals of the New York Academy of Sciences, vol. 332.

VARIATION IN TRANSPLANTABLE TUMOR GROWTH-PARAMETERS CAN BE REDUCED [1,2,3]

by DAVID G. MORRISON [a,b,4], MARY PAT MOYER[a,b], JAY C. DANIEL[b], WAID ROGERS[b], *and* REX C. MOYER[a]

[a]*Thorman Cancer Research Laboratory*
Trinity University, San Antonio, TX 78284
[b]*Department of Surgery, The University of Texas*
Health Science Center, San Antonio, TX 78284

ABSTRACT

The conventional procedure for transplanting rodent tumors was improved by continuous stirring of the tumor brei or ascites tumor cells with a magnetic stirrer at 500-800 rpm and 4 C, then vigorously shaking the suspension-filled syringe immediately prior to injection. In each case, these extra steps produced better results than the standard procedure without continuous stirring of the tumor brei. The standard and modified procedures were compared in four different transplantable tumor/mouse systems—C3H mammary adenocarcinoma (C3HMA) in C3H/HeJ mice, Lynd A/J mammary adenocarcinoma in A/J mice, P388 lymphocytic leukemia in CDF_1 mice. The modification required neither enzymatic treatments nor significantly more time and effort to yield reproducible results with regard to the uniformity of the resulting tumor growth parameters (survival and tumor growth). *Key Words:* transplantable tumors, mammary adenocarcinoma, transplantation techniques.

INTRODUCTION

Transplantable rodent tumors are used in many aspects of cancer research, including the screening of potential cancer chemotherapeutic agents. Statistically acceptable ranges of host survival time and solid-turmor growth-parameters have been well defined (Goldin et al. 1977). This paper describes a simple modificaiton of a widely used tumor transplantation technique (Goldin et al. 1977) that results in more uniform tumor growth-parameters. The few extra steps significantly reduce the amount of variability in host survival time and in solid tumor

[1]This work was supported by the Thorman Trust and The Robert J. Kleberg and Helen C. Kleberg Foundation of Trinity University and by the Department of Surgery of The University of Texas Health Science Center, San Antonio, TX 78284. The technical assistance of Mr. Gay Morrison, Jr., Miss Denise Miller, and Miss Leticia Soria is gratefully acknowledged.

[2]Address correspondence to Dr. Rex C. Moyer, Thorman Cancer Research Laboratory, Trinity Univeristy, 715 Stadium Drive, San Antonio, TX 78284.

[3]Lynd A/J mammary adenocarcinoma designated in memory of our deceased colleague, Dr. Frederick T. Lynd.

[4]Present Address: Depart. of Cell Biology, Baylor College of Medicine, Houston, TX 77030.

growth; therefore, the number of animals required to achieve statistically reliable results can be reduced.

MATERIALS AND METHODS

Solid and ascites tumors were harvested and prepared for injection essentially in accordance with the conventional method as described by Goldin et al. (1977). The only differences between the conventional method and the technique used in this study are that suspensions of tumor brei or ascites tumor cells were stirred continuously during preparation and loading of the syringes, each of which was vigorously agitated by hand immediately prior to injection to prevent clumps of tumor cells from plugging the needle. For injecting mice, we used 23 or smaller gauge needles to avoid creating large wounds that might result in tumor contamination. A magnetic stirrer and magnetic stir bar (Nalgene 6600-035), which minimizes air bubble formation, were used to stir the solutions at 500 to 800 rpm. The sterile vessel containing the diluted brei or ascites fluid was maintained at 4 C during preparation of transplant material and loading of syringes in a biohazard hood. In all experiments reported, the animals were injected with tumor material from the same donor, and samples of tumor preparation were inoculated into brain-heart infusion, tryptose phosphate, and thioglycollate broths to check sterility. One beaker of tumor material was kept at 4 C as described and the other beaker of tumor material was kept at 4 C and only gently agitated by hand, equivalent to 20 to 30 rpm, just prior to loading each syringe.

Animals were injected either subcutaneously or intraperitoneally with 0.05 grams harvested tumor brei or 10^6 ascites tumor cells. The C3HMA mammary adenocarcinoma (obtained from National Cancer Institute) was studied in female C3H/HeJ mice weighing 20-22 grams (Jackson Lab, Bar Harbor, Maine). The Lynd[3] A/J solid and ascites tumors were derived from a spontaneous mammary adenocarcinoma of an eight-week-old female A/J mouse in the laboratory of W. Rogers. The Lynd A/J solid and ascites tumors were tested in female A/J mice (Jackson Lab, Bar Harbor, Maine) weighing 20-22 grams. The P388 lymphocytic leukemia (obtained from EG & G Mason Research Institute, Worcester, Massachusetts) was studied in female CDF_1 mice (BALB/c $\times$ DBA/2, F_1; Lab Animal Supply Co., Indianapolis, Indiana) weighing 20-22 grams. The J774A.1 reticulum cell sarcoma (obtained from Mr. Bradly Fox, Cell Distribution Center, Salk Institute, San Diego, California) was studied in male and female CDF_1 mice (Lab Animal Supply Co., Indianapolis, Indiana) weighing 20-22 grams.

Animals were observed daily. Solid tumor diameters were measured every three days with a Vernier caliper, and the day of death was

TABLE 1. Reduction of variation in survival times (days).

Tumor	P388 Ascites		Lynd A/J Ascites Tumor		Lynd A/J Solid Tumor	
Method	Standard	Modified	Standard	Modified	Standard	Modified
Number of mice/group	50	50	12	12	11	12
Mean ± s.e.m.[a]	12 ± 0.2	12.0 ± 0.1	24.5 ± 0.9	22.3 ± 0.4	32.9 ± 3.2	34.2 ± 0.9
Median	12	12	25	22	33	33
Mode (times observed)	12(19)	12(35)	22(3)	21,22, or 23(3 ea)	31(2)	31,33 or 37(3 ea)
Range	9-14	11-13	21-32	20-25	18-57	30-39
Variance	1.4	0.3	10.5	2.0	109.7	10.3
Variance ratio for F test	4.67		5.25		10.65	
Level of significance of difference between variances	$P < 0.005$		$P < 0.010$		$P < 0.005$	
Calculated sample size (mice/group for future experiments)	13	3	25	5	105[b]	10[b]

[a]s.e.m.: standard error of the mean.

[b]$P = 0.001$ for confidence level in all tests except this one where $P = 0.050$ was used.

TABLE 2. Reduction of variation in solid-tumor growth-parameters.[a]

Tumor	Lynd A/J		C3HMA	
Method	Standard	Modified	Standard	Modified
Number of mice/group	11	12	25	25
Mean ± s.e.m.	3.4 ± 0.5[b]	4.9 ± 0.2[b]	6.3 ± 0.7[c]	7.0 ± 0.1[c]
Median	3.2	5.2	7.5	7.0
Mode	NA[d]	NA[d]	0(5)	7(18)
Range	0.8 - 6.1	2.9 - 6.0	0.0 - 12.0	6.0 - 8.0
Variance	2.8	0.8	13.3	0.30
Variance ratio for F test	3.5		44.33	
Level of significance of difference between variances	$p < 0.50$		$p < 0.005$	
Calculated sample size[e] mice/group for future experiments	27	8	32	3
Power of sample size test	$p = 0.001$		$p = 0.001$	

[a]The same conclusions were reached when the length and width were put into formulas used to calculate volume or estimate mass.

[b]Tumor area (cm^2) based on greatest perpendicular diameters 15 days after injection; mean ± s.e.m. (standard error of mean).

[c]Greatest diameter (mm) 10 days after injection; mean ± s.e.m.

[d]Not applicable.

[e]These are the "d" values used in the formula to calculate the number of mice needed per group in future experiments to obtain reliable results at the powers indicated.

recorded. Statistical analyses of experiments were performed according to Daniel (1977) to determine the number of mice per group that will probably provide statistically reliable data in the future according to this formula:

$$n = z^2 \cdot \sigma^2 / d^2$$

where n = expected number of animals needed in future experiments; z = desired level of confidence from standard normal table; σ^2 = variance in present experiment; and d = one-half of the width of the acceptable confidence interval selected by investigator.

We used d = 2 days for all projections relative to survival-time studies (Table 1) and d = 1. cm and 0.2 cm for the Lynd A/J and C3HMA projections (respectively) given in Table 2.

RESULTS AND DISCUSSION

The modified transplantation method effectively reduced the variation in survival times of animals injected with ascites or solid tumors (Table 1), when compared with the standard method. Favorable results

TABLE 3. Calculation of test power and sample size for future experiments using modified method.

Number Animals Injected[a]	Number Control Animals	Mean ± s.e.m.[b]	Median	Mode	Range	Power[c]	Estimated[d] Sample Size
44	5	13.2 ± 0.1	13	13(4)	13-14	0.05	5
68	6	13.3 ± 0.1	13	13(4)	13-14	0.01	3
83	5	13.4 ± 0.2	13	13(4)	13-15	0.05	4
83	7	13.7 ± 0.1	14	None	12-15	0.05	3

[a]All mice were injected i.p. with 10^6 viable J774A.1 reticulum-cell-sarcoma cells. Controls were chosen at random.

[b]Data collected from four different investigators using the modified technique. The means in this column represent the mean survival times of the control animals selected at random from their respective separate experiments.

[c]Indicates the probability that this test will reject a false null hypothesis (Daniel 1977).

[d]Number of mice necessary for future experiments to achieve reliable results at the power calculated (Daniel 1977).

also were obtained when tumor area or diameter was used to compare the standard and modified methods (Table 2). For both the Lynd A/J and C3HMA solid tumor systems, the range of sizes was narrower and the variance much less, for tumors injected by the modified method. The numbers of mice predicted as being necessary to achieve statistically reliable results at the $P = 0.001$ level in future experiments using the modified method were markedly reduced. For the modified method fewer animals were predicted as being necessary for future experiments using the Lynd A/J and C3HMA solid tumors. Follow-up experiments using these tumor systems and several others (Table 3) demonstrated that these predictions were accurate even when the technique was used by three other investigators.

The results shown in Tables 1, 2 and 3 (as well as those obtained in other studies where this method has been employed: Morrison et al. 1980, 1982) demonstrate that continuous stirring of the tumor cell suspension during the loading of syringes significantly reduces variability in host survival time and tumor growth. The viability of the cells treated with the modified technique was not reduced below that obtained by the standard technique as determined by trypan blue dye exclusion and tumor growth rates. Other advantages, with respect to growth variability and tumor heterogeneity (Fidler and Hart 1981), are that there is no selection for a specific tumor region and no need for proteolytic enzymes. Moreover, the demonstration that mean tumor size was not significantly different in separate experiments, suggests that "investigator-induced" variation can be reduced.

Implementation of our simple modification has the benefit of greatly decreasing the number of animals required to obtain reliable data. This

should be especially important to investigators conducting research with limited budgets and also should allow more consistent and reliable data to be obtained on novel anticancer drugs that are available only in small quantity. Use of this technique and other procedures that reduce variability in tumor growth parameters will allow one to recognize atypical test results and abnormally slow tumor growth earlier in the course of an experiment.

LITERATURE CITED

Daniel, W. W. 1977. Introductory statistics with applications. Houghton Mifflin Co., Boston. p. 122-125, 141-143, 272-275.

Fidler, I. J., and I. R. Hart. 1981. Biological and experimental consequences of the zonal composition of solid tumors. Canc. Res. 41:3266-3267.

Goldin, A., J. M. Venditti, and S. K. Carter. 1977. Screening at the National Cancer Institute, p. 37-48. *In* J. F. Saunders and S. K. Carter (Eds.), Methods of development of new anticancer drugs. National Cancer Institute Monographs, vol. 45, NIH, Bethesda, MD.

Morrison, D. G., F. T. Lynd, G. Morrison, D. R. Martel, K. A. Koester, S.C. Frink, M. M. MacDonell, J. W. G. LaValley, M. P. Moyer, W. Rogers, and R. C. Moyer. 1980. Host survival and tumor metastastes as affected by vitamin A, vitamin C, and a corticosteroid. Proc. 11th Internat. Congr. Chemotherapy: Current chemotherapy and infectious diseases, vol. 2: 1501-1503.

Morrison, D. G., M. P. Moyer, F. T. Lynd, W. Rogers, and R. C. Moyer. 1982. Susceptibility of BALB/c GnDu mice to transplantable tumors, in vitro transformed cells, BK and SV40 viruses, and chemical carcinogens. Oncology 39:228-233.

PALEOENVIRONMENTAL SIGNIFICANCE OF A NONMARINE PLEISTOCENE MOLLUSCAN FAUNA FROM SOUTHERN TEXAS

by RAYMOND W. NECK

Texas Parks and Wildlife Department
4200 Smith School Road
Austin, TX 78744

ABSTRACT

Examination of a non-marine molluscan fauna from the Beaumont Formation in Kleberg County, Texas, suggests that during Sangamon time a substantial water course existed in an area that presently has only intermittent drainages. During Sangamon time this general area received either greater effective precipitation that at present or inflow of water from more mesic areas.

INTRODUCTION

Recent excavation at a Pleistocene mammoth site in south Texas has produced a noteworthy non-marine molluscan fauna. Species recovered include freshwater mussels in addition to terrestrial and freshwater snails. The purpose of this report is twofold: 1) to provide paleoenvironmental interpretation of the fossil locality, and 2) to interpret the significance of this locality in relation to the present unionid clam fauna.

Few records of non-marine invertebrates of Pleistocene age have been reported from south Texas. Trowbridge (1932:219) reported several species of nonmarine molluscs from lower Rio Grande terraces. Richards (in Price 1958) reported a list of gastropods from the Ingleside Site; only modern species characteristic of shallow freshwater environments were recovered. Hubricht (1962) reported a fossil molluscan fauna from silt of Palo Blanco Creek in Brooks County, about 40 kilometers west of the Taylor Ranch Site. The terrestrial and aquatic gastropod fauna at Palo Blanco Creek consisted of species with both boreal and austral affinities indicating either an "ecologically incompatible" fauna (Holman 1976) or quite possibly a mixing of discrete depositional units. Neck (in Suhm 1978) reported only extant species characteristic of "reduced water currents and varying water quality" from the La Paloma Mammoth Site (8,000-10,000 years B.P.). Richards (1939) described several fossil localities in southern Texas but was concerned

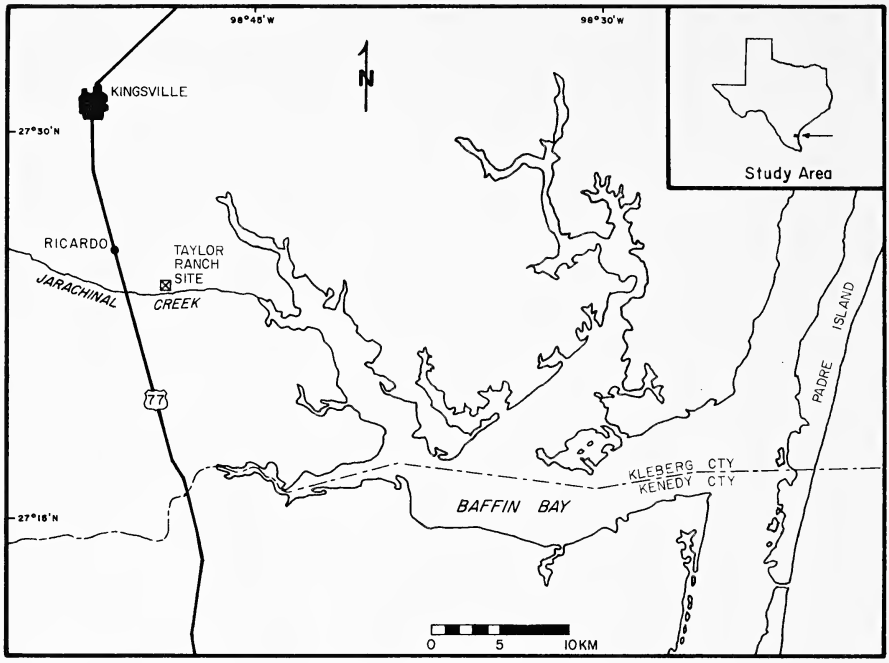

FIGURE 1. Location of Taylor Ranch site, Kleberg Co., Texas.

more with regional geological phenomena than with local environmental reconstruction.

Several Pleistocene fossil faunas are known from south central Texas. Nonmarine fossils of the Berclair Terrace (believed to be of Sangamon age) from Bee and Goliad Counties include species present in the area today (Conkin and Conkin 1962; Sellards 1940). Somewhat older (Pliocene) fossils from the Goliad Formation of DeWitt County do not represent living species although they may be immediately ancestral to present day forms (Marshall 1929).

FOSSIL LOCALITY

The Taylor Ranch Mammoth Site is located on a small tributary of Jarachinal Creek about three kilometers southeast of Ricardo, Kleberg County, Texas (Fig. 1). The skeleton of a mammoth, approximately fifty percent complete, has been excavated by Suhm (1980). Lack of dentition has prevented specific identification of the mammoth, but it is believed to be *Mammuthus imperator*. The mammoth appears to have died in a stream course. Although the bones have been somewhat disarticulated, probably by scavengers and/or moving water, rapid burial is suggested by partially natural orientation of the skeletal elements. Parts of the skeleton have been worn away by modern erosional events.

The fossils occur in deposits identified as belonging to the Beaumont Formation (Late Pleistocene) by Suhm (1980). The age of this formation in south Texas has not been well established. Brown et al. (1977) pointed out the difficulty in differentiating between the Sangamon Interglacial and the Peorian (an interglacial interlude during Mid-Wisconsin time). However, the Taylor Ranch fauna is probably Sangamon, given that the more recent dates from the Beaumont of Texas are non-typical (Aronow 1971). The Sangamon Interglacial Stage has been dated approximately 125,000 B.P. to 250,000 B.P. while the Peorian Interglacial Stage has been dated 60,000 B.P. to 80,000 B.P. (Bernard and LeBlanc 1965).

The Beaumont is lithologically somewhat variable in this portion of south Texas (Plummer 1932; Price 1933; Aronow 1971). The following description of the Taylor Ranch site is taken from Suhm (1980). Most sediment in the exposed section consists of sandy clays or clayey sands with gypsum granules. Modern bioturbation of upper layers due to burrowing activity by fiddler crabs has occurred. The bone/shell level also contains several lenses (up to 5 cm thick) of siliceous and calcareous fragments of granule-to-pebble size. The bone/shell bed is approximately 30 cm below the top of the floodplain deposit and 90 cm below the top of the modern soil. Above the bone/shell bed level is a layer of clayey sand with well-sorted, very fine quartz grains. An undated paleosol topped by modern wind-blown sand occurs at the top of the section.

The present environment is cattle-impacted grassland now dominated by weedy brush species. Most abundant are honey mesquite (*Prosopis glandulosa*), prickly pear (*Opuntia lindheimeri*), tasajillo (*Opuntia leptocaulis*) and lotebush (*Ziziphus obtusifolia*). Jarachinal Creek is an intermittent saline stream (see Russell and Wood 1976). No aquatic molluscs have been located in Jarachinal Creek during an ongoing survey of this portion of southern Texas. No survey of modern terrestrial gastropods has covered the area of the fossil site.

MOLLUSCAN FAUNA

Associated with the mammoth bones were a number of individuals of several molluscan species. Molluscan remains were recovered by R. W. Suhm from materials immediately adjacent to the mammoth skeleton.

Also, shells were visually detected in nearby sediments and collected by the author. No microfossil remains were recovered from the screened material, probably due to the coarseness of screen utilized. Discussed below are the species present and descriptions of the individual fossils.

Bivalvia: Eulamellibranchiata: Unionacea: Unionidae

Uniomerus tetralasmus (Say, 1831), 4 specimens. This clam today is found from Lake Erie through the Mississippi River drainage eastward

to the Coosa River, Alabama, and southwestward into Northern Mexico. The taxonomic situation within the genus *Uniomerus* is not yet clear. Johnson (1970) and Burch (1973) place all members in a single variable taxon, *tetralasmus*. Frierson (1903) separates two southern taxa, *tetralasmus* and *declivus* Say, 1832, stating that *tetralasmus* occurs in small streams and ponds while *declivus* is found in rivers; exceptions to this rule were considered erroneously curated specimens. Morrison (1977) also separates the above forms as species and included Texas in the range of both forms. Atlantic slope forms are classified as *carolinianus* Bosc, 1801. Given the tendency for unionid clams to express variable height and width indices under different environmental conditions (Isley 1914; Coker et al. 1921), these forms could be ecomorphs responding to differential environmental conditions.

Lack of preserved material with posterior margin of the shell intact precludes definitive assignment of *tetralasmus/declivus* classification to the Taylor Ranch *Unionmerus*. However, the lack of shell malformations or major growth ridges indicates permanent water (or nearly so) and lack of severe winters. One of the fossil shells exhibits minor growth ridges similar to those found on contemporary shells from permanent water. Intermittent ponds tend to produce "many variations and malformed specimens" (Frierson 1903), a circumstance which I also have observed. *Uniomerus* is able to withstand periods of dessication of its habitat (Strecker 1908; Van der Schalie 1940). *Uniomerus* can survive for more than six months in a non-aqueous environment under ambient laboratory conditions (Neck unpub. data).

Fossil remains of *Uniomerus* from the Taylor Ranch site consist of internal molds or "steinkerns" of variable completeness with associated original shell material. The remnant shell material has experienced dissolution to the extent that there has been separation of individual growth layers representing discrete active periods of secretion by mantle cells. The curved umbonal ridges typical of *Uniomerus* are detectable on several of the shells. No periostracum remains have been identified. The internal molds consist of calichified concretions containing sand, silt, clay and small pebbles which have become moderately indurated. These remains represent medium-to-large (full-sized) adult individuals. Living specimens of this size in the area of the Taylor Ranch site occur only in stock tanks; individuals from the various creeks are much smaller.

Gastropoda: Prosobranchiata: Archeogastropoda: Helicinidae

Helicina orbiculata (Say, 1818), 1 specimen. This snail is the only terrestrial operculate present today in south central North America. Geographical range includes the southeastern United States from Georgia and Oklahoma south to Texas and northeastern Mexico. A variety with a heavy apertural lip has been known as the variety or subspecies

tropica Pfeiffer, 1852. The individual recovered from the Taylor Ranch Mammoth Site (width 8.0 mm; height 7.0 mm) exhibits the expanded lip of *tropica*. Pilsbry (1948:1084) stated that although *tropica* reached its "fullest development" in the limestone area of central Texas, this form was absent in calcareous areas of Florida and Alabama. Pilsbry (1948:1084) concluded that "the modification is correlated with geographical range, therefore of subspecific significance." Considering that *tropica* is known from Tennessee and well-drained, acid sandy soils in East Texas, a phenotypic response to increased xeric conditions is likely (Fullington and Pratt 1974). This species today is found typically in woodlands and savannahs.

Gastropoda: Pulmonata: Basommatophora: Planorbidae

Helisoma trivolvis (Say, 1816),1 specimen. One large-sized individual (greatest diameter = 15.4 mm) of this aquatic snail was recovered at the Taylor Ranch site. *H. trivolvis* occurs today over a large part of North America from the southern plains and Gulf coast to New Mexico and south into Mexico. In Texas, this species has been found most commonly in shallow, slow-moving, usually permanent water, although it does occur in large floodplain pools.

Gastropoda: Pulmonata: Stylommatophora: Bulimulidae

Rabdotus alternatus alternatus (Say, 1830),2 specimen. The south Texas tree snail today is found throughout the south Texas plains from the Big Bend area to Corpus Christi (just north of the fossil locality) and south into northeastern Mexico. One of the fossil specimens appears to be an adult (only body whorl remaining; original height, 15-17 mm), although deposition of calcium carbonate as "apertural ridges" (MacMillan 1944) during periods of aestivation causes confusion in interpretation of maturity for this species. One juvenile specimen (height, 6.2 mm) was also recovered.

R. a. alternatus is known from variable habitats but generally occurs where there is significant woody vegetation. The vegetational character may vary from chaparral to open woodland. *R. a. alternatus* is characteristic of the Tamaulipan Biotic Province (see Dice 1943; Blair 1950, 1952); its presence indicates warm temperate or subtropical climatic conditions.

PALEOENVIRONMENTAL INTERPRETATION

The fossil molluscan assemblage recovered from the Taylor Ranch site suggests permanent or semi-permanent, slow-moving, shallow, non-brackish water with open woodland or chaparral present upstream or surrounding the actual site. The depositional environment of the Taylor Ranch site's fossil assemblage could have included periodic flooding, as suggested by Suhm (1980). A floodplain pool or backwater

slough is the most likely environment. Flowing water may have carried the snails to the site after they died. However, the clams lived very close to the place of deposition, because their valves were still articulated and closed when they were recovered.

In comparison to present conditions the molluscan fauna of the Taylor Ranch site indicates one of two alternatives: 1) higher effective precipitation or 2) inflow of a river from a more mesic region. Increased effective precipitation is produced by increased precipitation and/or decreased evaporation; alteration of seasonal distribution of precipitation may or may not be involved. The putative river with water originating from more mesic climes could be the Nueces River or one of several buried Pleistocene river valleys (associated with the Palo Blanco drainage to the south) known from the area.

BIOGEOGRAPHICAL SIGNIFICANCE

The Taylor Ranch site's, molluscan fauna has biogeographical significance because of the rarity of fossil sites in southern Texas. All of the molluscan species present in the Taylor Ranch fauna occur in the general area today. An ongoing survey (Neck unpub.) has revealed populations of *Uniomerus* south of the Nueces River in the drainage of Baffin Bay (which includes Jarachinal Creek), but these populations probably represent introductions. *Uniomerus* is known from the Nueces River (Taylor unpub.) but is not known from Lake Corpus Christi (Murray 1979). To the south, *Uniomerus* is known from the Rio Grande system (Strecker 1931). Age of origin of *Uniomerus* in south Texas is unknown but probably quite remote, as much of south Texas was probably suitable habitat for *Uniomerus* during the glacial maxima of the Wisconsin. Trowbridge (1932:219) reported *Uniomerus* from undated Pleistocene terraces of the lower Rio Grande. Prior to the Altithermal (a warm, dry episode of the Middle Holocene), significant water was available in the presently semi-arid Llano Mesteno southwest of the Taylor Ranch site (Suhm 1978). Quite possibly, *Uniomerus* existed in the Baffin Bay drainages until intense dessication during the Altithermal.

The Taylor Ranch Mammoth Site is peripheral or close to the Sangamon-age deposits of the migratory delta of the Nueces River (Aronow 1971). A Late Pleistocene route of the lower Nueces River to the Baffin Bay area was postulated by Bailey (1926). This hypothesis has not been widely accepted but is compatible with conclusions reached by Aronow (1971) concerning the Beaumont Nueces River deltaic deposits. Behrens (1963) reported the existence of several buried river valleys of undifferentiated Pleistocene age. One or all of these river valleys are channels of the Palo Blanco River, a broad meandering river which drained a large area of south Texas during the Wisconsin

(now without permanent water due to subsequent aridity); substantial water flow existed in this now intermittent creek as late as 8,000-10,000 years B.P. (Suhm 1978). The Taylor Ranch fauna may have lived in a floodplain pool along a water course; perhaps the Palo Blanco River existed during the Sangamon.

A number of marine molluscan Pleistocene faunas has been reported from the middle and upper portions of the Gulf coast of Texas. Pampe (1971) reported a Late Pleistocene (Sangamon or Early Wisconsin) molluscan fauna consisting of contemporary species on the Texas coast. Interglacial faunas tend to be similar or identical to present-day communities (Richards 1939; Parker 1959). Indeed, many of the present-day marine molluscs appear to have inhabited Texas waters since late Tertiary time (Parker 1959). The temporal dynamics of the freshwater molluscs of coastal Texas will remain unknown until additional interglacial and glacial period faunas have been discovered and investigated.

ACKNOWLEDGEMENTS

I thank Saul Aronow for constructive criticism of an early draft of this communication. Molluscan fossils described herein were kindly supplied by R. W. Suhm. T. B. Samsel III drafted Figure 1.

LITERATURE CITED

Aronow, S. 1971. Nueces River delta plain of the Pleistocene Beaumont Formation, Corpus Christi region. Texas. Bull. Amer. Assoc. Petrol. Geol. 55:1231-1248.

Bailey, T. L. 1926. The Gueydan, a new middle Tertiary formation from the southwestern coastal plain of Texas. Bull. Univ. Texas 2645. 187 p.

Behrens, E. W. 1963. Buried Pleistocene river valleys in Aransas and Baffin Bays, Texas. Publ. Mar. Sci. Inst. Univ. Texas 9:7-13.

Bernard, H. A., and R. J. LeBlanc. 1965. Resume of the Quaternary geology of the northwestern Gulf of Mexico province, p. 137-185. *In* H. E. Wright, Jr. and D. G. Frey (Eds.), The Quaternary of the United States, Princeton Univ. Press, Princeton, N.J.

Blair, W. F. 1950. The biotic regions of Texas. Tex. J. Sci. 2:93-117.

Blair, W. F. 1952. Mammals of the Tamaulipan biotic province in Texas. Tex. J. Sci. 4:230-250.

Brown, L. F. Jr., J. H. McGowen, T. J. Evans, C. G. Groat, and W. L. Fisher. 1977. Environmental geologic atlas of the Texas coastal zone-Kingsville area. Univ. Tex. Austin, Bur. Econ. Geol. 131 p.

Burch, J. B. 1973. Freshwater unionacean clams (Mollusca: Pelecypoda) of North America. U.S. Environ. Protect. Agency, Ident. Manual 11. 176 p.

Coker, R. E., A. F. Shira, H. W. Clark, and A. D. Howard. 1921. Natural history and propagation of freshwater mussels. U.S. Fish. Bull. 37:77-181.

Conkin, J. E., and B. M. Conkin. 1962. Pleistocene Berclair Terrace of Medio Creek, Bee County, Texas. Bull. Amer. Assoc. Petrol. Geol. 46:344-353.

Dice, L. R. 1943. The biotic provinces of North America. Univ. Mich. Press, Ann Arbor. 78 p.

Frierson, L. S. 1903. The specific value of *Unio declivus*, Say. Nautilus 17:49-51.

Fullington, R. W., and W. L. Pratt, Jr. 1974. The Helicinidae, Carychiidae, Achatinidae, Bradybaenidae, Bulimulidae, Cionellidae, Haplotrematidae, Helicidae, Oreohelicidae, Spiraxidae, Streptaxidae, Strobilopsidae, Thysanophoridae, Vallonidae (Gastropoda) in Texas. Bull. Dallas Mus. Nat. Hist. 1(3). 48 p.

Holman, J. A. 1976. Paleoclimatic implications of "ecologically incompatible" herpetological species (Late Pleistocene: southeastern United States). Herpetological 32:290-295.

Hubricht, L. 1962. Land snails from the Pleistocene of southern Texas. Sterkiana 7:1-3.

Isley, F. B. 1914. Experimental study of the growth and migration of freshwater mussels. Rpt. U.S. Comm. Fish. 1913, App. 3. 24 p.

Johnson, R.I. 1970. The systematics and zoogeography of the Unionidae (Mollusca: Bivalvia) of the southern Atlantic Slope Region. Bull. Mus. Comp. Zool. 140:263-450.

MacMillan, G. K. 1944. The "apertural ridge" in *Bulimulus*. Nautilus 57:98-99.

Marshall, W. B. 1929. New fossil land and fresh-water mollusks from the Reynosa Formation of Texas. Proc. U.S. Nat. Mus. 76:1-6.

Morrison, J. P. E. 1977. Species of the genus *Uniomerus*. Bull. Amer. Malacol. Union 1976:10-11.

Murray, H. D. 1979. Freshwater mussels of Lake Corpus Christi, Texas. Bull. Amer. Malacol. Union 1978:5-6.

Pampe, W. R. 1971. A new Pleistocene marine fossil locality in Chambers County, Texas. Trans. Gulf Coast Assoc. Geol. Soc. 21:395-410.

Parker, R. H. 1959. Macro-invertebrate assemblages of Central Texas coastal bays and Laguna Madre. Bull. Amer. Assoc. Petrol. Geol. 43:2100-2166.

Pilsbry, H.A. 1948. Land mollusca of North America (north of Mexico). Acad. Nat. Sci. Phil. Monog. 3, vol. II, pt. 2.

Plummer, F. B. 1932. Cenozoic systems in Texas, p. 519-818. *In* E. H. Sellards, W. S. Adkins and F. B. Plummer (Eds.), The geology of Texas. Bull. Univ. Texas 3232, Austin, TX.

Price, W. A. 1933. Lissie Formation and Beaumont Clay in south Texas. Bull. Amer. Assoc. Petrol. Geol. 18:948-959.

Price, W. A. 1958. Sedimentology and Quaternary geomorphology of South Texas. Trans. Gulf Coast Assoc. Geol. Soc. 8:41-75.

Richards, H. G. 1939. Marine Pleistocene of Texas. Bull. Geol. Soc. Amer. 50:1885-1898.

Russel, J. L., and C. E. Wood. 1976. The effects of Tropical Storm Fern (September, 1971) on Baffin Bay, Texas. Texas A&I Univ. Stud. 9:133-145.

Sellards, E. H. 1940. Pleistocene artifacts and associated fossils from Bee County, Texas. Bull. Geol. Soc. Amer. 51:1627-1664.

Strecker, J. K. 1908. The Mollusca of McLennan County, Texas. Nautilus 22:63-67.

Strecker, J. K. 1931. The distribution of the naiades of pearly freshwater mussels of Texas. Baylor Univ. Spec. Bull. 2. 69 p.

Suhm, R. W. 1978. Preliminary investigation of the La Paloma Mammoth Site (Late Pleistocene), Kenedy County, Texas. Texas A&I Univ. Stud. 11:13-35.

Suhm, R. W. 1980. Preliminary investigation of the Taylor Ranch Mammoth Site (Late Pleistocene), Kleberg County, Texas, p 46-51. *In* J. L. Russel and R. W. Suhm (Eds.), Geology of clay dunes, Baffin Bay and the South Texas Sand Sheet. (Geological field trip, Texas Acad. Sci. Meeting, Corpus Christi, Texas). Texas A&I Univ., Kingsville. 86 p.

Trowbridge, A. C. 1932. The Tertiary and Quaternary geology of the lower Rio Grande region, Texas. Bull. U.S. Geol. Surv. 837. 260 p.

van der Schalie, H. 1940. Aestivation of freshwater mussels. Nautilus 53:137-138.

CALORIC VALUE OF THE LIVER FLUKE, *FASCIOLA HEPATICA*

by JEREMY M. JAY *and* NORMAN O. DRONEN

Department of Biology
Texas A&M University
College Station, TX 77843

ABSTRACT

Adult liver flukes (*Fasciola hepatica*) from infected cattle yielded an average of 5.056 kcal/g dry weight, when combusted in a bomb calorimeter.

As part of a continuing investigation into the bioenergetics of *Fasciola hepatica*, caloric values for whole, adult flukes were determined in an oxygen bomb calorimeter. The flukes were removed alive from the livers of infected cattle, rinsed in distilled water and air dried at 60 C for 24 hours. Caloric values were determined in a Parr oxygen bomb calorimeter with a semi-micro adapter, using standard calorimetric techniques. Samples were desiccated before weighing, and to each was added a known amount of benzoic acid to increase burning efficiency. Finally, the mixture was pelleted to prevent loss during the initial stages of combustion.

Nineteen flukes were bombed individually. Mean caloric yield ± the 95% confidence limit ($t_{0.05,\ 18} \cdot s/\sqrt{n}$) was 5.056 ± 0.094 kcal/g dry weight. Calow and Jennings (1974) reported corresponding values of 5.205 ± 0.201 for *F. hepatica* they assayed. Our mean value is within 3% of theirs, but our confidence interval is less than half theirs. The latter difference may reflect the fact that our sample size was nearly double that of Calow and Jennings (1974).

The average dry weight of our flukes was 0.0255 g. Thus, the average energy content per fluke was 0.1289 kcal.

We thank Dr. Rural R. Bell and Les Dees, Department of Veterinary Microbiology and Parasitology, Texas A&M University, for their assistance in supplying specimens.

LITERATURE CITED

Calow, P. and J. B. Jennings. 1974. Calorific values in the phylum Platyhelminthes: The relationship between potential energy, mode of life and the evolution of entoparasites. Biol. Bull. 147:81-94.

STATUS OF BIGHORN SHEEP IN TEXAS

by BRUCE D. LEOPOLD *and* PAUL R. KRAUSMAN

Division of Wildlife, Fisheries and Recreation Resources
School of Renewable Natural Resources
University of Arizona
Tucson, AZ 85721

ABSTRACT

Native bighorn sheep (*Ovis canadensis*) last were observed in Texas in 1960. Attempts to reintroduce the bighorn to Texas have been largely unsuccessful, owing to predation and disease problems; however, escapees from the reintroduction experiment may account for infrequent sightings of bighorn sheep in Big Bend National Park between 1970 and 1980.

As human activities increased in west Texas, populations of bighorn sheep (*Ovis canadensis*) decreased (Davis and Taylor 1939; Carson 1941). Native bighorn sheep were last observed in Texas in Victoria Canyon, Culberson and Hudspeth Cos., in 1960 (Texas Parks and Wildlife Department 1980). Through cooperation of the U.S. Fish and Wildlife Service, the Boone and Crockett Club, the Wildlife Management Institute, the Arizona Game and Fish Department, and the Texas Parks and Wildlife Department, an effort began in the late 1950's to reintroduce desert bighorn sheep to Texas. The reintroduction program has been discussed in detail by the Texas Parks and Wildlife Department (1980), Kilpatrick (1980, 1981), and Winkler (1981). The present paper provides a brief history of the reintroduction effort and ends with a consideration of the bighorn sheep's present status in Texas.

Beginning in 1957, sheep were trapped on the Kofa Game Range in southwestern Arizona and transplanted to a 173 ha enclosure on the Black Gap Wildlife Management Area (BGWMA), Brewster Co., Texas. Sixteen sheep had been transplanted by 1959, but by December of that year only four rams and five ewes remained. The others had died from unknown causes (Texas Parks and Wildlife Department 1980).

From 1960 to 1971 the herd increased from the nine remaining sheep to an estimated 68 sheep. Twenty bighorn sheep were released from the enclosure into BGWMA in January 1971 (Kilpatrick 1980; Texas Parks and Wildlife Department 1980; Kilpatrick 1981). These 20 animals either fell prey to mountain lions (*Felis concolor*) or moved off the area (Kilpatrick 1980, 1981). Attempts to locate survivors have been largely unsuccessful.

The Texas Journal of Science, Vol. XXXV, No. 2, July 1983

In the summer of 1971 a die-off began in the enclosure, and 17 sheep perished. Probable causes included nutritional stress from poor range conditions complicated with penumonia and blue tongue. Problems with disease continued through 1975 when predators, primarily mountain lions, began killing desert sheep. Six additional ewes were captured in Mexico and transplanted to the enclosure in January 1977, but propogation efforts had to be terminated because predation was a serious limiting factor. Between 1975 and 1980, predators killed 21 sheep in the BGWMA enclosure.

In November 1977 most sheep were removed from the BGWMA brood pasture. Four ewes and three rams were moved to Chilicote Ranch, Presidio Co., Texas. Of the two rams still in the enclosure, one escaped in 1980. As of 1981 only one adult ram remained in the brood pasture. There are now approximately six free-ranging sheep on BGWMA (Winkler 1981).

Coincident with the sheep release at BGWMA was a series of observations in Big Bend National Park (BBNP), Brewster Co., Texas. The BGWMA is 8 km northeast of BBNP. Sixteen observations totaling 25 sheep were reported by park visitors from 4 October 1970 to 4 October 1980. No observations of sheep were reported prior to the BGWMA transplant. Not all visitor observations may have been accurate, but one of the observations was verified. On 4 October 1980 an adult male was observed and photographed (BBNP Case Incident Report) in Green Gulch approximately 45 km from BGWMA. Another observation of a sheep on the same day in the same area was reported.

The ram that escaped from the breeding pasture at BGWMA early in 1980 was last observed on BGWMA in March 1980. This may have been the same ram observed in BBNP in October 1980. This observation leads us to believe that some of the observations may be accurate and that some of the sheep leaving BGWMA moved into or through BBNP. Historically, bighorn sheep occupied Santa Elena Canyon in BBNP (Carson 1941) and probably also the surrounding rock outcrops and mesas (Borell and Bryant 1942). However, they were never common in BBNP, and they disappeared shortly after the first white settlers arrived (Borell and Bryant 1942). We doubt that desert bighorn sheep will naturally reestablish a population in BBNP due to the limited number of sheep entering the park, the small amount of suitable sheep habitat available, and the high density of predators (Krausman and Ables 1981).

LITERATURE CITED

Borell, A. E., and M. D. Bryant. 1942. Mammals of the Big Bend area of Texas. Univ. California Publ. 48:1-62.

Carson, B. 1941. Man—the greatest enemy of desert bighorn mountain sheep. Texas Game, Fish and Oyster Comm. Bull. No. 21:5-23.

Davis, W. B., and W. P. Taylor. 1929. The bighorn sheep of Texas. J. Mammal. 20:440-455.

Kilpatrick, J. S. 1980. Status of bighorn sheep. Fed. Aid Project No. W-109-R-3, Job No. 11. Texas Parks and Wildl. Dept., Austin, TX.

Kilpatrick, J. S. 1981. Status of bighorn sheep. Fed. Aid Project No. W-109-R-4, Job No. 11. Texas Parks and Wildl. Dept., Austin, TX.

Krausman, P. R., and E. D. Ables. 1981. Ecology of the Carmen Mountains white-tailed deer. National Park Serv. Sci. Monogr. 15:1-114.

Texas Parks and Wildlife Department. 1980. Status of desert bighorn sheep in Texas. Texas Parks and Wildl. Dept., Austin, TX., mimeo. 14 p.

Winkler, C. K. 1981. Status of desert bighorn sheep in Texas - 1981. Trans. Desert Bighorn Council. 25:63.

EGGS AND YOUNG OF SCHOTT'S WHIPSNAKE, *MASTICOPHIS TAENIATUS SCHOTTI*

by HUGH K. McCRYSTAL *and* JAMES R. DIXON

Department of Wildlife and Fisheries Sciences
Texas A&M University
College Station, TX 77843

ABSTRACT

A gravid female *Masticophis taeniatus schotti* (Serpentes: Colubridae) from Mexico laid five eggs in captivity. Three of the sand-textured eggs hatched 80, 81, and 81 days later, producing neonates that averaged 389 mm in total length and 9.85 g in weight. The neonates differed from typical adults in color and pattern of pigmentation.

There is little information regarding the reproductive biology of Schott's whipsnake, *Masticophis taeniatus schotti.* A report on one clutch of eggs and the subsequent hatchlings is presented here. This is apparently the first record of *M. t. schotti* hatchlings.

A gravid female [Texas Cooperative Wildlife Collections (TCWC) specimen 60760: snout-vent length 994 mm; total length 1479 mm] was collected from a site 419 m above mean sea level and 24.8 km south of Sabinas Hidalgo, Nuevo Leon, Mexico, on 14 June 1982. On 17 June 1983 she deposited five ellipsoidal, non-adherent eggs. The leathery shells were rough to the touch, resembling fine sandpaper. This unusual shell texture has been noted in *M. t. schotti* by Gloyd and Conant (1934) and also in *M. t. taeniatus* by Maslin (1947). The eggs were weighed, measured (Table 1) and incubated in a sealed three-liter French jar by the method described by Tryon (1975). Incubation temperature ranged from 25 to 27 C.

On 24 June egg number five was found to be infertile and was discarded. On 26 July egg number one ruptured and collapsed. A necrotic, but well-developed embryo was found inside. At 0800 hours on 5 September egg number two had pipped. The juvenile emerged by 1300 hours. Both eggs three and four pipped the following morning with the neonates emerging by 1400 hours. The hatchlings (TCWC 60761-763) were weighed, measured (Table 1) and housed in 3.8-liter glass jars. All three were males. Sex was determined by manually everting the hemipenes.

Gloyd and Conant (1934) reported egg clutches from four captive female *M. t. schotti.* Clutch size varied from three to twelve. The eggs were shorter than ours ($\bar{X}$ = 41.3 mm), slightly heavier ($\bar{X}$ = 16.8 g)

TABLE 1. Data on the eggs of *Masticophis taeniatus schotti* deposited 17 June 1982, and the young at hatching.

Egg	Width (mm)	Length (mm)	Weight (g)	Days to hatching	Snout-vent length (mm)	Total length (mm)	Weight (g)
1	19.7	62.4	15.87	—		(embryonic death)	
2	19.0	60.2	14.6	80	279	400	10.60
3	19.3	65.4	15.88	81	275	394	9.68
4	19.8	58.7	14.65	81	258	372	9.27
5	17.2	80.2	11.31	—		(infertile)	
$\bar{X}$	19.0	65.4	14.47	81	271	389	9.85

and all were apparently infertile. Maslin (1947) collected two gravid female *M. t. taeniatus* during June in Colorado; each contained four eggs. Parker and Brown (1972) reported clutch sizes for three *M. t. taeniatus* to be three, six and seven. They indicated that length of incubation in the wild ranged from 44-58 days. Minton (1959) reported that a gravid *M. t. ornatus*, collected in May, laid five eggs on 1 June, two of which hatched 62 days later. The neonates were slightly shorter in total length ($\bar{X}$ = 352 mm) than our hatchlings.

Our juvenile *M. t. schotti* differed in color and pattern from typical adults. Gloyd and Conant's (1934) color description of Schott's whipsnake makes no mention of juvenile color, pattern or ontogenetic color change. A color description, based on the color charts of Ridgeway (1912), of one of our live neonate *M. t. schotti* follows: dorsal area of head uniform raw umber, except parietals, which are antique brown with raw umber edges; upper half of rostral raw umber, lower half white; nasals blackish-brown posteriorly and white anteriorly; loreal, pre- and postoculars edged with blackish-brown and with white centers; temporals dark olive edged with white; a few dark olive dorsolateral scales immediately posterior to temporals also edged with white; iris black with yellow ocher ring around pupil; supralabials predominantly white with blackish-brown upper edges; most posterior supralabial with blackish-brown posterior edge; mental, infralabials, genials, gulars and throat (to about tenth ventral) white; white dorsolateral stripe with very pronounced light pinkish-cinnamon and blackish-brown borders immediately posterior to angle of jaw; this stripe interrupted at angle of jaw by dark olive ground color which descends to gulars; latter become progressively more light pinkish-cinnamon ventrally, grading into white throat color; color between dorsolateral stripes dark olive; lower two-thirds of scale row three and upper two-thirds of scale row four blackish-brown; white dorsolateral stripe occupies upper third of scale row three and lower third of scale row four; this stripe extends from angle of jaw to ventral 115 and fades completely by ventral 137 (47.2% total body length); diffuse cinnamon buff

spots found on adjacent scale rows above and below stripe; upper three-fourths of scale row one and scale row two dark olive, except anteriorly where upper three-fourths of scale row one blackish-brown; distinct ventrolateral light pinkish-cinnamon stripe extends posteriorly on lower scale row one and outer edge of adjacent ventrals from throat to ventral 107 fading completely by ventral 129 (40.9% total body length); tail dark olive above, fading to light pinkish-cinnamon on scale row two; subcaudals and scale row one light pinkish-cinnamon; ventrals change from white to pale pinkish-buff at about tenth ventral; at mid-body, color darkens to light pinkish-cinnamon; lateral edges of venter light pinkish-cinnamon throughout.

The other two neonates were virtually identical to the one described above, except that the ground color was blackish-brown instead of dark olive. There was no evidence of the anterolateral gold edging of the dorsal scales characteristic of adult *M. t. schotti* in any of the hatchlings.

We thank Michael McCoid and Edward Michaud for their comments on the manuscript.

LITERATURE CITED

Gloyd, H. K., and R. Conant. 1934. The taxonomic status, range and natural history of Schott's Racer. Occ. Pap. Mus. Zool., Univ. Michigan (287):1-17.

Maslin, T. P. 1947. Range extensions of three reptiles in Colorado. Copeia 1947:138.

Minton, S. A. 1959. Observations on amphibians and reptiles of the Big Bend Region of Texas. Southwest. Nat. 3:28-54.

Parker, W. S., and W. S. Brown. 1972. Telemetric study of movements and oviposition of two female *Masticophis t. taeniatus*. Copeia 1972:892-895.

Ridgeway, R. 1912. Color standards and nomenclature. Published by the author, Washington, D.C. 43 p.

Tryon, B. W. 1975. How to incubate reptile eggs: a proven technique. Bull. New York Herp. Soc. 11:33-37.

OBSERVATIONS ON HOST SELECTION BY *LYSATHIA LUDOVICIANA* (CHRYSOMELIDAE), A BEETLE WITH POTENTIAL FOR BIOLOGICAL CONTROL OF CERTAIN AQUATIC WEEDS

by JOHN M. CAMPBELL *and* WILLIAM J. CLARK

Department of Wildlife and Fisheries Sciences
Texas A&M University
College Station, TX 77843

ABSTRACT

Larvae of the beetle *Lysathia ludoviciana* were observed feeding selectively on the aquatic plant *Ludwigia peploides* in ponds of Brazos County, Texas. In experiments, the larvae readily consumed leaves and flowers of *L. peploides*, but refused leaves of *Juncus effusus*, *Hydrolea ovata*, and *Salix nigra*. Of these plants, only *L. peploides* contains dense accumulations of crystalline calcium oxalate, or raphides. Some insects (including other chrysomelids) have a dietary preference for biochemicals such as raphides.

Adults of the chrysomelid beetle *Lysathia ludoviciana* (Fall) have been collected from many species of plants, but only the aquatic plant *Myriophyllum aquaticum* has been observed to support larval development (Habeck and Wilkerson 1980). However, larvae were not very abundant on *M. aquaticum* in Florida, where the discovery was made, and Vogt and Cordo (1976) implied that *Ludwigia* may be the primary natural host. During an investigation of the microcrustacean fauna inhabiting submerged parts of the sprawling emergent plant *Ludwigia peploides* (H.B.K.) Raven (Onagraceae) in several ponds in Brazos County, Texas, we found evidence that this plant is the primary natural host for *L. ludoviciana.*

During the spring-summer periods of 1981 and 1982, we found larvae of the beetle feeding on *L. peploides* in three different ponds. Adults were seen on the plant at these and two additional locations—a fourth pond in Brazos County and at the narrow end of a small cove on Lake Conroe in Montgomery County. In all situations a variety of other plants was available to the insects, but *L. peploides* was the only plant utilized. The adult beetles never ventured very far from *Ludwigia* growing over the water, suggesting that this chrysomelid requires or prefers the humid environment above the water's surface.

The feeding larvae did not completely consume leaves, but rather ate small holes, then moved to other locations (or leaves) before eating again. Cells adjacent to the damaged part of a leaf died, and the zone of

The Texas Journal of Science, Vol. XXXV, No. 2, July 1983

dying cells progressed outward from the damaged point, eventually destroying the leaf.

The insects appeared not to be very mobile. In April 1981 we observed a dense population almost completely destroy the leafy foliage of a *L. peploides* mat that had covered the surface of a small (0.04 ha) pond located in College Station Central Park, while a pond only five meters away and containing abundant *L. peploides* had no infestation.

We collected healthy leaves from all of the plants present at the margin of one of the ponds and offered them to *L. ludoviciana* larvae of various sizes in repeated "no-choice" experiments. The larvae placed in chambers with leaves of *Juncus effusus* (Juncaceae), *Hydrolea ovata* (Hydrophyllaceae), or *Salix nigra* (Salicaceae) invariably ignored these potential foods; whereas, larvae placed with leaves or even flowers of *L. peploides* began feeding almost immediately.

Microscopic examination of the plants revealed that *L. peploides* differed from the others in having dense accumulations of raphides (needle-shaped crystals of calcium oxalate) throughout its leaves, stems and flowers. Raphides act as a deterrent to most plant feeders (Raven and Curtis 1970), but host specificity of some chrysomelid beetles and other plant-feeding insects has been attributed to these insects' preference for specific biochemical substances, such as raphides, in the plants (Feeny 1975; Hicks and Tahvanainen 1974). Some species of *Myriophyllum* contain calcium oxalate crystals in the form of druse (Hasman and Inanc 1957), which may account for the occurrence of *L. ludoviciana* on *Myriophyllum.*

The observed impact of *L ludoviciana* on *Ludwigia,* its apparent restriction to the "supra-aquatic" habitat, its lack of mobility and its host specificity suggest that this chrysomelid beetle has potential as a biological agent for control of *L. peploides* and other aquatic plants producing calcium oxalate. Habeck and Wilkerson (1980) report successful laboratory rearing of the insects, which suggests that large-scale production may be feasible.

This note is based on a paper presented at the Annual Technical Session of the Texas A&M Chapter of the American Fisheries Society, April 22, 1982, College Station, Texas. We thank Horace R. Burke (Department of Entomology, Texas A&M University) and Edward G. Riley (Department of Entomology, Louisiana State University), who assisted in identifying the insect.

LITERATURE CITED

Feeny, P. 1975. Biochemical coevolution between plants and their insect herbivores, p. 3-19. *In* L. E. Gilbert and P.H. Raven (Eds.), Coevolution of animals and plants. University of Texas Press, Austin, TX.

Habeck, D. H., and R. Wilkerson. 1980. The life cycle of *Lysathia ludoviciana* (Fall) (Coleoptera: Chrysomelidae) on parrot-feather, *Myriophyllum aquaticum* (Velloso) Verde. Coleopt. Bull. 34:167-170.

Hasman, M., and N. Inanc. 1957. Investigations on the anatomical structure of certain submerged, floating and amphibious hydrophytes. Rev. Fac. Sci. Univ. Istanbul Ser. B Sci. Nat. 22:137-153.

Hicks, K. L., and J. O. Tahvanainen. 1974. Biology of plants. Worth Publishers, Inc., New York, N.Y.

Vogt, G. B., and H. A. Cordo. 1976. Recent South American field studies of prospective biocontrol agents of weeds. Proceedings, Research Planning Conference on the Aquatic Plant Control Program, Charleston, S. C., U.S. Army Engineer Waterways Experiment Station Misc. Paper A-76-1, p. 36-55.

CHARACTERIZATION OF ERYTHROCYTE ESTERASES ON ELECTROPHORETIC GELS[1]

by JOHN P. CHERRY

Eastern Regional Research Center
ARS, U.S. Department of Agriculture
600 E. Mermaid Lane
Philadelphia, PA 19118

ABSTRACT

Polyacrylamide gel electrophoresis revealed a complex array of esterases in hypotonic washings and membrane fractions from rabbit erythrocytes prepared in the presence of Triton X-100. By the use of on-gel techniques, these esterases were characterized on the basis of substrate specificities, susceptibilities to inhibitors, and sensitivities to urea and heat. In addition to acetylcholinesterase, known to be present in erythrocyte membranes, the classes of enzymes were shown to be heteromorphic and examples were found for carboxylesterases, arylesterases, acetylesterases and cholinester hydrolases. These data establish electrophoretic patterns of rabbit erythrocyte esterases that may serve as standards to which enzymes from physiologically altered test animals might be compared.

INTRODUCTION

Enzymes distinguished qualitatively by gel electrophoretic techniques are useful as biological indicators of changes in composition of edible substances during preharvest, harvest, storage, and processing (Manwell and Baker 1970; Cherry 1977, 1978; Cherry et al. 1978). Changes include deletion of some enzymes, intensification of others, and/or production of new components as evidenced by quantitative and qualitative changes in bands appearing on electrophoretic gels. Enzymes in erythrocyte membrane and cytoplasm fractions may be useful in elucidating physiological changes due to nutritional inbalances in diets. Gel electrophoretic tests of enzymes in blood and other tissues are used to indicate the existence of certain disease-related physiological disorders (Wilkinson 1976; Ray and Cherry 1977). However, enzyme multiplicity that results from genetic variability, tissue ontogeny, and method of preparation (Cherry 1977, 1978) can complicate gel electrophoretic analysis. Thus, care should be taken to insure that known gel patterns

[1]This work was supported in part by contract F41609-C-0003 from the U.S. Air Force School of Aerospace Medicine, and by Grant A-003 of the Robert A. Welch Foundation while the author was in the Department of Biochemistry and Biophysics, Texas A&M University, College Station, TX. Special appreciation for the support is extended to John M. Prescott.

of enzymes are developed as standards for the materials to be examined prior to evaluation of treatment effects.

Previous workers (Markert and Hunter 1959; Augustinsson 1961; Holmes and Masters 1967, 1968) showed by non-gel-electrophoretic techniques that esterase activity in mammalian tissues is due to multiple enzyme forms with widely differing substrate specificities, susceptibilities to inhibitors, pH optima, and sensitivities to urea and heat. Esterases that have been observed by quantitative methods in tissues include carboxylesterases (E. C. 3.1.1.1), arylesterases (E. C. 3.1.1.2), acetylesterases (E. C. 3.1.1.6), acetylcholine hydrolases (E.C. 3.1.1.7), and cholinester hydrolases (E. C. 3.1.1.8). Erythrocytes of some mammalian species contain, in addition to the well-known membrane-bound acetylcholinesterases, other esterases that are relatively nonspecific, including arylesterases (Augustinsson et al. 1973). The present study was undertaken to demonstrate how the diversity of esterases present in rabbit erythrocytes can be standardized, using polyacrylamide disc gel electrophoretic techniques.

MATERIALS AND METHODS

Extraction of Erythrocyte Constituents

Blood from New Zealand white rabbits, 8 to 12 months old and weighing approximately 2500 g, was collected by cardiac puncture (approximately 45 ml per rabbit) in the presence of an anticoagulant acid-citrate-dextrose solution. Procedures for hemolyzing and washing the erythrocytes and preparing membrane ghosts were those of Cherry and Prescott (1974); membrane constituents were solubilized with 2.5% Triton X-100[2] in the presence of 1 mM EDTA, with or without 10 mM dithiothreitol (DTT).

Gel Electrophoresis and Detection of Esterases

Electrophoretic separation of these components was by a "standard" gel electrophoretic technique (Cherry and Prescott 1974). The identities of esterase bands on the electrophoretic gels were determined by direct on-gel staining techniques. Nonspecific esterases (general staining procedure for esterase activity) were detected by incubating duplicate gels in a mixture of α- and β-naphthyl acetate at room temperature for 30-60 min (Cherry and Katterman 1971). The substrate mixture contained 100 ml sodium phosphate (0.1 M, pH 6.1), 5 ml 1-propanol, 30 mg fast blue salt, 1.5 ml α-naphthyl acetate stock solution, and 1 ml

[2]Names of companies or commercial products are given solely for the purpose of providing specific information; their mention does not imply recommendation or endorsement by the U.S. Department of Agriculture over others not mentioned.

β-naphthyl acetate stock solution; the stock solutions contained 1 g of the respective naphthyl acetate in 100 ml of 50% acetone.

Acetylcholinesterase and butyrylcholinesterase activities were tested by modification of the method of Shafai and Cortner (1971). To 13 ml of sodium phosphate (0.5 M, pH 6.1) 50 mg acetylthiocholine iodide (for acetylcholinesterase) or 50 mg butyrylthiocholine iodide (for butyrylcholinesterase), 1 ml sodium citrate (1 M), 4 ml copper sulfate (0.15 M), and 2 ml potassium ferricyanide (0.05 M) were added in that order and mixed thoroughly; the gels were placed in this solution and kept at room temperature for 30-60 min.

Other substrates utilized to determine the specificities of individual esterase bands included α-naphthyl butyrate, β-naphthyl laurate, indoxyl acetate, thiophenyl acetate, and leucyl-β-naphthylamide. These preparations were made as stock solutions each containing 1 g of substrate per 100 ml 50% acetone, and fast blue salt was used as above (Cherry and Katterman 1971) to make the enzyme bands visible. Insoluble substrates were made as suspensions by subjecting the mixture to sonication.

Esterase Inhibition

Inhibitors of esterase activity tested in this study were diisopropylphosphorofluoridate (DPF), tri-o-tolyl phosphate (T-o-TP), phenylmethanesulfonylfluoride (PMSF), p-chloromercuribenzene sulfonic acid (CMBSA), eserine (physostigmine), mercuric chloride, and acetazolamide. The concentrations of inhibitors used for each experiment ranged from 0.01 to 1 mM, with each sample being subjected to the inhibitor for 15-20 min both before and after electrophoresis.

Heat Sensitivity

Sensitivity of esterases to heat was determined by incubating the electrophoretic gels in phosphate buffer (0.1 M, pH 6.1) at 55 C, and the effects of urea were investigated by soaking the gels in a solution of 10 M urea at room temperature. Both stability experiments were conducted for varying periods up to 40 min, after which the gels were equilibrated at room temperature in phosphate buffer, then incubated with the substrate that included fast blue salt for staining the enzyme bands.

RESULTS AND DISCUSSION

Electrophoretic gels of both the hypotonic washings and the membranes of rabbit erythrocytes showed multiple, discrete bands of nonspecific esterases (Fig. 1). Region 1.5 - 6.5 cm of the gel patterns revealed that several of the same enzyme bands were present both in the membranes (gels A-D) and in the washings (gels G-J). The membrane fraction, however, contained esterase activity in regions 0.5 - 1.5 cm and

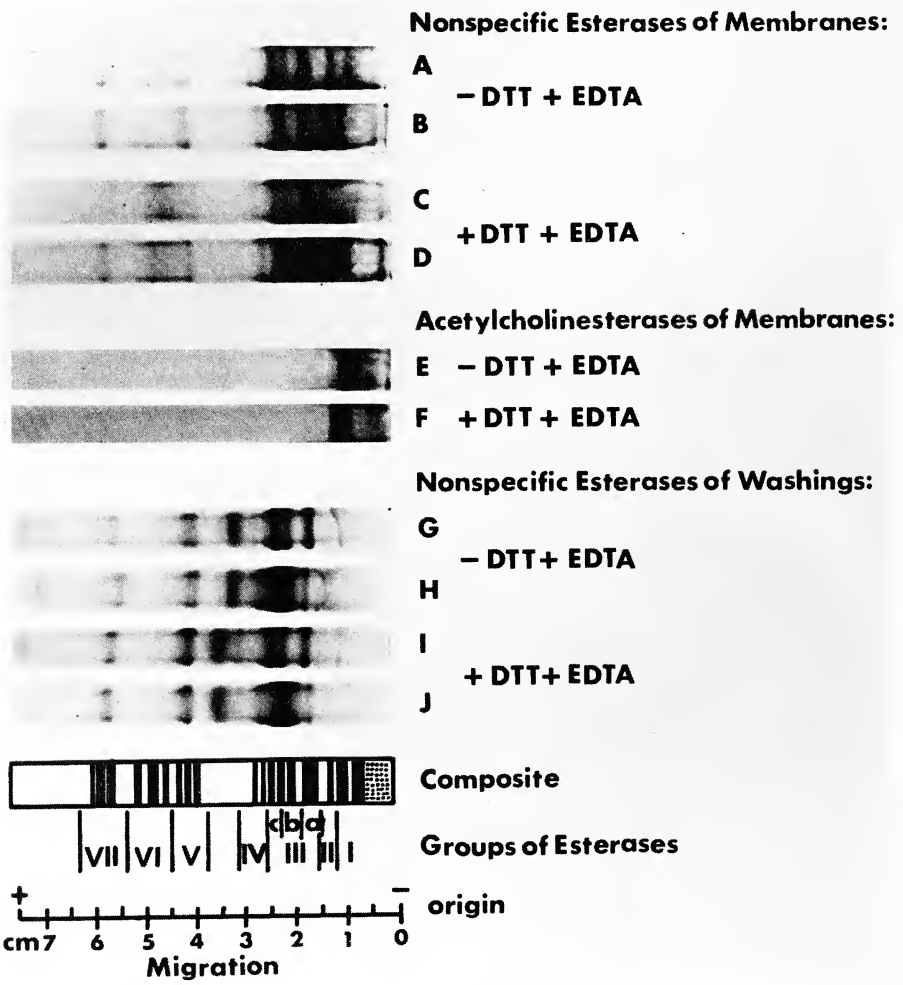

FIGURE 1. Standard polyacrylamide gel electrophoretic patterns of esterase activity in membranes and washings of rabbit erythrocytes. Esterases were solubilized in the presence of 2.5% Triton X-100 and 1 mM EDTA without (gels A, B, E, G, and H) or with 10 mM DTT (gels C, D, F, I, and J). Gels E and F were stained specifically for acetylcholinesterases, and the others were stained for nonspecific esterase activity with a mixture of α- and β-naphthyl acetate as the substrate solution. Gels A, C, G and I, and B, D, H and J distinguish the esterases of two groups of rabbits; E and F were the same for both groups. A composite drawing showing the classes of esterase activity (I, acetylcholinesterases; II, acetylesterases; III, a, b, and c, IV, and VI, carboxylesterases; V and VII, arylesterases). The bands in region 3.0 - 3.5 cm of gels G - J are hemoglobin.

4.5 - 5.5 cm, a result not clearly evident in the washings. Acetylcholinesterase activity (gels E-F; region 0 - 1.3 cm) was found only in the membrane fractions, as would be expected in light of previous reports showing that this enzyme is membrane-bound (Shafai and Cortner

1971; Wright and Plummer 1972; Ciliv and Ozand 1972; Srinivasan et al. 1972; Wheeler et al. 1972; Augustinsson et al. 1973).

Membranes and washings showed evidence of enzyme polymorphism in region 2.0 - 2.5 cm, possibly resulting from genetic variability among the rabbits (cf. gels A, C, G, and I to B, D, H, and J which distinguish two groups of rabbits). In addition, the presence of dithiothreitol (DTT) affected the number and intensity of bands in some of the samples (Fig. 1). These data indicate that the addition of reducing agents to samples, as well as genetic vaiability in tissues, can affect electrophoretic patterns (Carter 1973; Cherry and Ory 1973), which therefore should be interpreted cautiously, by careful comparison with adequate controls.

The results of testing the gels against various esterase substrates and with different inhibitors of esterase activity in membrane and wash fractions are presented in Table 1; the enzymes are grouped (I-VII) according to the mobilities shown in the diagram in Figure 1. The members of Group I, the slowest migrating enzymes, hydrolyze acetylthiocholine, butyrylthiocholine, thiophenyl acetate, and indoxyl acetate, in addition to the two substrates for nonspecific esterases (namely, α- and β-naphthyl acetate). This group of enzymes is inhibited by DPF, PMSF, and eserine but not by mercuric chloride or CMBSA, and it seems to be composed largely of acetylcholinesterases. Group II consists of esterases that did not hydrolyze acetylthiocholine or butyrylthiocholine and were not inhibited markedly by any of the inhibitors tested. The enzymes in Groups III (a, b, c), IV, and VI, consisting of slow, intermediate, and rapidly migrating carboxylesterases, respectively, were inhibited partially or completely by DPF and PMSF but not by mercurials or T-o-TP. Only Groups I and VI were inhibited by eserine. Groups V and VII showed specificity typical of arylesterases, being inhibited partially by DPF, PMSF, and the mercurial reagents. Acetazolamide did not alter the activity of any esterases distinguished in the gel patterns; thus, it seems that none of these enzymes was a carbonic anhydrase.

All of the esterases (Groups I-VII) showed some degree of activity against α-naphthyl acetate, β-naphthylacetate, and indoxyl acetate, but none showed arnidase activity toward leucyl—β-naphthylamide. Enzymes tentatively identified as acetylcholinesterases (I) showed specificity toward acetylthiocholine iodide and thiophenyl acetate, and all of the suggested carboxylesterases (III a, b, c, IV, and VI) were highly active toward α-naphthyl butyrate. Similar to the acetylcholinesterases (I), the carboxylesterases with intermediate mobilities in the gels (IV) showed activity toward butyrylthiocholine iodide, a substrate that is specifically hydrolyzed by butyrylcholinesterases. Bands in Region II

TABLE 1. Characterization of esterases from rabbit erythrocyte washings and membranes according to substrate specificity and susceptibility to inhibition and inactivation.

Treatment	Activity of Esterases of Group[a]							
	I	II	IIIa,c	IIIb	IV	V	VI	VII
Substrates								
α-Naphthyl acetate	++++	++++	++++	++++	++++	+++	++++	+++
β-Naphthyl acetate	+++	+++	+++	+++	+	+	++	+
α-Naphthyl butyrate	-	++	++++	++++	++++	-	++++	-
β-Naphthyl laurate	+	++	-	-	-	-	-	-
Indoxyl acetate	+++	++	++++	++++	+	++	+	++
Acetylthiocholine iodide	+++++	-	-	-	-	-	-	-
Butyrylthiocholine iodide	+++	-	-	-	++	-	-	-
Thiophenyl acetate	++++	+	+++	++	+	-	-	-
L-Leucyl-β-naphthylamide	-	-	-	-	-	-	-	-
Inhibitors[b]								
DPF	+	++++	+	-	-	+	-	++
T-o-TP	++++	++++	+++	+++	+++	++++	++++	++++
PMSF	+	++++	+	-	-	+	-	++
Eserine	+	++++	++++	++++	++++	++++	-	++++
CMBSA	++++	++++	++++	++++	++++	-	++++	-
Mercuric chloride	+++	+++	+++	+++	++	+	++	+
Acetazolamide	++++	++++	++++	++++	++++	++++	++++	++++
Minutes of exposure to 55 C								
0	++++	++++	++++	++++	++++	++++	++++	++++
3-7	++++	+++	+++	+	++	++	+++	++
12-18	+++	++	++	-	+	+	++	+
25-32	++	+	+	-	-	-	+	-
40	++	-	+	-	-	-	-	-
Minutes of exposure to 10 M urea								
3-7	++	++	++++	++++	++	++	++	++
12-18	+	+	+++	+++	+	-	+	-
25-32	-	-	++	++	-	-	-	-
40	-	-	+	+	-	-	-	-

[a]Groups I-VII denote bands with substrate specificities typical of acetylcholinesterases (I), acetylesterases (II), carboxylesterases (III a, b, and c, IV, and VI), and arylesterases (V and VII). Nonspecific esterase activity of each group, as determined with a mixture of α- and β-naphthyl acetate, is denoted by ++++; - indicates no detectable activity; + denotes trace activity; ++, +++ are intermediate amounts of activity; and +++++ is activity exceeding that observed toward the mixture of α- and β-naphthyl acetate substrates. The latter mixture was used also as the substrate to test the effects of inhibitors.

[b]Inhibitor concentrations used were as follows: DPF, 1 mM; T-o-TP, 1 mM; PMSF, 5 mM; eserine, 1 mM; CMBSA, 2 mM; and acetazolamide, 20 mM. Two replicates of triplicate gels of esterases were analyzed for substrate and inhibitor specificity.

were most active against esters of acetic acid but also showed some activity toward β-naphthyl laurate and thiophenylacetate.

Table I also shows results of characterization of esterases from rabbit erythrocytes on the basis of stability to heat and urea. The acetylcholinesterases (I) were stable in buffer at 55 C for 7 min and were still rela-

tively active after 18 min at this temperature; however, they were rapidly inactivated by 10 M urea at room temperature. Acetylesterases (II) and the slow (V) and fast (VII) migrating arylesterases revealed intermediate values for heat resistance and showed urea lability similar to the acetylcholinesterases (I). Most of the slow carboxylesterases (III a, c) were relatively stable to both heat and urea; however, the band in region 1.8 - 2.2 cm (III b) was extremely heat labile but remained active in the presence of urea. The intermediate (IV) and fast carboxylesterases (VIII) behaved similarly to the acetylesterases (II).

The on-gel enzymatic activities of the multiple forms of esterases from washings and membranes of rabbit erthrocytes were essentially constant over the pH range 5.7-7.4. At pH 8.0, however, all of the bands were approximately one-fourth to one-half as active as those observed at the other pH values.

CONCLUSIONS

These data from qualitative techniques of gel electrophoresis suggest that membranes of rabbit erythrocytes contain a complex array of esterases. Although some differences exist in the esterase patterns of washings and membranes, many of the enzymes exhibited similar mobilities and had corresponding substrate specificities, susceptibilities to inhibitors, pH optima, and sensitivities to heat and urea. The similarities of the banding patterns of esterases in the two fractions suggest that corresponding constituents were present in the cytoplasm and membranes of erythrocytes.

This investigation was done to standarize techniques (enzyme extraction, gel electrophoresis, detection, and identification) for examining cytoplasmic and membrane esterases of rabbit erythrocytes. Application of the techniques yielded results with good reproducibility—i.e., uniformity in intensity of gel staining, and repeatable spacial arrangement and identification of esterase bands between experiments. The electrophoretic patterns that were established may serve as standards to which those from physiologically altered test animals (e.g., due to nutritionally inbalanced diets) can be compared.

LITERATURE CITED

Augustinsson, K. B. 1961. Electrophoresis studies on blood plasma esterases. I. Mammalian plasmas. Acta Chem. Scand. 13:571-592.

Augustinsson, K. B., B. Axenfors, I. Anderson, and H. Eriksson. 1973. Arylesterase and acetylcholinesterase in the erythrocytes of man, cow and pig. Biochim. Biophys. Acta 293:424-433.

Carter, J. R. 1973. Role of sulfhydryl groups in erythrocyte membrane structure. Biochemistry 12:171-176.

Cherry, J. P. 1977. Oilseed enzymes as biological indicators for food uses and applications, p. 209-228. *In* R. L. Ory and A. J. St. Angelo (Eds.), Enzymes in food and beverage processing. American Chemical Society, Washington, D.C.

Cherry, J. P. 1978. Enzymes as quality indicators in edible plant tissues, p. 370-399. *In* H. O. Hultin and M. Milner (Eds.), Postharvest biology and biotechnology. Food Nutrition Press, Inc., Westport, CT.

Cherry, J. P., and F. R. H. Katterman. 1971. Nonspecific esterase isozyme polymorphism in natural populations of *Gossypium thurberi*. Phytochemistry 10:141-147.

Cherry, J. P., and R. L. Ory. 1973. Gel electrophoretic analysis of peanut proteins and enzymes. 2. Effects of thiol reagents and frozen storage. J. Agric. Fd. Chem. 21:656-660.

Cherry, J. P., and J. M. Prescott. 1974. Electrophoretic evaluation of various procedures for solubilizing erythrocyte membranes. Proc. Soc. Exptl. Biol. Med. 147:418-424.

Cherry, J. P., L. R. Beuchat, and P. E. Koehler. 1978. Soluble proteins and enzymes as indicators of change in peanuts infected with *Aspergillus flavus*. J. Agric. Fd. Chem. 26:242-245.

Ciliv, G., and P. T. Ozand. 1972. Human erythrocyte acetylcholinesterase purification, properties and kinetic behavior. Biochim. Biophys. Acta. 284:136-156.

Holmes, R. S., and C. J. Masters. 1967. The developmental multiplicity and isoenzyme status of cavian esterases. Biochim. Biophys. Acta. 132:379-399.

Holmes, R. S., and C. J. Masters. 1968. A comparative study of the multiplicity of mammalian esterases. Biochim. Biophys. Acta. 151:147-158.

Manwell, C., and C. M. A. Baker. 1970. Molecular biology and the origin of species: Heterosis, protein polymorphism and animal breeding. University of Washington Press, Seattle, WA. 394 p.

Markert, C. L., and R. L. Hunter. 1959. The distribution of esterases in mouse tissues. J. Histochem. Cytochem. 7:42-49.

Ray, L. E., and J. P. Cherry. 1977. Effects of hyperoxia on glutathione reductase activity, membrane proteins, and esterases of rabbit erythrocytes. Aviat. Space Environ. Med. 48:649-653.

Shafai, T., and J. A. Cortner. 1971. Human erythrocyte acetylcholinesterase. I. Resolution of activity into two components. Biochim. Biophys. Acta. 236:612-618.

Srinivasan, R., A. Karczmar, and J. Bernsohn. 1972. Activation of acetylcholinesterase by Triton X-100. Biochim. Biophys. Acta. 284:349-352.

Wheeler, G. E., R. Coleman, and J. B. Finean. 1972. Cholinesterase activities in subcellular fractions of rat liver. Biochim. Biophys. Acta. 255:917-930.

Wilkinson, J. H. 1976. Chemical enzymology: the state of the art. Lab. Manag. 14:21-24.

Wright, D. L., and D. T. Plummer. 1972. Solubilization of acetylcholinesterase from human erythrocytes by Triton X-100 in potassium chloride solution. Biochim. Biophys. Acta. 261:398-401.

OFFICERS

President:	Bernard T. Young, Angelo State University
President-Elect:	Michael Carlo, Angelo State University
Vice-President:	William J. Clark, Texas A&M University
Immediate Past President:	Elray S. Nixon, Stephen F. Austin State University
Secretary-Treasurer:	Everett D. Wilson, Sam Houston State University
Editor:	William H. Neill, Texas A&M University
AAAS Council Representative:	Arthur E. Hughes, Sam Houston State University

DIRECTORS

1981	Richard L. Noble, Texas A&M University
	Bob F. Perkins, University of Texas, Arlington
1982	Billy J. Franklin, Texas A&I University
	Ethel W. McLemore, Dallas
1983	D. Lane Hartsock, Austin
	Katherine Mays, Bay City

SECTIONS

I—*Mathematical Sciences*: Philip S. Morey, Jr., Texas A&I University
II—*Physical Sciences*: R. Charles Ivey, La Jet Corporation, Abilene
III—*Earth Sciences*: S. Christopher Caran, University of Texas, Austin
IV—*Biological Sciences*: Frank W. Judd, Pan American University
V—*Social Sciences*: Rollo K. Newsom, Southwest Texas State University
VI—*Environmental Sciences*: D. Lane Hartsock, Texas Air Control Board
VII—*Chemistry*: John T. Moore, Stephen F. Austin State University
VIII—*Science Education*: Rebecca Sparks, San Marcos
IX—*Computer Sciences*: Charles N. Adams, North Texas State University
X—*Aquatic Sciences*: G. Dan McClung, SK Engineering, San Angelo

Collegiate Academy Counselors: Shirley Handler, East Texas Baptist College
Helen Oujesky, University of Texas, San Antonio
Junior Academy Counselors: Ruth Spear, San Marcos
Peggy Carnahan, San Antonio

COVER PHOTO

Sediment Sampling
Device

by Ward, pp. 101-108

2nd CLASS POSTAGE
PAID AT HUNTSVILLE
TEXAS 77341
AND AT ADDITIONAL
MAILING OFFICE
AT LUBBOCK
TEXAS 79401

Volume XXXV, Number 3 September 1983

THE TEXAS JOURNAL OF SCIENCE

PUBLISHED QUARTERLY BY
THE TEXAS ACADEMY OF SCIENCE

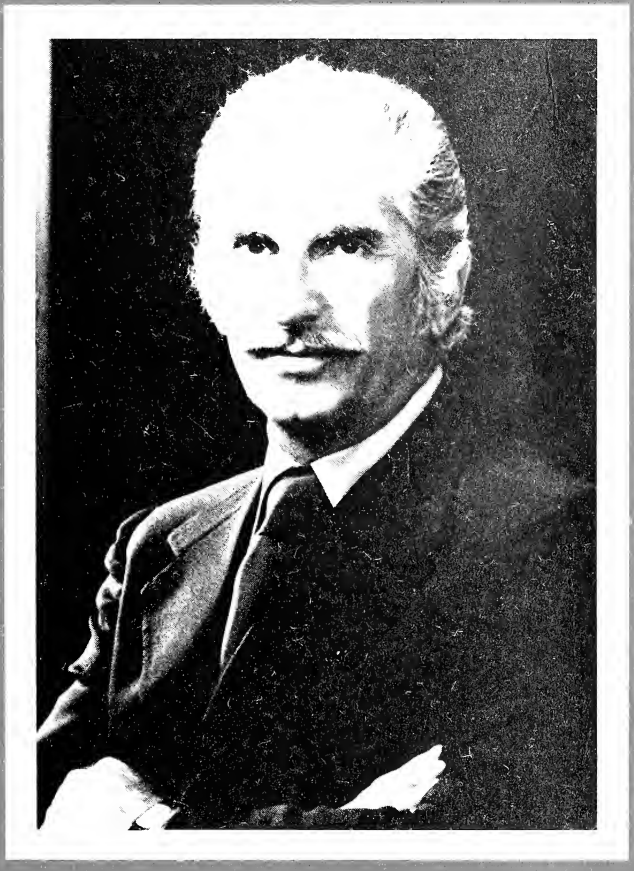

AFFILIATED ORGANIZATIONS
Texas Section, American Association of Physics Teachers
Texas Section, Mathematical Association of America
Texas Section, National Association of Geology Teachers

GENERAL INFORMATION

MEMBERSHIP. Any person or group engaged in scientific work or interested in the promotion of science is eligible for membership in The Texas Academy of Science. Dues for members are $20.00 annually; student members, $12.00 annually; sustaining members, at least $30.00 in addition to annual dues; life members, at least $400.00 in one payment; patrons, at least $500.00 in one payment; corporate members, $250.00 annually; corporate life members, $2000.00 in one payment. Library subscription rate is $45.00 annually. Payments should be sent to the Secretary-Treasurer, Box 2175, Huntsville, TX 77341.

The *Journal* is a quarterly publication of The Texas Academy of Science and is sent to all members and subscribers. Inquiries regarding back issues should be sent to Dr. Fred S. Hendricks, Dept. Wildlife & Fisheries Sciences, Texas A&M University, College Station, TX 77843.

The Texas Journal of Science (USPS 616740) is published quarterly at Huntsville, Texas U.S.A. Second class postage paid at Post Office, Huntsville, TX 77341, and at additional mailing office at Lubbock, TX 79401. Please send form 3579 and returned copies to Texas Tech Press, Box 4240, Lubbock, TX 79409.

THE TEXAS JOURNAL OF SCIENCE

Volume XXXV, No. 3 September 1983

CONTENTS

INSTRUCTIONS TO AUTHORS

Scholarly papers in any field of science, natural history, or technology are eligible for publication in *The Texas Journal of Science*. Before a paper can be accepted for publication, it must undergo critical review by at least 2 appropriate referees and the editor.

A manuscript intended for publication in the *Journal* should be prepared in accordance with the following instructions and then submitted to Dr. William H. Neill, TJS Editor, Department of Wildlife & Fisheries Sciences, Texas A&M University, College Station, TX 77843.

The manuscript is not to have been published elsewhere. Triplicate typewritten or machine-printed copies (or the original and 2 good xerographic reproductions) *must* be submitted. Text, table and figure captions, and references should be *double-spaced* with 2-3 cm margins (without right-justification) on 8½ X 11-inch paper. The title of the article should be followed by the name and business or institutional address of the author(s). *Be sure to include zip code* with the address. If the paper has been presented at a meeting, a footnote giving the name of the society, date, and occasion should be included but should not be numbered. Begin the body of the paper with a brief ABSTRACT to which is appended a list of key words (abstracting services pick this up directly), followed by the text subdivided into sections as appropriate. Use upper /lower case letters, italics (indicated by single underscore), and indentation in a way that mimics the pattern evident in the most recent issue of the *Journal*.

In the text, cite all references by author and date *in chronological order*, i.e., Jones (1971); Jones (1971, 1972); (Jones 1971); (Jones 1971, 1972); Jones and Smith (1971); (Jones and Smith 1971); (Jones 1971; Smith 1972; Beacon 1973). If there are more than 2 authors, use: Jones et al. (1971); (Jones et al. 1971).

References are then to be assembled, arranged *alphabetically*, and placed at the end of the article under the heading LITERATURE CITED. For a PERIODICAL ARTICLE use the form: Jones, A. P., and R. J. Smith. 1971. Persistence of chlorinated hydrocarbons. J. Soil Chem. 37:116-123. For a paper published in the PROCEEDINGS OF A SYMPOSIUM, etc., use the form: Jones, A. P. 1971. Persistence of chlorinated hydrocarbons, p. 155-181. *In* A. P. Jones (ed.), Pesticides in soils. Soc. Soil Chem., New York, NY. For a REPORT use: Jones, A. P. 1971. Persistence of chlorinated hydrocarbons. Texas Soils Institute (Austin, TX) Report No. 14, 46 p. A MASTERS OR Ph.D. THESIS should appear as: Jones, A. P. 1971. Persistence of chlorinated hydrocarbons in blackland soils. M.S. thesis, Texas A&M Univ., College Station, TX. For a BOOK, NO EDITORS, use: Jones, A. P. 1971. Environmental effects of chlorinated hydrocarbons. Academic Books, New York, NY, 439 p. For a CHAPTER IN A BOOK WITH

EDITORS: Jones, A. P. 1971. Persistence of chlorinated hydrocarbons, p. 13-39. *In* A. P. Jones, B. R. Smith, Jr. and T. S. Gibbs (eds.), Environmental effects of chlorinated hydrocarbons. Academic Books, New York, NY. For an IN-PRESS PERIODICAL ARTICLE use: Jones, A. P. In Press. Persistence of chlorinated hydrocarbons. J. Soil Chem. For an IN-PRESS BOOK use: Jones, A. P. In Press. Environmental effects of chlorinated hydrocarbons. Academic Books, New York, NY.

References to unpublished data or personal communications should not be listed in the LITERATURE CITED section. However, they should be presented within the text as: (unpubl. data from C. J. Jones, Dept. Zoology, Univ. Texas, Austin, TX) *or* (pers. comm. from R. C. Smith, P.O. Box 133, Mexia, TX).

Any footnotes (except those referenced in the body of a table) should appear on a separate sheet of paper, following the LITERATURE CITED.

All tables are to be typed with a carbon ribbon, free of error, without handwritten notations, and ready for photographic reproduction. Each table, headed by its caption, should be placed on a separate sheet of paper. Tables must have a text reference, i.e., Table 2 shows. . .*or* (Table 2).

Figures are to be *original inked drawings* or *photographic prints no larger than 4½ X 6½ inches* and mounted on standard 8½ X 11-inch paper. Each illustration should be marked on the back with the name of the first author and the figure number. Captions for figures are to be provided on a separate sheet of paper. Figures must have a text reference, i.e., Figure 3 illustrates. . .*or* (Fig. 3).

Authors will receive galley proofs plus the edited typescript and information concerning reprints and page charges. Proofs must be corrected (using ink) and returned to the editor within 5 days. Page charge payment (check or purchase voucher) or a publication-grant request must accompany return of the corrected proofs or a delay in printing the manuscript could occur. Reprint orders should be returned directly to Texas Tech Press, Box 4240, Lubbock, TX 79409.

THE EDITOR SHOULD BE NOTIFIED IMMEDIATELY OF ANY CHANGE IN THE PRINCIPLE AUTHOR'S ADDRESS OR TELEPHONE NUMBER.

NOTE: Authors are encouraged to contribute $35.00 per published page to defray printing costs, and authors of articles exceeding ten pages are expected to make *some* contribution to the publication fund. However, payment of printing costs is not a condition for publication in *The Texas Journal of Science*, and NO AUTHOR, WHO WOULD OTHERWISE SUBMIT A MANUSCRIPT, SHOULD HESITATE TO DO SO BECAUSE OF LACK OF FUNDS. Members without funds may apply to the Texas Academy of Science for a grant to cover some or all costs of publication.

GEOLOGY'S HERITAGE AND PROMISE[1]

by MICHEL T. HALBOUTY[2]

Chairman of the Board and Chief Executive Officer
Michel T. Halbouty Energy Co.
5100 Westheimer Road
Houston, TX 77056

As a geoscientist my career has been centered in geology, geophysics, and petroleum engineering. And, because of this affiliation, many of the other sciences have rubbed off on me. In reality, I have worn two hats since the day I graduated from Texas A&M University—one that of a geologist and the other that of a petroleum engineer. I have practiced diligently and studied continually so that I might add to my knowledge of those two disciplines to the best of my ability. To be more blunt, I can say that I gave my all to enhance them and add to their heritages.

I will take off my engineering hat now and leave the other hat on, because what I want to share with you today is the meaning of geology—the meaning of its heritage and what the science may mean for the future. Before proceeding, I want to make it clear that what I say here today you probably know already. I just want to review the "known with the knowing" so that we may all pause and reflect on the importance of the science of geology to mankind.

---

[1]Text of address presented in plenary session at the Texas Academy of Science 86th Annual Meeting, Stephen F. Austin State University, Nacogdoches, Texas, 4 March 1983. Mr. Halbouty presented the address upon the occasion of his being named "Distinguished Texas Scientist" for 1983 by the Academy. He became the fourth person to be so honored; the other three are heart surgeon Michael DeBakey (1979), physicist Ilya Prigogine (1980), and ecologist Perry Adkisson (1982).

The following synopsis of Mr. Halbouty's credentials is condensed from information compiled by Ann Benham, past president of the Academy.

[2]Michel Halbouty is among the world's foremost figures in geology and petroleum engineering. A native of Beaumont and a graduate of Texas A&M University, Mr. Halbouty not only has built one of the nation's most successful energy companies but also has authored or coauthored 5 books and over 240 professional papers. He is on the directoral boards of ten commercial, professional, and civic organizations. Active in more than 40 professional societies, Mr. Halbouty has been elected "Fellow" of four—The Texas Academy of Science, the American Association for the Advancement of Science, the Institute of Petroleum (London), and the Geological Society of America. He has also been awarded honorary membership in both the American Association of Petroleum Geologists and the American Institute of Mining, Metallurgical and Petroleum Engineers. Among numerous other awards and honors Mr. Halbouty has received are election to the National Academy of Engineering (1979) and appointment as leader of President Reagan's Transition Team on Energy.

The Texas Journal of Science, Vol. XXXV, No. 3, September 1983.

The story of the earth is the science of geology. Those of us who call ourselves geologists are fortunate that we have such a rich foundation upon which to base our studies. Others who have gone before us have lighted the way in unique but effective manners.

The procession of life, which for eons has passed over the earth's surface, and a thousand closely related themes have attracted countless men and women to the realm of the science. Their efforts have produced one of the most interesting records of human endeavor and achievement found in scientific history.

Geologists have the benefit of the accumulated knowledge of centuries of studies made by dedicated men and women who were not afraid to question the unknown, who had the courage of their convictions—the courage of stand up and be counted without fear. Geologists have a grand heritage upon which to rely.

I feel a close bond to and a great love for the earth. The almost unlimited facets of the geological sciences have fascinated me from my earliest boyhood. I have seen giant strides made in the understanding of the dynamics of the earth and I have witnessed a surge of scientific and technological breakthroughs once considered to be impossible or only in the realm of science fiction.

From the beginning, the discipline of geology has grown and advanced on the balance-scale of probability rather than in the rigid, less flexible framework of mathematics. Thus geology always has been an inexact, speculative science. Commonly suffering from speculation beyond the limits of observation and experience, geological hypotheses and theories have been promulgated and dissipated, but not without some benefit to each succeeding generation of earth scientists.

It is precisely this inexactness that makes geology such a great challenge. There were many who labored in this science who were maligned and criticized for their observations but who courageously weathered the storm of derision to prove that they were right. Although their efforts at times were impeded by ignorance and human fallibility, their observations, failures and successes helped forge the study of the earth into a fascinating science.

We can trace recorded observations of nature from those of Herodotus in the 5th century. Since that time students have searched, probed, and charted the earth to unlock her past and to record her secrets for the benefit of mankind. Our early observers of the earth were called, and even referred to themselves as, "philosophers of nature", and their efforts to prove and disprove their observations and beliefs are legendary.

The philosophers of nature during the Middle Ages undoubtedly were influenced by the "Aristotelian elements" of fire, air, earth, and water. Werner and Hutton gained many of their ideas on minerology

from the published works of George Bauer, better known as Agricola. Werner and Hutton debated their respective philosophies and fought for the minds of their colleagues, each in the belief that he was right.

Each of these men, whether right or wrong, had a heritage upon which he laid the foundation for his own pursuits. These men, their forebearers, their colleagues, and their successors all contributed in some measure to the heritage by continuously ferreting out the unknown and adding to the knowledge which we all share today.

The names of other great men of long ago come to mind, men such as John Playfair, James Hall, Robert Jameson, Nicholas Steno, William Smith, Thomas Chamberlin, William Davis, Willard Libby, Norman Bowen, James Walker, and so many more—a roll-call so long that no list could ever be completely accurate. Innumerable men and women through their discoveries, their mistakes, their confusions, and their solutions have given to us the total results of their efforts which have added immeasurably to our heritage.

Simply, our heritage consists of geologic truths, and carries no obligation except that we carry on from where our predecessors left off. Thus, there must be a continuum, based on more study, exploration, curiosity, failure, success, and total effort so that we, in turn, may hand down to our geological successors a heritage greater than that which we received. We must not break the continuum. This is our responsibility to the future of the science of geology and to the peoples of the earth.

Geology and its associated sciences have continued through the centuries to move forward to serve nations and their people. The rush of activity that began during the 19th century toward in-depth study of the earth heralded the beginning of various geoscience fields, and it is indeed significant to note that today geology has split into numerous scientific disciplines. The science has become so diversified that men and women working in one area may neither know nor understand those whose specialty lies in another field. This in turn has led to significant accomplishments for the betterment of the world's people. Let us review some of them.

In the fields of energy supply, geology was responsible for the discoveries of raw energy fuels which have been so important to the progress and prosperity of the world. Based largely on the pioneering of Israel Charles White and a handful of others in the latter part of the 19th century, geology has been the foundation of the worldwide search for oil and gas. Petroleum is probably the most dramatic modern contribution of geology to the needs of mankind.

In nuclear energy, itself based on the results of geological exploration for fissionable materials such as uranium, a whole new age of human progress has been opened.

The space program, the most conceptual field of science today, will lean more and more on geology as it progresses. We are becoming more involved in the studies of the other planets and astronaut-geologists are a regular feature of any space exploration team. Also in the realm of space, programs such as the land satellite project (LANDSAT) and the observation satellites for ocean coverage (SEASAT) have become invaluable tools in the exploration for various minerals and fuels.

The earliest photographic experiments in space on the Mercury, Gemini, Apollo and Skylab flights showed the value of the space perspective for study of the earth. The coverage provided from these missions, however, was never sufficient to do anything more than to tantalize the prospective users of space data. The Land Satellite launched in 1972 extended the application of space remote sensing to all areas of the earth and to spectral regions never seen before by man. LANDSAT provided the repetitive coverage necessary to the study of dynamic phenomena on land, in the oceans and in the atmosphere.

LANDSAT 4, now orbiting the earth with its Thematic Mapper, is providing the scientist new data with better resolution which will materially assist in the discovery of the world's energy and mineral resources of the future. As a geoscientist who has used and appreciated the value of LANDSAT data, and one who has been involved in the project since its inception, I am of the opinion that in terms of benefit to the world's people, the United States' LANDSAT program is probably the most significant mission ever launched by NASA.

Even more sophisticated satellites, some already designed and some now on the drawing boards, will provide new and spectacular data which will aid us enormously in our further search for energy and mineral resources from the land and the seas.

Oceanographers have given us valuable information of the seas and more is yet to come. We know that the seas make up one of this planet's richest ecological units and comprise scarcely touched reservoirs of resources that will absorb increasing proportions of man's research and development energies for generations to come. These untold stores of minerals and life are already creating far-reaching challenges to the geologists, biologists, and oceanographers.

In association with the paleontologists, we have recorded the age of man and developed a fascinating story of the evolution of all past living things, and working with the archeologists, geologists have made untold contributions to the culture of the entire world.

Geologists have also been responsible, along with engineers, for the development of major building and construction programs, such as changing the courses of rivers, locating dams, harbors, high-rise structures, housing developments, railroads, highways, sites for new cities

and untold other taken-for-granted activities in the advancement of human progress.

Geologists and seismologists currently are involved in studies of past earthquakes and are seeking criteria for the possible prediction of future earthquakes. This includes the study of the areas most vulnerable to earthquakes and could result in recommendations for the actual removal of major cities or portions of them to other locations where the likelihood of earthquakes would be negligible.

The spreading deserts of the world call attention to the need for protection of crops and grazing lands. As a result of using innovative land designs, new irrigation techniques, and methods of controlling wind damage, much desert land is now arable and habitable. The forests of many nations have been depleted by industrialization and natural disasters. This affects the overall agriculture by disrupting soil conditions and water balance, and we are now actively involved in reforestation to speed nature's progress in renewing and reclaiming the land.

Geologists and the aquatic scientists are also recycling and protecting our planet's most precious resource—water. We have recognized that the world's fresh water is not inexhaustible and that a problem of both the present and the future is how to meet an increasing demand with a limited supply. The problem has been approached in many ways—cloud seeding to produce rainfall, extracting fresh water from seawater, decreasing evaporation from reservoirs, building strong earthen reservoirs to hold seasonal excesses, transferring water from one basin to another and storing it in permeable rocks for future use. Through the use of three-dimensional analysis of groundwater flow, subsidence of land areas, which until recently were considered unsalvageable, is being controlled.

"Dead" lakes and waterways are being cleaned up and are being repopulated to provide new marine food supplies. Geologists have studied the effect of weather on certain land areas and have established methods to control the erosion and destruction of the land.

All of these activities and many, many more, too long a list to mention, are in some measure controlled by the proper applications of geology. Therefore, it is appropriate to state that there is no area of human interest where geology does not explore or participate in some manner.

Our science is constantly working to understand the needs of mankind and how they can be met. Through the studies of historical and physical geology, through investigations into the many branches of the earth sciences, from the deepest parts of the oceans to the heights of the atmosphere, we are finding clues to the solution of mankind's problems.

We are constantly examining the internal and external phenomena of nature to further adapt the environment to man to meet his needs and assure his continued presence upon the earth. Although all of our past efforts required diligent research and careful examination of detail in all areas of geology, we must strive for better understanding of man's future needs and ways of fulfilling these needs.

It is appropriate here to mention that the Geological Society of America's Centennial Decade Study of North America will add new chapters to what has been handed down to us by our predecessors. The investigations of this continent will write remarkable new pages in the history of the geology of this landmass. The investigation of the North American continent alone is a Herculean task. Covering more than 9 million square miles and representing slightly over 16% of the earth's land area, it poses a formidable challenge to every aspect of geoscience.

The geological endowments of North America cover the spectrum of features of terrestrial continental evolution in space, time and style. Its history is a compendium of spectacularly diverse fragments of time, each punctuated by momentus events. Its landscape has been sculptured by a staggering variety of elemental forces.

Its mosaic of natural monuments conveys an infinity of moods—awesome like Death Valley, turbulent like the Colorado River rapids, placid like Canada's Athabasca Glacier, luxuriant like the Yucatan jungle, austere like the Dakota Badlands. Mountain ranges, plains, and lakes stand out as the most obvious aspects of the terrain. Large rivers drain the interior of the continent, carrying sediments to the seas that border it. The face of the continent today is only the most recent of many profiles the continent has shown since the earth took shape.

Whatever its origins, North America was first a lifeless landmass in the turbulent process of being formed and shaped. Towering mountains were thrust up by volcanic action. The mountains were capped with smoldering craters which spewed torrents of lava. The crust of the continent coiled and contracted, buckled and buckled again, shifting and lifting mountain spires. Then earthquakes shattered and rearranged the continent. The primal seas washed the surface and hid the landscape. Throughout the billions of years, the forces of nature continued in restless surges to remold and strip and lift and submerge again the land.

The rainbow of rock stripes in the Grand Canyon marks the passage of time. Billions of sand particles from ancient seas became sandstone layers, mud transformed into shale, enormous masses of marine skeletons and shells compressed to form limestone. Every color and every layer signifies small eternities that mock our conventional calendars.

From the Canadian Shield carved by ice after milenia of folding, faulting and compression, to the Central Lowland of arches and domes,

basins and troughs, to the Appalachian Highlands uplifted by extensive moutain building, to the soft, young Coastal Plain and to the rugged Western Cordillera, the face of the continent presents endless opportunities for exploration and investigation.

What happened so long ago is impossible to determine with certainty. The sequence of events, and the events themselves, are still disputed by scholars and scientists. Time is a tease when it comes to contemplating these events. A thousand years is a fleeting instant, barely worth mentioning. A million years is a brief moment, leaving the barest of legacies.

It is noteworthy to observe that what is visible of our continent is awesome in its grandeur, and its unsurpassed surface beauty is challenged only by its geological history. What we have already uncovered of the once unseen has intrigued and amazed both scientist and layman alike. What is still yet to be uncovered will amaze us even more.

As I stated in the beginning of this presentation, my intention was to review the "known with the knowing" and what I have just outlined about the Continent are things you already know. This audience today is comprised of scientists from many fields, but we all have the common bond as probers who are constantly searching for better solutions to old problems and searching for new methods of unlocking the secrets of our world.

Mankind today relies more than ever before on the endeavors of scientists for survival. The world within us and the world around us are the realms of science. In looking toward the future, it is vitally important that we realize that the quality of the lives of the world's people is directly linked to the scientific and technological progress which are made day after day. This progress must be never-ending, a continuance without interruption or cessation, an everlasting hand-down procedure. This is the obligation each one of us here owes to our respective science.

The scientific endeavor is the most optimistic of all human activities. It can have no end—only continual challenge and only continual amazement in what the mind of man can imagine, change, or create. The future scientific accomplishments are limited *only* by the imagination of the men and women involved in the ever changing, ever challenging world of science. Today's science is tomorrow's hope.

TRANSLATION OF C SHELL SCRIPTS TO C FOR FASTER EXECUTION OF UNIX COMPUTER PROGRAMS

by GRADY EARLY

Department of Mathematics and Computer Science
Southwest Texas State University
San Marcos, TX 78666

and JANE GAMBILL *and* TERESA THOMAS

Department of Computer Science
University of North Carolina
Chapel Hill, NC 27514

ABSTRACT

Many UNIX computer programs are, in reality, *shell scripts*—text files interpreted at run-time by the generalized UNIX command-language interpreter, the shell. Although this mechanism provides great flexibility, it tends to slow execution because some shell scripts are executed frequently and iteratively. In this paper, we describe a translator for one of the available UNIX shells, the C shell. Given a C shell script as input, the translator produces a C program to accomplish the same job. The program binds C shell scripts for fast execution, avoids interpretive overhead, and performs some operations in-line that otherwise would be done by invoking a subprogram.

INTRODUCTION

The C shell (Joy 1979, 1980) is a generalized command-language interpreter that is somewhat more powerful and more flexible for the interactive user of UNIX[1] than the regular shell (Bourne 1978; Ritchie and Thompson 1978). The C shell provides a very convenient, interactive mechanism for command execution and file manipulation. A multitude of C shell commands, UNIX system commands, and user-written programs (including shell scripts) may be invoked and executed by the C shell. Commands may be executived singly, in parallel (pipelining), or in tandem. C shell and user variables may be defined and manipulated. These variables may be used as normal program variables or may be used to specify files (either explicitly or via pattern-matching metacharacters) that are to be created, modified, or deleted as dictated by the commands being executed. Late binding (e.g., of file names) allows the flexibility that one expects of an interpretive system.

However, the C-shell mechanism has the usual disadvantages of a purely interpretive system. One primary disadvantage is the relatively

[1]UNIX is a trademark of Bell Laboratories.

slow speed of execution as compared to compilation or partial compilation. Many UNIX programs are, in fact, C shell scripts that are frequently or iteratively invoked. It would be desirable to bind such sequences and thus reduce execution time by removing much of the interpretive overhead. The purpose of this project was to investigate the feasibility of producing a translator to effect early binding.

DESIGN DECISIONS

Target Language

The design of any programming system necessitates many decisions that affect the form of the finished product. Perhaps the most important decision, in the present case, was the choice of language. Translation to a high-level language is often much easier than translation to an assembly or machine language. Three considerations led to the selection of C. First, the C shell was designed with a C-like syntax. Thus, the formulation of C shell commands into corresponding C statements is nicely effected. Second, the code generation routines, being written in C, reduced the confusion inherent in writing, in one language, a translator for a second language, to produce code in yet a third language. The presence of a very powerful C compiler in the UNIX system made the decision almost foreordained. Third, the use of C throughout means that the translator is at least potentially transportable.

Translation Aids

The spirit of UNIX programming insists that there be no "reinvention of the wheel." In this case, there were two clear choices of preexisting 'wheels.' The UNIX system contains two state-of-the-art translation aids that greatly simplify the translation task. The first is 'lex' (Lesk and Schmidt 1979), which is a lexical analyzer generator. Use of lex requires only that one define the rules and associated actions to produce tokens that can be recognized by the parser. The function of lex is to take the rules specified by the user and generate a program (in C) that reads the input script and breaks off appropriate tokens, passing them to the parser.

The second is 'yacc' (Johnson 1981), which generates a parsing algorithm (also in C). The user specifies a grammar and associated actions to be performed upon recognition of a grammatical rule. The grammar may be ambiguous, but should be context-free. As we shall see, C shell constructs are not necessarily context-free. However, this difficulty can be avoided.

Modularity and Information Hiding

Another decision, which was almost foreordained, required that the translator be written in clearly-defined and easily-interfaced modules.

This decision allowed development of the translator to proceed on three fronts—lexical analysis, parsing, and code-generating. Crisp module definition and interfacing thus accomplished two goals. First, the amount of programmer interaction was reduced because, given carefully controlled interface specifications, each programmer was free to develop his part of the translator in the most efficient way. Algorithm modifications in one module had minimal effect on other modules. Second, consistent modularity resulted in a translator that is easily enhanced.

Incremental Development

There were actually twelve versions of the translator developed. Each version, beginning with the implementation of comments only (!), added yet another C shell feature to the translator. The decision to proceed in this manner resulted in the attainment of three goals. First, beginning with the very simplest construct (the comment) allowed the programmers to become familiar with the use of the various translation aids and with the source and target languages. Interface specification problems were resolved at a very low level, and it was possible to achieve a working system very quickly. Second, it was possible to fix overall goals as development proceeded. Rather than attempt the implementation of a grand, predetermined goal, features were added in a fairly natural manner. And it was possible to stop at an arbitrary point—when the system was judged to be powerful enough to be useful and when it had been demonstrated that translation was feasible as well as useful. Third, the experience gained with incremental development resulted in a system that can be easily enhanced. The steps required to add yet another feature to the translator are by now somewhat stylized. Enhancement of the system can actually take the form of addition of new features or of increasing the capabilities of features already implemented. In either case, the overall system need not be redesigned; only those modules affected by the enhancement need be scrutinized.

Error Handling

One of the most elegant design decisions concerns the error handling capabilities of the translation system: There are none. However, the system does detect and report C shell constructs, or forms therof, that are not implemented within the current version of the translator. Error handling within those constructs that are implemented was deliberately avoided. The goal was to reduce the complexity of the translation system itself, and the goal was attained. The elegance of the decision arises from the attempt to produce C programs that faithfully mimic, insofar as possible, the results produced by the C shell as it interprets the scripts being translated. The presence of the C shell makes it very easy to require that, prior to translation, the script be executed interpre-

tively. Thus, syntactic or semantic errors will be detected during interpretation. Given an input script that has been debugged by the C shell, the translator need not concern itself with the correctness of that script. If the script is executable by the C shell, then it is by fiat correct.

Binding

The stage at which a particular bit of information is bound can range from very early binding of complete compilation versus very late binding of pure interpretation. The translator pursues a moderate course between these two extremes. The primary area in which binding time was a concern was in the specification of file names. On the UNIX system, there is no particular differentiation among files: At one and the same time, a specific file may contain a command which is to be executed, or it may be taken as the argument to a command. We treat these two areas separately. For example, the command

```
cat *.c>outfile
```

means to catenate all files, in the current directory, that have the .c suffix and to store that catenation in the specified output file. In most scripts the command itself (e.g., cat) is subject to little if any change. That is, the command to be executed is generally known and specified explicitly. Hence, command file names are bound at translation time. Command arguments, on the other hand, often are not known at translation time. They are specified, as in the above example, with the help of pattern-matching metacharacters. The intent is that all files whose names match the pattern, including those that did not exist when the command was written, be used as arguments to the command. A run-time routine effects this file name expansion (globbing) at the time the translated script is actually executed.

Context Sensitivity

The decision to use the C shell interpreter to debug scripts before subjecting them to translation yielded yet another advantage in the implementation of the translator. Because all scripts input to the translator are assumed to be correct, the translation of one line of a script has little or no effect on the translation of subsequent lines. For example, an 'if' statement implies that a corresponding 'endif' is also in the script. This arrangement simplified the design of the translator in that code could be generated for each line as it was encountered in the script. Not only did this simplify code-generation, but also parsing. In effect, the translator can proceed as if each script consists of only a single line. Of course, some information can be common to more than one line of a script. A crucial example of this lies in the variables typically defined in one line, modified in others, and utilized in still others.

The handling of this problem simply required the maintenance of a user symbol table for collecting the names of all variables specified by the user. No auxiliary information was required since the translator, like the C shell, maintains all variables as arrays of 0 or more strings. Thus, variable handling simply required keeping a table of variable names so that the appropriate C declarations could be produced once the entire script had been translated.

Futher, the line-by-line translation of scripts allowed resolution of a conflict created by the use of yacc, which requires a context-free grammar, to parse C shell commands, which are not context-free. For example, in the commands

```
set x==
echo x==
```

the 'x==' mean entirely different things. In the first command, the meaning is to store the string '=' in the variable x. In the second command, the string 'x==' is to be displayed. However, by processing each script line separately, it is possible to handle such problems by interpreting each character string in terms of the type of line in which it is encountered. Thus, the 'set' command is a signal that the first equal sign be taken as a replacement operator, while the 'echo' command is a signal that equal signs have no special meaning within words.

IMPLEMENTATION

The current version of the translator implements more than enough C shell features to verify the effectiveness and the feasibility of translation. These features are variables, comments, simple commands, pipelines, input/output redirection, globbing (metacharacter pattern matching for file names), set/unset, arithmetic and string expressions, if/else if/else/endif, while/end, and goto/label.

The features implemented are quite adequate for many UNIX programming applications. And they are adequate to demonstrate the advantages of translation through the comparison of execution times of interpreted versus translated scripts. It would be desirable to implement other C shell features; but for purposes of this project, the above list is adequate.

EXAMPLES

A perhaps atypical C shell script is shown in Figure 1. While a more common use of scripts is for file manipulation, this example is nevertheless appropriate to illustrate the form of the generated code. The C code which corresponds to the example of Figure 1 is shown in Figure 2.

```
#Example 2:  Calculate n! where n is a command line argument.
set n = $argv[1]
set f = 1
loop:
      if($n <= 0)then
         goto output
   else
         @ f *= $n
         @ n--
   endif
   goto loop
output:
      echo $argv[1] factorial equal $f
```

FIGURE 1. C shell script example.

Note that the execution of a command is effected by means of the UNIX *exec* command which does not return control to the calling program unless, for some reason, it is not possible to execute the specified command. Thus, the system *fork* command creates a clone, an almost exact duplicate, of the running program. The original program, called the parent, waits for the clone, called the child, to execute the specified command. When that command completes execution, the child dies with a signal to the parent that it can resume execution. Note also that two separate exec's are generated. The reason for this is that a command may itself be a shell script or it may be an executable binary file such as the output of the C compiler. The *execv* attempts command execution under the assumption that the command is an executable binary file. If this assumption is incorrect, then the execv will fail and

```
#include     <stdio.h>
#define      MAXVEC       100
#define      MAXLINE      512
char  *strcpy();
char  *strcat();
char  *malloc();
int   tmp;
char  cmdline[MAXLINE];
int   execvecc;
char  *execvecc[MAXVEC];
int   pid;
int   ivec;
/*
 *User-defined variable
 *declarations
 */
char  *n[MAXVEC];
int    n;
char  *f[MAXVEC];
int   _f;
main(_argv,argv)
int   _argv;
char  *argv[];
{
      _argv--;
/*
#Example 2:  Calculate n!
             where n is a
             command line
             argument.

 */
     n[1]=argv[1];
     _n=1;
     f[1]="1";
     _f=1;
loop:;
     if(atoi(n[1])<=0){
     goto output;
     }
     else{
     tmp=atoi(f[1])*atoi(n[1]);
     if(strlen(f[1])<10)
        f[1]=malloc(10);
     sprintf(f[1],"%d",tmp);
     _f=1;
     tmp=atoi(n[1])-1;
     if(strlen(n[1])<10)
        n[1]=malloc(10);
     sprintf(n[1],"%d",tmp);
     _n=1;
     }
     goto loop;
output:;
     execvec[0]="echo";
     execvec[1]=argv[1];
     execvec[2]="factorial";
     execvec[3]="equal";
     execvec[4]=f[1];
     execvec[5]=NULL;
     execvecc=5;
     if((pid=fork())==0){
        execv("/bin/echo",execvec);
        strcpy(cmdline,"/bin/echo");
        for(ivec=1;ivec<execvecc;ivec++){
           strcat(cmdline," ");
           strcat(cmdline,execvec[ivec]);
        }
        execl("/bin/csh","csh","-c",cmdline,NULL);
        exit(-1);
     }
     while(wait(0)!=pid);
     exit(0);
}
```

FIGURE 2. Example in figure 1 translated to C.

TABLE 1. Relative sizes of C shell script, C program, and object program.

file name	lines	words	characters
ex1	7	32	159
ex1.c	84	125	1505
ex1.out	17	64	8883
ex2	13	45	236
ex2.c	69	106	1131
ex2.out	19	58	8598
ex3	12	50	238
ex3.c	163	304	3058
ex3.out	23	73	10029

will return control to the child which will then attempt to execute the command via the *execl* under the assumption that the command is a C shell script. If this assumption is incorrect, then the entire program will exit. If the script has been debugged using the C shell interpreter, then such problems as these should not arise.

RESULTS

Table 1 gives information typical of the additional cost in file space required by translated and compiled scripts. The first row in each triple represents the original script, the second row represents the generated C program, and the third row represents the compiled binary file. Example 2 is the script exhibited in Figures 1 and 2. The script of Example 1 effects the counting of all lines, words, and characters in those files whose names are listed on the command lines. The script of Example 3 effects the counting of all lines, words, and characters of all files, in the current directory, whose names match the *.c pattern.

Table 2 gives typical times of translation and compilation, and execution time gains through reduction of interpretive overhead. The first row gives the interpretive execution times for the three scripts. The last three rows give the times for translation, compilation, and execution, respectively. Column 1 gives execution times for Example 1 (three files processed). Columns 2-4 give execution times for Example 2 (5!, 10!,

TABLE 2. Relative execution time (seconds) of C shell scripts, translator (cshp), C compiler (cc), and object code.

	ex1	ex2			ex3
file	3 files	n=5	n=10	n=15	8 files
script	2.0	2.1	3.1	3.5	8.2
cshp	1.2		1.4		1.6
cc	3.9		3.2		6.7
.out	.4	.1	.1	.1	6.2

15!; only one translation and compilation required). Column 5 gives execution times for Example 3 (eight files processed).

CONCLUSION

The C shell was designed primarily for easy, interactive use. However, that ease of use encourages—almost guarantees—inefficient use of the UNIX system. Because it is so much easier to create C shell scripts than equivalent C programs (as evidenced by the relative sizes of the script and the C program in Figures 1 and 2), it is much more programmer-efficient to create scripts. But if these scripts are frequently invoked, then there exists the possibility of an unacceptably inefficient use of system resources. The clear solution then is the development of a translator that preserves the programmer-efficiency achieved by the usage of scripts while preventing the system-inefficiency produced by repetitive and unnecessary interpretation. The prototype translator described above accomplishes these objectives at the relatively modest cost of additional file space required by the translated and compiled versions of the script.

ACKNOWLEDGEMENT

Many thanks are due to Dr. Fred Brooks, Jr. and to Mr. Mike Pique, whose advice and encouragement contributed significantly to the success of the project.

LITERATURE CITED

Bourne, S. R. 1978. The UNIX shell. The Bell System Technical Journal 57:1971-1990.

Johnson, S. C. 1978. Yacc: Yet another compiler compiler. *In* UNIX programmer's manual. Bell Telephone Laboratories, Holmdel, NJ.

Joy, W. 1979. Csh. *In* UNIX programmer's manual, seventh edition, University of California, Berkeley, CA.

Joy, W. 1980. An introduction to the C shell. *In* UNIX programmer's manual, seventh edition, University of California, Berkeley, CA.

Lesk, M. E., and E. Schmidt. 1979. Lex: A lexical analyzer generator. *In* UNIX programmer's manual, Bell Telephone Laboratories, Holmdel, NJ.

Ritchie, D. M., and K. Thompson. 1978. The UNIX time-sharing system. The Bell System Technical Journal 57:1905-1929.

VEGETATIONAL ANALYSIS OF A POST OAK—BLACK HICKORY COMMUNITY IN EASTERN TEXAS[1]

by K. L. MARIETTA *and* E. S. NIXON

Department of Biology
Stephen F. Austin State University
Nacogdoches, TX 75962

ABSTRACT

A well-stratified, upland post oak (*Quercus stellata* Wang.) and black hickory (*Carya texana* Buckl.) community in Jasper County, Texas, had an overstory dominated by *Quercus stellata* and *Carya texana*, and a well developed shrub layer composed primarily of *Forestiera liqustrina* (Michx.) Poir., *Crataegus marshallii* Eggl., *Vaccinium arboreum* Marsh., and *Ilex vomitoria* Ait. The woody seedling layer was dominated by *Gelsemium sempervirens* (L.) Ait. and *Parthenocissus quinquefolia* (L.) Planch. The sparse herbaceous layer was composed primarily of *Chasmanthium sessiliflorum* (Poir.) Yates. Although this community was located within the Longleaf Pine Forest region, its woody vegetation closely resembled that of the Oak-Hickory region to the northwest.

INTRODUCTION

Eastern Texas exhibits a great diversity of woodland habitats including dry uplands, mesic uplands, mesic creek bottoms, wet creek bottoms, spring and seepage areas, river bottomlands, and swamps. Vegetation on all of these sites must be analyzed to assess the forest resources of east Texas. The neglected habitats are the uplands. Sullivan and Nixon (1971) and Langston (1974) have characterized a few mesic upland communities in Nacogdoches County. Because there is a noticeable void in the literature on xeric upland communities, this study focused on a mature forest community in the dryer uplands.

East Texas has a mild mesohumid climate with 100 to 125 cm of annual precipitation that is fairly evenly distributed, with driest months in the summer and slight highs in precipitation during December and May (Carr 1967). The average free air temperature is 18 C, with extremes rarely beyond 40 C and -10 C. The average growing season is 245 days.

The study area was within the Longleaf Pine Forest region of Tharp (1939) and the Southeastern Evergreen Forest region of Braun (1950). Geologically, the area is part of the Catahoula formation, which was formed during the Tertiary Period and is composed of tuffaceous mud-

[1]This paper is part of a thesis presented by the senior author in partial fulfillment of the requirements for the Master of Science degree, Stephen F. Austin State University.

stone and sand (Geologic Atlas of Texas 1967). The general topography is gently rolling, with elevations of 70 to 170 m. The soil is a sandy loam of the Corrigan Series (Raymond Dolezel, U.S.D.A. Soil Conservation Service, Nacogdoches, TX, pers. comm.) The Corrigan Series is a moderately deep, somewhat poorly drained upland forest soil. Taxonomically it is a fine, montmorillonitic, thermic Typic Albaqualf.

The post oak-black hickory community was located in northern Jasper County near its boundary with Angelina County, about 27 km southeast of Zavalla, Texas. Disturbed *Pinus taeda* forest surrounded the small, undisturbed community on three sides while the southeast portion bordered Texas highway 63. The 0.4 ha study site was a relatively flat (maximum slope to 5 %) upland adjacent to a small creek.

METHODS

The study site was sampled during 1978 with transects composed of contiguous 25 m^2 (5 $\times$ 5 m) plots randomly placed in an east-west direction. A total of 54 plots was analyzed. Woody seedling and herbaceous plants were sampled from smaller plots nested in the northwest corner of each 25 m^2 quadrat. In the 25 m^2 plots, the diameters of all trees, shrubs, and woody vines, with diameters equal to or greater than 0.5 cm at about 1.4 m above the ground (diameter at breast height = dbh $\geq$ 0.5 cm), were recorded by species during the summer. Concurrently, seedlings of woody species with dbh of less than 0.5 cm were counted in 4 m^2 (2 $\times$ 2 m) plots. Herbaceous species data were recorded from 1 m^2 (1 $\times$ 1 m) plots every two weeks during the growing season, from February through October. The herbaceous species rooted in each plot were identified and counted as they flowered. Shoots of rhizomatous plants were treated as individual plants.

Plot data were used to determine importance values for each species. Importance values were based on relative frequency, relative density, and relative basal area for those woody species with measured dbh and on relative frequency and relative density for woody seedling and herbaceous plants. The Shannon-Weiner diversity index (Shannon and Weaver 1949) was computed for each layer of the community and for the community as a whole. Nomenclature followed Correll and Johnston (1970).

Soil samples collected from the A horizon at three selected locations within the study site were analyzed for pH, Ca, P, K, and Mg by the Stephen F. Austin State University Soil Testing Lab. Particle size distribution was determined by the hydrometer method (Bouyoucos 1962).

TABLE 1. Physical and chemical properties of the A Horizon (0-15 cm) of the soil at the study site.

		Exchangeable cations (ppm)				Distribution (%) of particle size			
Sample	pH	Ca	P	K	Mg	sand	silt	clay	Texture
1	5.2	600	1.5	50	75	75.6	15.4	9.0	sandy loam
2	4.6	200	2.0	42	35	78.0	13.2	8.8	sandy loam
3	5.2	300	0.7	37	60				

RESULTS AND DISCUSSION

Soils

The physical and chemical properties of the top soil are reported in Table 1. These results indicate the soil is low in phosphorus, a condition often encountered in east Texas soils (Nixon et al. 1977). Such low levels of P, however, do not appear to restrict the growth of native east Texas plants.

Woody Vegetation

The community was well stratified with distinct overstory, shrub, woody seedling, and herbaceous layers. The overstory layer was composed of large trees up to 50 cm dbh and 25 m in height. Several of the largest *Quercus stellata* trees were cored and found to range in age from 85 to 100 years. The larger trees were scattered over the area, forming a relatively closed canopy with occasional openings. *Quercus stellata* and *Carya texana* dominated this layer, along with occasional *Ulmus alata* and *Quercus nigra* (Table 2).

The shrub layer of the community was quite prominent, as indicated by the presence of six shrubby species among the top-10 dominant woody species (Table 2). Most common were *Forestiera ligustrina, Crataegus marshallii,* and *Vaccinium arboreum.* With a combined density of 13.4 plants/25 m^2 plot, these species formed occasional thickets in the area and represented 98.0 % of the individuals with dbh from 1-5 cm.

The woody seedling layer was dominated by small vines of *Gelsemium sempervirens* and *Parthenocissus quinquefolia,* which together made up 40.2 % of the total importance value of this stratum. The other eight of the top-10 dominants were seedlings of the canopy and shrub dominants. All the remaining species in this layer, except for five, were seedlings of the woody overstory and shrub layer species. The five exceptions were *Rhus toxicodendron, Bignonia capreolata, Rubus trivialis, Trachelospermum difforme,* and *Ascyrum hypericoides.* Woody seedling species had a total density of 40.4 plants/4 m^2 plot (253 plants/25 m^2 plot). *Gelsemium sempervirens* had a density of 18.7

TABLE 2. Data on frequency, density, basal area, and importance value for woody species in the canopy and shrub layers.

Species	Frequency (%)	Relative Frequency (%)	Density (No./25m²)	Relative Density (%)	Relative Basal Area (%)	Importance Value[a]
Quercus stellata	46.3	7.1	1.0	5.5	41.3	53.9
Carya texana	48.2	7.4	0.8	4.2	24.1	35.7
Forestiera ligustrina	81.5	12.5	3.4	18.9	1.6	33.0
Crataegus marshallii	68.5	10.5	2.7	15.0	1.7	27.2
Vaccinium arboreum	48.2	7.4	2.2	12.3	4.4	24.1
Ilex vomitoria	59.3	9.1	1.9	10.4	1.5	21.0
Ulmus alata	29.6	4.5	0.4	2.1	13.2	19.8
Crataegus spathulata	50.0	7.7	1.9	10.3	1.3	19.3
Ilex decidua	50.0	7.7	1.4	7.5	0.8	16.0
Quercus nigra	13.0	2.0	0.2	0.8	8.0	10.8
Others[b]		24.4	2.4	13.1	2.1	39.6
Total		100.3	18.3	100.1	100.0	300.4

[a]Sum of relative frequency, relative density, and relative basal area.

[b]Other species, listed in order of decreasing importance value, were *Chionanthus virginica, Viburnum rufidulum, Callicarpa americana, Vitis rotundifolia, Crataegus crus-galli, Pinus taeda, Quercus marilandica, Campsis radicans, Fraxinus americana, Bumelia lanuginosa, Gelsemium sempervirens, Smilax bona-nox, Berchemia scandens, Ilex opaca, Juniperus virginiana, Cissus incisa, Lonicera japonica, Parthenocissus quinquefolia, Smilax rotundifolia.*

plants/4 m² plot (117 plants/25 m² plot), which was three times higher than *Parthencissus quinquefolia* and nine times higher than any other species in the woody seedling layer.

Herbaceous Vegetation

The herbaceous layer of the community was completely dominated by *Chasmanthium sessiliflorum*—a caespitose, rhizomatous, shade tolerant, perennial grass of sandy forests (Gould 1975). It occurred in all 54 plots and made up 53.9 % of the total importance value and 77.0 % of the total density for herbaceous species (Table 3).

Including *Chasmanthium sessiliflorum*, 34 species, representing 18 families, flowered in the plots. Eleven of these species were represented by a single individual. An additional 10 species were represented by only two individuals. Thus 61.8 % of the species present in the community had an importance value of less than 1.0 % of the total. A density of 31.0 plants/m² plot (775 plants/25 m² plot) was tabulated (Table 3).

Eighteen species (52.9 %) flowered before the trees produced mature leaves in the spring. During the late spring and summer months, 12 species, including *Chasmanthium sessiliflorum*, flowered. The remaining 4 species flowered in September and early October. Of the 34 species present, 3 were annuals and 31 perennials. Only the perennial

TABLE 3. Frequency, density, and importance values for the herbaceous species.

Species	Frequency (%)	Relative Frequency (%)	Density (No./m²)	Relative Density (%)	Importance Value[a]
Chasmanthium sessiliflorum	100.0	30.9	23.9	77.0	107.9
Ranunculus fascicularis	38.9	12.0	1.6	5.1	17.1
Stipa avenacea	37.0	11.4	0.9	3.1	14.5
Carex nigromarginata	18.5	5.7	0.5	1.5	7.2
Sanicula canadensis	9.3	2.9	0.6	1.9	4.8
Aster patens	9.3	2.9	0.6	1.8	4.7
Carex flaccosperma	11.1	3.4	0.3	0.9	4.3
Vicia minutiflora	11.1	3.4	0.2	0.5	3.9
Scutellaria parvula	5.6	1.7	0.6	2.0	3.7
Galium uniflorum	7.4	2.3	0.2	0.5	2.8
Others[b]		23.4	1.8	5.7	29.1
Total		100.0	31.2	100.0	200.0

[a]Sum of relative frequency and relative density.

[b]Other species, listed in order of decreasing importance value, were *Nothoscordum bivalve, Claytonia virginica, Galactia volubilis, Allium canadense, Oxalis violacea, Dichanthelium oligosanthes, Sporobolus asper, Carex complanata, Dichanthelium angustifolium, Asplenium platyneuron, Aristida longespica, Dichanthelium lindheimeri, Dichanthelium laxiflorum, Cardamine bulbosa, Ruellia humilis, Passiflora lutea, Oxalis dillenii, Anemone caroliniana, Spiranthes X laciniata, Cyperus globulosus, Polygala polygama, Acalypha gracilens, Panicum anceps, Cyperus ovularis.*

grass and sedge species such as *Chasmanthium sessiliflorum, Stipa avenacea,* and *Carex nigromarginata* were present in the vegetative form throughout the growing season.

Diversity

Diversity indices for each layer and a combined index were computed (Table 4). The herbaceous layer was much less diverse than the woody or woody seedling layer. This reflected the complete dominance of *Chasmanthium sessiliflorum.* The combined index as well as the herbaceous layer index is lower for this community than for more open upland communities studied in the same area (Marietta and Nixon unpublished data).

Community Comparisons

Dry upland sites are scattered throughout eastern Texas. They occur in Tharp's (1939) Pine-Oak and Oak-Hickory Forest regions as well as in the Longleaf Pine Forest region. In the Oak-Hickory region, *Quercus stellata* is the universal dominant usually accompanied by *Q. marilandica* and *Carya texana* (Tharp 1925; McBryde 1933). *Quercus stellata* and *Carya texana* were dominants in the present study. Other associated species listed by Tharp (1939) and McBryde (1933) were also found in this study.

TABLE 4. Shannon-Wiener diversity indices for the community's layers, separately and combined.

Layer	Diversity index	Number of species
Woody	3.63	29
Woody seedling	2.95	29
Herbaceous	1.69	34
Combined	3.82	66

Our post oak-black hickory community was also similar to communities in the Western Cross Timbers region of Texas (Dyksterhuis 1948), and to communities in the Oak-Hickory region of Oklahoma (Rice and Penfound 1959). Rice and Penfound (1959) compiled a list of species for upland forest in Oklahoma. We found all the listed woody species, plus *Ilex vomitoria* and *Forestiera ligustrina,* which are more coastal in their distribution and therefore would not be expected in Oklahoma.

The paucity of quantitative studies of dry upland communities in the Pine-Oak and Longleaf Pine regions makes comparisons difficult. However, a great deal of similarity is likely. Sullivan and Nixon (1971) analyzed the vegetation of an upland site in the Pine-Oak region which was more mesic than the present site. The community was dominated by *Pinus echinata, Quercus stellata, Sassafras albidum, Cornus florida,* and *Carya* spp. The canopy layer of the more mesic community had a greater diversity of species than our post oak-black hickory community.

The dominance of *Chasmanthium sessiliflorum* in the herbaceous layer of our community is not surprising. It is frequently encountered in the shade of east Texas forests and has been listed among the dominant species of other communities (Stransky et al. 1974; Nixon et al. 1981).

LITERATURE CITED

Bouyoucos, G. J. 1962. Hydrometer method improved for making particle size analyses of soil. Agron. J. 54:464-465.

Braun, E. L. 1950. Deciduous forests of eastern North America. The Blakiston Company, Philadelphia, PA. 596 p.

Carr, J. T. 1967. The climate and physiography of Texas. Texas Water Development Board Report 53. 27 p.

Correll, D. S., and M. C. Johnston. 1970. Manual of the vascular plants of Texas. Texas Research Foundation, Renner, TX. 1881 p.

Dyksterhuis, E. J. 1948. The vegetation of the Western Cross Timbers. Ecol. Monogr. 18:325-376.

Geologic Atlas of Texas. 1967. Palestine sheet. Bureau of Economic Geology, University of Texas, Austin, TX. 1 p.

Gould, F. W. 1975. The grasses of Texas. Texas A&M University Press, College Station, TX. 653 p.

Langston, S. A. 1974. Woody vegetation of mesic uplands in Nacogdoches and Rusk counties, Texas. Masters thesis, Stephen F. Austin State University, Nacogdoches, TX. 40 p.

McBryde, J. B. 1933. The vegetation and habitat factors of the Carrizo sands. Ecol. Monogr. 3:247-297.

Nixon, E. S., R. L. Willett, M. L. Butts, and C. L. Burandt, Jr. 1981. Early seral development following partial clearcutting in east Texas. Texas J. Sci. 33:25-32.

Nixon, E. S., R. L. Willett, and P. W. Cox. 1977. Woody vegetation of a virgin forest in an eastern Texas river bottom. Castanea 42:227-236.

Rice, E. L., and W. T. Penfound. 1959. The upland forest of Oklahoma. Ecology 40:593-608.

Shannon, C. E., and W. Weaver. 1949. The mathematical theory of communication. University of Illinois Press, Urbana, IL. 117 p.

Stransky, J. J., E. S. Nixon, C. L. Burandt, Jr., and R. L. Willett. 1974. First year revegetation following timber harvest in east Texas. USDA For. Serv. Res. Note SO-173. Southern For. Exp. Sta., New Orleans, LA. 7 p.

Sullivan, J. R., and E. S. Nixon. 1971. A vegetational analysis of an area in Nacogdoches County, Texas. Texas J. Sci. 23:67-79.

Tharp, B. C. 1925. Structure of Texas vegetation east of the 98th meridian. Ph.D. dissertation, University of Texas, Austin, TX. 125 p.

Tharp, B. C. 1939. The vegetation of Texas. Texas Academy of Science Nontechnical Publication Series. The Anson Jones Press, Houston, TX. 74 p.

WOODY, STREAMSIDE VEGETATION OF PRAIRIE CREEK IN EAST TEXAS

by E. S. NIXON, R. L. EHRHART, S. A. JASPER, J. S. NECK *and* J. R. WARD

Department of Biology
Stephen F. Austin State University
Nacogdoches, TX 75962-3003

ABSTRACT

The woody vegetation of upper Prairie Creek in east Texas was analyzed by the plot method, with communities being sampled along a moisture gradient from wet to mesic. Dominant woody species at the creek's origin, a wet site, were *Nyssa sylvatica, Magnolia virginiana, Persea borbonia, Pinus taeda,* and *Rhododendron canescens.* Downstream, at a deeper and more clearly defined channel, *Pinus taeda, Rhododendron canescens, Magnolia grandiflora, Quercus alba,* and *Fagus grandifolia* emerged as dominants. The lower, mesic-site communities of Prairie Creek were dominated by *Fagus grandifolia, Pinus taeda, Magnolia grandiflora, Carpinus caroliniana,* and *Ostrya virginiana.* Shannon-Wiener species diversity indices increased down the moisture gradient.

INTRODUCTION

The gently rolling terrain of east Texas supports a variety of upland and bottomland communities. Variable and quite distinct from the regional forest cover is the woody vegetation along the frequent creek-bottoms (Sullivan and Nixon 1971; Nixon and Raines 1976; Nixon et al. 1980). These creek bottoms generally have been neglected and need further vegetational characterization. Understanding creek-bottom vegetation requires elucidation of creekside floristic changes along the length of individual creeks. Prairie Creek—a small continuously flowing stream which begins and extends for about 3.3 km within the Angelina National Forest in east Texas—is appropriate for such a study. The area along Prairie Creek outside the National Forest could not be included because of recent clearcutting.

Prairie Creek is located vegetationally within Tharp's (1939) Longleaf Pine region near its border with the Pine-oak Forest region. It is in San Augustine County just southeast of the junction of Texas Highway 103 and FM 1277. The creek runs from north to south, generally paralleling (at approximately 0.5 km) FM 1277. The study was conducted in the fall of 1980.

Except for a band of trees immediately bordering the creek, the forest associated with Prairie Creek was clearcut in 1935. Since that time, the creek-bottom forest was subjected to occasional thinning, selective cutting, prescribed burning, and wildfire (personal communication, U.S.

The Texas Journal of Science, Vol. XXXV, No. 3, September 1983

Forest Service, Lufkin, Texas). It appears, however, that disturbance was minor immediately along the creek as evidenced by a rather mature forest, and the absence of stumps. Thus, the study was restricted to this creekside forest.

The east Texas climate is mild, with temperatures generally ranging from 41 C to -12 C and a mean relative humidity of 73%. Precipitation, of which rainfall is the dominant form, is 119 cm annually and fairly evenly distributed throughout the year. The growing season averages about 240 days. The soil of upper Prairie Creek, at the sites of our communities 1, 2, and 3 (see below), is a Renzel loamy fine sand (Dolezel and Holt 1979). This soil generally occurs on both sides of spring-fed, flowing streams and at times marks the starting point of continuously flowing springs. The soil is somewhat poorly drained and has a high available water capacity. Just north of community 4, the Renzel soil grades into an Iuka fine sandy loam. Communities 4 and 5 were located on this rather deep, occasionally flooded Iuka soil, which is generally found on nearly level bottomlands of small streams and creeks (Dolezel and Holt 1979). Iuka soils are moderately well drained and have a high available water capacity.

STUDY SITES

Five segments of woody vegetation along Prairie Creek were designated as communities. Each community was located approximately equidistant (about 0.8 km apart) along the creek channel starting at the creek's head and ending near its exit from the National Forest. The first community (Community 1) was at the creek's origin, where small springs and seepages feed water into a shallow channel 0.3-0.6 m deep and usually not more than a meter wide. Ferns were common at this rather wet site. At Community 2 the stream channel was 1-1.5 m deep and up to 2 m wide. Further downstream at Community 3 there was a channel depth of 2-2.5 m and a channel width to 3-3.5 m. The banks were quite steep and the creek began to meander. Communities 4 and 5, as a result, were positioned along a winding channel about 3 to 3.5 m deep, respectively. The channel bottoms in communities 4 and 5 were about 2 m wide, widening to about 5 m across at the top. Prairie Creek contained only a small amount of water at the time of this study but high levels of water and some flooding occur during heavy rains. A soil moisture gradient exists moving from the wet stream head (Community 1) to the more mesic communities of lower Prairie Creek.

METHODS

Woody vegetation of the 5 communities was sampled by the plot method. Fifty 5 × 5 m plots located in belt transects, 25 immediately

paralleling each side of the creek, were analyzed in each community, giving a total of 250 plots. Where the creek meandered, some plots were irregularly shaped to contain 25 m^2. All trees, shrubs and woody vines with diameters at breast height (dbh at 140 cm above ground) equal to or greater than 0.5 cm were measured to the nearest centimeter. Scientific nomenclature followed Correll and Johnston (1970).

Data obtained from plots included frequency, density and basal area. By summing relative frequency, relative density, and relative basal area, an importance value for each species in each community was calculated and used in organizing composition tables and in determining community ordination (Cox 1980). Dominance, as used in this study, is based on importance value. Pairs of communities were compared by calculating a coefficient of community (C). The formula followed was $C = 2w/(a+b)$, where w equals the sum of the lower of the two quantitative values (importance values) for species shared by the two communities, a equals the sum of all importance values for the first community and b the sum of all importance values for the second community (Cox 1980). Shannon-Wiener diversity indices also were calculated for the 5 communities (Shannon and Weaver 1949).

RESULTS

A community ordination was constructed and community similarity coefficients calculated to determine if vegetation on east and west banks within each of the 5 communities was different. Results indicated a high degree of similarity; therefore each community was treated as a whole. The same ordination indicated 3 groupings involving the 5 communities. The more hydric Community 1 separated from all the downstream study sites, Communities 2 and 3 clustered together, and Communities 4 and 5 clustered together. These three groupings will be referred to as upper, middle, and lower Prairie Creek communities.

Upper Prairie Creek

The dominant species, based on importance value, at upper Prairie Creek (Community 1) were *Nyssa sylvatica* and *Magnolia virginiana* (Table 1). Overstory constituents were *N. sylvatica, M. virginiana, Pinus taeda,* and *Liquidambar styraciflua.* The middle layer was composed mainly of *Persea borbonia, Ilex opaca, Chionanthus virginica, Acer rubrum* and *Fraxinus pennsylvanica.* Prevalent in the shrub layer were *Rhododendron canescens, Vaccinium arkansanum, Alnus serrulata* and *Viburnum nudum.* The distribution of both *P. borbonia* and *R. canescens* was characterized by a clumping pattern as indicated by a high density to frequency ratio. The vine most frequently encountered was *Smilax laurifolia.* The vegetation of upper Prairie Creek was represented by fewest number of species (27) and the highest average density (10.8 plants per plot) of any of the communities studied.

TABLE 1. A comparison of density, basal area, species richness and species diversity and of the importance values of dominant woody species in the five communities along Prairie Creek.

	Community				
	1 Upper Wet	2	3 Middle	4	5 Lower mesic
	Importance Value[a]				
Persea borbonia	29.8				
Vaccinium arkansanum	13.3				
Alnus serrulata	10.2				
Smilax laurifolia	10.1				
Ilex opaca	13.3	13.8			
Magnolia virginiana	34.7		15.4		
Nyssa sylvatica	46.0	16.8	20.6		
Rhododendron canescens	25.8	39.9	27.9		
Liquidambar styraciflua	20.0	11.4			13.8
Pinus taeda	27.9	45.0	45.9	27.2	37.7
Fagus grandifolia		25.4	35.0	50.0	35.1
Quercus alba		29.5	31.0		11.0
Magnolia grandiflora		30.7		20.6	10.9
Morus rubra		20.2			
Acer rubrum			15.3	11.3	
Chionanthus virginica		12.3	13.9		
Quercus lyrata			15.9		
Fraxinus pennsylvanica			14.9		
Quercus phellos				26.0	
Quercus nigra				12.9	
Symplocos tinctoria				11.9	
Ostrya virginiana				24.3	17.5
Carpinus caroliniana				20.2	26.1
Ulmus alata				14.0	11.3
Vitis rotundifolia					14.4
Styrax americana					11.4
Density (No/Plot)	10.84	8.08	6.74	7.04	7.48
Basal area (sq. m)	6.62	8.35	6.27	6.94	5.65
Species richness (no. of species)	27	30	34	37	38
Species diversity (H′)	4.01	3.95	4.16	4.49	4.58

[a]Sum of relative frequency, relative density and relative basal area.

Middle Prairie Creek

A middle Prairie Creek (Communities 2 and 3), *P. taeda* emerged as the dominant species, because of its high relative basal area (Tables 1 and 2). Other overstory species were *Fagus grandifolia, Quercus alba, Magnolia grandiflora, Pinus echinata* and *M. virginiana.* The middle layer was composed primarily of *P. borbonia, I. opaca, C. virginica, F. pennsylvanica, A. rubrum,* and *Morus rubra.* The dominant shrub was

TABLE 2. Importance values and size-class distribution of woody plant species of Prairie Creek.

Species	Importance Value[a]	Size Class (cm)						
		1-10	11-20	21-30	31-40	41-50	51-60	>60
Pinus taeda	36.3	3	15	11	10	14	14	6
Fagus grandifolia	27.5	25	19	19	13	14	4	
Rhododendron canescens	22.1	267						
Nyssa sylvatica	18.2	60	23	8	5	7		
Quercus alba	15.7	50	10	10	2	4	2	1
Magnolia virginiana	14.9	69	22	13	6	1	2	1
Magnolia grandiflora	14.8	28	4	6	4	5	5	1
Liquidambar styraciflua	12.4	51	14	10	1	1	1	
Acer rubrum	11.4	60	19	8				
Persea borbonia	9.9	117	2	1				
Others[b]	117.4	923	50	7	11	3	3	1
Total	300.6	1653	178	93	52	49	31	10

[a]Sum of relative frequency, relative density and relative basal area.

[b]Other species present, listed in order of decreasing importance value (in parentheses), were *Quercus phellos* (9.7), *Fraxinus pennsylvanica (9.6)*, *Ilex opaca* (9.1), *Chionanthus virginica* (8.9), *Carpinus caroliniana* (8.4), *Ostrya virginiana* (7.5), *Vitis rotundifolia* (5.5), *Quercus nigra* (5.2), *Ulmus alata* (4.9), *Alnus serrulata* (4.5), *Vaccinium arkansanum* (3.9), *Symplocos tinctoria* (3.8), *Styrax americana* (3.2), *Smilax laurifolia* (3.2), *Viburnum dentatum* (2.8), *Callicarpa americana* (2.8), *Cornus florida* (2.7), *Myrica cerifera* (2.4), *Viburnum nudum* (2.2), *Pinus echinata* (1.9), *Acer saccharum* (1.6), *Vaccinium arboream* (1.6), *Quercus falcata* (1.6), *Ilex decidua* (1.4), *Hamamelis* sp. (.9), *Arundinaria gigantea* (.8), *Pinus palustris* (.7), *Prunus serotina* (.6), *Gelsemium sempervirens* (.6), *Viburnum rufidulum* (.5), *Castanea* spp. (.4), *Crataegus marshallii* (.4), *Bignonia capreolata* (.4), *Sassafras albidum* (.4), *Quercus prinus* (.4), *Tilia americana* (.3), *Rhamnus caroliniana* (.3), *Morus rubra* (.3), *Ilex montana* (.3), *Vaccinium amoenum* (.3), *Smilax rotundifolia* (.3), *Berchemia scandens* (.3), *Campsis radicans* (.2), *Ulmus americana* (.1), *Bumelia lanuginosa* (.1), *Ulmus rubra* (.1), *Euonymous americanus* (.1), *Juniperus virginiana* (.1), *Celtis laevigata* (.1).

R. canescens, which again displayed a clumping pattern of distribution like that observed at upper Prairie Creek. *A. serrulata, Symplocos tinctoria, Callicarpa americana, V. arkansanum* and *Ilex decidua* also were present in the shrub layer. The middle portion of Prairie Creek contained a total of 42 woody species with an average density of 7.41 plants per plot.

Lower Prairie Creek

Lower Prairie Creek (Communities 4 and 5) was dominated by *F. grandifolia* and *P. taeda.* These species, along with *Quercus phellos, L. styraciflua, Quercus nigra,* and *M. grandiflora* characterized the overstory. The midlayer consisted chiefly of *Carpinus caroliniana, Ostrya virginiana, A. rubrum, Ulmus alata,* and *C. virginica. Acer saccharum* also was encountered occasionally in that stratum. The shrub layer was

composed primarily of *Styrax americana, Viburnum dentatum, S. tinctoria,* and *R. canescens.* The vine, *Vitis rotundifolia,* was among the dominants because of its high frequency and density. A total of 49 species of woody plants was recorded, with an average density of 7.26 plants per plot.

Combined Prairie Creek Communities

When one considers the woody creekside vegetation of Prairie Creek as a single community, the following species emerge as dominants in order of importance value: *P. taeda, F. grandifolia, R. canescens, N. sylvatica, Q. alba, M. virginiana, M. grandiflora, L. styraciflua, A. rubrum,* and *P. borbonia* (Table 2). The presence among the dominants of *R. canescens,* a shrub, is due to its high relative frequency and density. All 267 plants of this species were in the 1-10 cm size class (Table 2). A well represented size class distribution existed for the other dominant species with the exception of *P. taeda,* which had only 3 individuals in the 1-10 cm size class.

Comparative Analysis

A total of 59 woody species was recorded in plots at Prairie Creek. On average, there were 8.1 plants per plot. Upper Prairie Creek contained 27 species, the middle portion 42 and the lower portion 49. This increase in species richness from the wet habitat to mesic habitat was reflected in an accompanying increase in species diversity (Shannon-Wiener indices increased from 3.95 to 4.58—Table 1). The more hydric species common to upper Prairie Creek occurred less frequently with distance downstream and were confined to seepages or to the creek bank. Conversely, 16 species were found only at lower Prairie Creek.

An ordination was made of other east Texas creek-side and creek-bottom communities to compare them with creek-side communities of this study (Fig. 1). Three general groupings occurred—those associated with very wet creek bottoms, wet to somewhat wet creek bottoms and mesic creek bottoms. The very wet creek-bottom site was wide and flat with much running water. It was dominated by *Nyssa aquatica* and *Taxodium distichum* (Nixon and Willett 1974). The wet to somewhat wet grouping included communities 1, 2 and 3 of the present study and a wet creek-branch community analyzed by Nixon et al. (1980). The wet creek branch community consisted chiefly of *M. virginiana* and *N. sylvatica.* The 2 communities of lower Prairie Creek clustered with other mesic area communities. *C. caroliniana, L. styraciflua, Q. alba* and *O. virginiana* generally dominated these communities (Sullivan and Nixon 1971; Nixon and Raines 1976).

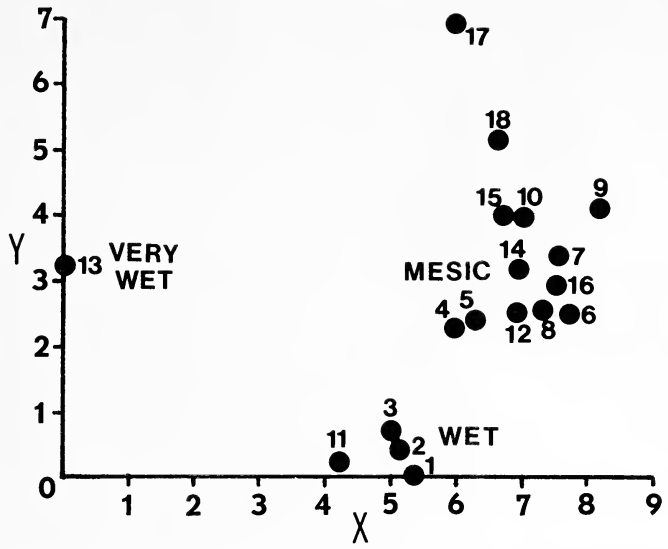

FIGURE 1. Ordination of 18 east Texas creek-side and creek-bottom communities (communities 1-5, present study; 6-10 and 14-15, Nixon and Raines 1976; community 11, Nixon et al. 1980; community 12, Sullivan and Nixon 1971; community 13, Nixon and Willett 1974; communities 16-18, Nixon unpublished data).

DISCUSSION

The wet area associated with the origin of Prairie Creek was dominated by *N. sylvatica, M. virginiana, P. borbonia, P. taeda* and *R. canescens.* The designation of a Sweetbay-Swamp tupelo-Redbay Forest Cover type by the Society of American Foresters (Eyre 1980) indicates the high frequency with which this kind of community occurs. This aggregation of species mainly occurs at branch heads (Nixon et al. 1980), creek heads, wet creek bottoms and seepages in eastern Texas and then may be found eastward and northeastward in these same kinds of habitats throughout the southern Coastal Plain to Maryland and Virginia (Eyre 1980). Downstream on mesic sites of Prairie Creek, *P. taeda* and *F. grandifolia* dominate the streamside vegetation in association with *Q. alba, M. grandiflora* and *L. styraciflua.* At the lower communities *C. caroliniana* and *O. virginiana* become prevalent. With the exception of *M. grandiflora,* these are the principal species associated with creeks in Nacogdoches County, Texas (Sullivan and Nixon 1971; Nixon and Raines 1976).

Although Glascock and Ware (1979) observed numerous floristic and vegetational differences among bottom-land communities of the eastern U.S., they concluded that *A. rubrum, Fraxinus* spp., *N. sylvatica, L. styraciflua, M. virginiana,* and *Ulmus* spp. are the most consistently important species of small stream bottoms in Alabama, Florida, Virgi-

nia, and New Jersey. This remarkable floristic uniformity appears to extend into eastern Texas, as evidenced in this study, and also northward to some extent. Upwards to 40% of the species in streamside forests of Illinois were in common with Prairie Creek vegetation, with taxa such as *Q. alba, O. virginiana, F. pennsylvanica, U. rubra,* and *U. americana* occurring at times among the dominants (Boggess and Geis 1967; Bell and del Moral 1977; Johnson et al. 1978).

As a part of Gemborys and Hodgkins' (1971) analyses of forests of small stream bottoms in the Coastal Plain of southwestern Alabama, they associated taxa with a moisture gradient. The following selected species occurred along a gradient from drier to wet: *Cornus florida, Pinus palustris, S. tinctoria, Q. nigra, L styraciflua, M. grandiflora, I. opaca, N. sylvatica, M. virginiana,* and *A. serrulata.* These species generally followed the same pattern at Prairie Creek.

Oftentimes there is an increase in species diversity associated with a decrease in stress (Barbour et al. 1980). Assuming that the water-saturated soils of upper Prairie Creek provide a more stressful environment than those of mesic sites, species diversity should increase, at least for some distance, with distance from the creek's headwaters. This was demonstrated in that both species richness and diversity increased as apparent soil moisture decreased. Bell (1974) and Bell and del Moral (1977) found that species richness and diversity tended to increase with decreasing flood stress.

LITERATURE CITED

Barbour, M. G., J. H. Burk, and W. P. Pitts. 1980. Terrestrial plant ecology. The Benjamin/Cummings Publishing Company, Inc., Menlo Park, CA. 604 p.

Bell, D. T. 1974. Tree stratum composition and distribution in the streamside forest. Amer. Midl. Nat. 92:35-45.

Bell, D. T., and R. del Moral. 1977. Vegetation gradients in the streamside forest of Hickory Creek, Will County, Illinois. Bull. Torrey Bot. Club 104:127-135.

Boggess, W. R., and J. W. Geis. 1967. Composition of an upland, streamside forest in Piatt County, Illinois. Amer. Midl. Nat. 78:89-97.

Correll, D. S., and M. C. Johnston. 1970. Manual of the vascular plants of Texas. Tex. Res. Found., Renner, TX 1881 p.

Cox, G. W. 1980. Laboratory manual of general ecology. William C. Brown Co., Dubuque, IA. 195 p.

Dolezel, R., and T. Holt. 1979. Angelina National Forest study area soil survey in San Augustine Co., Texas. U.S. Department of Agriculture Soil Conservation Service, Nacogdoches, TX 68 p.

Eyre, F. H. 1980. Forest cover types of the United States and Canada. Society of American Foresters, Washington, D.C. 148 p.

Gemborys, S. R., and E. J. Hodgkins. 1971. Forests of small stream bottoms in the Coastal Plain of southwestern Alabama. Ecology 52:70-84.

Glascock, S., and S. Ware. 1979. Forests of small stream bottoms in the Peninsula of Virginia. Virginia J. Sci. 30:17-21.

Johnson, G. R., D. R. Pelz, and G. L. Rolfe. 1978. Woody vegetation of a streamside forest in Illinois. Trans. Ill. State Acad. Sci. 71:412-419.

Nixon, E. S., and J. A. Raines. 1976. Woody creekside vegetation of Nacogdoches County, Texas. Tex. J. Sci. 27:443-452.

Nixon, E. S., and R. L. Willett. 1974. Vegetative analysis of the floodplain of the Trinity River, Texas. U.S. Army Corps of Engineers, Fort Worth District, Fort Worth, TX. 267 p.

Nixon, E. S., J. W. Higgins, P. L. Blanchette, and F. A. Roth. 1980. Woody vegetation of a wet creek branch in east Texas. Tex. J. Sci. 32:337-341.

Shannon, C. E., and W. Weaver. 1949. The mathematical theory of communication. University of Illinois Press, Urbana, IL. 117 p.

Sullivan, J. R., and E. S. Nixon. 1971. A vegetational analysis of an area in Nacogdoches County, Texas. Tex. J. Sci. 23:67-79.

Tharp, B. C. 1939. The vegetation of Texas. The Anson Jones Press, Houston, TX. 74 p.

GLOBAL INVERSE FUNCTION THEOREM

by JOHN D. MILLER

Department of Mathematics
Texas Tech University
Lubbock, TX 79409

ABSTRACT

A global inverse function theorem is obtained here which is equivalent to one due to Hadamard.

INTRODUCTION

Let f: $R^n \to R^n$ be a differentiable function of n-dimensional Euclidean space into itself. The classical Inverse Function Theorem states that, at points x in R^n where $f'(x)$ is nonsingular, the function f maps a sufficiently small open set U about x diffeomorphically onto an open set f(U).

It is well known that even if $f'(x)$ is nonsingular for each x in R^n, f may fail to be either one-one or onto (e.g., take $f(x)=e^x$ for $x \in R$, R the reals, in one case and $x \in C$, C the complex numbers, in the other). That is to say, even if $f'(x)$ is everywhere nonsingular, f may fail to be a global diffeomorphism.

The purpose of this paper is to provide a short proof of a global inverse function theorem that is equivalent to a version of one due to Hadamard (1968). Whereas in Hadamard's theorem the given function is required to be proper, I require the seemingly stronger but equivalent condition of having a homotopy associated with the given function to be proper.

DEFINITIONS

Before stating and proving the theorem, I establish some definitions: A differentiable map f *on* R^n into R^n is a *diffeomorphism* if it is one-one, onto, and has a differentiable inverse. A continuous map f is *proper* if $f^{-1}(K)$ is compact whenever K is compact. Continuous maps f and g between spaces X and Y are *homotopic* if there is a continuous map H, called a homotopy, defined on I x X into Y, I the unit interval, such that $H(0,x) = f(x)$ and $H(1,x) = g(x)$ for all x in X. Let $f:R^n \to R^n$ be a C^2 map with $f(0) = 0$. A homotopy H can be defined between f and $f'(0)$ by the rule

The Texas Journal of Science, Vol. XXXV, No. 3, September 1983

$$H(t,x) = \begin{cases} \dfrac{f(tx)}{t} & 0 < t \leq 1 \\ f'(0)(x) & t = 0. \end{cases}$$

Since $f'(0)(x) = \lim_{t \to 0} \frac{f(tx)}{t}$ it may be checked that H is indeed a differentiable homotopy (cf. Milnor 1965, p. 34).

Finally, if $v_1, v_2, \ldots, v_n$ are n-vectors, the symbol $(v_1, \ldots, v_n)^t$ denotes the nxn matrix whose i^{th} row consists of the components of v_i, and det $(v_1, \ldots, v_n)^t$ denotes its determinant.

THEOREM

Let $f: R^n \to R^n$ be a C^2 map with $f(0) = 0$. Suppose further that the Jacobian of f never vanishes. Then a necessary and sufficient condition that f is a diffeomorphism is that the homotopy H defined above is proper.

PROOF

It suffices to show f is one-one and onto, because the non-vanishing of the Jacobian of f implies, by virtue of the Local Inverse Function Therorem, that f is a local diffeomorphism.

Now, since $f'(x)$ is nonsingular everywhere in R^n, the linear map $H'(t,x)$ has full rank for all (t,x) in $I \times R^n$. Thus, if H is proper, for any y in R^n, a variation on an argument due to Milnor (1965, section 5) implies $H^{-1}(y)$ is a finite union of arcs and circles, with the endpoints—and only the endpoints—of the arcs lying in the set $0 \times R^n \cup 1 \times R^n$. More precisely, on this last point, $H^{-1}(y) \cap 0 \times R^n = 0 \times R^n = 0 \times f'(0)^{-1}(y)$ and $H^{-1}(y)$ and $H^{-1}(y) \cap 1 \times R^n = 1 \times f^{-1}(y)$:

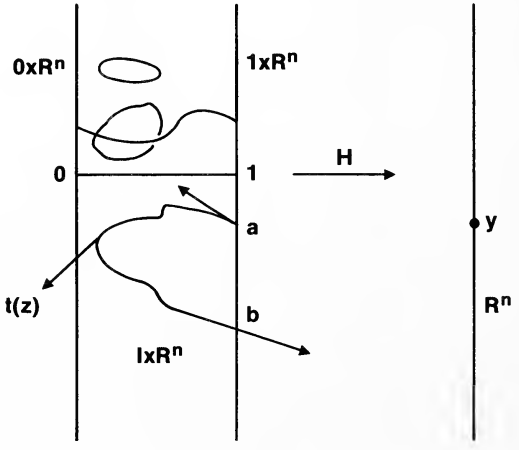

Now it is clear that $H^{-1}(y) \cap 0 \times R^n$ consists of exactly one point (since $f'(0)$ is nonsingular); that is the endpoint of an arc whose other endpoint must lie in the set $1 \times f^{-1}(y)$. Hence, f is onto. Moreover, if the set $1 \times f^{-1}(y)$ consisted of more than one point, there would have to be an arc A, $A \subset H^{-1}(y)$, with endpoints a and b lying in $1 \times R^n$. But, according to Milnor (1965, Lemma 1, section 5), this implies the Jacobian of f must have opposite signs at a and b. Hence it must vanish somewhere in R^n contrary to hypothesis.

At each point z on the arc A there is to be selected an ordered basis from the n+1-dimensional tangent plane at z consisting of unit vectors $t(z), v_2, \ldots, v_{n+1}$, where t(z) is tangent to the arc at z. The selection process is carried out in the following manner: First, select $v_2, \ldots, v_{n+1}$, such that $\det (H'(V_2), \ldots, H'(V_{n+1}))^t$ is positive; second, select t(z) such that $\det (t(z), v_2, \ldots, v_{n+1})^t$ is positive, also. Note that the former matrix is indeed nonsingular, since the vector t(z) spans the null space of the linear mapping H'(z). Also, more importantly, note that the assignment of points z along the curve to tanget vectors t(z) is unique and independent of the selection of the vectors $v_2, \ldots, v_{n+1}$ up to the manner of their choice.

Now let $e_1, e_2, \ldots, e_{n+1}$ be the usual unit vectors in R^{n+1} which lie along the positive coordinate axes. Form an ordered basis for the tangent plane at the indicated point a as in the figure by choosing an appropriate permutation of $e_2, \ldots, e_{n+1}$, say $e_{i_1}, \ldots, e_{i_n}$, and t(a) according to the given prescription. Since $H(1,x) = f(x)$, the value of $\det(H'(a)(e_{i1}), \ldots, H'(a)(e_{i_n}))_t$ is either the value of the Jacobian of f at a or its negative.

One does the same at the point b, and notes that since the assignment of points z to tanget vectors t(z) along the arc A in the fashion indicated is differentiable, t(a) and t(b) have e_1 components opposite in sign. This means that the permutation of the vectors $e_2, \ldots, e_{n+1}$, say $e_{j_1}, \ldots, e_{j_n}$, which together with t(b) forms an ordered basis at b and for which $\det (t(b), e_{j_1}, \ldots, e_{j_1}, \ldots, e_{j_n})^t$ is positive, is opposite to that at a. Hence the Jacobian of f at a and at b must have opposite signs as asserted.

REMARKS

1. Finding conditions that imply when differentiable functions are diffeomrophisms seems to be of some importance in engineering applications. For an extensive bibliography of such applications see the paper by Wu and Desoer (1972).

2. For other proofs of Hadamard's Global Inverse Function Theorem, which for all practical purposes my theorem is, consult Gordon (1972), Palais (1959), and Wu and Desoer (1972). See Schwartz (1956) for yet

another theorem of Hadamard on global inverses but generalized to a Banach space setting. It is this theorem, in an R^n setting, that is known by many as Hadamard's Theorem.

LITERATURE CITED

Gordon, W. B. 1972. On the diffeomorphisms of Euclidean space. Am. Math. Mon. 79:755-759.

Hadamard, J. S. 1968. Oeures, p. 383-384. *In* Editions Du Centre National de La Recherche Scientifique, Paris.

Minor, J. W. 1965. Topology from the differential viewpoint. The University Press of Virginia, Charlottesville, VA. 57p.

Palais, R. S. 1959. Natural operations on differential forms. Trans. Amer. Math. Soc. 92:125-141.

Schwartz, J. T. 1965. Nonlinear functional analysis. N.Y.U. Courant Institute of Mathematical Sciences, New York, NY, p. 21-22.

Wu, F. F., and C. A. Desoer. 1972. Global inverse function theorem. I.E.E.E. Trans. on Circuit Theory, March: 199-201.

NEW RECORDS OF INVERTEBRATE SAPROVORES FROM BARN OWL PELLETS

by KIRK L. HAMILTON[1] *and*
ANNEMARIE B. HAMILTON[1]

Department of Biology, UMC 53
Utah State University
Logan, UT 84322

ABSTRACT

Barn owl (*Tyto alba*) pellets were examined for presence of invertebrate saprovores. Specimens of Insecta and Acarina were found. Ours appear to be the first records of *Ataenius* sp., *Cheletomorpha lepidopterorum*, and *Tydeus* sp. associated with barn owl pellets. *Dermestes caninus* also was identified.

Philips and Dindal (1977, 1979) have classified raptor-nest invertebrates into three major groups—parasite fauna, animal saprovores, and humus fauna. The parasite fauna includes raptor and prey parasites and their respective parasites and predators. The animal saprovores include invertebrates responsible for the decomposition of pellets, excreta, and molted feathers. The humus fauna includes invertebrates associated with decomposition of nest litter and wood. Philips and Dindal (1977, 1979) reported that invertebrates known from barn owl (*Tyto alba*) nests and pellets represent approximately 40 species and 22 families [based on work of Hicks (1959, 1962, 1971)]. Here we present additional records of invertebrates from barn owl pellets.

Pellets (248) were removed biweekly from a barn owl nest in an abandoned water tower 16 km NE of Fort Worth, Tarrant County, Texas, from 26 March to 20 August 1976. Thirty living invertebrates were collected from the pellets by two methods: Insects and insect larvae were captured by hand, and mites were collected with a moistened fine-point artist's brush. All specimens were stored in 70% ethanol. For examination, insects were pinned and mites were cleared with a warm lacto-phenol solution held over low heat for 15-20 min; then, isolated individuals were mounted on slides with Hoyer's solution (Krantz 1970). All mites were identified under a phase microscope.

The 21 specimens thus far identified represent two groups of arthropods—Insecta and Acarina (mites). Insect saprovores included the coleopterans (beetles) *Dermestes caninus* (2 adults and 10 larvae) and *Ataenius* sp. (1 adult). Wallace (1948) previously has recorded *Dermestes* spp. in association with barn owl debris; however, ours appears

[1]Present address: 7301 Brompton B103, Houston, TX 77025.

to be the first recorded incidence of *Ataenius* sp. associated with barn owl pellets. One specimen (an adult) belonging to the coleopteran family Histeridae also was collected.

Acarine specimens included 4 individuals each of *Cheletomorpha lepidopterorum* (Cheyletidae) and *Tydeus* sp. (Tydeidae), which also are saprovores. Neither *C. lepidopterorum* nor *Tydeus* sp. seems to have been reported previously from barn owl pellets. Individuals of the acarine families Parasitidae (5), Cunaxidae (1), and Laelapidae (2) also were found and are currently under taxonomic investigation.

We thank J. R. Philips for his helpful discussion and criticism of this manuscript. We thank G. S. Spicer and C. C. Hall (Univ. of Texas at Arlington) for the mite identification and H. R. Burke (Texas A&M Univ.) and H. W. Boodée for their assistance with the insect identification. This study was funded in part by a Grant-in-Aid of Research award from the Society of Sigma Xi.

LITERATURE CITED

Hicks, E. A. 1959. Check-list and bibliography on the occurrence of insects in birds's nests. Iowa State Press, Ames, IA. 681 p.

Hicks, E. A. 1962. Check-list and bibliography on the occurrence of insects in birds' nests. Suppl. I. Iowa State J. Sci. 36:233-344.

Hicks, E. A. 1971. Check-list and bibliography on the occurrence of insects in birds' nests. Suppl. II. Iowa State J. Sci. 46:123-338.

Krantz, G. W. 1970. A manual of acarology. Oregon State Univ., Corvallis, OR.

Philips, J. R., and D. L. Dindal. 1977. Raptor nests as a habitat for invertebrates: a review. Raptor Res. 11:86-96.

Philips, J. R., and D. L. Dindal. 1979. Decomposition of raptor pellets. Raptor Res. 13:102-111.

Wallace, G. J. 1948. Barn owl in Michigan. Mich. Agr. Exp. Sta. Tech. Bull. 208:1-61.

A NEW EDGEWORTH-TYPE EXPANSION

by JAMES G. GALLOWAY *and* E. D. McCUNE

Department of Mathematics and Statistics
Stephen F. Austin State University
Nacogdoches, TX 75962

ABSTRACT

In this paper, a new Edgeworth-type expansion is developed in which the necessity of knowing cumulants is eliminated and which always gives nonnegative values for the probability distribution function to be approximated. Asymptotic order properties also are discussed.

INTRODUCTION

The Edgeworth expansion is an important representation for approximating one probability distribution function in terms of another. In this expansion the cumulants of the distributions involved must be known. The Edgeworth expansion has been used in statistical applications as well as in theoretical developments (Bickel 1974; Gotze 1981; Singh 1981; McCune and Gray 1982).

Coberly (1972) and Gray, Coberly and Lewis (1975) introduced an Edgeworth-type expansion which in this paper will be called the Gray-Coberly-Lewis expansion. In this expansion, the requirement of knowing the cumulants is eliminated and the derivatives of the distribution functions are used instead. In some cases, this expansion reduces the error of approximation.

Both of the above expansions can give negative values for the approximated distribution function, which is an undesirable feature. In this paper, a new Edgeworth-type expansion is introduced for which it is also not necessary to know the cumulants, but which always gives nonnegative values and has the same asymptotic order properties as the previous two expansions.

EDGEWORTH EXPANSION

Let $F(\ ;\lambda)$ be the probability distribution function to be approximated and let ψ be a limiting distribution for $F(\ ;\lambda)$. That is,

$$\lim_{\lambda \to \infty} F(x;\lambda) = \psi(x) \tag{1}$$

for all x in the support of $F(\ ;\lambda)$. In practice, the limiting distribution most often used is the standard normal. Let κ_i and α_i be the cumulants of $F(\ ;\lambda)$ and ψ respectively, and let $\beta_i = \kappa_i - \alpha_i$. Also, assume that $\beta_i = O(\lambda^{1-i/2})$, $i = 3,4 \cdots$. Now (see Gray, Coberly and Lewis, 1975) in many instances $F(x;\lambda)$ can be written as

$$F(x;\lambda) \sim \psi(x) + \sum_{i=1}^{\infty} Q_i(x;\lambda) \tag{2}$$

or equivalently as

$$F(x;\lambda) = \psi(x) + \sum_{i=1}^{n} Q_i(x;\lambda) + O(\lambda^{-(n+1)/2}) \tag{3}$$

where the Q_i's are functions of λ and x determined by the derivatives of ψ and by the β_i, and satisfies the relation $Q_i(x;\lambda) = O(\lambda^{-i/2})$. See McCune and Adams (1979) for a table defining Q values. The Edgeworth expansion corresponding to this $F(x;\lambda)$ can be written as

$$E_n(x;\lambda) = \psi(x) + \sum_{i=1}^{n} Q_i(x;\lambda). \tag{4}$$

Throughout this paper we will tacitly assume that (3) holds, that is

$$F(x;\lambda) - E_n(x;\lambda) = O(\lambda^{-(n+1)/2}). \tag{5}$$

It is this asymptotic property which will be desired in subsequently derived expansions. For $n = 1$, equation (4) becomes

$$E_1(x;\lambda) = \psi(x) + \frac{-\beta_3 \psi^{(3)}(x)}{3!} \tag{6}$$

where

$$F(x;\lambda) - E_1(x;\lambda) = O(\lambda^{-1}). \tag{7}$$

For $n > 1$, similar equations may be written. Now $E_n(x;\lambda)$ may be difficult to obtain if the cumulants associated with $F(\ ;\lambda)$ and ψ are difficult to calculate. This approximation also can take on negative values for certain values of x and λ (Table 1).

TABLE 1. Approximations of the probability distribution function $F(x;\lambda)$, for various values of λ and x, given by the Edgeworth expansion $E_1(x;\lambda)$, the Gray-Coberly-Lewis expansion $C_1(x;\lambda)$, and our expansion $G_1(x;\lambda)$.

λ	x	$F(x;\lambda)$	$E_1(x;\lambda)$	$C_1(x;\lambda)$	$G_1(x;\lambda)$
15	-3.5	.000000	-.000612	-.000071	.000000
25	-3.5	.000000	-.000422	-.000069	.000000
50	-3.5	.000009	-.000230	-.000048	.000008
100	-3.5	.000034	-.000095	-.000005	.000032
15	-3.0	.000003	-.001702	-.000603	.000001
25	-3.0	.000047	-.001014	-.000457	.000035
50	-3.0	.000211	-.000321	-.000105	.000190
100	-3.0	.000430	.000168	.000255	.000413
15	-2.5	.000426	-.001710	-.003081	.000268
25	-2.5	.001193	.000075	-.001007	.000971
50	-2.5	.002348	.001872	.001251	.002166
100	-2.5	.003353	.003142	.002814	.003238
15	-2.0	.007763	.008810	-.005579	.004829
25	-2.0	.011165	.011952	.004012	.008847
50	-2.0	.014662	.015115	.011464	.013297
100	-2.0	.017111	.017351	.015629	.016375
15	-1.5	.047968	.052873	.056274	.057332
25	-1.5	.053176	.056014	.057684	.058487
50	-1.5	.057808	.059175	.059864	.060337
100	-1.5	.060746	.061411	.061712	.061971
15	- .5	.331368	.331263	.333184	.332195
25	- .5	.326208	.326141	.327257	.326680
50	- .5	.321020	.320985	.321526	.321245
100	- .5	.317365	.317339	.317604	.317466
15	.5	.714060	.714188	.712694	.713496
25	.5	.708989	.709066	.708147	.708638
50	.5	.703871	.703910	.703438	.703689
100	.5	.700233	.700264	.700024	.700151
15	1.5	.922877	.919259	.918588	.916045
25	1.5	.924639	.922400	.921917	.920449
50	1.5	.926717	.925561	.925273	.924571
100	1.5	.928386	.927796	.927633	.927294
15	2.0	.965281	.963310	.970750	.970082
25	2.0	.967625	.966452	.971204	.970628
50	2.0	.970192	.969614	.972152	.971745
100	2.0	.972129	.971851	.973183	.972924
15	2.5	.985576	.985870	.988057	.986923
25	2.5	.987403	.987655	.988998	.988201
50	2.5	.989283	.989452	.990137	.989670
100	2.5	.990620	.990723	.991068	.990807
15	3.0	.994416	.995599	.995748	.994950
25	3.0	.995517	.996286	.996337	.995812
50	3.0	.996563	.996979	.996979	.996695
100	3.0	.997249	.997468	.997458	.997308
15	3.5	.997969	.998922	.998603	.998184
25	3.5	.998528	.999112	.998893	.998637
50	3.5	.999009	.999305	.999179	.999052
100	3.5	.999292	.999440	.999372	.999310
15	4.0	.999301	.999796	.999567	.999386
25	4.0	.999551	.999834	.999691	.999590
50	4.0	.999741	.999874	.999799	.999754
100	4.0	.999839	.999901	.999864	.999844

GRAY-COBERLY-LEWIS EXPANSION

The Gray-Coberly-Lewis expansion is another representation of $F(\ ;\lambda)$ in terms of ψ, but in this case it is not necessary to know the cumulants. Only the first-order expansion will be derived, but higher orders can be derived in a similar fashion. Using the Edgeworth expansion for n = 1, it follows that (see Coberly 1972)

$$F(x;\lambda) = \psi(x) + \frac{-\beta_3\psi^{(3)}(x)}{3!} + O(\lambda^{-1}) \tag{8}$$

and

$$F'(x;\lambda) = \psi'(x) + \frac{-\beta_3\psi^{(4)}(x)}{3!} + O(\lambda^{-1}). \tag{9}$$

This implies that

$$\psi(x) = (1)F(x;\lambda) + \frac{\beta_3\psi^{(3)}(x)}{3!} - O(\lambda^{-1}) \tag{10}$$

and

$$\psi'(x) - F'(x;\lambda) = (0)F(x;\lambda) + \frac{\beta_3\psi^{(4)}(x)}{3!} - O(\lambda^{-1}). \tag{11}$$

Now in equations (10) and (11), treating $F(x;\lambda)$ and $\frac{\beta_3}{3!}$ as unknowns, and ignoring order terms, application of Cramer's Rule gives the Gray-Coberly-Lewis expansion

$$C_1(x;\lambda) = \frac{\begin{vmatrix} \psi(x) & \psi^{(3)}(x) \\ \psi'(x) - F'(x;\lambda) & \psi^{(4)}(x) \end{vmatrix}}{\begin{vmatrix} 1 & \psi^{(3)}(x) \\ 0 & \psi^{(4)}(x) \end{vmatrix}}, \tag{12}$$

provided the denominator is not 0, i.e. $\psi^{(4)}(x) \neq 0$. Solving these determinants, the first order Gray-Coberly-Lewis expansion becomes

$$C_1(x;\lambda) = \psi(x) - \frac{\psi^{(3)}(x)}{\psi^{(4)}(x)}(\psi'(x) - F'(x;\lambda)) \tag{13}$$

and for the case in which ψ is the standard normal distribution,

$$C_1(x;\lambda) = \psi(x) + \frac{H_2(x)}{H_3(x)}(\psi'(x) - F'(x;\lambda)) \tag{14}$$

where $H_2(x) = x^2 - 1$ and $H_3(x) = x^3 - 3x$ are so-called Hermite polynomials.

Higher order approximations C_n can be derived in a similar manner. Gray, Coberly and Lewis (1975) show that

$$F(x;\lambda) - C_n(x;\lambda) = O(\lambda^{-(n+1)/2}), \tag{15}$$

which is the same asymptotic property as that in (5). Note that the Gray-Coberly-Lewis expansion does not require the cumulants; instead only derivatives of $\psi(x)$ and $F(x;\lambda)$ are needed. As with the Edgeworth expansion, the Gray-Coberly-Lewis expansion can take on negative values (Table 1).

A NEW EXPANSION

A new Edgeworth-type expansion in which it is not necessary to know the cumulants can be derived as follows: Rewrite (8) as

$$F(x;\lambda) = \psi(x)\{1 + \frac{-\beta_3}{3!}\frac{\psi^{(3)}(x)}{\psi(x)} + O(\lambda^{-1})\} \tag{16}$$

and

$$1 - F(x;\lambda) = (1 - \psi(x))\{1 + \frac{\beta_3}{3!}\frac{\psi^{(3)}(x)}{1 - \psi(x)} + O(\lambda^{-1})\}. \tag{17}$$

Now by careful application of the series expansion for natural logarithms to $\log\{1 - F(x;\lambda)\} - \log F(x;\lambda)$, we obtain

$$\log\frac{1 - F(x;\lambda)}{F(x;\lambda)} = \log\frac{1 - \psi(x)}{\psi(x)} + \frac{\beta_3}{3!}\frac{\psi^{(3)}(x)}{\psi(x)\{1 - \psi(x)\}} + O(\lambda^{-1}). \tag{18}$$

In a similar manner, we rewrite (9) as

$$F'(x;\lambda) = \psi'(x)\{1 + \frac{-\beta_3}{3!}\frac{\psi^{(4)}(x)}{\psi'(x)} + O(\lambda^{-1})\} \tag{19}$$

$$\log\frac{F'(x;\lambda)}{\psi'(x)} = \frac{-\beta_3}{3!}\frac{\psi^{(4)}(x)}{\psi'(x)} + O(\lambda^{-1}). \tag{20}$$

Applying a similar procedure to that used in the derivation of the Gray-Coberly-Lewis expansion, we rewrite (18) and (19) as

$$\log \frac{1-\psi(x)}{\psi(x)} = 1 \cdot \log \frac{1-F(x;\lambda)}{F(x;\lambda)} + \frac{\beta_3}{3!} \frac{\psi^{(3)}(x)}{\psi(x)\{\psi(x)-1\}} - O(\lambda^{-1}) \tag{21}$$

and

$$\log \frac{\psi'(x)}{F'(x;\lambda)} = 0 \cdot \log \frac{1-F(x;\lambda)}{F(x;\lambda)} + \frac{\beta_3}{3!} \frac{\psi^{(4)}(x)}{\psi'(x)} - O(\lambda^{-1}). \tag{22}$$

Using Cramer's Rule on (21) and (22) we have an approximation for $\log \frac{1-F(x;\lambda)}{F(x;\lambda)}$:

$$\log \frac{1-G_1(x;\lambda)}{G_1(x;\lambda)} = \log \frac{1-\psi(x)}{\psi(x)} + \frac{\psi^{(3)}(x)\psi'(x)}{\psi^{(4)}(x)\psi(x)(1-\psi(x))} \cdot \log \frac{\psi'(x)}{F'(x;\lambda)} \tag{23}$$

which can be written as

$$\log \frac{1-G_1(x;\lambda)}{G_1(x;\lambda)} = \log \frac{1-\psi(x)}{\psi(x)} \cdot \left\{ \frac{F'(x;\lambda)}{\psi'(x)} \right\}^{M(x)} \tag{24}$$

where

$$M(x) = \frac{-\psi^{(3)}(x)\psi'(x)}{\psi^{(4)}(x)\psi(x)\{1-\psi(x)\}} \tag{25}$$

provided $\psi^{(4)}(x) \neq 0$.

After exponentiating (24) and solving for $G_1(x;\lambda)$, we may define the new approximation of $F(x;\lambda)$ as the expansion

$$G_1(x;\lambda) = \left[1 + \frac{1-\psi(x)}{\psi(x)} \left\{ \frac{F'(x;\lambda)}{\psi'(x)} \right\}^{M(x)} \right]^{-1} \tag{26}$$

for all values of x for which $0 < \psi(x) < 1$, $\psi'(x) > 0$, $F'(x;\lambda) > 0$, and $\psi^{(4)}(x) \neq 0$. Also, $M(x)$ is defined in (25).

At this point a few remarks are in order concerning the new approximation. It is not necessary to know the cumulants of the distributions involved in order to use G_1; and, unlike the Edgeworth and Gray-Coberly-Lewis expansions, this new expansion will never give negative

values as approximations for $F(x;\lambda)$. In fact, for all x in the domain of G_1, we have $0 < G_1(x;\lambda) < 1$, the required range for approximation of a probability value.

In most applications the limiting distribution ψ is the standard normal distribution, for which $\psi^{(4)}(x) = (3x - x^3)\psi'(x)$. When this is the case and when $F'(x;\lambda) > 0$, C_1 and G_1 are defined for all real x except where $\psi^{(4)}(x) = 0$, that is except for $x \in \{-\sqrt{3}, 0, \sqrt{3}\}$. Hence, when ψ is the standard normal C_1 and G_1 will be defined at all values of x in the left and right tails of the distribution; however, when selecting values "near" $-\sqrt{3}$, 0, or $\sqrt{3}$, some numerical problems in calculating C_1 or G_1 may arise. Thus, in these regions the user should use some caution. We will return to this matter later in an example of numerical calculations comparing E_1, C_1, and G_1.

We would hope that G_1 has the same asymptotic property as C_1; this turns out to be the case. Substituting (21) and (22) into (23) we obtain

$$\log \frac{1 - G_1(x;\lambda)}{G_1(x;\lambda)} = \log \frac{1 - F(x;\lambda)}{F(x;\lambda)} - O(\lambda^{-1}) \tag{27}$$

and then exponentiating and using the elementary properties of the order function, it follows that

$$F(x;\lambda) - G_1(x;\lambda) = O(\lambda^{-1}), \tag{28}$$

which is the desired result.

ILLUSTRATIVE EXAMPLE

Let ψ be the standard normal distribution function, and let

$$F(x;\lambda) = \int_{-\infty}^{x} \lambda^{1/2}\, g(t\,\lambda^{1/2} + \lambda)dt \tag{34}$$

where

$$g(u) = \begin{cases} \dfrac{1}{\Gamma(\lambda)} u^{\lambda-1}\, e^{-u} & u > 0 \\ 0 & \text{otherwise.} \end{cases} \tag{35}$$

Note that $F(\ ;\lambda)$ is the standard Gamma distribution, for which it can be shown that $F(x;\lambda) \to \psi(x)$ as $\lambda \to \infty$ for all real x in the support of $F(\ ;\lambda)$.

TABLE 2. Extension of Table 1 for values of x near zero.

λ	x	$F(x;\lambda)$	$E_1(x;\lambda)$	$C_1(x;\lambda)$	$G_1(x;\lambda)$
15	-.10	.494221	.493995	.487416	.487228
	-.09	.498210	.498063	.490569	.490408
	-.08	.502312	.502125	.493510	.493376
	-.07	.506347	.506180	.496152	.496046
	-.06	.510373	.510228	.498347	.498268
	-.05	.514390	.514268	.499834	.499781
	-.04	.518400	.518300	.500084	.500056
	-.03	.522401	.522323	.497870	.497863
	-.02	.526394	.526337	.489510	.489509
	-.01	.530376	.530341	.456585	.456633
	.01	.538307	.538320	.611695	.610298
	.02	.542258	.542293	.578742	.578486
	.03	.546199	.546256	.570332	.570287
	.04	.550129	.550207	.568050	.568096
	.05	.554046	.554146	.568212	.568315
	.06	.557952	.558072	.569591	.569737
	.07	.561846	.561987	.571660	.571842
	.08	.565726	.565888	.574156	.574369
	.09	.569596	.569776	.576931	.577174

The cumulants of $(F\ ;\lambda)$ are

$$\kappa_i = \begin{cases} 0 & i = 1 \\ 1 & i = 2 \\ \lambda^{1-i/2}(i-1)! & i = 3,4,\cdots \end{cases} \tag{36}$$

and those for ψ are

$$\alpha_i = \begin{cases} 1 & i = 2 \\ 0 & i = 1,3,4,\cdots. \end{cases} \tag{37}$$

Therefore,

$$\beta_i = \begin{cases} 0 & i = 1,2 \\ \lambda^{1-i/2}\,(i-1)! & i = 3,4,\cdots \end{cases} \tag{38}$$

The Edgeworth expansion can easily be calculated from (38). Likewise, the Gray-Coberly-Lewis expansion and the new expansion can readily be found. Selected results for first order calculations (n = 1) are shown in Table 1. The accuracy of the new expansion seems to be quite satisfactory, especially for negative values of x. In fact, this point is clearly made by observing in Table 1 that for x = -3.0 and $\lambda = 50$, we have $F(x;\lambda) = .000211$, $E_1(x;\lambda) = -.000321$, $C_1(x;\lambda) = -.000105$, and

$G_1(x;\lambda) = .000190$. Also, by observing Table 1, it appears that for this example G_1 is uniformly better than E_1 or C_1 for $x \leq -3.0$ and $x \geq 3.0$, which seems to support its application in approximating tail probabilities.

Since in this example the limiting distribution is the standard normal, the approximations are not defined at points where $\psi^{(4)}(x) = (3x - x^3)\psi'(x) = 0$, that is at $x = -\sqrt{3}, 0$, or $\sqrt{3}$. In fact, as mentioned earlier, when selecting values of x "near" these points we might expect numerical problems to arise. In Table 2 we have selected values of x near 0 in order to illustrate the erratic behavior of C_1 amd G_1. Similar behavior also exists for x values near $-\sqrt{3}$ or $\sqrt{3}$. Hence in small neighborhoods about these points, we again emphasize that caution should be taken by the user. Fortunately, the expansion G_1 is defined at *all* points in the tails of the distribution.

ACKNOWLEDGEMENTS

This research was supported by a Stephen F. Austin State University Faculty Research Grant. The authors would like to thank the referees for their detailed criticisms and helpful comments on an earlier version of the paper.

LITERATURE CITED

Bickel, P. J. 1974. Edgeworth expansions in nonparametric statistics. The Annals of Statistics 2(1):1-20.

Coberly, W. A. 1972. On Edgeworth expansions with unknown cumulants. Ph.D. dissertation, Texas Tech University, Lubbock, TX.

Gotze, F. 1981. On Edgeworth expansions in Banach spaces. The Annals of Probability 9(5):852-859.

Gray, H. L., W. A. Coberly, and T. O. Lewis. 1975. On Edgeworth expansions with unknown cumulants. The Annals of Statistics 3(3):741-746.

McCune, E. D., and J. E. Adams. 1979. The practitioner's approach to obtaining generalized Cornish-Fisher expansions. The Texas Journal of Science. 31(4):303-308.

McCune, E. D., and H. L. Gray. 1982. Cornish-Fisher and Edgeworth expansions. Encyclopedia of Statistics 2:188-193.

Singh, K. 1981. On the asymptotic accuracy of Efron's bootstrap. The Annals of Statistics 9(6):1187-1195.

Terrell, R., and D. W. Scott. 1980. On improving convergency rates for nonnegative kernel density estimators. The Annals of Statistics 8(5):1160-1163.

RELATIONSHIPS OF SUGAR MAPLES (*ACER SACCHARUM* AND *A. GRANDIDENTATUM*) IN TEXAS AND OKLAHOMA WITH SPECIAL REFERENCE TO RELICT POPULATIONS

by FREDERICK R. GEHLBACH *and*
ROBERT C. GARDNER[1]

Department of Biology
Baylor University
Waco, TX 76798

ABSTRACT

Leaf shape and leaf flavonoid compounds suggest that southwestern sugar maples (*Acer saccharum* complex) have a common gene pool. *A. s. floridanum* (mature leaves larger than 50 mm in mid-vein length and with fewer than 14 blade points on the average) occurs in Arkansas, eastern Oklahoma and across Texas; whereas, *A. s. grandidentatum* (smaller leaves with 14 or more blade points) is present in Arizona, western New Mexico, and the Wichita Mountains, Oklahoma. An intermediate population lives in the Caddo Canyons, Oklahoma. The leaf features vary environmentally but remain diagnostic in McKittrick Canyon, Guadalupe Mountains, Texas, where *A. s. floridanum* is temporally and spatially diverse.

INTRODUCTION

Relict maple populations in central Texas are called *Acer saccharum* var. *grandidentatum* (Nutt.) Sarg., var. *sinuosum* (Rhed.) Little, var. *brachypterum* (Woot. and Standl.) E. J. Palm., or simply *A. grandidentatum* (Correll and Johnston 1970). Similar isolates in western Oklahoma are referred to *A. saccharum* March or *A. grandidentatum* Nutt., usually without varietal or subspecific epithets (Dent 1969). All live in restricted, comparatively mesic habitats (Rice 1962) between the range of *A. saccharum floridanum* (Chapm.) Small and Heller (sugar maple) in the forests of eastern Texas and Oklahoma and montane populations of *A. grandidentatum* (bigtooth maple) in trans-Pecos Texas and westward.

Desmaris' (1952) revision of sugar maples in the eastern U. S. and Canada designated *grandidentatum* as a western subspecies of *saccharum*, relegating *sinuosum* and *brachypterum* to its synonymy, although the bigtooth maple was not studied quantitatively. Leaf characteristics were used to combine all named taxa of the sugar maple complex with *A. saccharum*, but southwestern floras do not concur taxonomically (Kearney and Peebles 1960; Correll and Johnston 1970; Martin and

[1]Deceased 2 October 1981

Hutchins 1981). Confusion results, in part, from using qualitative leaf features that may be modified temporally and spatially by local environments (Fig. 1).

A newly discovered population of the sugar maple complex at Owl Creek Mountain, Coryell County, Texas (U.S. Army's Fort Hood) is of special interest, because it is isolated between the range of the sugar maple in east Texas and the presumed bigtooth maples of Bandera, Kendall, and Uvalde counties in central Texas. So that we might identify it and provide a quantitative appraisal of southwestern populations, the senior author analyzed leaf features (Anderson and Hubricht 1938; Desmaris 1952) with multivariate statistics, while the junior author compared flavonoid compounds from leaves of the same samples from Arkansas, Oklahoma, Texas, and Arizona.

EASTERN SUGAR MAPLES

Preliminary to our study of southwestern sugar maples, we used a principal components analysis (BMDP4M, Dixon and Brown 1979) to reexamine Desmaris' (1952) extensive information on eastern sugar maples. His table-3 data, appropriately transformed, on 22 populations containing 5,254 specimens in a transect from Arkansas through Ohio to Maine provided a test of critical leaf characteristics. Shape (*floridanum* and *saccharum* outline classes 1 and 3, respectively, with correlation coefficients of 0.91 and -0.88) plus number of teeth ($r = 0.86$) and size ($r = 0.83$) were the highly significant ($P < 0.001$) features comprising PC I, which explained 31 percent of the variance; hence these features were selected for examination in our southwestern samples.

Also, the principal components analysis suggested that *A. nigrum* Michx. is a distinct species that hybridizes with *A. saccharum*, rather than a non-geographic subspecies as postulated by Desmaris (1952). Midwestern populations, most influenced by *nigrum* (*fide* Desmaris and pers. observ.), fall between and overlap Arkansas-Tennessee samples (*A. s. floridanum*) and those from Pennsylvania through New England (*A. s. saccharum*) on PC I but segregate completely on PC II, defined by erect leaf hairs ($r = 0.80$) and a pubescent, *nigrum*-type leaf (Desmaris outline class 5, $r = 0.85$, $P < 0.001$). PC II explains 27 percent additional variance.

SOUTHWESTERN SUGAR MAPLES

Methods

Following Desmaris (1952), two stands from Arkansas (Benton and Randolph counties, $N = 62$) and two from Arizona (Chiricahua and Huachuca mountains, Cochise Co., $N = 83$) were chosen to represent sugar maple versus bigtooth maple influence, respectively. Unbiased

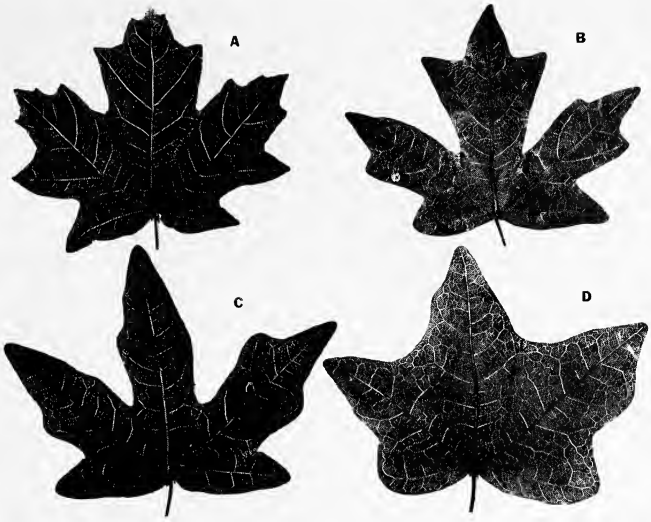

FIGURE 1. Extreme variation in the mature leaf shape of *Acer saccharum* from 1560-1650 m in McKittrick Canyon, Guadalupe Mountains, Culberson County, Texas, 1981. Specimen (A) resembles *A. s. saccharum*; (B) *A. grandidentatum;* (C), var. *sinuosum;* and, (D), *A. barbatum* Michx. (Leaves have 17, 10, 9, and 7 blade points, respectively, and are 61-70 mm in mid-vein length; all are from the outer twigs of trees at least 10 cm dbh.)

samples of leaves from McCurtain Co., Oklahoma (N = 30) and Nacogdoches Co., Texas (N = 42) represented sugar maple features near the western limit of range; whereas, a sample from McKittrick Canyon, Guadalupe Mountains, Culberson Co., Texas (N = 55) presumably represented bigtooth features near their eastern limit. Relict maples of the complex from Owl Creek Mountain (N = 60); Sabinal Canyon, Bandera Co., Texas (N = 65); Caddo Canyon, Canadian Co., Oklahoma (N = 30); and the Wichita Mountains, Comanche Co., Oklahoma (N = 30).

Stratified random samples of mature, undamaged leaves, larger than 40 mm in mid-vein length, were taken from the outer twigs of trees at least 10 cm in diameter at breast height (dbh) in Texas and Arizona (vouchers in Baylor University herbarium). Data for Arkansas and Oklahoma trees were obtained by measuring presumably unbiased samples of mature leaves in the Robert Bebb Herbarium, University of Oklahoma. A minimum of 10 leaves from each of 3 trees per locale provided data on number of blade points (teeth), mid-vein length (size), maximum middle and right lateral lobe widths, distance from edge of blade in the right lateral sinus to petiole insertion, and angle of the right lateral vein relative to the mid-vein. These six features were subjected to a discriminant function analysis with BMDP7M (Dixon and Brown 1979), using the Arkansas and Arizona samples for reference.

Flavonoids from 3-5 leaves of at least 2 trees per locale were extracted. Paper chromatography methods followed Mabry et al. (1970). Eleven compounds were located by means of their R_f values and color in ultraviolet light with and without ammonia vapor. A single linkage cluster analysis of the leaves was based on the simple matching coefficient of their compounds (Sneath and Sokal 1973).

Results and Discussion

Number of blade points was the only feature of leaf shape that differed significantly among the nine populations ($F = 36$, $P < 0.001$). Mid-vein length, a criterion of leaf size, was significant ($F = 9$, $P < 0.001$) when considered together with number of blade points but did not distinguish the samples by itself. None of the remaining measurements differed significantly among the samples ($F = 0.1\text{-}1.9$, $P > 0.05$). Arizona and Oklahoma trees had smaller leaves with more blade points in comparison with Arkansas and Texas populations (Table 1).

The discriminant function analysis separated Arizona maples from all other ($F = 8\text{-}52$, $P < 0.05$) except those in Comanche Co., Oklahoma ($F = 5$, $P > 0.05$). Arkansas samples differed significantly from those of Arizona, and Comanche and Canadian counties, Oklahoma ($F = 11\text{-}36$, $P < 0.05$). When individual leaves were classed according to reference sample, Arizona and Arkansas were 90 percent distinct; all Texas samples fell with those from Arkansas, as did those from McCurtain Co., Oklahoma (55-100% of leaves); the Canadian Co., Oklahoma sample was exactly intermediate; and, Comanche Co., Oklahoma, leaves fit largely with those from Arizona (60%).

On the basis of leaf shape, therefore, Arkansas sugar maples seem distinct from Arizona bigtooth maples. Eastern Texas and Oklahoma maples resemble the sugar maple in leaf-type (larger with fewer blade points) as predicted, but the montane and canyon isolates in central and trans-Pecos Texas are also allied with this type. Western or bigtooth maple influence (smaller leaf with more blade points) is more apparent in the Oklahoma relicts; although, varying degrees of intermediacy exist in the Texas and Oklahoma populations we examined (Table 1), thereby uniting the sugar and bigtooth maples as suggested by Desmaris (1952).

The analysis of flavonoid compounds grouped leaves within populations and closely assembled the Texas populations. In addition, it suggested greater intermediacy among the Oklahoma samples while failing to group any of the samples convincingly with either the sugar or bigtooth maple-types (Table 1). One-way ANOVAs of the arcsine-transformed matching coefficients suggested that neither the Texas nor Oklahoma samples were significantly closer to those of Arkansas ($F = 1.0$, $P > 0.05$) or Arizona ($F = 2.1$, $P > 0.05$).

TABLE 1. Distinguishing features of leaf shape ($\bar{x} \pm SD$) and mean matching coefficients (Sneath and Sokal 1973) of leaf flavonoid compounds in selected southwestern populations of *Acer saccharum* (Arkansas references sample) and *A. grandidentatum* (Arizona reference sample) arranged by mean coordinate on canonical variable 1 of a discriminant function analysis (in parentheses below population). See text for sample sizes.

Feature	Bandera County Texas (-3.3)	Arkansas (-2.8)	McCurtain County Oklahoma (-2.4)	Nacogdoches County Texas (-2.1)	Culberson County Texas (-1.5)	Coryell County Texas (-0.8)	Canadian County Oklahoma (-0.07)	Comanche County Oklahoma (0.6)	Arizona (2.3)
Leaf Blade Points	10.8 ± 0.8	11.3 ± 2.3	11.6 ± 2.1	11.9 ± 1.7	12.5 ± 1.9	13.2 ± 1.8	13.8 ± 1.9	14.3 ± 2.3	15.9 ± 1.9
Mid-vein Length (mm)	51.0 ± 9.1	59.4 ± 8.7	57.6 ± 7.4	58.0 ± 7.7	57.1 ± 5.9	57.8 ± 6.4	55.1 ± 5.6	50.9 ± 5.5	49.9 ± 8.1
Flavonoid Similarities									
Within population	91	73	70	91	73	95	100	82	65
Within state	87		60	76	77	76	69	62	
With Arkansas	50		55	45	55	68	68	63	55
With Arizona	32	55	55	34	41	40	68	56	

TABLE 2. Within-and between-years comparison of the diagnostic features of leaf shape ($\bar{x} \pm SD$) in *Acer saccharum* from McKittrick Canyon, Guadalupe Mountains, Culberson Co., Texas. (N = 10 leaves from each of three trees per elevation per year.)

		Elevation (m)			
Feature	Year	1560	1567	1650	Grand Mean ± SD
Mid-vein Length	1981	61.8 ± 6.8	53.6 ± 3.9	63.6 ± 7.1	
	1982	55.1 ± 7.1	48.0 ± 6.3	55.5 ± 7.5	54.3 ± 6.4
Leaf Blade Points	1981	16.1 ± 2.5	13.8 ± 1.6	13.6 ± 1.2	
	1982	13.7 ± 2.3	13.3 ± 1.2	13.1 ± 1.3	13.4 ± 1.7

The general evidence of intermediacy, yet morphologic distinctiveness, of the Arizona maples requires us to consider *grandidentatum* as the westernmost subspecies of *A. saccharum* (*sensu* Desmaris 1952), recognizable in southeastern Arizona and adjacent New Mexico (pers. observ.) but not widespread in Oklahoma and certainly not in Texas. Moreover, our findings do not support recognition of var. *sinuosum* or var. *brachypterum*, thus corroborating Desmaris' (1952) synonymy of these forms with *grandidentatum*.

The newly found relict population in Coryell Co., Texas, represents the eastern sugar maples, i.e. *A. s. floridanum* in eastern Texas, Oklahoma, and Arkansas. This too obtains for the other canyon and montane isolates in Texas, while the Canadian Co., Oklahoma, relict must be called *floridanum* × *grandidentatum*, and the Wichita Mountains population is strictly *grandidentatum*. The primacy of eastern sugar maple influence in Oklahoma and Texas, undoubtedly a mixture of genetic and environmental factors (Rice 1962), agrees with the postulated Pleistocene history of temperate zone biotas in the region (Martin and Harrell 1957).

As a guide for discerning the two subspecies of sugar maples in Texas and Oklahoma, we suggest that mature, outer leaves (at least 40 mm in mid-vein length) from several trees at least 10 cm dbh will average 14 or more blade points and 50 mm or less in mid-vein length if closest to *grandidentatum*. If more like *floridanum* the leaves will be larger and have fewer than 14 blade points on the average. We emphasize the importance of replicated blade point (tooth) counts, especially when the key features give conflicting information.

Because of the potential for environmental modifications, both within and between growing seasons, two additional year-samples from three sites in the 1560-1650 m elevational gradient of McKittrick Canyon, Texas, were studied (Fig. 1, Table 2). A two-way ANOVA revealed significant differences between years and among sites ($F = 4.8 - 9.6$, $P < 0.05$) except for the inter-site comparison of leaf blade points ($F = 1.4$, $P > 0.05$). No significant site by year interactions were apparent ($F = 0.01 - 1.2$, $P > 0.05$).

Despite these findings, only one measure of one sample (16.1 blade points in 1981) was at variance with our earlier designation of the McKittrick Canyon sugar maples as largely eastern in character (above and see Gehlbach 1981). Furthermore, when the grand means of 1981-1982 (Table 2) were compared with those of 1980 (Table 1), the result confirmed that the McKittrick Canyon trees resemble *A. s. floridanum* more than *A. s. grandidentatum* (two-way $t = 1.1, 1.5$, $P > 0.05$). Thus, we suggest that local temporal and spatial gradients do not alter the diagnostic value of our taxonomic criteria.

ACKNOWLEDGEMENTS

Robert Gardner extracted the flavonoids and qualitatively assessed their similarities before his untimely death. The senior author is responsible for all other aspects of this study, which benefitted from the comments of James Estes and Thomas Dent. Estes, Vincent Roth and Carroll Peabody sent specimens; Brenda Harvey and Daniel Turner helped in the laboratory; and Harold Beaty, Owen Lind, Richard Meyerhoff, Elray Nixon, and Roger Reisch aided the field work.

LITERATURE CITED

Anderson, E., and L. Hubricht. 1938. The American sugar maples. I. Phylogenetic relationships as deduced from a study of leaf variation. Bot. Gaz. 100:312-323.

Correll, D. S., and M. C. Johnston. 1970. Manual of the vascular plants of Texas. Texas Research Foundation, Renner. 1881 p.

Desmaris, Y. 1952. Dynamics of leaf variation in the sugar maples. Brittonia 7:347-387.

Dent, T. C. 1969. Relationships of two isolated groups of sugar maples in central Oklahoma to eastern and western species. Ph.D. dissert., Univ. Oklahoma, Norman, OK. 50 p.

Dixon, W. J., and M. B. Brown. 1979. Biomedical computer programs: P-series. Univ. California Press, Berkeley, CA. 880 p.

Gehlbach, F. R. 1981. Mountain islands and desert seas: A natural history of the U.S.-Mexican borderlands. Texas A&M University Press, College Station, TX. 298 p.

Kearney, T. H., and R. H. Peebles. 1960. Arizona flora. Univ. California Press, Berkeley, CA. 1085 p.

Mabry, T. S., K. R. Markham, and M. B. Thomas. 1970. The systematic identification of flavonoids. Springer-Verlag Publ. Co., New York, N.Y. 354 p.

Martin, P. s., and B. H. Harrell. 1957. The Pleistocene history of temperate biotas in Mexico and eastern United States. Ecology 38:468-480.

Martin, W. C., and C. R. Hutchins. 1981. A flora of New Mexico, vol. 1. J. Cramer, W. Germany. 1276 p.

Rice, E. L. 1962. The microclimate of sugar maple stands in Oklahoma. Ecology 43:19-25.

Sneath, P. H., and R. R. Sokal. 1973. Numerical taxonomy; the principles and practice of numerical classification. W. A. Freeman Publ. Co., San Francisco, CA. 573 p.

RECENT POPULATION TRENDS OF CORMORANTS (AVES: PELICANIFORMES) IN TEXAS

by MICHAEL L. MORRISON

Department of Forestry and Resource Management
University of California
Berkeley, CA 94720

and BRENDA S. HALE[1]

Department of Fisheries and Wildlife
Oregon State University
Corvallis, OR 97331

and R. DOUGLAS SLACK

Department of Wildlife and Fisheries Sciences
Texas A&M University
College Station, TX 77843

ABSTRACT

Data from Christmas Bird Counts and statewide nest surveys suggest that cormorants have maintained relatively high numbers in Texas during the late 1970's, 1980, and 1981.

Cormorant populations in Texas underwent an apparent decline during the early 1960's (Oberholser 1974), followed by a fluctuating but generally increasing trend in numbers by the end of the decade (Morrison and Slack 1977). However, data presented by Morrison and Slack (1977) indicated that numbers of Olivaceous Cormorants (*Phalacrocorax olivaceus*) might have been entering another period of decline as recently as the winter of 1973-74. This note examines population trends of Olivaceous and Double-crested (*P. auritus*) Cormorants in Texas through 1981.

Specific methods are given in Morrison and Slack (1977). Briefly, data were recorded from nine Texas coastal areas in which Audubon Christmas Bird Counts (CBCs) consistently have been conducted since 1949 (Morrison and Slack 1977: Table 1). (CBCs are 1-day counts conducted by volunteers in 15-mile-radius areas throughout much of North America sometime during late December and early January each year. CBC data are published annually in *American Birds*.) Data transcribed

---

[1]Present Address: Arizona Cooperative Wildlife Research Unit, University of Arizona, Tucson, Arizona 85721.

from each count were number of parties, total party-hours, total party-miles, and numbers of Olivaeous and Double-crested Cormorants seen. Although Raynor (1975) has cautioned that varying levels of observer effort over time can make interpretation of CBC data difficult, we felt justified in using the acutal numbers of birds counted in the nine areas for trend analysis because (1) count effort has remained relatively constant from 1975 to 1981 in the nine CBC areas used, and (2) the general trends shown for cormorants in Texas are similar for both standardized and raw data (Morrison and Slack 1977). Numbers of birds were reported by 3-year means to smooth the data series (Raynor 1975). To supplement wintering data for Olivaceous Cormorants, nesting colony surveys of the Texas Colonial Waterbird Society (TCWS) through 1981 were analyzed in the same way as the CBC data. (Double-crested Cormorants wintering in Texas nest primarily outside of the state.) The TCWS has conducted a formal census of colonial nesting waterbirds in Texas since 1967. Data by colony are made available to the public annually and have been compiled for the period 1973-1980 (Texas Colonial Waterbird Society 1982).

Although numbers of wintering Olivaceous Cormorants declined during the first half of the 1970's, they rose to a historic high by the end of the decade (1979-81; Table 1). The decline in the early 1970's was not as severe in magnitude nor duration as that noted during the 1960's. Although the total number of Olivaceous Cormorants (for the nine areas analyzed) prior to 1970 often dropped below 100 individuals per winter (range = 14-1682), total numbers since 1970 have remained above 100 birds (range = 125-1807).

After nesting Olivaceous Cormorants attained a mean population of more than 900 pairs in 1973-75, they apparently declined slightly through 1981 (Table 1). However, the number of nesting pairs still is considerably higher than that recorded during the 1960's. The data given for 1979-81 should be considered a minimum number of nesting pairs; coverage (survey) of nesting colonies during 1980 was incomplete, with several colonies not included in the count.

After wintering (coastal) Double-crested Cormorant populations reached a historic maximum in the mid-1970's, they declined during the latter part of the decade (Table 1). However, numbers of Double-crested Cormorants in the mid-1970's still were about twice as great as population levels previously reported. Numbers of this species were never above 1000 individuals/winter (for the nine count areas) until 1968 (range = 8-937). During the 1970's numbers usually were greater than 2000 individuals/winter (range = 572-7872), with a historic high of 7872 birds recorded during the winter of 1977-78.

Morrison and Slack (1977) summarized possible factors responsible for the fluctuations in populations of cormorants in Texas. Although

TABLE 1. Mean number of Olivaceous and Double-crested Cormorants wintering (data from nine Christmas Bird Count areas) and nesting (Texas Colonial Waterbird Society 1982) in Texas[a].

Period	Mean number of Olivaceous Cormorants		Mean number of Double-crested Cormorants
	nesting	wintering	wintering
1949-51	—[b]	188	15
1952-54	—	101	45
1955-57	—	190	134
1958-60	—	773	449
1961-63	—	78	64
1964-66	0[c]	153	301
1967-69	99	116	1560
1970-72	435	750	794
1973-75	943	351	4365
1976-78	648	424	3860
1979-81	607	994	2549

[a]Data for 1949-51 to 1973-75 adapted from Morrison and Slack (1977).
[b]Survey not conducted.
[c]Data for 1966 only; surveys not conducted prior to 1966.

further speculation is not appropriate, apparently populations of cormorants in Texas maintained (on the average) high numbers during the 1970's. For Olivaceous Cormorants, a nesting population of at least 500 pairs and a wintering population of about 500 individuals (for the nine CBC areas) should be considered average. For Double-crested Cormorants, a winter total of more than 2000 individuals (for the nine areas) should be expected. Continued monitoring of winter (CBC) and nesting (TCWS) cormorants will allow early detection of significant departures from expected population sizes. Wintering Double-crested Cormorants in the coastal regions analyzed herein deserve special attention, given the probable decline in their numbers during the late 1970's. Double-crested Cormorants also winter in inland Texas. Therefore, monitoring of inland populations of Double-crested Cormorants is especially important because it is possible that a certain segment of their population may shift between coastal and inland wintering areas among years. Such shifting between wintering areas, if it occurs, could have resulted in an under- or overestimate of populations of this species in the coastal areas monitored in this study.

LITERATURE CITED

Morrison, M. L., and R. D. Slack. 1977. Population trends and status of the Olivaceous Cormorant. American Birds 31:954-959.

Oberholser, H. C. 1974. The bird life of Texas. Vol. 1. University of Texas Press, Austin. 530 p.

Raynor, G. S. 1975. Techniques for evaluating and analyzing Christmas birds count data. American Birds 29:626-633.

Texas Colonial Waterbird Society. 1982. An atlas and census of Texas waterbird colonies 1973-1980. Caesar Kleberg Wildlife Research Institute, Kingsville, Texas. 358 p.

OCCURRENCE OF THE CADDISFLY *ATOPSYCHE ERIGIA* IN TEXAS' GUADALUPE RIVER BELOW CANYON RESERVOIR

by ROBERT A. SHORT

Aquatic Station
Southwest Texas State University
San Marcos, TX 78666

ABSTRACT

Larvae of the caddisfly *Atopsyche erigia*, which previously had been reported in south-central Texas only from spring-fed streams, were collected from the Guadalupe River below Canyon Reservoir. Recent colonization of the Guadalupe River by *A. erigia* apparently has been enabled by hypolimnial flow from the reservoir, which causes the tailwater's thermal regime to resemble that of a spring-fed stream.

The caddisfly (Trichoptera) genus *Atopsyche* Banks contains about 30 mostly South and Central American species (Ross 1953). *Atopsyche erigia* Ross occurs in the southwestern United States and has been collected in several Texas counties (Edwards 1973). All previous larval collections in Texas have been from spring-fed streams emanating from the Edwards Aquifer in the south-central part of the state, most notably the San Marcos River. Adults always have been taken in areas near a spring-fed stream (Edwards 1973).

During 1981, I collected larvae of *A. erigia* from the Guadalupe River, Comal County, Texas. Larvae were first collected during September, about 24 km downstream of Canyon Dam, a hypolimnial-release reservoir constructed in 1964. Occurrence of *A. erigia* at this site is interesting for several reasons. Kent (1971) collected extensively at the same site during 1969-70, some five years after Canyon Dam was closed, but did not report finding any *A. erigia*. Furthermore, collections by Kent (1971) and myself from the Guadalupe River above Canyon Reservoir did not yield any *A. erigia*. Apparently, the hypolimnial release has modified environmental conditions such that *A. erigia* has been able to colonize the Guadalupe River below the dam. Furthermore, this colonization has occurred within the past ten years, probably from the Comal River some 20 km downstream or from a smaller spring-fed tributary of the Guadalupe River.

Streams below hypolimnial-release reservoirs may exhibit thermal and flow characteristics similar to those of springbrooks (Ward and Short 1978). When compared to upstream sections, reservoir tailwaters

The Texas Journal of Science, Vol. XXXV, No. 3, September 1983

tend to have a more constant thermal regime, with winter-warm and summer-cool conditions. Kent (1971) reported an annual range of 8.0-29.5 C for the Guadalupe River above Canyon Reservoir and 12.5-17.7 C for the section below the dam.

The restriction of *A. erigia* to spring-fed streams may reflect their need for relatively low summer temperatures (Edwards 1973); the family to which it belongs, Rhyacophilidae, is said to be cool-adapted (Wiggins 1977). Thus, the establishment of *A. erigia* in the Guadalupe River below Canyon Dam may have been in response to the lower water temperatures provided by the hypolimnial release during summer. However, the winter-warm conditions below Canyon Reservoir and in spring-fed streams may also be of importance, considering that *A. erigia* belongs to a caddisfly genus with tropical affinities. Edwards (1973) reported collecting adult *A. erigia* from January through May, indicating that growth and/or pupal development continues through the winter, which might require winter-warm conditions. Life history studies of *A. erigia* are needed to more fully establish its habitat requirements.

I thank Steve Canton and James Ward for helpful suggestions regarding the manuscript.

LITERATURE CITED

Edwards, S. W. 1973. Texas caddisflies. Tex. J. Sci. 24:491-516.

Kent, D. H. 1971. The effects of a deep-storage reservoir on the benthic macroinvertebrate community of the Guadalupe River, Texas. M.S. thesis, Southwest Texas State University, San Marcos, Texas.

Ross, H. H. 1953. Additional material on the phylogeny and dispersal of *Atopsyche* (Trichoptera: Rhyacophilidae). J. Wash. Acad. Sci. 43:287-293.

Ward, J. V., and R. A. Short. 1978. Macroinvertebrate community structure of four special lotic habitats in Colorado, U.S.A. Verh. Int. Verein. Limnol. 20:1382-1387.

Wiggins, G. B. 1977. Larvae of the North American caddisfly genera (Trichoptera). University of Toronto Press, Toronto, Ontario, Canada.

HERPETOFAUNA OF THE PEDRO ARMENDARIZ LAVA FIELD, NEW MEXICO

by TROY L. BEST[1], HERMAN C. JAMES

Llano Estacado Center for Advanced Professional Studies and Research
Eastern New Mexico University
Portales, NM 88130

and FRANK H. BEST

P.O. Box 4571
Eastern New Mexico University
Portales, NM 88130

ABSTRACT

Notes on the distribution, relative abundance, habitat, and the relative degree of melanism are presented for 26 species of amphibians and reptiles collected at the Pedro Armendariz lava field, New Mexico. *Crotaphytus collaris, Sceloporus undulatus, Uta stansburiana, Phrynosoma cornutum, P. modestum, Crotalus atrox,* and *C. molossus* exhibited noticeable melanism. The 718 specimens analyzed represent the first comprehensive herpetofaunal study of the lava field.

INTRODUCTION

Three large basaltic lava fields occur in south-central New Mexico—the Tularosa malpais in Lincoln and Otero Counties, the Afton lava flows in Dona Ana County, and the Pedro Armendariz lava field in Socorro and Sierra Counties. Several authors (e.g., Dice 1929, 1930, 1942; Benson 1932, 1933; Bradt 1932; Dice and Blossom 1937; Burt 1939; Blair 1941, 1943; Lewis 1949; Shields and Crispin 1956) have investigated the biota of the Tularosa malpais. Lewis (1951), Prieto and Jacobson (1968), Koschmann (1972), and Elder (1977) have studied reptiles and mammals on the Afton flows. However, no biological investigations of the Pedro Armendariz lava field have been published.

The earliest account of collecting activities on the Pedro Armendariz lava field was that of Seth Benson of the University of California at Berkeley (unpublished); according to his field notes, Dr. Benson and his wife spent a few days there in July 1933. These field notes contain references to nearly black forms of *Phrynosoma, Crotalus,* and *Crotaphytus,* as well as dark forms of mammals such as *Peromyscus eremi-*

[1]Present address: Department of Biology and Museum of Southwestern Biology, The University of New Mexico, Albuquerque, NM 87131.

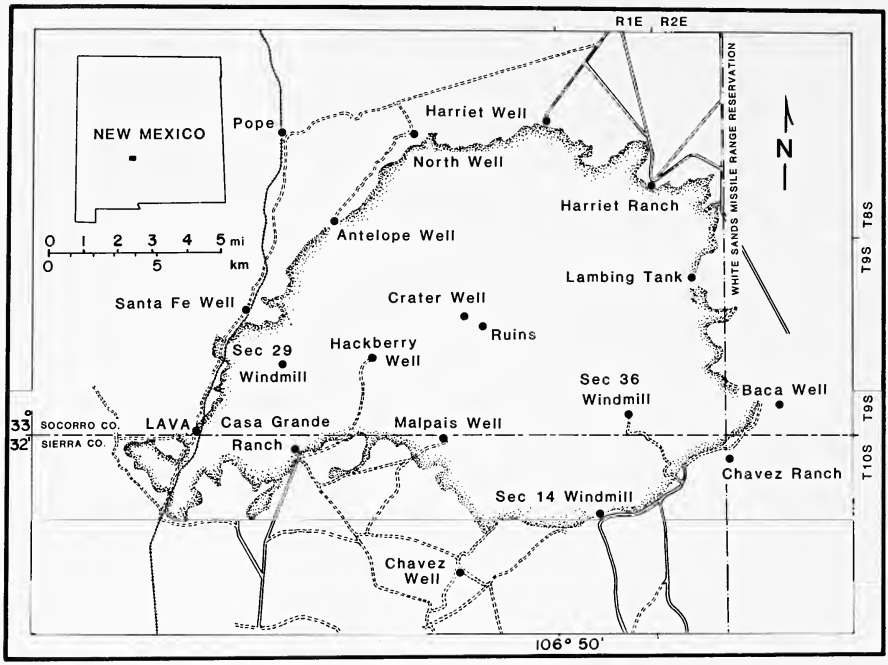

FIGURE 1. The Pedro Armendariz lava field, New Mexico.

cus and *Perognathus intermedius*. It was not until the late 1970s that additional collecting was done; mammals were collected by Melvin and Felecia Beard of Eastern New Mexico University under a contract with the New Mexico Department of Game and Fish.

Our study is the first comprehensive survey of the amphibians and reptiles of the Pedro Armendariz lava field. The purposes of our study were to determine which amphibian and reptile species occur on and near the lava field, the relative abundance of these, the habitats occupied by each, and the relative degree of melanism within the populations.

MATERIALS AND METHODS

A map of the Pedro Armendariz lava field, including place names mentioned in the text, is presented in Figure 1. The age of the field is approximately 760,000 years (Bachman and Mehnert 1978). It is 15 to 20 km in diameter, and there is a large crater near its center (elevation 1,566 m). The lava abruptly meets the plains on all sides. However, on the west and southwest sides there is a great deal of sandy soil on the lava. The edge of the lava is 3 to 5 m high and rises gradually toward the crater in a series of low hills. Between the low hills are soil-filled flats that hold water following heavy rains (Dr. S. Altenbach, Univer-

sity of New Mexico, Albuquerque, pers. comm. 1982). The soil here is mostly sandy although there is enough clay to make passage of vehicles difficult after rain showers. The surface of the lava field consists of broken pieces of lava embedded in soil. Much of the field is well vegetated with shrubs and grasses. Small lava pebbles form desert pavement between shrubs in many areas. The mosaic of lava and soil areas is extensive, especially near the edges of the lava field, and extends into the crater itself.

During April, July, and August of 1981 and May and June of 1982, 718 specimens of amphibians and reptiles were collected on or within 300 m of the lava field. Specimens were collected by hand, by rubber bands (launched ballistically from the collector's finger), and with .22 caliber no. 12 shot. All specimens were preserved in 10% formalin in the field, stored in 40% isopropyl alcohol, and permanently deposited in the Eastern New Mexico University Natural History Museum.

Although we might have been more successful in capturing some species had rocks been overturned systematically, rock-turning was avoided to minimize disturbance of the lava habitat. Unless stated, the species listed below did not exhibit melanism.

ACCOUNTS OF SPECIES

Ambystomidae, Mole Salamanders

Ambystoma tigrinum, Tiger Salmander

Specimen examined, 1—Socorro Co.: Antelope Well. Sight records—Socorro Co.: Lambing Tank. Sierra Co.: Malpais Well. Remarks—Tiger salamanders (larvae and adults) occurred regularly in small numbers in earthen stock tanks. All specimens were observed at night.

Pelobatidae, Spadefoot Toads

Scaphiopus couchi, Couch's Spadefoot

Specimens examined, 12—Socorro Co.: Lambing Tank. Remarks—Couch's spadefoots were locally abundant at only one of the four temporary rainwater ponds where we collected in August 1981.

Scaphiopus multiplicatus, Western Spadefoot

Specimens examined, 32—Socorro Co.: Harriet Well; North Well; Lambing Tank; T9S R2E NE 1/4 Sec 20; Sec 29 Windmill. Sierra Co.: Chavez Ranch. Remarks—We have followed Brown (1976) in assigning the species name to this taxon. Western spadefoots occurred regularly in small numbers at earthen stock tanks and abundantly in temporary rainwater ponds.

Scaphiopus bombifrons, Plains Spadefoot

Specimens examined, 21—Socorro Co.: Harriet Well; Lambing Tank; T9S R2E NE 1/4 Sec 20. Remarks—These spadefoots were locally

abundant following heavy rains, and were found in three of the four temporary rainwater ponds where we collected in August 1981.

BUFONIDAE, Toads

Bufo cognatus, Great Plains Toad

Specimens examined, 26—Socorro Co.: North Well; 2.4 km (1.5 mi) S North Well; Antelope Well; T9S R2E NE 1/4 Sec 20; Sec 29 Windmill. Sierra Co.: Malpais Well; Chavez Ranch. Remarks—The Great Plains toad occurred regularly in small numbers at earthen stock tanks and temporary rainwater ponds throughout the region. One specimen was found under a 20 cm diameter lava boulder 2.4 km (1.5 mi) south of North Well, the nearest water. The soil under the rock was moist from a recent rain. This was the only specimen of *Bufo* or *Scaphiophus* actually collected on the lava field proper.

Bufo debilis, Green Toad

Specimens examined, 12—Socorro Co.: Lambing Tank; T9S R2E NE 1/4 Sec 20. Remarks—Green toads were locally abundant following heavy rains, and were found in two of four temporary rainwater ponds in August 1981.

TESTUDINIDAE, Box and Water Turtles, Tortoises

Terrapene ornata, Box Turtle

Specimens examined, 13—Socorro Co.: North Well; 0.8 km (0.5 mi) W Antelope Well; Antelope Well; 7.7 km (4.8 mi) NE Lava; Santa Fe Well; 4.2 km (2.6 mi) S Hackberry Well; 1.9 km (1.2 mi) SW Baca Well; Lava. Sierra Co.: 1.0 km (0.6 mi) NE Casa Grande Ranch; Malpais Well; 0.5 km (0.3 mi) NW Windmill, T10S R1E NW 1/4 Sec 14; 3.2 km (2 mi) N Chavez Well. Remarks—Box turtles were common, especially in sand-filled lava areas on the south and west side of the lava field. They were present on the lava field proper in smaller numbers, and were most common in periods following rainfall. During late May and early June 1982, when it was very dry, no box turtles were observed.

IGUANIDAE, Iguanid Lizards

Holbrookia maculata, Lesser Earless Lizard

Specimens examined, 34—Socorro Co.: Harriet Well; 2.4 km (1.5 mi) S North Well; Antelope Well; Lambing Tank; 0.6 km (0.4 mi) N Malpais Well; Lava. Sierra Co.: Malpais Well; 1.0 km (0.6 mi) NE Casa Grande Ranch; 6.4 km (4 mi) SW Casa Grande Ranch; 2.9 km (1.8 mi) SW Casa Grande Ranch; 4.8 km (3 mi) SW Casa Grande Ranch; 3.2 km (2 mi) N Chavez Well. Remarks—Individuals of this species were locally abundant near the edge of the lava field, but were not common on the lava field proper. They preferred sandy soils with sparse vegeta-

tion, and were often observed at entrances to banner-tailed kangaroo rat (*Dipodomys spectabilis*) burrows. Within the lava field, lesser earless lizards were found only on the flat, sandy-soiled areas. They were most active during the warmest part of the day.

Crotaphytus collaris, Collared Lizard

Specimens examed, 145—Socorro Co.: Harriet Well; 0.8 km (0.5 mi) W North Well; 2.4 km (1.5 mi) S North Well; 2.9 km (1.8 mi) SW North Well; Antelope Well; T9S R1E NE 1/4 Sec 1; T9S R2E N 1/2 Sec 5; Lambing Tank; Santa Fe Well; 0.2 km (0.1 mi) SE Crater Well; Ruins, 1.1 km (0.7 mi) SE Crater Well, 1.6 km (1 mi) SW Crater Well; 1.9 km (1.2 mi) SW Crater well; 3.1 km (1.9 mi) NE Hackberry Well; 2.4 km (1.5 mi) NE Hackberry Well; 1.8 km (1.1 mi) NE Hackberry Well; 2.1 km (1.3 mi) E Hackberry Well; 2.9 km (1.8 mi) E. Hackberry Well; Hackberry Well; Sec 29 Windmill; 1.1 km (0.7 mi) SE Hackberry Well; 1.4 km (0.9 mi) SE Hackberry Well; 3.1 km (1.9 mi) SSW Hackberry Well; 7.6 km (4.7 mi) SSW Hackberry Well; 50.7 km (31.5 mi) N, 18.5 km (11.5 mi) E Engle; T9S R2E S 1/2 Sec 19; T9S R2E N 1/2 Sec 29; T9S R2E N 1/2 Sec 33; 1.9 km (1.2 mi) SW Baca Well; Sec 36 Windmill; 3.9 km (2.4 mi) NNW Malpais Well; 3.4 km (2.1 mi) NNW Malpais Well; 3.2 km (2 mi) NNW Malpais Well; 3.1 km (1.9 mi) NNW Malpais Well; 2.9 km (1.8 mi) NNW Malpais Well; 0.6 km (0.4 mi) N Malpais Well; Lava. Sierra Co.: 1.9 km (1.2 mi) E Casa Grande Ranch; T10S R2E NW 1/4 Sec 6; T10S R2E SW 1/4 Sec 6; T10S R2E SE 1/4 Sec 6; T10S R2E NW 1/4 Sec 7; 0.5 km (0.3 mi) NW Windmill, T10S R1E NW 1/4 Sec 14; 6.4 km (4 mi) SW Casa Grande Ranch; T10S R1E W 1/2 Sec 15; 3.2 km (2 mi) N Chavez Well. Remarks—The collared lizard was probably the most abundant reptile on the lava field; most lava outcrops had one or more individuals present. Collared lizards also were found perched in tops of *Rhus* and *Atriplex*, and on man-made objects such as cement blocks, corrals, and old boards. This species was restricted mostly to the lava field, although specimens were collected 50 to 80 m from the lava border. They were most active during the warmest part of the day. Specimens ranged from almost black dorsally to pale green. The majority of specimens was dark and many were approximately the same color as the lava. Ventrally, all specimens were pale.

Crotaphytus wislizenii, Leopard Lizard

Specimens examined, 7—Socorro Co.: Antelope Well; Santa Fe Well. Sierra Co.: 1.9 km (1.2 mi) E Casa Grande Ranch; Malpais Well; 0.5 km (0.3 mi) NW Windmill, T10S R1E NW 1/4 Sec 14. Remarks—Leopard lizards were not common. They seemed to prefer sandy soils and were most active during the warmest portion of the day. This spe-

cies was never found on the lava field, but was collected within 20 m of lava at all localities.

Sceloporus undulatus, Fence Lizard

Specimens examined, 13—Socorro Co.: Harriet Well; T9S R2E N 1/2 Sec 5. Sierra Co.: 3.2 km (2 mi) N Chavez Well. Remarks—These lizards were found in only three localities. Fence lizards were common on the sides and tops of large lava boulders at the Harriet Well and Chavez Well sites, and their absence at other localities is puzzling. Although specimens at the lava field were all found on or near the lava, one specimen was collected from the top of a fence post in a sandy soiled area several miles north of the lava field (Socorro Co., T7S R2E SW 1/4 Sec 21). Specimens from the lava field were dark. However, the two light colored dorsolateral stripes were visible.

Uta stansburiana, Side-blotched Lizard

Specimens examined, 185—Socorro Co.: Harriet Well; North Well; 2.1 km (1.3 mi) SW North Well; 2.4 km (1.5 mi) S North Well; 2.1 km (1.3 mi) N Harriet Ranch Hdqts.; T9S R2E N 1/2 Sec 5; Antelope Well; Santa Fe Well; Lava; Malpais Well. Sierra Co.: 1.9 km (1.2 mi) E Casa Grande Ranch; Malpais Well; 2.9 km (1.8 mi) SW Casa Grande Ranch; 0.5 km (0.3 mi) NW Windmill, T10S R1E NW 1/4 Sec 14; 6.4 km (4 mi) SW Casa Grande Ranch; 3.2 km (2 mi) N Chavez Well. Remarks—Side-blotched lizards were locally abundant, especially in areas with considerable sand on the lava. The area on the east side of the lava field had relatively little sand, and no *U. stansburiana* was collected there. Since *U. stansburiana* is relatively dark colored, it was difficult to assess the degree of melanism in this species. Specimens exhibited some melanism, but were extremely variable. In collecting specimens we qualitatively observed that darker specimens came from areas with less sand on the lava, and vice versa. We believe this species would be valuable in studying color variation between populations occurring on and off the lava field.

Phrynosoma cornutum, Texas Horned Lizard

Specimens examined, 7—Socorro Co.: 2.4 km (1.5 mi) S North Well; 0.8 km (0.5 mi) W Antelope Well; Santa Fe Well; Sec 29 Windmill; Lava. Sierra Co.: 3.2 km (2 mi) S Lava. Sight record—Socorro Co.: 2.1 km (1.3 mi) N Harriet Ranch Hdqts. (eviscerated and mummified body on *Rhus*; not saved). Remarks—Texas horned lizards were common only on the west and northwest portions of the lava field in both lava and sand covered areas. The species seemed most common on sandy sites, and many were observed in sandy habitat north of the lava field. Some of the specimens exhibited a slight degree of melanism.

Phrynosoma modestum, Round-tailed Horned Lizard

Specimens examined, 15—Socorro Co.: Harriet Well; 2.4 km (1.5 mi) S North Well; T9S R1E NE 1/4 Sec 1; Antelope Well; T9S R2E N 1/2 Sec 5; Hackberry Well; Sec 29 Windmill; 41.0 km (25.5 mi) N, 8.9 km (5.5 mi) E Engle; 1.9 km (1.2 mi) SW Baca Well. Sierra Co.: 6.4 km (4 mi) SW Casa Grande Ranch; 3.2 km (2 mi) N Chavez Well. Sight record—Sierra Co.: 0.5 km (0.3 mi) NW Windmill, T10S R1E NW 1/4 Sec 14 (eviscerated and mummified body on *Prosopis*; not saved). Remarks—This was one of the most abundant reptiles on the lava field proper. It occupied lava flats and sandy flats next to lava outcrops. Some specimens were nearly black and others were paler, but all of them exhibited some melanism.

Teiidae, Whiptails

Cnemidophorus neomexicanus, New Mexico Whiptail

Specimens examined, 48—Socorro Co.: Harriet Well; North Well; 2.1 km (1.3 mi) N Harriet Ranch Hdqts.; 2.4 km (1.5 mi) S North Well; Antelope Well; 2.3 km (1.4 mi) NNE Santa Fe Well; Santa Fe Well; T9S R2E N 1/2 Sec 29; 1.9 km (1.2 mi) SW Baca Well; Lava. Sierra Co.: 1.9 km (1.2 mi) E Casa Grande Ranch; T10S R2E NW 1/4 Sec 7; 0.5 km (0.3 mi) NW Windmill, T10S R1E NW 1/4 Sec 14; 4.8 km (3 mi) SSW Lava; 6.4 km (4 mi) SW Casa Grande Ranch. Remarks—New Mexico whiptails were most abundant on the extreme north side of the lava field near Harriet Well and North Well. The species was common throughout the rest of the region, but in lesser numbers. It occurred on both lava and soiled sites, but seemed to prefer soil-covered areas.

Cnemidophorus inornatus, Seven-striped Whiptail

Specimens examined, 62—Socorro Co.: Harriet Well; North Well; 2.1 km (1.3 mi) N Harriet Ranch Hdqts.; 2.4 km (1.5 mi) S North Well; T9S R1E NE 1/4 Sec 1; Antelope Well; T9S R2E N 1/2 Sec 5; Lambing Tank; Santa Fe Well; Hackberry Well; Sec 29 Windmill; 2.3 km (1.4 mi) SW Hackberry Well; 5.3 km (3.3 mi) SW Hackberry Well. Sierra Co.: Malpais Well; T105 R2E SE 1/4 Sec 6; T10S R2E NW 1/4 Sec 7; 2.9 km (1.8 mi) SW Casa Grande Ranch; 0.5 km (0.3 mi) NW Windmill, T10S R1E NW 1/4 Sec 14; 6.4 km (4 mi) SW Casa Grande Ranch; 3.2 km (2 mi) N Chavez Well. Remarks—This lizard was one of the most common species on the lava field; it was also common in adjacent areas.

Cnemidophorus tigris, Marbled Whiptail

Specimens examined, 2—Socorro Co.: 2.1 km (1.3 mi) N Harriet Ranch Hdqts.; Santa Fe Well. Remarks—Marbled whiptails were rare, and were never found on the lava field. The specimen from near Harriet Ranch was collected on top of a banner-tailed kangaroo rat mound,

near some broomweed (*Xanthocephalum*) and grass; the substrate was sandy with desert pavement of caliche and lava. The Santa Fe Well specimen was collected in creosote bush (*Larrea*) habitat north of the lava field, again with caliche desert pavement.

Cnemidophorus tesselatus, Checkered Whiptail

Specimens examined, 51—Socorro Co.: Harriet Well; 2.1 km (1.3 mi) N Harriet Ranch Hdqts.; 2.4 km (1.5 mi) S North Well; Lambing Tank; Santa Fe Well; Hackberry Well; T9S R2E N 1/2 Sec 29; Sec 36 Windmill; 1.9 km (1.2 mi) SW Baca Well; Malpais Well. Sierra Co.: 1.9 km (1.2 mi) E Casa Grande Ranch; Malpais Well; T10S R2E SE 1/4 Sec 6; T10S R2E NW 1/4 Sec 7; 0.5 km (0.3 mi) NW Windmill, T10S R1E NW 1/4 Sec 14; 3.2 km (2 mi) N Chavez Well. Remarks—This species was common, especially on soil-covered areas in and near the lava field. It seemed to prefer areas with sand and at least some lava nearby, but several were collected on sandy soils away from the lava.

COLUBRIDAE, Colubrid Snakes

Sonora semiannulata, Ground Snake

Specimens examined, 2—Socorro Co.: T9S R2E N 1/2 Sec 33. Sierra Co.: T10S R2E NW 1/4 Sec 7. Remarks—Because we elected not to systematically overturn rocks, this species may have been more common than was indicated by our observations. One specimen was collected from under a 20 cm diameter lava rock on a lava outcrop; the other was collected as it crawled across the desert pavement on a soil-filled lava flat.

Heterodon nasicus, Western Hognose Snake

Specimen examined, 1—Socorro Co.: North Well. Remarks—These snakes are common in the general region, but they probably are not abundant on the lava field. Our specimen was collected as it crawled along the cement base of the large stock tank at North Well.

Masticophis flagellum, Coachwhip

Specimens examined, 5—Socorro Co.: North Well; 2.1 km (1.3 mi) N Harriet Ranch Hdqts.; 2.4 km (1.5 mi) S North Well. Sierra Co.: 4.0 km (2.5 mi) SW Casa Grande Ranch; T10S R1E NE 1/4 Sec 13. Remarks—Coachwhips were common on the lava field and throughout the region. They seemed to prefer sandy-soiled areas.

Pituophis melanoleucus, Gopher Snake

Specimens examined, 3—Socorro Co.: 0.8 km (0.5 mi) W Antelope Well. Sierra Co.: Malpais Well; T10S R2E NW 1/4 Sec 7. Remarks—Gopher snakes were common on the lava field and throughout the region.

VIPERIDAE, Pit Vipers

Crotalus atrox, Western Diamondback Rattlesnake

Specimens examined, 14—Socorro Co.: Harriet Well; 2.1 km (1.3 mi) N Harriet Ranch Hdqts.; Hackberry Well; T9S R2E N 1/2 Sec 33; Sec 29 Windmill; 41.0 km (25.5 mi) N, 8.9 km (5.5 mi) E Engle; Sec 36 Windmill. Sierra Co.: 0.5 km (0.3 mi) NW Windmill, T10S R1E NW 1/4 Sec 14. Remarks—This is probably the most common snake species on the lava field. Lava outcrops and soil-covered areas next to lava were preferred, but some western diamondbacks occurred in adjacent sandy areas at dusk. All specimens exhibited melanism. The variation ranged from nearly black to moderately dusky. The diamond-shaped dorsal markings were visible on all specimens. Often the ventral sides were pinkish rather than cream colored.

Crotalus molossus, Black-tailed Rattlesnake

Specimen examined, 1—Socorro Co.: 50.7 km (31.5 mi) N, 18.5 km (11.5 mi) E Engle (=Ruins). Remarks—Our specimen was coiled in a rockpile in the mining ruins near the center of the lava field, and was darker than those examined from adjacent areas in New Mexico.

Crotalus viridis, Prairie Rattlesnake

Specimens examined, 6—Socorro Co.: Harriet Well; Antelope Well; Santa Fe Well; T9S R2E NE 1/4 Sec 20; Lava. Remarks—Prairie rattlesnakes were common, especially on sandy areas, throughout the region. They preferred sandy soils away from the lava, but the specimen from Antelope Well was collected from the top of a large lava outcrop where it was coiled on the sand in a lava crevice.

MELANISM IN REPTILES FROM NEW MEXICO LAVA FLOWS

Coloration of reptiles on New Mexico lava fields has received little attention. Lewis (1949) briefly reported on the coloration of reptiles from the Tularosa malpais, and Lewis (1951) and Prieto and Jacobson (1968) provided comments on specimens they collected on the Afton lava flows. These studies provide a basis for comparisons of coloration between the three southern New Mexico lava fields.

We observed some degree of melanism in seven reptile species on the Pedro Armendariz lava field; these were *Crotaphytus collaris, Sceloporus undulatus, Uta stansburiana, Phrynosoma cornutum, P. modestum, Crotalus atrox,* and *C. molossus.* Of these species, Lewis (1951) collected *U. stansburiana* and *C. collaris* on the Afton lava flows and also found them to be malanistic. However, his *C. atrox* was not melanistic. Prieto and Jacobson (1968) subsequently collected additional nonmelanistic specimens of *C. atrox* from the Afton lava flows, but their *C. molossus* were melanistic. For the Tularosa malpais, Lewis (1949) col-

lected specimens of *U. stansburiana, S. undulatus, C. collaris,* and *C. molossus;* all exhibited melanism. Thus, *C. collaris, U. stansburiana,* and *C. molossus* were darker on all three fields, *S. undulatus* was darker on both lava fields where they occurred (the Pedro Armendariz field and the Tularosa malpais), and the only darkly pigmented populations of *P. cornutum, P. modestum,* and *C. atrox* were on the Pedro Armendariz field.

ACKNOWLEDGEMENTS

We are grateful to Dr. G. Sanchez, Dean of Graduate Studies and Research, Llano Estacado Center for Advanced Professional Studies and Research, Eastern New Mexico University, who provided a major portion of the financial support for this project. N. J. Scott verified our identifications of specimens, A. L. Gennaro provided some of the equipment, and W. R. Barber, D. G. Beard, H. F. Pearson, and F. W. Weckerly provided valuable assistance in the field. Joe Williams and Johnnie Mounyo allowed us to collect specimens on the land in their care; we sincerely appreciate their assistance. L. L. DeVries typed the manuscript, D. J. Hafner helped prepare the figure, S. A. Reza assisted in proofreading, and N. J. Scott provided valuable criticism and consultation throughout the study.

LITERATURE CITED

Bachman, G. O., and H. H. Mehnert. 1978. New K-Ar dates and the late Pliocene to Holocene geomorphic history of the central Rio Grande region, New Mexico. Geol. Soc. Amer. Bull. 89:283-292.

Benson, S. B. 1932. Three new rodents from lava beds of southern New Mexico. Univ. California Publ. Zool. 38:335-345.

Benson, S. B. 1933. Concealing coloration among some desert rodents of the southwestern United States. Univ. California Publ. Zool. 40:1-69.

Blair, W. F. 1941. Annotated list of mammals of the Tularosa Basin, New Mexico. Amer. Midl. Nat. 26:218-229.

Blair, W. F. 1943. Ecological distribution of mammals in the Tularosa Basin, New Mexico. Contrib. Lab. Vert. Biol., Univ. Michigan No. 20, 24 p.

Bradt, G. W. 1932. The mammals of the malpais, an area of black lava rock in the Tularosa Basin, New Mexico. J. Mammal. 13: 321-328.

Brown, H. A. 1976. The status of California and Arizona populations of the western spadefoot toads (genus *Scaphiopus*). Nat. Hist. Mus. Los Angeles Co., Contrib. Sci. No. 286, 15 p.

Burt, W. H. 1939. A new woodrat (*Neotoma mexiana*) from the lava beds of southern New Mexico. Occas. Pap. Mus. Zool., Univ. Michigan No. 400, 3 p.

Dice, L. R. 1929. Description of two new pocket mice and a new woodrat from New Mexico. Occas. Pap. Mus. Zool., Univ. Michigan No. 203, 4 p.

Dice, L. R. 1930. Mammal distribution in the Alamogordo region, New Mexico. Occas. Pap. Mus. Zool., Univ. Michigan No. 213, 32 p.

Dice, L. R. 1942. Ecological distribution of *Peromyscus* and *Neotoma* in parts of southern New Mexico. Ecology 23: 199-208.

Dice, L. R., and P. M. Blossom. 1937. Studies of mammalian ecology in southwestern North America with special attention to the colors of desert mammals. Carnegie Inst. Washington Publ. No. 485, 129 p.

Elder, F. F. B. 1977. The ecological distribution of the rock pocket mouse *Perognathus intermedius* Merriam, in the Afton lava flows of southern New Mexico. Stud. Nat. Sci., Eastern N. Mex. Univ. 2(3):1-23.

Koschmann, J. R. 1972. Melanism in rodents of the Afton lava flows, Dona Ana County, New Mexico. M.S. Thesis, Univ. Texas El Paso, 50 p.

Lewis, T. H. 1949. Dark coloration in the reptiles of the Tularosa malpais, New Mexico. Copeia 1949:181-184.

Lewis, T. H. 1951. Dark coloration in the reptiles of the malpais of the Mexican border. Copeia 1951:311-312.

Prieto, A. A., and E. R. Jacobson. 1968. A new locality for melanistic *Crotalus molossus molossus* in southern New Mexico. Herpetologica 24:339-340.

Shields, L. M., and J. Crispin. 1956. Vascular vegetation of a recent volcanic area in New Mexico. Ecology 37:341-351.

TAXONOMIC STATUS OF THE BRAZILIAN COLUBRID SNAKE, *XENODON SUSPECTUS* COPE

by JAMES R. DIXON

Department of Wildlife and Fisheries Sciences
Texas A&M University
College Station, TX 77843

ABSTRACT

Xenodon suspectus is proposed to be conspecific and synonymous with *X. rhabdocephalus.*

In 1968 Cope questioned the relationship of several species of *Xenodon* and agreed with Gunther (1863) that the species in British India belonged to another genus. However, Cope argued that Jan's (1863) removal of *Xenodon gigas* to a separate genus was in error. When Cope (1868) described the single known specimen of *Xenodon suspectus,* he had before him two specimens of *X. gigas* (= *Hydrodynastes gigas*), five of *X. severus,* one of *X. neovidii* (= *X. neuwiedii*), three of *X. colubrinus* (= *X. rhabdocephalus*), and four of *X. angustirostris* (= *X. rhabdocephalus*). Cope stated that the type locality of *X. suspectus* was Lake Jose Azzu, Brazil. Amaral (1929), in his list of neotropical snakes, gave the distribution of *X. suspectus* as "eastern Peru", and this suggestion was followed by Peters and Orejas-Miranda (1970). A review of the literature indicates that only one specimen of *X. suspectus,* other than the holotype, has been recorded. This specimen was reported by Boulenger (1894) from Moyobamba, N.E. Peru.

Dick (1977), in his account of the stations of the Thayer Expedition to Brazil during 1865-1866, states that Agazziz, Burkhardt, Thayer, and Coutinho traveled to Lago Jose Assu (=Acu), Brazil, during August 27-30, 1865. This locality is approximately 02°51′S — 57°00′W. It is no longer named Lago Jose Assu on modern maps and gazetteers for Brazil. The locality now may be recognized as the body of water formed at the confluences of Igarape Acu, Rio Ariau, and Rio Andira, on the extreme eastern edge of the Brazilian state of Amazonas. This lake is located just west and south of the confluence of the Rio Ramos and Rio Andira.

The Peruvian locality is either the town or province of Moyobamba. The town lies at 854 meters and the lowest part of the province is at an

The Texas Journal of Science, Vol. XXXV, No. 3, September 1983

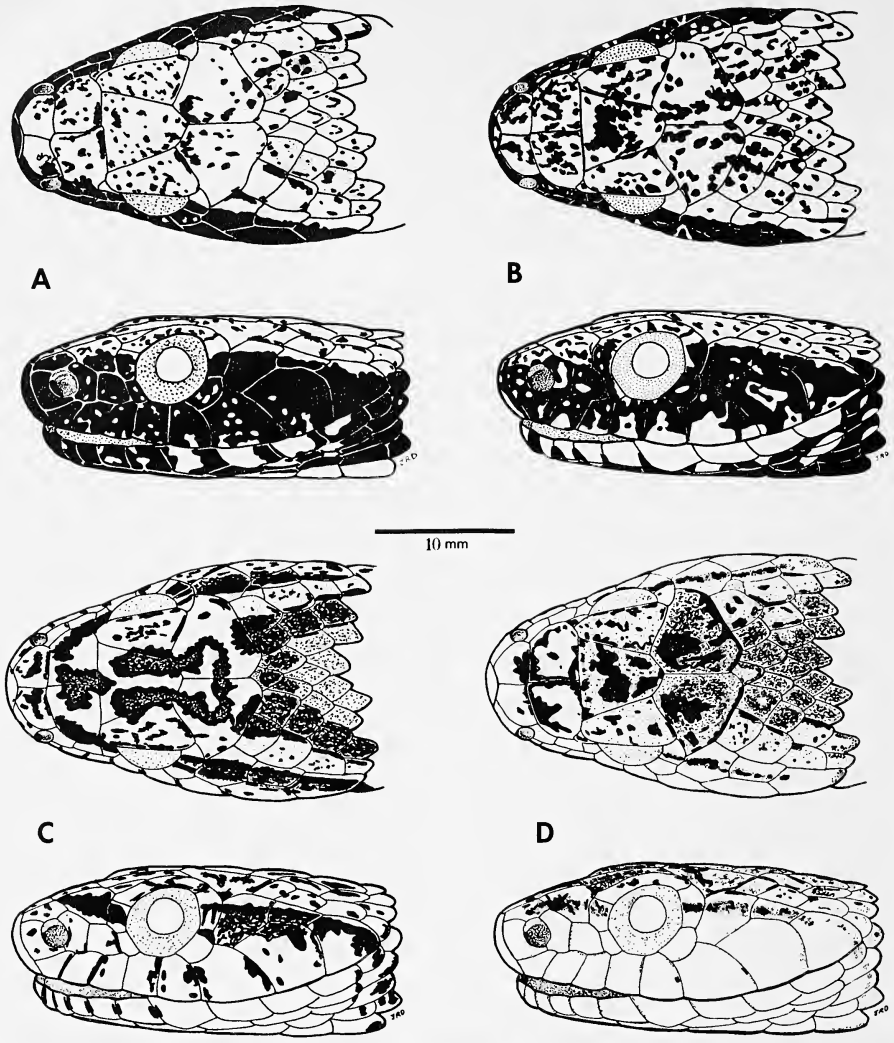

FIGURE 1. Dorsal and lateral views of the heads of three *Xenodon rhabdocephalus* from Iquitos region, Peru, and of the holotype of *X. suspectus*. A) TCWC 38213, female; B) MCZ 362, female (holotype of *X. suspectus*); C) TCWC 42103, male; D) TCWC 42100, male.

elevation of approximately 200 meters, well within the known altitudinal distribution of *Xenodon*.

Boulenger (1894) diagnosed *X. suspectus* and separated it from *X. columbrinus* (= *rhabdocephalus*) only on the basis of the width and depth of the rostral scale, i.e., one and one-third as broad as deep in *X. suspectus* versus one and one-half to one and two-thirds as broad as deep in *X. rhabdocephalus*. The two species are essentially identical in scutellation and color pattern. The only other species of *Xenodon*

TABLE 1. Range of variation in external characters of *Xenodon rhabdocephalus* and *X. suspectus*, taken from specimens. Number in parenthesis below name represents sample size.

	X. r. rhabdocephalus (40)	*suspectus* (2)	*r. mexicanus* (10)
Scale Rows	19-19-15	19-19-15	19-19-17
Ventrals	135-155	132-140	124-144
Subcaudals	36-50	36-41	35-42
Supralabials	8	8	8
Infralabials	9-11	9	9-10
Infral. Chin Shield Contact	5-7	6	5-6
Preoculars	1-3	1	1
Postoculars	2-3	2	2
Temporals	1 + 2/2 + 3	1 + 2	1 + 2
Max. Teeth	14-19	16	15-16
Blotches	13-18	14	13-15
Tail/Total Length Ratio	.132 − .152	.134	.138 − .168
Supral/Orbit	4 + 5	4 + 5	4 + 5
Anal Plate	E	E	E
Rostral Width/Height	1.32 − 1.80	1.33	1.40 − 1.60

(sensu stricto) that have the essential external characters of *X. suspectus* are *X. bertholdi* and *X. guentheri.* Of these, *X. guentheri* has a higher number of ventrals (170) and subcaudals (57), and a divided anal plate. *Xenodon bertholdi* has, on each side of the trunk, a series of large oval spots that are separated from each other medially.

A sample of 28 *Xenodon rhabdocephalus* that I examined from a 100 km radius of Iquitos, Peru, exhibited several color patterns. The dorsum ranged from a very light ground color with dark blotches to a uniform blackish brown. The venter was almost immaculate yellow to dusky dark brown. The dorsum of the head varied from light brown freckles and mixed dark spots to uniform brown. The side of the head was almost completely black to almost completely light tan or yellow.

Of the 28 specimens, 21.4% had wide (Fig. 1A), 28.6% medium (Fig. 1C), and 50.0% narrow (Fig. 1D) temporal dark stripes from the snout to the temporal region of the head. The dorsum of the head was densely freckled (Fig. 1A) in 60.7%, had a spear-shaped mark (Fig. 1C) in 14.3%, and an ill-defined spear with freckles (Fig. 1D) in 25.0% of the individuals. The infralabials and supralabials were scored as freckled (light on dark or dark on light), streaked (black edging), or unmarked. The labials were freckled in 25.0%, streaked in 64.3%, and unmarked in 10.7% of the sample. The ventral color was dark in 14.3%, moderately dark in 21.4%, moderately light in 17.9%, and light in 46.4% of the sample. Twenty-seven of the 28 individuals contained 13-18 (mean = 14.7) body blotches; one individual was unicolored.

The single specimen in the British Museum identified as *X. suspectus* from Moyobamba, Peru, and the holotype of *X. suspectus* (Fig. 1B), appear very similar to the dark phase color pattern of *X. rhabdocephalus* (Fig. 1A). This—together with the broad overlap of count-data from the two forms (Table 1)—leads me to propose that *Xenodon suspectus* be considered a junior subjective synonym of *X. rhabdocephalus.*

I thank E. E. Williams for the loan of the type specimen of *X. suspectus.* I also thank W. W. Lamar for data on Colombian *Xenodon* and R. Dean, H. McCrystal and E. Michaud for reviewing the manuscript.

LITERATURE CITED

Amaral, A., do. 1929. Estudos sobre ophidios Neotropicos XVII. Valor systematico de varias formas de ophidios neotropicos. Mem. Inst. Butantan 4:1-68.

Boulenger, A. G. 1894. Catalogue of the snakes in the British Museum (Natural History). Vol 2. Trustees of the Museum, London, England, xi + 382 p.

Cope, E. D. 1868. An examination of the Reptilia and Batrachia obtained by the Orton Expedition to Ecuador and the upper Amazon, with notes on other species. Proc. Acad. Nat. Sci. 20:96-140.

Dick, M. M. 1977. Stations of the Thayer expedition to Brazil 1865-1866. Brevoria 444:1-37.

Gunther, A. 1863. Third account of new species of snakes in the collection of the British Museum. Ann. Mag. Nat. Hist. (3)12:348-365.

Jan, G. 1863. Enumerazione sistematica degli ofidi appartenenti al gruppo Coronellidae. Arch. Zool. Anat. Fisiol. 2(2):213-330.

Peters, J. A., and B. Orejas-Miranda. 1970. Catalogue of the neotropical Squamata. Part 1. Snakes. Bull. U.S. Natl. Mus. 297:v-347.

VISCOMETRIC MEASUREMENT OF THE CELLULASE ACTIVITY OF A SOIL FUNGUS

by J. ORTEGA *and* E. J. BACA

School of Sciences and Mathematics
Pan American University
Edinburg, TX 78539

ABSTRACT

A simple viscometric technique for the determination of the cellulase activity of fluids from liquid cultures of fungi was developed. Because results were expected to follow Michaelis-Menten kinetics for enzyme activity, the data obtained from the viscosity tests were fitted to an exponential function. Significantly high coefficients of correlation were obtained. The inital rates of the reactions were calculated from these functions. The Michaelis-Menten constant (Km) of the test fungus was estimated from a Lineweaver-Burk plot.

INTRODUCTION

Fungi vary greatly in their ability to decompose cellulosic materials (Mandels and Weber 1969; Mandels 1975; Rosenberg 1978). Because the number of species of fungi found in most agricultural soils tends to be large, there is a need for a simple and direct method that will permit the screening of large numbers of fungal isolates for cellulolytic activity with a minimum of laboratory equipment and time. This work is an attempt to develop such a method.

Several methods based on viscometric techniques have been proposed for the evaluation of cellulase activity of fungi and other microorganisms. One of these mehtods (Levinson and Reese 1950) relates cellulase activity to the changes in fluidity of a cellulose-derivative test solution. This method does not seem to equate cellulase activity with the rate at which depolymerization of the substrate occurs. Another method (Almin and Eriksson 1967; Almin et al. 1967) is complicated by the calculation and introduction of an exponent (a) based on the empirical relationship between the intrinsic viscosity of the test solution and time. A final method (Hulme 1971) offers a somewhat similar approach to that described here. It relates cellulase activity to specific viscosity of a test solution and to the average molecular weight of the substrate; Lineweaver-Burk plots for the velocity of depolymerization of the substrate are calculated as the reciprocals of the units of cellulase activity versus concentration of the substrate.

In this work, the proposed method for measuring cellulase activity is based on the Michaelis-Menten equation as described by Laidler (1965).

With the use of this equation and the Lineweaver-Burk plot as described by Williams and William (1973), the maximum velocity of substrate degradation (a measure of enzyme activity) for a given enzyme concentration can be calculated. Furthermore, the Michaelis-Menten constant, which is an approximate measure of the enzyme-substrate bonding affinity, can be evaluated.

THEORY

In the study of reactions affected by enzymes, it is necessary to measure the initial rate of the reaction at variable substrate concentrations while the concentration of the enzyme is kept constant. The initial rate of the reation can be determined by fitting the concentration and time data for each experiment to the exponential function.

$$C_s = a \cdot e^{bt}$$

where C_s represents the concentration of the substrate, a and b are the constants fo the function, e is the base of natural logarithms and t is the time. The inital rate, V_o, then can be evaluated by computing dC_s/dt at time = 0, which is,

$$V_o = dC_s(0)/dt = a \cdot b.$$

The Michaelis-Menten equation can be used to relate the initial rate to the concentration of the substrate. This equation leads to the following expression for the rate:

$$V_o = V_m \cdot C_s/(K_m + C_s)$$

where V_o is the initial rate, V_m the maximum reaction velocity, C_s the concentration of the substrate and K_m the Michaelis-Menten constant. This expression can be rearranged to obtain

$$1/V_o = K_m/(V_m \cdot C_s) + 1/V_m.$$

The Michaelis-Menten constant (K_m) can be determined from the slope and the intercept of the linear regression of $1/V_o$ versus $1/C_s$.

The specific viscosity (N_{sp}) determined experimentally for each of the test solutions can be used to determine the average molecular weight (M_n) and the concentration (C_s) of the substrate using the method proposed by Hulme (1971).

MATERIALS AND METHODS

The fungus *Fusarium roseum* was isolated from soil taken from an agricultural field near Edinburg, Texas, in March of 1982. The initial culture was purified and identified following the methods of Toussoun and Nelson (1976).

The liquid culture medium had the following composition: $(NH_4)_2SO_4$, 4.5 g; KH_2PO_4, 2.0 g; $MgSO_4 \cdot 7H_2O$, 0.8 g; $Ca(NO_3)_2 \cdot 4H_2O$, 0.5 g; $Fe(NO_3)_3 \cdot 9H_2O$, 1.44 mg; $ZnSO_4 \cdot 7H_2O$, 0.88 mg; $MnSO_4 \cdot 4H_2O$, 0.40 mg; Neo Peptone (Difco), 5.0 g; powdered cellulose (Sigma 50), 20.0 g; distilled water, 1000 ml. The pH of the medium was adjusted to 5.0 with 0.01 M K_2HPO_4 buffer. The medium was dispensed in 500-ml flasks, 250 ml per flask, and sterilized for 15 minutes at 121 C and 15 psi.

Solid medium for the inoculum was prepared by adding 15 g of agar to the ingredients listed above. Seven-day-old cultures of the test fungus grown in petri dishes on solid medium were used as sources of inoculum. Each culture flask was inoculated as described before (Ortega 1980) by aseptically transferring four 5 mm inoculum disks carrying hyphae and spores. All cultures were incubated at 25 C.

Samples from the fungus cultures were taken after eight days of cultivation by pipetting 15 ml of the fluid into sterile test tubes. The samples were centrifuged at 6000 **g** for 15 minutes at 20 C. After centrifugation, the clear supernatant was carefully pipetted into sterile test tubes and frozen until the cellulase assays were made.

Samples of the culture fluids were assayed for carboxymethyl cellulase (CM cellulase; EC 3.2.1.4) as described before (Ortega 1980), by measuring the change in the viscosity of a buffered solution of sodium carboxymethyl cellulose, when the fluid from the test fungus was mixed with it and the reaction mixture was kept at constant temperature. The test solution consisted of 7.0 g of sodium carboxymethyl cellulose (CMC, type 7HF with a D.S. of 0.7, by Hercules, Inc.) dissolved in 1000 ml of 0.055 M sodium citrate buffer with a pH of 5.0. A series of test solutions with different CMC concentrations (0.2% to 0.8%) was also prepared for the determination of the Michaelis-Menten constant. The reaction mixture consisted of 9 ml of CMC test solution and 1 ml of a 50% dilution of the fungus fluid in 0.055 M sodium citrate buffer.

The changes in the viscosity of the reaction mixture were determined with a Cannon-Fenske routine viscometer. All tests were made at 37 C, at intervals of 1 to 3 minutes for 25 to 30 minutes. The efflux time of the viscometer was determined in seconds. The data obtained from the viscosity tests were used to determine the specific viscosity of the substrate, the rate of the reaction and the activity of the enzyme. Specific viscosity (N_{sp}) was determined as suggested by Levinson and Reese

(1950). Reaction rates were determined as the time-derivatives of the exponential functions of the substrate concentrations versus the incubation time.

The measurement of the cellulase activity was based on the amount of substrate hydrolyzed as inferred from viscosity reduction, not on the formation of any intermediate or end product of the reaction. The unit of enzyme activity was that amount of cellulase that produces a 0.1 mg per ml decrease in the substrate concentration per minute at 37 C, under the conditions described for the assay.

The Michaelis-Menten constant was estimated from a Lineweaver-Burk plot of the reciprocals of substrate concentrations against the reciprocals of the reaction rates at different substrate concentrations and constant amount of enzyme, at the start of the reaction.

RESULTS AND DISCUSSION

The data presented in Table 1 show the changes in viscosity and inferred substrate concentration with respect to time for a typical experiment in which the initial substrate concentration was 4.71 g per liter. The viscosity of the reaction mixture was reduced 23.5 % during the first 90 seconds of incubation.

A plot of substrate concentration (C_s) versus time for this experiment is shown in Figure 1. This plot, as well as those obtained for other experiments with different initial substrate concentrations, resulted in a good fit to the exponential model. The units of cellulase activity shown in Table 1 can be determined directly from this plot or from the data of Table 1. Initial reaction rates (V_0) were determined from the plots of a series of tests with different initial substrate concentrations and constant amount of enzyme (Table 2).

The relationship between the reciprocal of V_0 and substrate concentration (C_s) is shown in Figure 2. This Lineweaver-Burk plot illustrates that the reaction followed the Michaelis-Menten model for enzyme activity. The Michaelis-Menten constant ($K_m = 2.84 \times 10^{-2}$) for the test fungus was determined from the resulting slope and intercept of a linear regression of the plot. Maximum velocity (77.9 units per ml per minute) of substrate degradation was determined from the intercept of the plot.

The method described above permits one to determine the activity of fungal cellulases from simple viscometric measurements and a few calculations. The present method is more precise than that of Levinson and Reese (1950) and less cumbersome than that of Almin and Eriksson (1967) and Almin et al. (1967). Its advantage over the method of Hulme (1971) is that the initial reaction rate can be estimated directly, by fitting experimental viscosity data to an exponential model.

TABLE 1. Decline in viscosity of a solution of sodium carboxymethyl cellulose due to cellulase activity of *Fusarium roseum*.

Time in minutes	Efflux, seconds	Specific viscosity[a]	C_s, g per liter $x10^{-1}$	Activity Units[b]
0.00	281	55.88	4.71	
1.49	216	42.72	4.04	45
5.58	192	37.87	3.76	17
9.35	173	34.02	3.54	13
12.78	159	31.19	3.36	11
16.02	147	28.76	3.20	10
18.89	138	26.94	3.08	9
21.79	130	25.32	2.97	8
24.51	124	24.10	2.88	7
27.05	118	22.89	2.79	7
29.48	114	22.08	2.73	7
32.10	109	21.06	2.66	6

[a]Centistokes

[b]Each unit equals a 0.1 mg per ml decrease in the substrate concentration per minute, as described in the text.

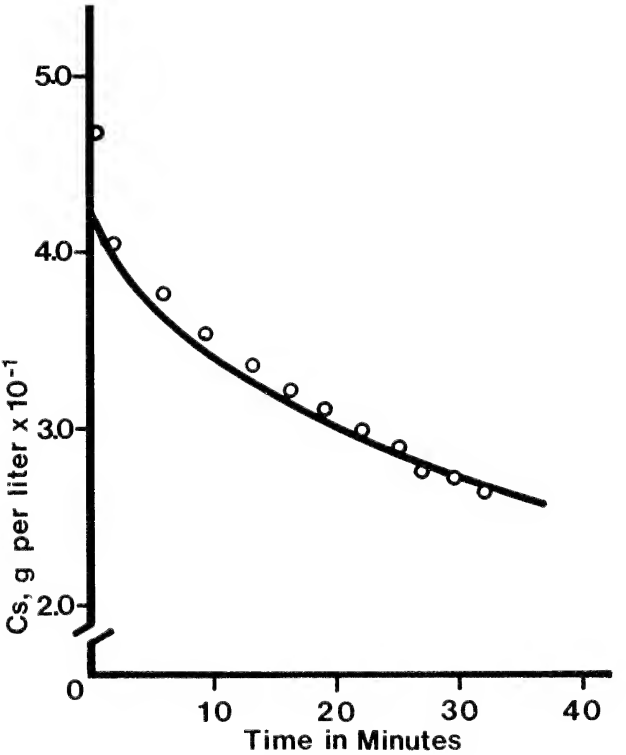

FIGURE 1. Substrate concentration (C_s, in g per liter) versus time (t, in minutes). Equation of the line is $C_s = 0.404 \cdot e^{-0.0136 \cdot t}$; $r^2 = 0.99$.

TABLE 2. Data for a Lineweaver-Burk plot of the cellulase activity of *Fusarium roseum*.

N_{sp}[a]	C_s, g per liter	$1/C_s$, (g per liter)$^{-1}$	V_o, (g per liter per minute)	$1/V_o$, (g per liter per minute)$^{-1}$
2.6	0.64	1.56	1.45	0.69
5.9	1.16	0.86	2.22	0.45
11.5	1.82	0.55	3.09	0.32
19.4	2.53	0.40	3.83	0.26
27.7	3.13	0.32	4.67	0.21
33.9	3.53	0.28	4.03	0.25
44.4	4.13	0.24	4.99	0.20
56.0	4.71	0.21	5.49	0.18
68.7	5.29	0.19	5.31	0.19
54.7	4.65	0.22	3.72	0.27

[a]Specific viscosity in Centistokes.

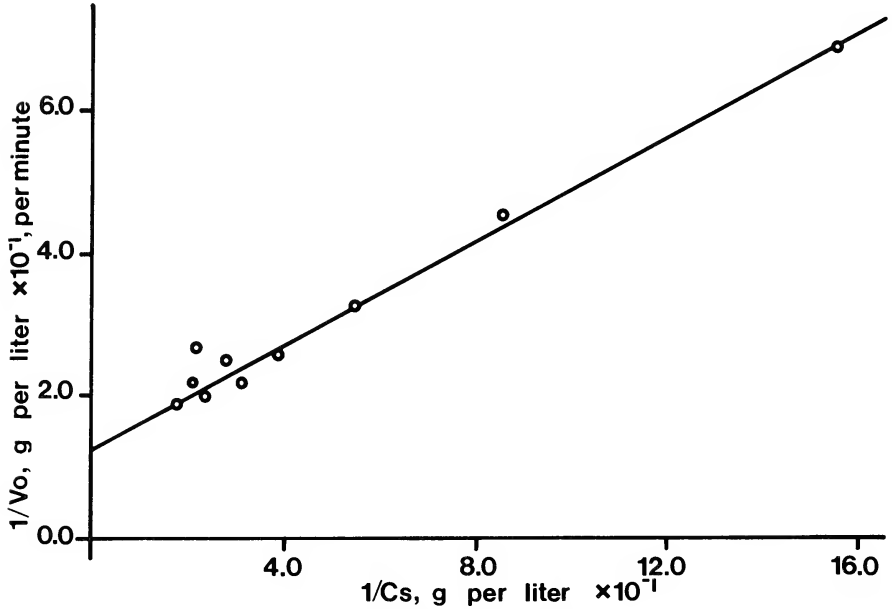

FIGURE 2. Lineweaver-Burk plot of the reciprocals of the initial reaction rate (V_o, in g per liter per minute) and substrate concentration (C_s, in g per liter). Equation of the line is $1/V_o = 0.128 + 0.360 \cdot (1/C_s)$; $r^2 = 0.97$.

LITERATURE CITED

Almin, K. E., and K. E. Eriksson. 1967. Enzymic degradation of polymers. I. Viscometric method for the determination of enzymic activity. Biochim. Biophys. Acta 139:238-247.

Almin, K. E., K. E. Eriksson, and C. Jansson. 1967. Enzymic degradation of polymers. II. Viscometric determination of cellulase activity in absolute terms. Biochim. Biophys. Acta 139:248-253.

Hulme, M. A. 1971. Viscometric determination of carboxymethyl cellulase in standard international units. Arch. Biochem. Biophys. 147:49-54.

Laidler, K. J. 1965. Chemical kinetics. McGraw-Hill Book Co., New York, N.Y., p. 475-478.

Levinson, H. E., and E. T. Reese. 1950. Enzymatic hydrolysis of soluble cellulose derivatives as measured by changes in viscosity. J. Gen. Physiol. 33:601-628.

Mandels, M., and J. Weber. 1969. The production of cellulases, p. 391-413. *In* R. F. Gould (Ed.), Cellulases and their applications. Advances in chemistry series 95. Am. Chem. Soc., Washington, D.C.

Mandels, M. 1975. Microbial sources of cellulase, p. 81-105. *In* Biotechnol. Bioeng. Symp. No. 5. John Wiley and Sons, Inc. New York, N.Y.

Ortega, J. 1980. Cellulase activities of soil fungi. Texas J. Sci. 32:241-246.

Rosenberg, S. L. 1978. Cellulose and lignocellulose degradation by thermophilic and thermotolerant fungi. Mycologia 70:1-13.

Toussoun, T. A., and P. E. Nelson. 1976. Fusarium. A pictorial guid to the identification of *Fusarium* species according to the taxonomic system of Snyder and Hanson. Second Edition. The Pennsylvania State University Press, University Park, PA.

Williams, V. R., and H. R. Williams. 1973. Basic physical chemistry for the life sciences. W. H. Freeman and Co., San Francisco, CA. p. 299-302.

NEW RECORDS OF THE FRESHWATER ECTOPROCT *PECTINATELLA MAGNIFICA* IN EASTERN TEXAS

by RAYMOND W. NECK

Texas Parks and Wildlife Department
4200 Smith School Road
Austin, TX 78744

and RICHARD W. FULLINGTON

Dallas Museum of Natural History
P.O. Box 26193, Fair Park Station
Dallas, TX 75205

ABSTRACT

We present additional records of the freshwater ectoproct, *Pectinatella magnifica*, from the eastern part of Texas. Apparent proliferation of this animal in Texas may have resulted from an increase in suitable habitat comprised by numerous artificial impoundments constructed since 1932.

The lophophorate phylum Ectoprocta largely consists of marine forms, although the class Phylactolaemata contains approximately 50 freshwater species (Ryland 1970). Many ectoprocts live as loosely-developed, mat-like colonies. However, *Pectinatella magnifica* (Leidy) forms large gelatinous masses with maximum diameters as great as one meter. Only limited records of *P. magnifica* in Texas have been published. The first Texas report seems to be one by Geiser (1934), who had specimens from Caddo Lake near Jefferson, Marion and Harrison counties (collected by E. P. Cheatum and W. M. Longnecker in 1933) and from a locality in Lake Worth, Tarrant County (collected by B. B. Harris on 29 October 1933). Everitt (1975) also reported colonies in "Caddo Lake, Texas." More recently, Casto and Johnson (1982) reported a population in Belton Lake, Bell County, in the Brazos River drainage. Here we report additional localities and speculate on what may be an increase in abundance of this species in Texas waters.

On 23 September 1982, one of us (RWN) encountered several colonies of *Pectinatella magnifica* on small tree-branches floating in the water and on bald cypress (*Taxodium distichum*) knees in a slough of Lake Houston off Caney Creek south of the fork known as Peach Creek, San Jacinto River drainage, Montgomery County. Water level was approximately one meter below normal due to severe drought conditions. Colonies were variable in size; the largest was 28 cm by 11 cm.

Over the past several years the other of us (RWF) has encountered colonies of *Pectinatella magnifica* in a number of localities as follows (with date of collection): Lake Murvaul, Murvaul Creek, Sabine River drainage, Panola County, 1968; Lake Tawakoni, Sabine River, Hunt County, 1974; Toledo Bend Reservoir, Sabine River, Shelby County, 1976; Lake Palestine, Neches River, Henderson County, 1977; Cedar Creek Lake, Cedar Creek, Trinity River drainage, Kaufman County, 1978; Lake Hawkins, Little Sandy Creek, Sabine River drainage, Wood County, 1980; and Beaver Lake (private lake on Patton farm), Sabine River drainage, Wood County, 1982.

These observations of *Pectinatella magnifica* in widely separated portions of Texas may reflect a recent increase in suitable microhabitat due to the large number of reservoirs now present in Texas. Records now exist for all major Texas drainages from the Sabine west to the Brazos. The large globular colonies are conspicuous and certainly evince interest and curiosity among biologists and non-biologists alike.

Several environmental factors have been implicated as controlling agents in distribution of *Pectinatella magnifica.* The most comprehensive study of this species is by Brown (1933), who found it in warm, well-lighted waters of less than 3 meters depth in quiet, protected areas. In seeming contradiction of Brown's (1933) findings, Davenport (1904) reported that *P. magnifica* prefers shady conditions and running water. Williams (1921) reported that young colonies in aquarium jars prefer dark areas. Brown (1933) observed that *P. magnifica* was not found in acidic waters and that colonies planted in bogs soon died because organic debris accumulated in the region of the mouth and tentacles. However, Everitt (1975) found no *P. magnifica* in waters with pH over 7.1. Marcus (1925) reported that a temperature of 20 C was required for proper colony development; destruction of colonies observed by Marcus (1925) occurred when temperature declined to 16-17 C. Bushnell (1974) stated that *P. magnifica* "is known only from uncontaminated water." Hubschman (1970) investigated substrate discrimination and demonstrated that *P. magnifica* prefers pebbles over glass which is preferred over sand.

While the Caddo Lake and Lake Houston localities are both in eastern Texas, which is characterized by acidic waters, the Belton Lake locality is located in the limestone region of central Texas with alkaline waters. The key habitat factor in Texas appears to be a permanent body of quiescent water. Such habitats were relatively rare in Texas until the construction of numerous reservoirs beginning in the 1930's.

Dispersal mechanisms employed by *Pectinatella magnifica* are not well understood. Asexual reproduction of freshwater ectoprocts involves production of resistant bodies known as statoblasts which may float, sink to the bottom or adhere to the parent colony. Statoblast viability is

reduced following ingestion by various vertebrates, but significant numbers survive (Brown 1933). Introductions into Germany (Schachanowskaja 1929) probably involved transport by ships (Hyman 1959). Dried statoblasts are able to survive for several years (Rogick 1940).

Fluctuations in population density and sudden appearances at new localities are typical for *Pectinatella magnifica* (Geiser 1937). A dramatic appearance of this species in Iowa was associated with low water levels during the cool season (Geiser 1937). Lack of overflow Iowa ponds during winter resulted in a larger than normal percentage of the statoblasts remaining in the pond at the intiation of the spring growing season. Nutrients similarly retained in the pond allowed maximum production of suitable food organisms.

LITERATURED CITED

Brown, C J. D. 1933. A limnological study of certain fresh-water Polyzoa. Trans. Amer. Micros. Soc. 52:271-313.

Bushnell, J. H. 1974. Bryozoans (Ectoprocta), p. 157-194. *In* C. W. Hart. Jr. and S. L. H. Fuller (Eds.), Pollution ecology of freshwater invertebrates. Academic Press, New York, N.Y.

Casto, S. D., and K. W. Johnson. 1982. A second record of the ectoproct *Pectinatella magnifica* in Texas. Texas J. Sci. 34:192.

Davenport, C. B. 1904. Fresh-water Bryozoa of the United States. Proc. U.S. Natl. Mus. 27:211-221.

Everitt, B. 1975. Freshwater Ectoprocta: Distribution and ecology of five species in southeastern Louisiana. Trans. Amer. Micros. Soc. 94:130-134.

Geiser, S. W. 1937. *Pectinatella* an occasional river pest in Iowa. Field and Laboratory 5(2):65-76.

Hubschman, J. H. 1970. Substrate discrimination in *Pectinatella magnifica* Leidy (Bryozoa). J. Exp. Biol. 52:603-607.

Hyman, L. H. 1959. The invertebrates: Smaller coelomate groups. Vol. V. McGraw-Hill, New York, N.Y. 783 p.

Marcus, E. 1925. Bryozoa, p. 1-46. *In* P. Schulze (Ed.), Biologie der Tiere Deutschlands, Lief. 14, Teil 25.

Rogick, M. D. 1940. Studies of freshwater Bryozoa. XI. The viability of dried statoblasts of several species. Growth 4:315-322.

Ryland, J. S. 1970. Bryozoans. Hutchinson Univ. Library, London, England. 175 p.

Schachanowskaja, M. 1929. *Pectinatella magnifica* Leidy in Bohmen. Zool. Anzeiger 80:296-297.

Williams, S. R. 1921. Concerning "larval" colonies of *Pectinatella.* Ohio J. Sci. 21:123-127.

THE TEXAS ACADEMY OF SCIENCE, 1983-84

OFFICERS

President:	Bernard T. Young, Angelo State University
President-Elect:	Michael J. Carlo, Angelo State University
Vice-President:	William J. Clark, Texas A&M University
Immediate Past President:	Elray S. Nixon, Stephen F. Austin State University
Secretary-Treasurer:	Everett D. Wilson, Sam Houston State University
Editor:	William H. Neill, Texas A&M University
AAAS Council Representative:	Arthur E. Hughes, Sam Houston State University

DIRECTORS

1981	Richard L. Noble, Texas A&M University
	Bob F. Perkins, University of Texas, Arlington
1982	Billy J. Franklin, Texas A&I University
	Ethel W. McLemore, Dallas
1983	D. Lane Hartsock, Austin
	Katherine Mays, Bay City

SECTIONAL CHAIRPERSONS

I—*Mathematical Sciences*: Barbara Schreur, Texas A&I University
II—*Physical Sciences*: Virginia L. Rawlins, North Texas State University
III—*Earth Sciences*: James C. Grenda, Angelo State University
IV—*Biological Sciences*: Edward Schenider, Southwest Texas State University
V—*Social Sciences*: James O. Standley, Stephen F. Austin State University
VI—*Environmental Sciences*: Robert D. Larsen, Southwest Texas State University
VII—*Chemistry*: John T. Moore, Stephen F. Austin State University
VIII—*Science Education*: Fred L. Fifer, University of Texas, Dallas
IX—*Computer Sciences*: H. P. Haiduk, Amarillo College
X—*Aquatic Sciences*: Fred L. Rainwater, Stephen F. Austin State University

COUNSELORS

Collegiate Academy: Shirley Handler, East Texas Baptist College
Helen Oujesky, University of Texas, San Antonio
Junior Academy: Ruth Spear, San Marcos
Peggy Carnahan, San Antonio

COVER PHOTO

Michel T. Halbouty, the Academy's Distinguished Texas Scientist for 1983

Text of Mr. Halbouty's address to the Academy appears on pages 181-187.

2nd CLASS POSTAGE
PAID AT HUNTSVILLE
TEXAS 77341
AND AT ADDITIONAL
MAILING OFFICE
AT LUBBOCK
TEXAS 79401

ISSN 0040-4403

ume XXXV, Number 4 January 1984

THE TEXAS JOURNAL OF SCIENCE

PUBLISHED QUARTERLY BY
THE TEXAS ACADEMY OF SCIENCE

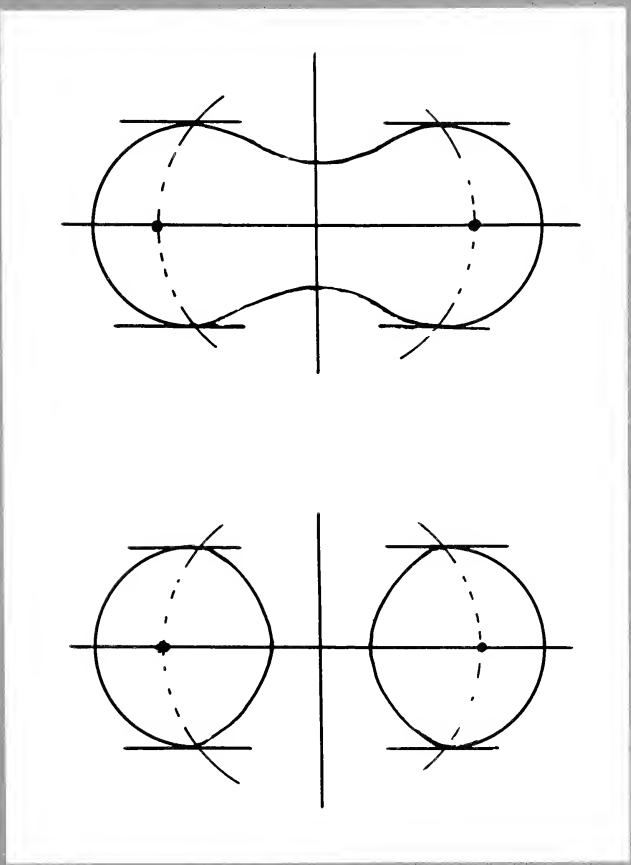

AFFILIATED ORGANIZATIONS
Texas Section, American Association of Physics Teachers
Texas Section, Mathematical Association of America
Texas Section, National Association of Geology Teachers

GENERAL INFORMATION

MEMBERSHIP. Any person or group engaged in scientific work or interested in the promotion of science is eligible for membership in The Texas Academy of Science. Dues for members are $20.00 annually; student members, $12.00 annually; sustaining members, at least $30.00 in addition to annual dues; life members, at least $400.00 in one payment; patrons, at least $500.00 in one payment; corporate members, $250.00 annually; corporate life members, $2000.00 in one payment. Library subscription rate is $45.00 annually. Payments should be sent to the Secretary-Treasurer, Box 2175, Huntsville, TX 77341.

The *Journal* is a quarterly publication of The Texas Academy of Science and is sent to all members and subscribers. Inquiries regarding back issues should be sent to Dr. Fred S. Hendricks, Dept. Wildlife & Fisheries Sciences, Texas A&M University, College Station, TX 77843.

The Texas Journal of Science (USPS 616740) is published quarterly at Huntsville, Texas U.S.A. Second class postage paid at Post Office, Huntsville, TX 77341, and at additional mailing office at Lubbock, TX 79401. Please send form 3579 and returned copies to Texas Tech Press, Box 4240, Lubbock, TX 79409.

THE TEXAS JOURNAL OF SCIENCE

Volume XXXV, No. 4 January 1984

CONTENTS

INSTRUCTIONS TO AUTHORS

Scholarly papers in any field of science, natural history, or technology are eligible for publication in *The Texas Journal of Science.* Before a paper can be accepted for publication, it must undergo critical review by at least 2 appropriate referees and the editor.

A manuscript intended for publication in the *Journal* should be prepared in accordance with the following instructions and then submitted to Dr. William H. Neill, TJS Editor, Department of Wildlife & Fisheries Sciences, Texas A&M University, College Station, TX 77843.

The manuscript is not to have been published elsewhere. Triplicate typewritten or machine-printed copies (or the original and 2 good xerographic reproductions) *must* be submitted. Text, table and figure captions, and references should be *double-spaced* with 2-3 cm margins (without right-justification) on 8½ X 11-inch paper. The title of the article should be followed by the name and business or institutional address of the author(s). *Be sure to include zip code* with the address. If the paper has been presented at a meeting, a footnote giving the name of the society, date, and occasion should be included but should not be numbered. Begin the body of the paper with a brief ABSTRACT to which is appended a list of key words (abstracting services pick this up directly), followed by the text subdivided into sections as appropriate. Use upper / lower case letters, italics (indicated by single underscore), and indentation in a way that mimics the pattern evident in the most recent issue of the *Journal.*

In the text, cite all references by author and date *in chronological order*, i.e., Jones (1971); Jones (1971, 1972); (Jones 1971); (Jones 1971, 1972); Jones and Smith (1971); (Jones and Smith 1971); (Jones 1971; Smith 1972; Beacon 1973). If there are more than 2 authors, use: Jones et al. (1971); (Jones et al. 1971).

References are then to be assembled, arranged *alphabetically*, and placed at the end of the article under the heading LITERATURE CITED. For a PERIODICAL ARTICLE use the form: Jones, A. P., and R. J. Smith. 1971. Persistence of chlorinated hydrocarbons. J. Soil Chem. 37:116-123. For a paper published in the PROCEEDINGS OF A SYMPOSIUM, etc., use the form: Jones, A. P. 1971. Persistence of chlorinated hydrocarbons, p. 155-181. *In* A. P. Jones (ed.), Pesticides in soils. Soc. Soil Chem., New York, NY. For a REPORT use: Jones, A. P. 1971. Persistence of chlorinated hydrocarbons. Texas Soils Institute (Austin, TX) Report No. 14, 46 p. A MASTERS OR Ph.D. THESIS should appear as: Jones, A. P. 1971. Persistence of chlorinated hydrocarbons in blackland soils. M.S. thesis, Texas A&M Univ., College Station, TX. For a BOOK, NO EDITORS, use: Jones, A. P. 1971. Environmental effects of chlorinated hydrocarbons. Academic Books, New York, NY, 439 p. For a CHAPTER IN A BOOK WITH

EDITORS: Jones, A. P. 1971. Persistence of chlorinated hydrocarbons, p. 13-39. *In* A. P. Jones, B. R. Smith, Jr. and T. S. Gibbs (eds.), Environmental effects of chlorinated hydrocarbons. Academic Books, New York, NY. For an IN-PRESS PERIODICAL ARTICLE use: Jones, A. P. In Press. Persistence of chlorinated hydrocarbons. J. Soil Chem. For an IN-PRESS BOOK use: Jones, A. P. In Press. Environmental effects of chlorinated hydrocarbons. Academic Books, New York, NY.

References to unpublished data or personal communications should not be listed in the LITERATURE CITED section. However, they should be presented within the text as: (unpubl. data from C. J. Jones, Dept. Zoology, Univ. Texas, Austin, TX) *or* (pers. comm. from R. C. Smith, P.O. Box 133, Mexia, TX).

Any footnotes (except those referenced in the body of a table) should appear on a separate sheet of paper, following the LITERATURE CITED.

All tables are to be typed with a carbon ribbon, free of error, without handwritten notations, and ready for photographic reproduction. Each table, headed by its caption, should be placed on a separate sheet of paper. Tables must have a text reference, i.e., Table 2 shows...*or* (Table 2).

Figures are to be *original inked drawings* or *photographic prints no larger than 4½ X 6½ inches* and mounted on standard 8½ X 11-inch paper. Each illustration should be marked on the back with the name of the first author and the figure number. Captions for figures are to be provided on a separate sheet of paper. Figures must have a text reference, i.e., Figure 3 illustrates...*or* (Fig. 3).

Authors will receive galley proofs plus the edited typescript and information concerning reprints and page charges. Proofs must be corrected (using ink) and returned to the editor within 5 days. Page charge payment (check or purchase voucher) or a publication-grant request must accompany return of the corrected proofs or a delay in printing the manuscript could occur. Reprint orders should be returned directly to Texas Tech Press, Box 4240, Lubbock, TX 79409.

THE EDITOR SHOULD BE NOTIFIED IMMEDIATELY OF ANY CHANGE IN THE PRINCIPLE AUTHOR'S ADDRESS OR TELEPHONE NUMBER.

NOTE: Authors are encouraged to contribute $35.00 per published page to defray printing costs, and authors of articles exceeding ten pages are expected to make *some* contribution to the publication fund. However, payment of printing costs is not a condition for publication in *The Texas Journal of Science*, and NO AUTHOR, WHO WOULD OTHERWISE SUBMIT A MANUSCRIPT, SHOULD HESITATE TO DO SO BECAUSE OF LACK OF FUNDS. Members without funds may apply to the Texas Academy of Science for a grant to cover some or all costs of publication.

TORIC SECTIONS

by ALI R. AMIR-MOEZ *and* GREGORY A. FREDRICKS

Department of Mathematics
Texas Tech University
Lubbock, TX 79409

ABSTRACT

Plane sections of a torus are described with techniques of vector algebra. Then, the result is generalized to an n-dimensional Euclidean space.

INTRODUCTION

The study of plane sections of a torus is relevant to both pure and applied mathematics and suggests, through vector algebra, many generalizations. Yeates (1947) states, without proof, that certain sections of tori are Cassini ovals. In this note we explore this idea for R_3 and give a generalization to R_n.

NOTATION

We employ standard notation. Vectors are denoted by Greek letters and scalars by Latin letters. The inner product of α and β is denoted by (α, β) and the norm of α is denoted by $\| \alpha \|$. The subspace spanned by the set $\{\alpha_1, \ldots, \alpha_k\}$ is indicated by $[\alpha_1, \ldots, \alpha_k]$.

TORIC SECTIONS

Suppose that T is a torus in R_3. Then there exists an orthonormal basis $\{\alpha_1,\alpha_2,\alpha_3\}$ of R_3 for which the leading circle S of T lies in $[\alpha_1,\alpha_2]$ and has its center τ on the α_2-axis (Fig. 1). Let $a>0$ be the radius of S and suppose that $\tau = p\alpha_2$. The equation of S is

$$\gamma = h\alpha_1 + k\alpha_2, \ \|\gamma - \tau\| = a.$$

The generating circle of T lies in the plane which is parallel to α_3 and passes through the endpoints of τ and γ. If the endpoint of ξ is on T, then

$$\begin{cases} \xi = m(\gamma - \tau) + s\alpha_3 + \tau \\ \|\xi - \gamma\| = b > 0, \end{cases} \tag{1}$$

The Texas Journal of Science, Vol. XXXV, No. 4, January 1984

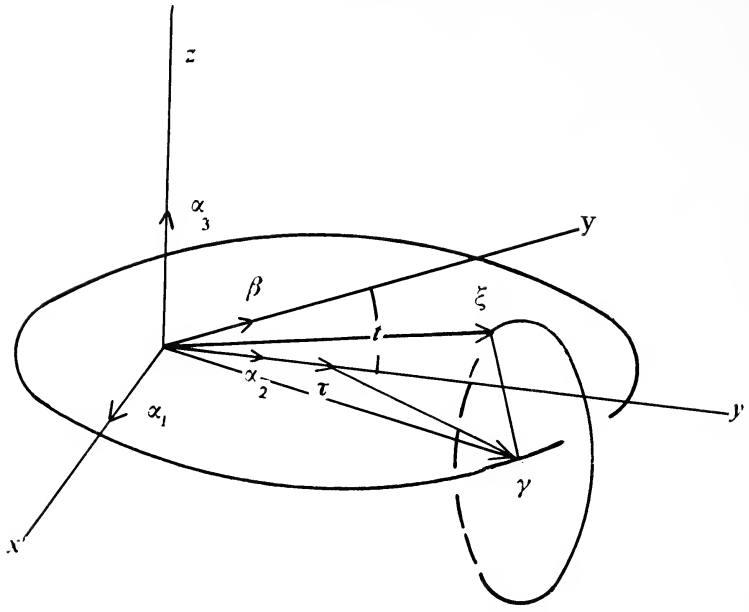

FIGURE 1. Leading and generating circles of the torus.

where b is the radius of the generating circle of T. One can write (1) as

$$\begin{cases} \xi = mh\alpha_1 + [mk + (1 - m)p]\,\alpha_2 + s\alpha_3 \\ h^2 + (k - p)^2 = a^2 \\ (m - 1)^2\, a^2 + s^2 = b^2. \end{cases} \tag{2}$$

Note that p,a and b are fixed, while m,s,h and k are parameters.

It suffices to consider the intersection of T with planes of the form $[\alpha_1,\beta]$, where $\beta\epsilon[\alpha_2,\alpha_3]$ and $\| \beta \| = 1$. Let t denote the angle between β and α_2. The intersection of the torus and such a plane is given by

$$\begin{cases} \xi = mh\alpha_1 + [mk + (1 - m)p]\,\alpha_2 + s\alpha_3 \\ \xi = x\alpha_1 + (y\ \cos t)\,\alpha_2 + (y \sin t)\,\alpha_3 \\ h^2 + (k - p)^2 = a^2,\ a^2(m - 1)^2 + s^2 = b^2, \end{cases} \tag{3}$$

where (x,y) is the set of components of ξ with respect to the orthonormal set $\{\alpha_1,\beta\}$. Eliminating the parameters, we obtain

$$\begin{aligned} &(x^2 + y^2)^2 + 2[p^2 - (a^2 + b^2)\text{-}2\ (p \cos t)y]\,(x^2 + y^2) \\ &+ (p^2 - a^2 - b^2)^2 - 4\,(p^2 - a^2 - b^2)\,(p \cos t)y \\ &\qquad + 4\,p^2(\cos^2 t)\,y^2 = 4a^2(b^2 - y^2 \sin^2 t). \end{aligned} \tag{4}$$

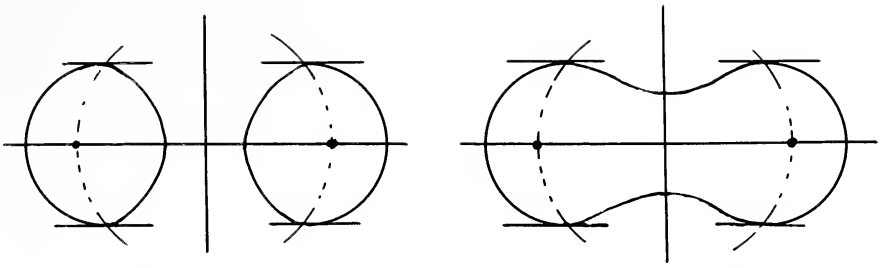

FIGURE 2. Cassini ovals in the cases $a > 2b$ (left) and $a < 2b$ (right).

Thus, toric sections in R_3 are curves which satisfy equations of the form (4). We will discuss only some simple cases.

When $t = \pi/2$ and $p = b$ we obtain the equation

$$(x^2 + y^2)^2 = 2a^2(x^2 - y^2) + 4a^2b^2 - a^4, \tag{5}$$

which is a Cassini oval (Fig. 2). When the shape of the torus changes, the shape of the Cassini oval given by (5) also changes. For example, when $a = 2b$ the Cassini oval is a Bernoulli lemniscate (Fig. 3). For those interested in convexity, we remark that it can be shown by elementary techniques that the Cassini oval (5) is the boundary of a convex set when $b \geq a$.

HYPERTORIC SECTIONS

We now generalize the study of the previous section to R_n. Let T be a torus in R_n, i.e., T is as in the previous section except that the "leading circle" of T is a sphere of dimension n-2. Then there exists an orthonormal basis $\{\alpha_1, \ldots, \alpha_n\}$ of R_n for which the leading sphere S of T has center at $\tau \in [\alpha_2]$ and is given by

$$S = \{\gamma \in R_n \mid \gamma \in [\alpha_1, \ldots, \alpha_{n-1}] \text{ and } \|\gamma - \tau\| = a > 0\}.$$

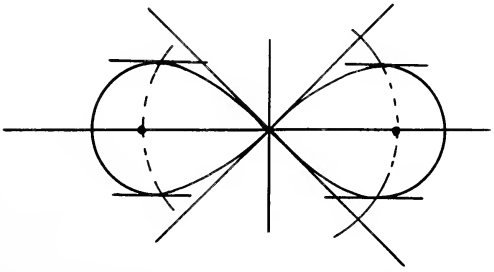

FIGURE 3. Lemniscate of Bernoulli.

The torus T is given by

$$T = \{\xi \epsilon R_n | \xi \epsilon \tau + [\gamma - \tau, \alpha_n],$$
$$\|\xi - \gamma\| = b > 0 \text{ for some } \gamma \epsilon S\}.$$

Let $\tau = p\alpha_2$ for a fixed $p \epsilon R$ and let

$$\xi = m(\gamma - \tau) + s\alpha_n + \tau \epsilon T$$

for some $\gamma \epsilon S$ and $m, s \epsilon R$. Since

$$\xi - \gamma = (m - 1)(\gamma - \tau) + s\alpha_n$$

we see that

$$b^2 = \|\xi - \gamma\|^2 = (m - 1)^2 \|\gamma - \tau\|^2 + s^2 = (m - 1)^2 a^2 + s^2,$$

and hence

$$ma = a \pm \sqrt{b^2 - s^2}. \tag{6}$$

Since $\xi - \tau = m(\gamma - \tau) + s\alpha_n$, we see that

$$\|\xi - \tau\|^2 = m^2 \|\gamma - \tau\|^2 + s^2 = m^2 a^2 + s^2.$$

Moreover, since $\tau = p\alpha_2$, we see that

$$\|\xi - \tau\|^2 = \|\xi\|^2 - 2p(\xi, \alpha_2) + p^2$$

and hence have

$$\|\xi\|^2 - 2p(\xi, \alpha_2) + p^2 = m^2 a^2 + s^2. \tag{7}$$

Substituting for ma in (7) from (6) and replacing s by (ξ, α_n) we obtain the vector equation of T

$$\|\xi\|^2 - 2p(\xi, \alpha_2) + p^2 - (a^2 + b^2)$$
$$= \pm 2a \sqrt{b^2 - (\xi, \alpha_n)^2}. \tag{8}$$

It suffices to consider intersections of T with planes which are hinged on α_1, i.e., planes $H = [\alpha_1, \beta_2, \ldots, \beta_k]$, where $\{\beta_2, \ldots, \beta_k\}$ is an orthonormal family in $[\alpha_2, \ldots, \alpha_n]$. If $\xi \epsilon H$, say

$$\xi = x_1\alpha_1 + \sum_{i=2}^{k} x_i\beta_i,$$

then

$$\xi = x_1\alpha_1 + \sum_{j=2}^{k}\sum_{i=2}^{k} x_i(\beta_i,\alpha_j)\alpha_j$$

and hence

$$(\xi,\alpha_j) = \sum_{i=2}^{k} x_i(\beta_i,\alpha_j) \text{ for } j = 2, \ldots, n. \tag{9}$$

If $\xi \in T \cap H$, we can substitute (9) into (8) and obtain the equation

$$\sum_{i=1}^{k} x_i^2 - 2p \sum_{i=2}^{k} (\beta_i,\alpha_2)x_i + (p^2 - a^2 - b^2)$$

$$= \pm 2a \sqrt{b^2 - [\sum_{i=2}^{k} (\beta_i,\alpha_n)x_i]^2}. \tag{10}$$

Thus toric sections obtained by intersecting a torus in R_n with a k-dimensional plane satisfy an equation of the form (10).

We now discuss some interesting cases. For example, if $\beta_i = \alpha_{i+1}$ for $i = 2, \ldots, k$, one obtains

$$\sum_{i=1}^{k} x_i^2 + (p^2 - a^2 - b^2) = 0 \text{ if } k < n - 1$$

and

$$\sum_{i=1}^{k} x_i^2 + (p^2 - a^2 - b^2)$$

$$= \pm 2a \sqrt{b^2 - x_k^2} \text{ if } k = n - 1. \tag{11}$$

Thus we obtain spheres for this choice of $\beta_2, \ldots, \beta_k$ if $k < n - 1$. Note, however, that a choice of $\beta_i = \alpha_{i+n-k}$ for $i = 2, \ldots, k$ gives equations of the form (11) for any k.

As in the case $n = 3$, we set $p = b$ in (11) and get the equation

$$[\sum_{i=1}^{k} x_i^2]^2 = 2a^2(x_1^2 + \ . \ . \ . \ + x_{k-1}^2 - x_k^2) + 4a^2b^2 - a^4. \qquad (12)$$

Note that the intersection of (12) with each plane $[\alpha_i,\alpha_k]$ for $i = 1, \ . \ . \ . \ ,k-1$ is a Cassini oval and hence (12) is a surface of revolution generated by a Cassini oval. In the case $a = 2b$ we obtain a surface of revolution generated by a Bernoulli lemniscate. Finally, note that a toric section of the form (12) is the boundary of a convex set if $b \geq a$.

LITERATURE CITED

Yates, R.C. 1947. A handbook on curves and their properties. J. W. Edwards, Ann Arbor, MI. (Republished by National Council of Teachers of Mathematics, Washington, DC, 1952.)

USE OF FISSIOGENIC STABLE RUTHENIUM VERSUS XENON ISOTOPES IN THE DETERMINATION OF INDUCED FISSION IN URANIUM ORES

by MOSES ATTREP, JR., *and* KUNG HSING-TUNG

Department of Chemistry
East Texas State University
Commerce, TX 75428

ABSTRACT

We compare the use of fissiogenic stable isotopes of the inert gas, xenon, to those of the transition metal, ruthenium, as an indication of the ratio of thermal-neutron-induced fission of ^{235}U to the spontaneous fission of ^{238}U. Xenon isotopes provided an internally consistent ratio from different sets of xenon isotopes that was not observed when different ruthenium isotope pairs were used. The range of the ratios deduced from the xenon isotopes was from aproximately 0 (no induced fission) to a value of 0.47 (about 45% induced fission); values derived from ruthenium isotopes ranged from negative values to 0.93. Other, graphic analyses also indicated that xenon isotopes probably provide a more accurate picture of the nuclear geo-fission history of the ores.

INTRODUCTION

Uranium ores are unique in geological deposits: they represent chemical-physical phenomena as well as nuclear events in nature. Uranium-238, the most abundant isotope of uranium, undergoes both α decay and spontaneous fission, with half-lives of 4.5×10^9 years and 1.0×10^{16} years, respectively. The result is a complex, natural uranium-decay series produced by α and β emissions, and a wide variety of nuclides produced from the fission process. The other, less abundant isotope of uranium,^{235}U, also decays by α emission. Another nuclear phenomenon is observed under certain conditions, namely neutron capture by ^{235}U, leading to fission. The cross-section for capture of thermalized neutrons is large, leading to a fission rate in many instances as great as that of spontaneous fission of ^{238}U. The fission yield curves for the spontaneous fission of ^{238}U and neutron induced fission of ^{235}U are both primarily asymmetric. The fission yield curves are not superimposable because of differences in the yields of the fission products.

Although neutron-induced fission is of great importance, we consider the origin of the neutrons causing that fission to be equally important. Alteration of uranium assemblies by certain elements causes changes in the amount of neutron-induced fission of ^{235}U: (α,n)

reaction on low Z elements increases the neutron flux and hence the amount of neutron-induced fission of ^{235}U (Attrep and Sherwood 1972; Attrep et al. 1979; Raut and Attrep 1975; Attrep et al. 1981). The inverse effect operates when neutron absorbing elements are added, in which case the neutron-induced fission component is eliminated, leaving only spontaneous fission of ^{238}U (Attrep et al. 1981).

The Oklo phenomenon marks the only known occurrence of a uranium deposit having functioned successfully as a self-sustaining reactor (Baudin et al. 1972). Obviously, in this case, the amount of induced fission must have exceeded the amount of spontaneous fission. Patterns of isotopic fission products identified in the deposit confirm reaction status. For the reactor to have operated it would have had certain physical and nuclear requirements—sufficient moderator (probably water), enriched fuel, a mechanism to remove the heat generated, and a suitable chemical composition. This combination existed some 1.2 billion years ago.

One must consider the possibility both of uranium assemblies with no induced fission and others which could have undergone reactor status as in the case of the Oklo mine. We focus on cases in which induced fission rate is of the same order as the spontaneous fission rate of ^{238}U. For these, 0.42 fissions per minute per gram of uranium occur.

To elucidate these conditions, we have taken a two-fold approach. The first is to simulate uranium assemblies in the laboratory, controlling the chemical-physical parameters. These experiments have led to the conclusion that elements such as lithium, boron, beryllium, and carbon can undergo (α,n) reactions, leading to increased neutron-induced fission of ^{235}U. Conversely, the introduction of samarium, a neutron absorber, reduced the total neutron flux by reduction of neutrons from (α,n) reactions and neutrons from neutron-induced fission of ^{235}U. The other line of investigation centers around the use of stable isotopes of fissiogenically produced elements. Earlier we showed that xenon extracted from uranium minerals and analyzed mass spectrometrically provides the basis for the development of a model that could be used to measure the amount of induced fission in the system (Attrep et al. 1977).

Maeck et al. (1978 a,b) used stable fissiogenic ruthenium isotopes as a means of dating uranium ores and of determining if a uranium deposit had undergone nuclear reactor status. The ruthenium analysis has been described by Delmore (1980). Mass spectrometry of ruthenium is difficult, requiring extreme caution during the separation procedure; otherwise interferences result from other elements.

Here we compare xenon isotopes to ruthenium isotopes as indicators of neutron-induced fission of ^{235}U. Fissiogenic products accumulated

and analysis of these provide an understanding of the nuclear dynamics of the uranium ores.

METHODS AND EQUATIONS

To calculate the ratio of thermal-neutron-induced fission of ^{235}U to the spontaneous fission of ^{238}U, we assume only these two fission sources. Tasa and Attrep (1974) indicated that fast-neutron fission of ^{238}U existed at ~6% when conditions were adjusted to a large fast-neutron flux.

Attrep et al. (1977) derived equations which related the experimentally observed ratios of fissiogenic nuclides, fission yields, both spontaneous and thermal-neutron induced, and R, the ratio of induced to spontaneous fission. Here we give only the equations essential to understanding the relationships between these factors.

The total number of fission-produced atoms in the geological sample, N_t, is a sum of those atoms coming from the spontaneous fission process, N_s, and those coming from the thermal-neutron-induced process, N_i; hence, $N_t = N_s + N_i$. The overall ratio (R), the thermal-neutron-induced fission of ^{235}U to the spontaneous fission of ^{238}U in the ore, is expressed in terms of the accumulated atoms from one process divided by the atoms accumulated from the other process. Specifically, the ratio for two fissiogenic isotopes of a given element are conveniently expressed as

$$\frac{N'_t}{N''_t} = \frac{(Y'_s + RY'_i)}{(Y''_s + RY''_i)}$$

where N'_t is the number of atoms determined experimentally in the uranium sample for one fissiogenic isotope; N''_t is that observed for another fissiogenic isotope; Y'_s and Y'_i, and Y''_s and Y''_i are the spontaneous fission yield and induced fission yield for the two respective fissiogenic isotopes.

This equation will be used to indicate the sensitivity of the method of ruthenium isotopes to measure R. Fissiogenic ruthenium isotopes used in this study are mass 99, 101, 102, and 104. The fission yields for these are given in Table 1 as reported by Maeck et al. (1978a).

RESULTS AND DISCUSSION

Of the six possible ratios of ruthenium isotopes, the three which indicated the most significant change in the isotopic ratio over the R values from 0 to 1.0 are 101/99, 102/99, and 104/99 (Fig. 1). Consequently, these three sets of values are the best indicators of R.

TABLE 1. Percent fission yields of stable ruthenium isotopes from spontaneous fission of ^{238}U and from thermal-neutron-induced fission of ^{235}U. (Reported in Maeck et al. 1978a.)

Ruthenium Mass Number	^{238}U Spontaneous Fission Yield (Percent)	^{235}U Neutron Induced Fission (Percent)
99	6.0	6.10
101	7.25	5.08
102	8.01	4.23
104	4.21	1.83

The slopes for ruthenium 104/102, 104/101 and 102/101 are nearly zero; thus, these are poor indicators of induced fission. We chose 101/99, 102/99, and 104/99 for determining values of R.

A small variation in R is reflected much more significantly in the xenon isotopes where a change from 0 to 0.1 gives rise to a change of N′/N″ ratio from 12 to 7 for the 134/131 xenon isotope pair (Attrep et al. 1977). A comparable R value change in ruthenium 102/99, the most promising of the ruthenium isotopes, produces a change of only 1.34 to 1.28. The xenon system changes ~42% compared to 4.5% for the ruthenium system. Clearly, the xenon system is more sensitive and therefore more valuable for detecting variations in the values of R.

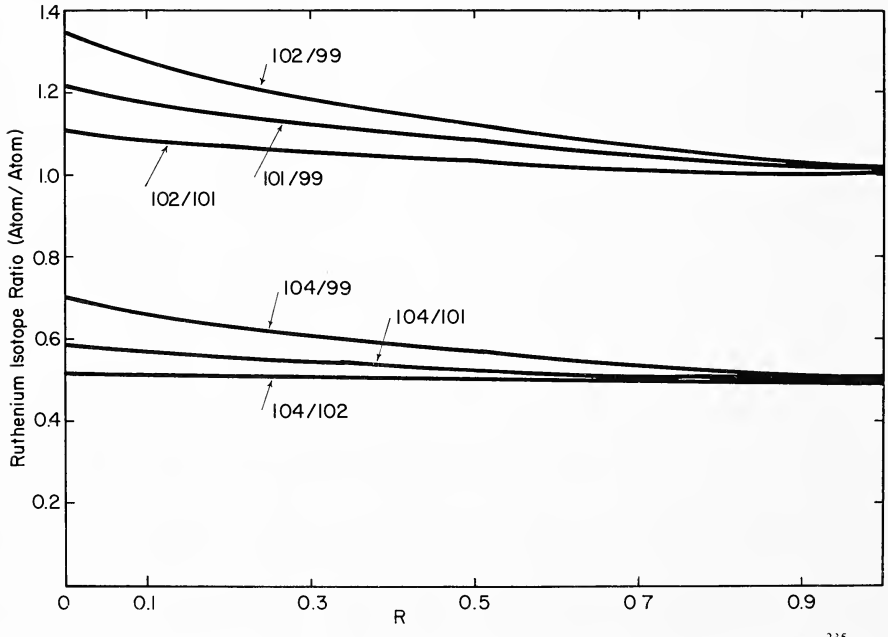

FIGURE 1. Ruthenium isotope ratios as functions of the ratio of induced fission of ^{235}U to spontaneous fission of ^{238}U (R).

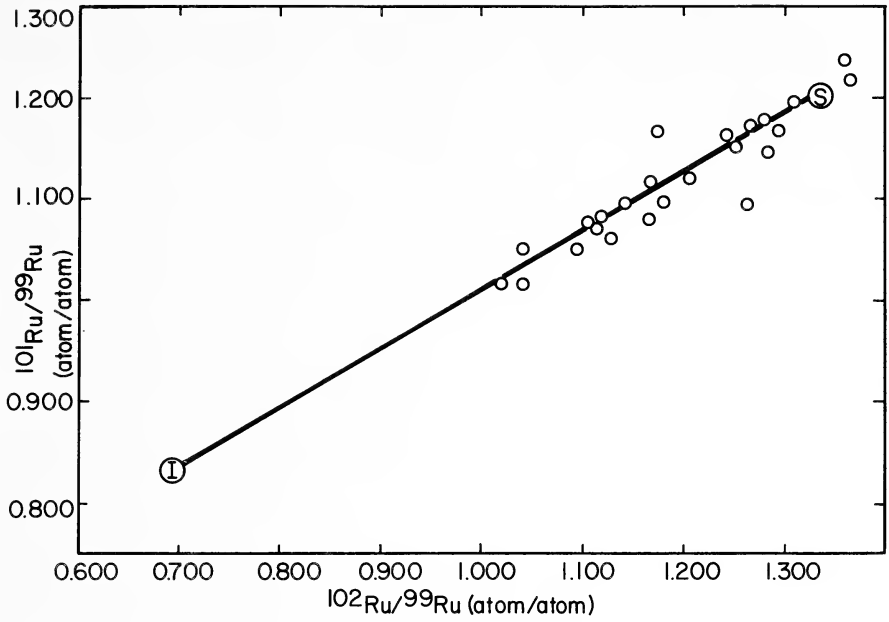

FIGURE 2. $^{101}Ru/^{99}Ru$ versus $^{102}Ru/^{99}Ru$ plot for uranium ores.

Points on the graphs of the plots $^{101}Ru/^{99}Ru$ versus $^{102}Ru/^{99}Ru$, $^{102}Ru/^{99}Ru$ versus $^{104}Ru/^{99}Ru$, and $^{102}Ru/^{101}Ru$ versus $^{104}Ru/^{101}Ru$ (Fig. 2, 3, 4, respectively) generally lie between the induced-fission point (marked by I) and the spontaneous fission point (marked by S). Scatter of the points on these graphs arises from the reported values of abundances of the ruthenium isotopes.

A similar plot of $^{134}Xe/^{131}Xe$ versus $^{136}Xe/^{131}Xe$ yields a well-defined spontaneous fission system; however, the $^{134}Xe/^{132}Xe$ versus $^{136}Xe/^{132}Xe$ plot exhibits as much scatter as those of the ruthenium plots (Attrep et al. 1977). The trends in Figures 2, 3, and 4 indicate that accumulated fissiogenic ruthenium isotopes in the uranium ores originate primarily from spontaneous fission of ^{238}U and thermal-neutron-induced fission of ^{235}U.

Table 2 shows calculated values of R for the three selected ruthenium pairs. The samples used were those analyzed by Maeck et al. (1978a). Listed below each pair are the calculated R values using the fission yields in Table 2. The average of the three sets of data is given in the last column.

The R values vary considerably when calculated from the ruthenium 101/99 ratio, 102/99 ratio, or the 104/99 ratio. Use of the ruthenium isotopes is apparently not accurate enough. In contrast, the xenon system provides R values that varied insignificantly.

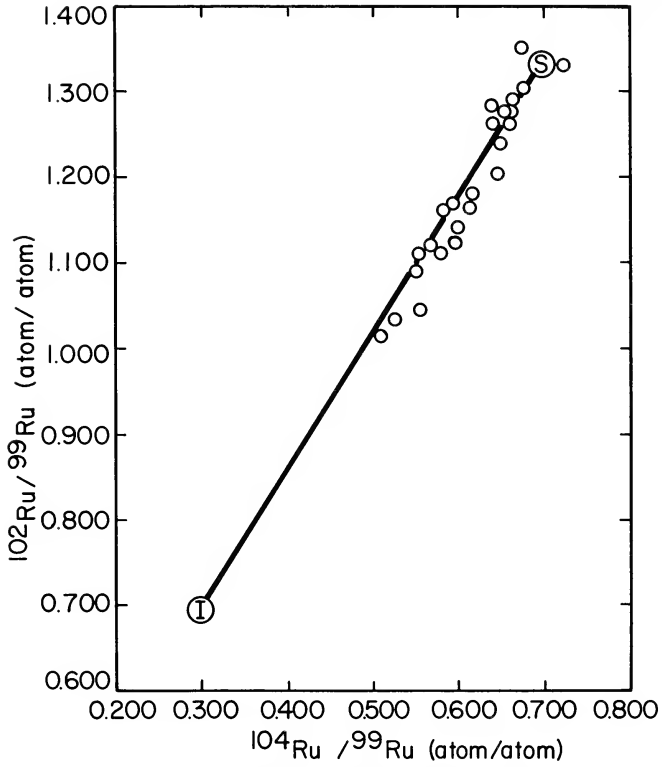

FIGURE 3. $^{102}Ru/^{99}Ru$ versus $^{104}Ru/^{99}Ru$ plot for uranium ores.

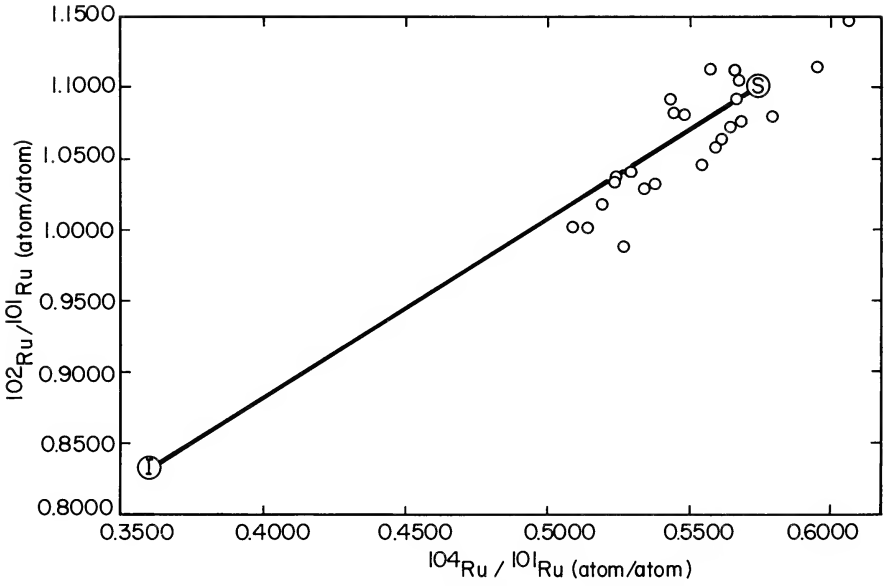

FIGURE 4. $^{102}Ru/^{101}Ru$ versus $^{104}Ru/^{101}Ru$ plot for uranium ores.

TABLE 2. Derived values for the ratio of thermal-neutron-induced fission of ^{235}U to the spontaneous fission of ^{238}U in uranium samples. (Ru isotopic data reported in Maeck et al. 1978b.)

Sample		R from Ruthenium Isotope Ratio 101/99	102/99	104/99	Average ± s.d.
Wilberforce, Ont.*		−0.03	−0.04	−0.06	−0.04 ± 0.02
Rio Grande do Norte, Brazil*		0.03	0.04	0.06	0.05 ± 0.02
Shinkolbwe, Zaire		0.32	0.24	0.16	0.27 ± 0.08
Kasolo, Zaire		0.41	0.31	0.26	0.33 ± 0.08
Gordonia, SWA		0.12	0.34	0.34	0.26 ± 0.13
NT, Australia	a	0.31	0.36	0.37	0.35 ± 0.03
	b	0.70	0.84	0.57	0.70 ± 0.13
Jabiluka, Australia	a	0.56	0.53	0.52	0.54 ± 0.02
	b	1.01	0.95	0.83	0.93 ± 0.09
	c	1.03	0.87	0.76	0.89 ± 0.14
Nabarlek, Australia		0.51	0.36	0.28	0.38 ± 0.12
Wilberforce, Ont.		−0.07	−0.03	−0.08	−0.01 ± 0.08
Fay Mine, Sask.		0.70	0.61	0.59	0.63 ± 0.06
Cluff Lake, Sask.	a	0.61	0.48	0.36	0.48 ± 0.13
	b	0.44	0.43	0.31	0.39 ± 0.07
Rabbit Lake, Sask.	a	0.19	0.09	0.15	0.14 ± 0.05
	b	0.49	0.51	0.44	0.48 ± 0.04
	c	0.53	0.54	0.44	0.51 ± 0.06
	d	0.13	0.17	0.14	0.15 ± 0.02
	e	0.16	0.08	0.17	0.14 ± 0.05
	f	0.43	0.13	0.10	0.21 ± 0.18
Port Radium, NWT	a	0.12	0.07	0.11	0.10 ± 0.02
	b	0.09	0.10	0.17	0.12 ± 0.05
	c	0.10	0.12	0.18	0.13 ± 0.04

*Reference Samples indicated by Maeck et al. 1978a.

Use of ruthenium isotopes yielded negative values of R in samples 1 and 12, which is physically unrealistic. By definition these samples are near zero since sample 1 was used to define the spontaneous-fission yield. The negative values reflect error associated with values used in the equation, the fission yields assigned to the spontaneous fission process, or the ratio of ruthenium isotopes.

Jabiluka, Australia, samples b and c show unusually high values—0.93 and 0.89, respectively. These are the highest values yet observed for the ratio of neutron-induced fission of ^{235}U to the spontaneous fission of ^{238}U, except for the Oklo samples which had experienced self-sustaining nuclear reactor status ($R>>1$). Because slight variations in the ruthenium yield can cause large variations in R, these high values may simply represent error.

For non-Oklo samples, xenon isotopes yielded R values from ~0 to 0.47. This is significantly different from that of the ruthenium isotopes (~0 to 0.93). Because so few R values are available from other methods,

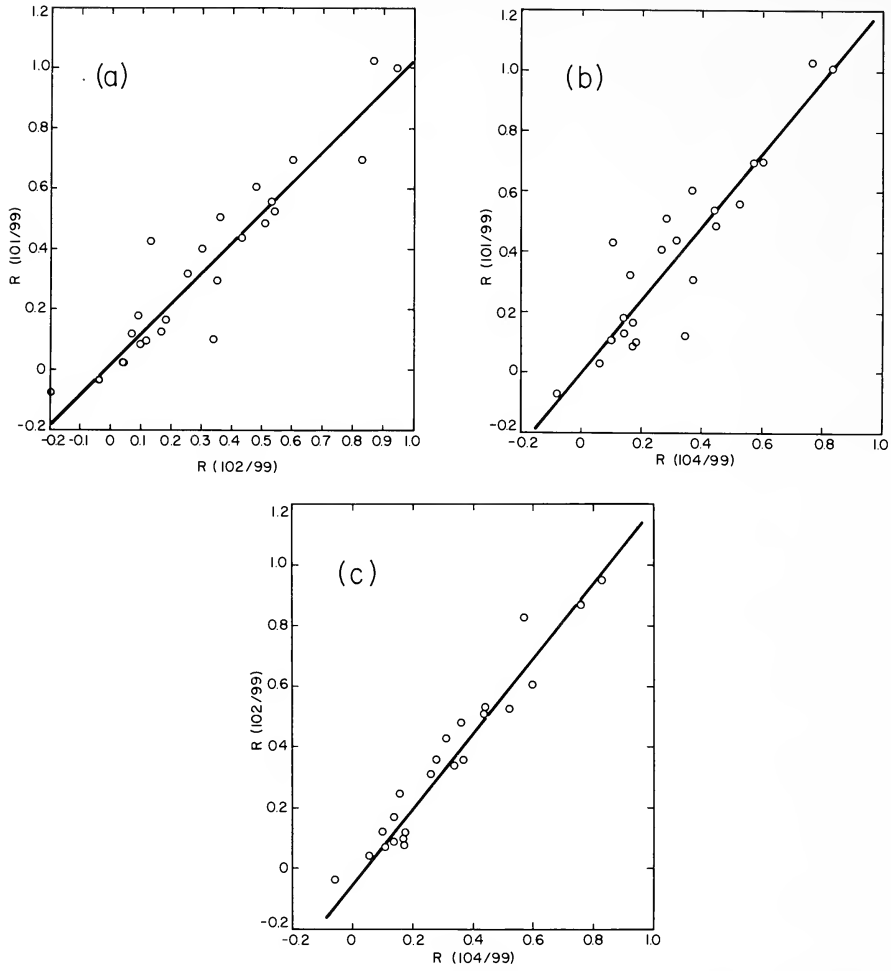

FIGURE 5. (a) R(101/99) versus R(102/99), (b) R(101/99) versus R(104/99), and (c) R(101/99) versus R(104/99) for uranium samples.

it is extremely difficult to compare one method with another. There is only one case in which two separate methods were used to determine R for a single sample. For the African pitchblende sample, R was reported from radio-chemical data using ^{99}Tc and ^{36}Cl (Kenna and Attrep 1966) and the xenon method by Attrep et al. (1977) with R = 0.33 and R~ 0.45, respectively. Different samples were analyzed which may account for the discrepancy. A xenon analysis of the identical African pitchblende, where R was determined to be 0.33 radio-chemically, yielded R of 0.38 (Sumerlin and Kuroda 1978). Although a single agreement does not provide conclusive evidence as to the validity of the xenon approach, it gives credence to the method.

To check the validity of the two-fission system for ruthenium isotopes, R values were plotted for different sets of ruthenium isotopes versus the R values from other sets. These are shown in Figure 5 for the R values originating from the following ruthenium isotope pairs: (a) R(102/99) versus R(101/99), (b) R(101/99) versus R(104/99), and (c) R(102/99) versus R(104/99). Least-squares analysis was used to find the line best fitting each set of data. If the scatter were due to random error a straight line, slope = 1, would be expected. The plot of R(101/99) versus R(102/99) had a slope of 1.04, which supports our original assumption of a simple two-component system of spontaneous fission of ^{238}U and thermal-neutron-induced fission of ^{235}U. The slopes of the lines in figures 5b and 5c are 1.56 and 1.59, respectively.

CONCLUSIONS

Although it is possible to measure neutron-induced fission in uranium ores by using ruthenium isotopes that are produced in the fission process, this method does not provide the precision observed when xenon isotopes are used. This does not, however, eliminate the usefulness of ruthenium isotopes as indicators of other nuclear geochemical events. As pointed out earlier, the age of the ore can be estimated using the fissiogenic ruthenium isotope abundance.

Ruthenium is attractive because it is a non-volatile metal as compared to xenon, a gas. However, the radio-precursor in the mass 99-chain, technetium-99, has been shown to be environmentally mobile (Ehrhardt and Attrep 1979). This fact, along with the observation that there are anomalous amounts of ^{99}Ru involving the migration of ^{99}Tc in the Oklo Mine samples (Gancarz et al. 1979), provides an additional uncertainty in using the ruthenium isotopes to calculate R. The fractional loss of isotopes of xenon cannot be measured easily. Funk et al. (1967) showed that xenon loss in an ore occurs almost equally among all the fissiogenic isotopes with no significant isotopic fractionation. Since ratios are being used in measures of this type, the absolute amounts are inconsequential.

In conclusion, the use of xenon isotopes to measure small amounts of thermal-neutron-induced fission is easier and more reliable than that of ruthenium isotopes. However, it is reassuring that the model first established for the xenon isotopes also holds, in principle, for the case of ruthenium isotopes.

ACKNOWLEDGEMENT

This research was supported by the Robert A. Welch Foundation, grant number T-291.

LITERATURE CITED

Attrep, M., Jr., C. A. Ao, A. I. Safa, and J. G. Griffin. 1981. Induced fission factors in natural uranium assemblies. J. Inorg. Nucl. Chem. 43:2623-2627.

Attrep, M., Jr., W. B. Ledbetter, and D. K. Riddle. 1979. The effects of boron and lithium on the ratio of induced to spontaneous fission in natural uranium. J. Inorg. Nucl. Chem. 41:1-3.

Attrep, M., and J. D. Sherwood. 1972. The effect of (α,n) reactions on the ratio of induced to spontaneous fission in natural uranium. J. Inorg. Nucl. Chem. 34:435-438.

Attrep, M., Jr., K. S. Tasa, and J. D. Sherwood. 1977. Estimations of the ratio of induced to spontaneous fission in uranium ores. Texas J. Sci. 29:109-120.

Baudin, C., C. Bain, R. Hagemann, M. Kremer, M. Lucas, L. Merlivat, R. Molina, C. Nief, F. Prost-Marcehal, F. Regnaud, and E. Roth. 1972. Quelques donnees nouvelles sur les reactions nucleaires en chain que se sont produites dan le gisement d'Oklo. C. R. Acad. Sci. Paris 275:2291-2297.

Delmore, J. E. 1980. The mass spectrometric analysis of nanogram levels of ruthenium. Proceedings of the Twenty-Third Conference on Analytical Chemistry in Energy Technology, Ann Arbor Science Publishers, Inc., Ann Arbor, MI. p. 51-356.

Ehrhardt, K. C., and M. Attrep, Jr. 1978. Technetium-99 in the atmosphere. Environ. Sci. Tech. 12:55-57.

Funk, H., F. Podosek, and M. W. Rowe. 1967. Fisssiogenic xenon in the Renazzo and Murray meteorites. Geochim. Cosmochim. Acta 31:1721-1732.

Gancarz, A. J., G. A. Cowan, D. B. Curtis, and W. J. Maeck. 1979. ^{99}Tc, Pb and Ru migration around the Oklo natural fission reactors. International Symposium on the Scientific Basis for Nuclear Waste Management, Boston, MA.

Kenna, B. T., and M. Attrep, Jr. 1966. The ratio of induced fission *vs.* spontaneous fission and the trace element analysis in pitchblende. J. Inorg. Nucl. Chem. 28:1491-1500.

Maeck, W. J., J. E. Delmore, R. L. Eggleston, and F. W. Spraktes. 1978a. The measurement of ruthenium in uranium ores and ^{238}U fission yields. Proceedings of a meeting of the Technical Committee on Natural Fission Reactors, International Atomic Energy Agency, Vienna, Austria. p. 521-533.

Maeck, W. J., K. E. Apt, and G. A. Cowan. 1978b. A possible uranium-ruthenium method for measurement of ore age. Proceedings of a meeting of the technical committee on natural fission reactors, International Atomic Energy Agency, Vienna, Austria. p. 535-541.

Raut, M. K., and M. Attrep, Jr. 1975. (α,n) Reactions in uranium solutions. J. Inorg. Nucl. Chem. 37:274-275.

Sumerlin, N. G., and P. K. Kuroda. 1978. Isotopic compositions of xenon and krypton in Belgian Congo pitchblende. Geochem. J. 12:279-285.

Tasa, K. S., and M. Attrep, Jr. 1974. Fast neutron studies in uranium. J. Inorg. Nucl. Chem. 36:1699-1703.

THE DEATH DIP AMONG ORDINARY FOLKS: A STUDY OF THE DIP/PEAK PHENOMENON FOR TEXANS DYING IN 1979

by ROLLO K. NEWSOM, ALVIN P. SHORT, LOUIS M. TANNER, *and* T. C. BORELLI

Department of Sociology and Anthropology
Southwest Texas State University
San Marcos, TX 78666

ABSTRACT

This paper explores the death dip/death peak phenomenon as it may have applied to ordinary persons dying in the State of Texas during 1979. Thirteen comparisons were made using conventional probability techniques. A death dip was not found for the overall group of Texans, but significant dips occurred for Black females and Spanish-surnamed males. In the case of Spanish-surnamed males, a death peak also was associated with the death dip. Speculations are made as to why the dip occurred in some subgroups but not in the total group. In addition, we consider the overall importance of this phenomenon to ordinary persons in view of our general findings.

INTRODUCTION

In 1973 a curious concept known as the death dip was introduced to sociologists (Phillips and Feldman 1973). With the usual obligatory accolades to E. Durkheim, it was argued that differing degrees of integration into one's group and society are accompanied by differing degrees of obligation to participate in the celebrations considered important by that society. Phillips and Feldman "extended" Durkheim's argument to suggest that more integrated persons *may* be able to postpone their deaths in order to experience significant social events. Birthdays, presidential elections and the Jewish Day of Atonement were examined for association with a death dip among various populations. In particular, Phillips and Feldman examined deaths of the famous to see if fewer than the expected number of these people have died immediately before some significant social event.

Using birth and death dates of several groups of "famous persons" in the United States and Europe, Phillips and Feldman (1973) found not only a death dip before the month of birth, but also a rise in the number of deaths in the month of birth and the three following months. The researchers used only "famous persons" because their birth and death dates were readily available in various biographical sources and because, as they stated, "The famous may be more likely

The Texas Journal of Science, Vol. XXXV, No. 4, January 1984

than the non-famous to produce a death dip." (Phillips and Feldman 1973; see also Phillips 1970:7).

Here we report our efforts to determine whether the death dip-peak phenomenon may occur among "ordinary" people.

THE DATA

Recent developments in the application of computer technology at the Texas Department of Health[1] have made data traditionally recorded only on death certificates available on tape for any given year since 1979. These data include the dates of birth and death for all 101,196 resident deaths in Texas during the year 1979. In addition, the tapes are coded for the sex, race, and ethnicity of the individual decedent. These data permit one to address the question as to whether or not the death dip occurs in ordinary people.

Before beginning analysis, individual cases involving death before the twenty-fifth birthday were eliminated in order to better replicate the Phillips and Feldman (1973) analysis. Phillips (1970) was unable to find the death dip for infants and children even in samples where the dip was present for adults. A preliminary analysis of the Texas data (Tanner and Newsom 1981) had indicated that an extraordinary number of persons die during the month of actual birth. This was, of course, due to infant mortality. Further, as has been indicated by Short and Borelli (1981), the suggested sentiments that may influence somatic functions in adults have not likely had the chance to fully develop in the very young. Also, deaths from the chronic diseases amenable to somatic control account for only a small portion of deaths among young people and children. For the above reasons the authors decided to exclude from the analysis those persons who died prior to their twenty-fifth birthday. This resulted in a total sample of 96,093 Texans who were over twenty-five years of age when they died in 1979.

MEASURING THE DIP AND PEAK

The Dip

To identify a death dip before bithdays, it is necessary to know the number of deaths by the month of birth and by the month of death. Also, one must determine the number of deaths expected probabilistically if in fact there were really no association between the individual's month of birth and month of death. These expected deaths may be computed by use of contingency table techniques, or by a much

[1]The authors wish to thank the Texas Department of Health and Mr. W. D. Carroll, Chief of the Bureau of Vital Statistics, as well as others in the Department who assisted us in obtaining these data.

simpler and more straightforward procedure in which one simply makes the assumption that the probability of dying in any given month is roughly 0.0833, or 1 in 12. We found that results obtained from the simple 1/12 assumption and by the more involved contingency table technique were virtually indistinguishable as was the case in the study by Phillips and Feldman (1973) on the death patterns of notable people.

Using the assumption stated above, one would expect that 8,005 of the deaths in the total sample of 96,093 should have occurred in the month prior to the birth month.[2] Actually, the number of deaths in the month prior to birth was 8,019 (Table 1). This is almost identical to what one would expect (z test, $P = 0.44$). There clearly is no death dip indicated for the total group of Texans dying in 1979.

The Peak

Phillips and Feldman (1973) also found that the existence of a death dip may lead to another phenomena known as the "death peak." That is, if people were to "hang on" long enough to experience a significant social event like the birthday, then we might expect them to die shortly after the event. Since there was no death dip in our Texas population, we would not expect a death peak. The test for a death peak was made using the same types of probability assumptions as for the death dip; however, in the case of the peak we assumed that any peak might occur in the month of birth and persist for three months thereafter. After eliminating the data from the month prior to birth (to minimize dependence of any peak on a preceding dip), we computed the probability of dying in an eleven-month year (dip month removed) as roughly 1 chance in 11 in any given month. The expected chances of dying in the birth month and the three following months was therefore simply 4/11. The expected frequency was then compared with that observed (Table 1) and a z score computed in the usual manner. There was no significant death peak ($P = 0.25$).

THE DIP AND PEAK BY SEX, RACE, AND ETHNICITY

Table 2 provides z scores for death dips and peaks associated with sex, race, and ethnicity. We divided the total number of Texans dying in 1979 into groups according to sex, race, and ethnicity to ascertain

[2]Different calendar months have different numbers of days and hence either more or fewer opportunities (days) on which one can die. We, therefore, computed "expected deaths" on a 1/13 assumption dividing the year into 13 twenty-eight day months. These adjustments made no difference in results; so, the data in this paper are reported by calendar month.

TABLE 1. Number of deaths by month of birth and month of death for all Texans dying in 1979, 25 years of age of older. Dip z = 0.16; P = 0.44. Peak z = 0.66; P = 0.25.

Month of Birth	Month of Death												
	Jan.	Feb.	Mar.	Apr.	May	June	July	Aug.	Sep.	Oct.	Nov.	Dec.	Row Total
Jan.	806	696	852	689	646	613	770	812	857	816	672	750*	8979
Feb.	670*	668	690	648	585	608	662	759	729	650	630	672	7971
Mar.	803	697*	776	631	645	646	641	797	708	776	661	684	8455
Apr.	680	664	659*	608	588	537	625	724	726	736	607	677	7831
May	646	658	735	589*	576	555	690	732	717	707	619	699	7923
June	665	655	607	572	552*	561	596	712	692	656	639	666	7573
July	670	637	695	589	582	600*	657	690	729	678	664	680	7871
Aug.	667	607	677	594	574	552	642*	733	730	652	597	624	7649
Sep.	662	581	658	541	541	546	620	652*	698	647	584	667	7397
Oct.	700	676	720	604	577	583	641	690	722*	690	647	644	7894
Nov.	685	661	714	620	577	571	656	720	733	766*	651	707	8061
Dec.	742	681	756	652	647	574	696	778	775	772	720*	696	8489
Total	8396	7881	8529	7337	7090	6946	7896	8799	8816	8546	7691	8166	96093

*Month prior to birth month

TABLE 2. Number of deaths and z scores for the death dip and death peak by sex, race and ethnicity.

Population	Number of Deaths	z Scores	
		Death Dip	Death Peak
Sex			
Male	52,946	.84	.57
Female	43,147	−.17	.88
Anglo[a]	73,711	1.57	.09
Male	40,069	1.58	−.48
Female	33,642	1.16	1.65*
Black	12,480	−.90	1.14
Male	7,029	1.21	1.33
Female	5,451	−2.63**	.93
Spanish-surnamed	9,753	−2.91**	1.12
Male	5,772	−3.19***	1.91*
Female	3,981	−.80	−.50
Other[b]	149	.77	1.29

* $P \leq 0.05$; ** $P \leq 0.01$; *** $P \leq 0.001$.

[a]The term Anglo is used in a general sense here and throughout the discussion to indicate those formally coded as white, non-Spanish-surnamed persons.

[b]The Texas Department of Health uses the term "other" with no explanation.

whether a death dip and/or a death peak was present for the individual group. As before, the z scores for real dips and peaks should be in the correct direction and of significant magnitude.[3] Five of the twenty-four comparisons reported in Table 2 were in the right direction and of sufficient magnitude to be declared statistically significant.

Comparison by Sex

Looking first at the male-female comparisons for the total population, it may be observed that the z score for males was in the wrong direction for a dip, and even though the score for females was in the correct direction, it was still far from being statistically significant. The scores for the peaks for both males and females were in the right direction, but neither score was high enough to have an associated level of probability less than 0.05.

It begins to become clear that we were unable to replicate Phillips and Feldman's (1973) findings in this much larger group.

[3]It is appropriate to make these comparisons since these variables are routine in specifying the operation of social relationships in almost all aspects of society. We are aware of the fact that computing enough scores for various sub-divisions of the population may yield some significant scores with little real meaning. We believe, however, that these are the minimal comparisons necessary to examine possible variations among important sub-groupings in the population.

Racial and Ethnic Comparisons

With reference to racial and ethnic comparisons, it can be seen that the death dip scores for Anglos were in the wrong direction. This reverse dip pattern was slightly more accentuated for the Anglo males. The small death-peak score for the Anglo male sub-sample was also in the wrong (negative) direction. Although the dip score for Anglo females was in the wrong direction, the peak score was in the correct direction and was significant. However, a peak alone is not indicative of a death dip. Apparently, there was no marked dip/peak phenomenon for the larger Anglo sub-sample of Texans dying in 1979.

Another interesting phenomena is found in the data concerning Black females. The Black females show a significant death dip, but there is no associated peak with the dip. Blacks overall, however, show insignificant relationships, or in the case of Black males, a relationship in the wrong direction. The one significant relationship for Blacks is the dip relationship for Black females.

More significant relationships appear for Spanish-surnamed persons than for any other group. Computations for Spanish-surnamed females do not show significant relationships and the peak computation for Spanish-surnamed females is in the wrong direction. A significant dip is observed for the entire Spanish-surnamed group, but the peak computation (even though in the right direction) is not significant. Overall, three of the computations for the Spanish-surnamed group are significant. It is the Spanish-surnamed males that show the dip.

There is only one set of computations in the entire table where one can observe both a significant dip and peak for the same group. Spanish-surnamed males, who in Texas would be primarily of Mexican and/or Mexican-American origin, do show the death dip/peak phenomenon at a level that is statistically impressive. Certainly, the findings shown in Table 2 are contrary to the idea that the death dip/peak phenomenon is associated only with notability. The birthday appears to be a more important event for Black women and Spanish-surnamed men, particularly for Spanish-surnamed men, since a significant death peak can also be demonstrated for this group.

Searching for a Pattern

Examination of the comparisons within the race/ethnicity categories reveals an interesting pattern. Two computations based on factors of race, sex, and ethnicity may really be considered significant statistically in terms of the death dip. In the order of magnitude of the relationships, male Spanish-surnamed persons show the greatest dip and Black females a slightly lower dip.

As Staples (1981:234) has indicated, "As a result of the declining fertility rate among Blacks, the elderly represent a larger proportion of the total Black population than in previous times." This population is also becoming more disproportionately female than is the case with Anglos. In spite of the observation that poverty falls disproportionately upon Blacks in general, the Black elderly have more often than the Anglo elderly described themselves as happy because of their role in the extended family and community (Staples 1981:235). For example, elderly women often take care of children who have no other place to go. The fact that these women are vitally enmeshed in the community rather than in isolated retirement or home settings may influence attitudes about age and the significance of certain social events. Perhaps feelings about birthdays are accentuated by the family and neighborhood position of the older Black woman. This in turn could be translated into the phenomenon that we are calling a death dip prior to the birthday month.

The data for the Spanish-surnamed population show both the dip and the peak. The partriarchy of the traditional Mexican-American family has been widely noted (Alvirez et al. 1981:274-277). And, as we have speculated for Black females, the status of the Mexican-American husband/father is such that some individuals may manage to "hang on" to receive birthday compliments "one more time."

CONCLUSIONS

There are two possible ways to conclude this report. The first is obvious: We could state that the death dip was not manifest for a sample composed of 96,093 Texans who died in 1979 after their twenty-fifth birthday. We could, of course, emphasize the presumptive death dip for Black females in the same year and one that was definitely present (at least statistically) for Spanish-surnamed males during 1979.

While the latter conclusion is important in terms of the implications for further inquiry into the effects of ethnicity on social and even biological behavior, the former conclusion has at least hidden implications for research endeavors in sociology, social demography, and death and dying research. Data like those in this report have been available in county courthouses across the United States for many years. Data collection would be tedious and time consuming, but certainly not impossible. Also, we suspect that other states have records of birth and death on tape and probably have had this information available for the past several years. Why then have we not seen more published on the applicability of the death dip/peak phenomenon to various populations? The phenomenon is often mentioned in the

literature on death and dying and is alluded to in other sociologically relevant literature. In short, the research is feasible and the topic is certainly relevant to sociologists. Why then has not more been written? We suspect that much more research has been done than meets the eye and that small papers such as our own works cited in the reference section have been presented and written as tentative reports; however, few if any of these works—aside from the original Phillips and Feldman (1973) investigation of notables—have apparently been published in widely read journals in the field. We suggest that the findings may not have been published because the findings were either consistently negative, or mixed and somewhat ambiguous as in the case of our own Texas data.

We have completed preliminary analysis for the death dip in association with specific causes of death and also using social events other than the birthday of the individual. We can merely state that the results of these analyses were consistently negative, and we suspect that may have been the result with other investigations. It seems that sociologists may be reluctant to submit important research that has a negative outcome and we, of course, cannot ascertain to what degree this feeling is shared totally or partially by editors and referees for various professional publications.

Let us now return to our first conclusion emphasizing the positive findings. Spanish-surnamed males in Texas who died in 1979 do show the death dip/peak phenomenon. Perhaps we need to further investigate how patterns of ethnicity and social class may influence dying behavior in general and the specific timing of death. Perhaps the death dip does not apply to the majority of urban Americans, in these modern times, but can be found among ordinary people in more traditional societies under certain circumstances. Until we have better death reporting in more traditional societies, and better socio-economic indicators for American mortality data, some important relationships may remain only tentatively explored.

LITERATURE CITED

Alvirez, D., F. D. Bean, and D. Williams. 1981. The Mexican-American family, p. 269-292. *In* C. H. Mindel and R. W. Habenstein (eds.), Ethnic families in America: Patterns and variations, 2nd edition. Elsenier, New York, NY.

Phillips, D. P. 1970. Dying as a form of social behavior. Ph.D. dissertation, University of Michigan, Ann Arbor, MI.

Phillips, D. P., and K. A. Feldman. 1973. A dip in death before ceremonial occasions: Some new relationships between social integration and mortality. American Sociological Review 38:678-696.

Short, A. P., and T. C. Borelli. 1981. The death dip in selected Texas counties. Unpublished paper presented at the Texas Academy of Science Meetings, Austin, TX.

Staples, R. 1981. The Black-American family, p. 217-244. *In* C. H. Mindel and R. W. Habenstein (eds.), Ethnic families in America: Patterns and variations, 2nd edition. Elsenier, New York, NY.

Tanner, L. M., and R. K. Newsom. 1981. Do Texans really die with their boots on? Unpublished paper presented at the Southwestern Sociological Association Meetings, Dallas, TX.

CATTLE EGRETS (*ARDEOLA IBIS* = *BUBULCUS IBIS*) IN TEXAS

by RAYMOND C. TELFAIR II *and* LARRY E. MARCY

Department of Wildlife and Fisheries Sciences
Texas A&M University
College Station, TX 77843

ABSTRACT

African Cattle Egrets reached Texas by 1954, via South America and the southeastern U.S. By 1979, there were about 300,000 breeding pairs in Texas, mostly east of the Balcones Escarpment. These birds use heronries established by native egrets and herons, but there appears to be little competition between the newcomers and their relatives. Cattle Egrets arrive at the heronries later in the spring (mid-April) and are less selective of nest sites and materials than native ardeids. Furthermore, Cattle Egrets feed primarily on terrestrial organisms, particularly grasshoppers and crickets, and consume few fish and crayfish. Consistent with their food habits, Cattle Egrets are vulnerable to agricultural pesticides. Cattle Egrets benefit cattle, with which they often associate, by preying on competing herbivorous insects and on such biting pests as horseflies (but not ticks). Cattle Egrets seem to pose little threat as vectors of disease and, by eating tabanid flies, may even help to control bovine anaplasmosis. On balance, Cattle Egrets are beneficial birds, but their heronries can be a serious nuisance to nearby human communities.

INTRODUCTION

The phenomenal, almost worldwide range expansion of the Cattle Egret (*Ardeola ibis* = *Bubulcus ibis*) has been of interest to scientists and laymen alike. Cattle Egrets were first seen in Texas in 1954; today, their breeding population in the state is about 300,000 pairs. As this exotic bird has proliferated, so have questions about its orgin, rapid range expansion, population dynamics, food habits, competition with native herons and egrets, and economic importance. Our purpose here is to provide basic information about this unique bird, and to dispel some of the common misbeliefs concerning it—e.g., that the Cattle Egret consumes ticks, spreads livestock diseases, out-competes native herons and egrets, and feeds in pastures that are relatively free of pesticides. More complete treatment of these subjects is provided in Telfair (1979) and Telfair (1983).

DISTINGUISHING CHARACTERISTICS

The Cattle Egret is gregarious and usually associates with grazing cattle. Compared to similar-sized herons and egrets, it is short-legged and thick-necked, the throat appearing swollen. Adults are about 17

The Texas Journal of Science, Vol. XXXV, No. 4, January 1984

inches (43.2 cm) in length, have a wingspan of about 37 inches (94.0 cm) and weigh about 0.6 to 1.0 pounds (0.27-0.45 kg). At rest, whether standing or perched, the Cattle Egret has a "hunched" posture.

Plumage of the Cattle Egret is generally white; but, during the breeding season, orange-buff plumes appear on the breast, forehead, nape, and mantle. In non-breeding birds, the bill, lores, and irises are yellow, and the legs are very dark green, appearing black at a distance. In breeding birds, the legs become more yellow-green and the iris darker yellow; for a brief period during the peak of the breeding season, the bill, legs, and irises turn bright red, and the lores turn purple-pink.

GLOBAL RANGE EXPANSION

During the last 100 years, the Cattle Egret has spread from centers of distribution in Africa and southern Asia to many parts of the world, including places as remote as Australia (by 1948), Tierra del Fuego (by 1977), and Alaska (by 1981).

Although details of the Cattle Egret's expansion to the New World are not known, the African subspecies (*A. i. ibis*) apparently spread from the west coast of Africa across the Atlantic to coastal areas of northeastern South America. They were noted between 1877 and 1882 in Surinam (Dutch Guiana) and in 1911-1912 in British Guiana. Several were seen and collected in this region during 1937-1947; they were common in 1947 and 1948; and by 1950, were well established.

The first sight records of Cattle Egrets in North America were in Florida in 1941 or 1942, but proof via photographs was not established until 1952, and the first nest was not found until 1953. Cattle Egrets were well established in the United States by 1954, even before they were first reported from the West Indies. They may have flown to Florida directly from South America, rather than island-hopping through the Carribbean.

Band recovery data suggest that Texas originally received Cattle Egrets from the eastern Gulf Coast states, probably as a result of west-southwestward coastal wanderings and/or migrations, rather than via routes through Central America and Mexico. Cattle Egrets spread into Texas in 1954 (Fig. 1) and established breeding populations by 1959. Along the Texas coast, they increased from 10 pairs in 1959 to more than 20,000 pairs by 1965. The 1970 population in Texas was at least 35,500 pairs and by 1979 there were about 300,000 breeding pairs in the state.

Today, in North America, Cattle Egrets are found nesting in most eastern states, throughout the Gulf Coast states, along the west coast of California, and inland as far north as Saskatchewan. They now nest in

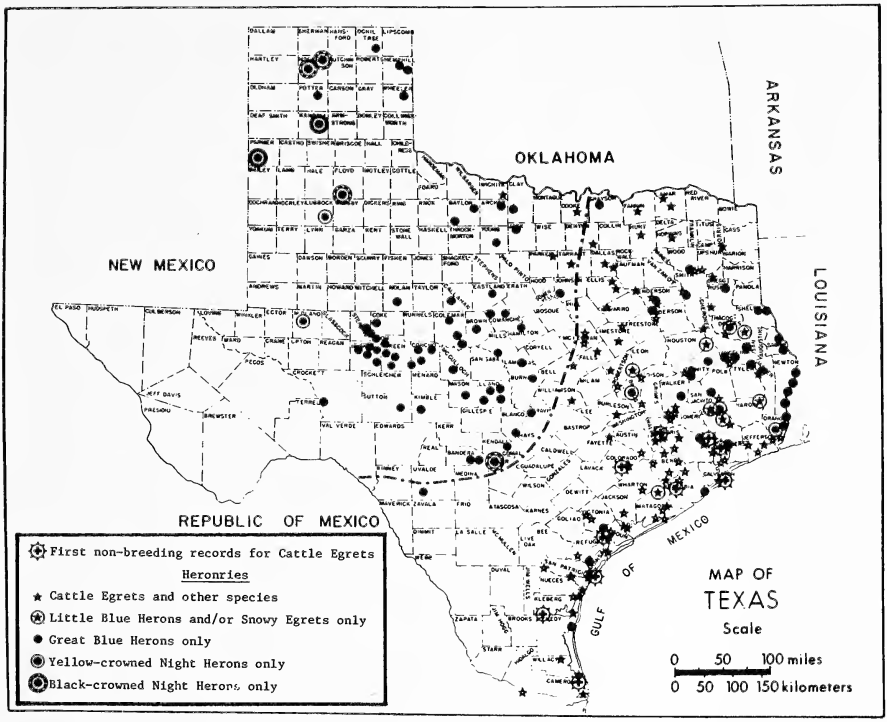

FIGURE 1. Locations of the first confirmed occurrences of Cattle Egrets in Texas and the subsequent breeding distribution of Cattle Egrets in relation to other ardeids. The dot-dash line marks location of the Balcones Escarpment. Only 208 of the 302 known heronries (68.9%) are represented because of the small scale of the map. Most of the omitted heronries are coastal, especially in bay systems. Data are from Mullins et al. (1982). Map updated from Telfair (1979).

all but 14 of the United States (Alaska, Arizona, Indiana, Iowa, Maine, Massachusetts, Michigan, Montana, Nebraska, New Hampshire, Oregon, Washington, West Virginia, and Wyoming).

DISTRIBUTION IN TEXAS

The current breeding range of Cattle Egrets in Texas is largely east of the Balcones Escarpment (Fig. 1). Breeding distribution and the western inland boundary of the breeding range correspond with those of Little Blue Herons (*Egretta caerules*) and Snowy Egrets (*E. thula*). In fact, Cattle Egrets are attracted to inland heronries already established by native species, primarily Little Blue Herons and Snowy Egrets; the latter species, in turn, are limited by the distribution and abundance of crayfish upon which they feed (Telfair 1981).

Data assembled by Mullins et al. (1982), and plotted in Figure 2, indicate that Texas Cattle Egrets nest mostly along the Gulf Coast and

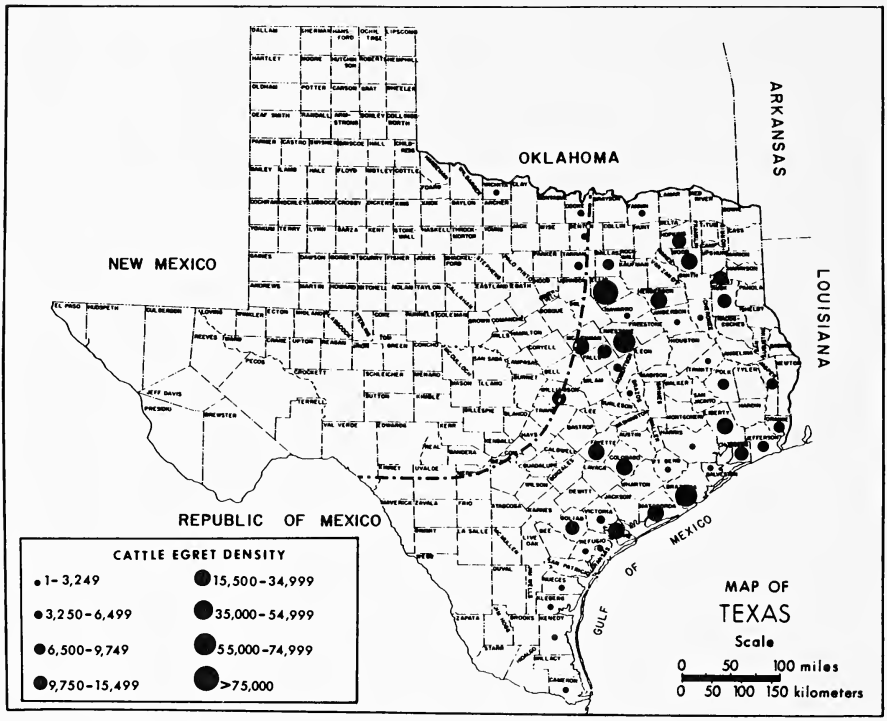

FIGURE 2. Distribution and density of Cattle Egrets per county in Texas (black dots). The dot-dash line marks location of the Balcones Escarpment. Data are from Mullins et al. (1982). Map copied from Telfair (1983).

coastal drainages (31.8% of the breeding population), and inland in the Trinity River system (40.5%). A smaller fraction of the population occupies heronries in the Sabine, Neches, Brazos, and Red River systems (27.8% combined).

FOOD HABITS

The diet of Cattle Egret chicks reflects that of adult birds. Telfair (1979) analyzed 500 undigested boluses regurgitated by chicks at 10 heronries to determine the diet during the nesting season. Analyses of prey items included occurrence (frequency), total numbers, average number per bolus, maximum number per bolus, total volume, and average volume per bolus.

Diet composition was as follows: by frequency of occurrence—93.6% invertebrates, 53.8% vertebrates; by total number of food items—94.9% invertebrates, 5.1% vertebrates; and by total volume—69.2% invertebrates, 30.0% vertebrates. Most prominent in the diet were grasshoppers and crickets (78.6% by number). With the exception of aquatic organisms (4.5% by number), almost all prey items are common

inhabitants of farm pastures and ranches (94.7% by number). Ticks, earthworms, crayfish, and fish were rare.

During the breeding season, aquatic habitats (often away from cattle) provide vertebrate food, especially frogs and toads. These items are important during the critical period of maximum growth and energy requirement of chicks. Cattle Egrets, especially during the fall, often feed away from cattle in cotton and grain fields and follow cutting machines and tractors plowing under harvested crops.

OCCURRENCE OF PESTICIDES IN EGGS AND TISSUES

Egg-shell thinning and toxicosis of breeding birds are important factors related to successful reproduction (Telfair 1979). In several heronries, I found thin-shelled eggs and breeding birds that exhibited symptoms of chlorinated hydrocarbon toxicosis. For analyses, 4 eggs were randomly selected from a sample of 185 eggs lost from nests during storms, and 12 adult birds were randomly selected from a sample of 59 birds exhibiting signs of pesticide toxicosis.

The most significant pesticide residues in eggs were DDE (0.20-12.45 ppm) and DDT (0.02-0.04 ppm). Lindane was found in all four eggs, but concentrations were small (0.006-0.02 ppm). Tissues from adult birds contained DDE in amounts varying from 0.01 to 297.32 ppm. Some brain tissue contained more DDE than did livers. Residues of PCB's (trace to 8.0 ppm) were found in only 2 birds. Trace amounts of 2, 4, 5-T occurred in livers.

Two apparently normal adults obtained in the field were almost devoid of pesticide residues; viz., DDE, dieldrin, and DDT occurred in amounts from trace to 0.01 ppm, and no other residues were found.

These observations suggest that some Cattle Egrets feed regularly in areas that have been treated with chlorinated-hydrocarbon pesticides. The presence of greater than trace amounts of DDT residues in brain and liver tissues of some adult birds and in eggs indicates intake of the pesticide was recent since it had not been metabolized into DDE or DDD. Presence of lindane in tissues and eggs suggests feeding by Cattle Egrets in cotton-producing areas.

NESTING AND REPRODUCTION

The following account relies mainly on observations of Telfair (1979, 1983), who studied the breeding biology of Texas Cattle Egrets from 1972 through 1982. Most field work was conducted during the breeding seasons of 1972-1975, from the arrival of birds at the heronries in late February and March to their departure in October and November. The study area encompassed most parts of Texas in which Cattle Egrets breed (Fig. 1). Data were taken from 29 heronries.

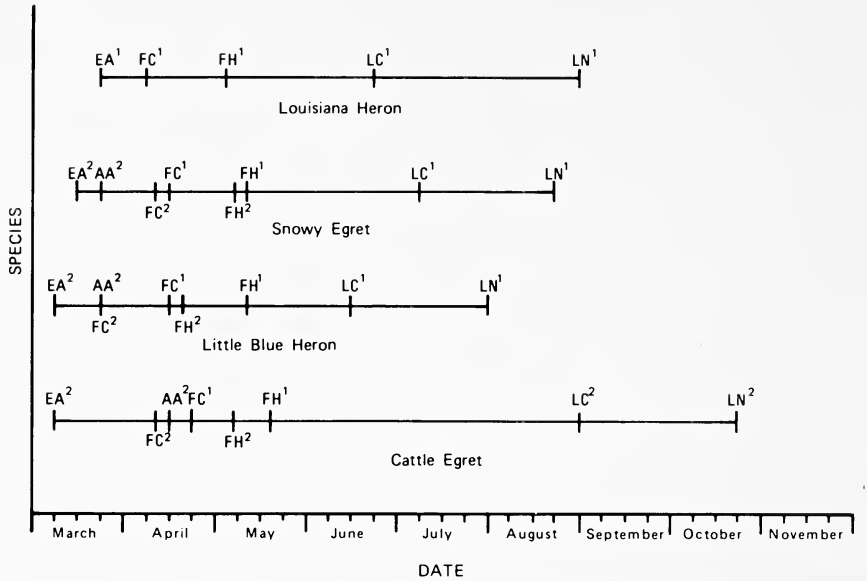

FIGURE 3. Average phenologies and sequences of major events during the breeding seasons of Cattle Egrets, Little Blue Herons, Snowy Egrets, and Louisiana Herons in Texas heronries. EA = early arrival, AA = average arrival, FC = first clutches, FH = first hatchlings, LC = last clutches, and LN = last nestlings. Data are from (1) Oberholser (1974) and from (2) this study. Figure from Telfair (1979).

Beginning at the time of nest construction, nests were marked individually. When feasible, the condition and contents of nests were recorded each day during egg laying and at the time of hatching, and on alternate days at other times. To facilitate study of stick-stealing activity, foundation and protruding sticks of occupied nests were spray-painted from beneath, and entire unoccupied nests were lightly sprayed with the same bright-orange paint.

Since 1963, over 18,000 Cattle Egret chicks have been banded or banded and color-marked in Texas. In May 1974, the Texas Parks and Wildlife Department initiated a large-scale banding and color-marking program to investigate movements and population dynamics of colonial water birds in 3 coastal and 3 inland regions of eastern Texas. Methods were described by Swepston et al. (1978). The Saflag leg tag used to color-mark birds was described by Frentress (1975). Of a total of 15,765 chicks banded and color-marked, 8,143 were Cattle Egrets. Since 1975, I have marked 9,976 additional Cattle Egrets, using a more durable tagging material, Herculite "80".

Cattle Egrets are usually the last species to arrive in Texas heronries, about 1 month after the mid- to late March return of native species (Fig. 3). By the time Cattle Egrets appear, most native species have already established nests and laid eggs. Early arrival and breeding of

native species in inland heronries appears to be synchronized with the average of maximum spring rains during May and the subsequent availability of aquatic prey. The later arrival and subsequent nesting of Cattle Egrets is apparently synchronized with the cumulative increase of pasture-dwelling insect populations, especially grasshoppers and crickets, during mid- to late summer.

Cattle Egrets use a wide variety of sites and substrates for nesting. Preferred nest sites are old platforms of nests from the previous year. In swamp heronries, nests often are built in basket-like growths of limbs of common buttonbush (*Cephalanthus occidentalis*), water elm (*Planera aquatica*), and swampprivet (*Forestiera acuminata*); the basketlike growths result from pruning of therminal shoots by nesting birds in previous years.

Cattle Egrets select unused nest sites or, in the case of late arrivals, nests vacated by native species. In coastal island heronries, Cattle Egrets prefer shrubs and tall herbaceous plants; whereas, native species generally nest lower, preferring sites in low herbs, in grasses, and on the ground.

Precariously sited nests are often destroyed in wind gusts of 25 to 60 mph (40.2-96.5 kph) that occur during spring-summer thunderstorms. Since most Cattle Egrets nest several weeks later than native herons and egrets, nests of the native species are more subject to storm destruction. However, both Cattle Egrets and native species usually renest and thus replace early nest losses.

Cattle Egrets usually build their nests in living vegetation about 1 m below the highest part of the nest-site plant, but they are less selective of nest sites than are native species. Consistent with the Cattle Egret's late arrival, many live twigs bearing leaves are often incorporated into their nests. Both Cattle Egrets and native species build nests resembling shallow saucers or bowls, but there is much variation. Cattle Egrets spend about 2 more days in nest construction than native species of similar size, and Cattle Egret nests are more complete when the first egg is laid. Thus, Cattle Egrets seldom lose their first egg through the nest floor.

The average clutch size of Cattle Egrets in heronries monitored by Telfair (1979) was 3.6; the average interval between laying of successive eggs was 2.0 days; and average incubation period was 24.0 days. The highest hatching success occurred on coastal islands (90.0%); in descending order, lesser success occurred on wooded inland islands (84.1%), in swamps (82.1%), and in woodlands (79.6%). Success for 26 heronries over a period of 5 breeding seasons (1970 through 1974) averaged 83.4%.

Fledging success for Texas Cattle Egrets (percentage of chicks fledged in relation to the number of eggs hatched) also was highest in

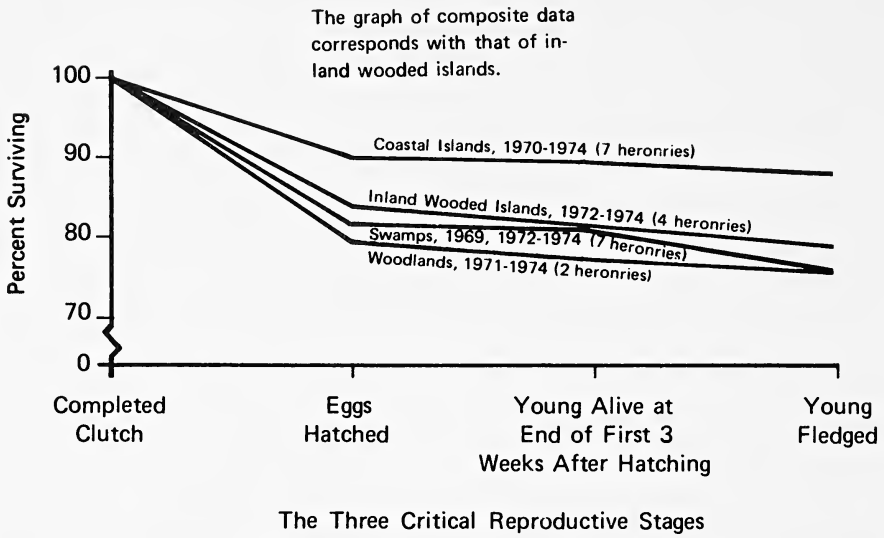

FIGURE 4. Comparison of the breeding success of Cattle Egrets in 4 types of heronries. The composite graph is the average of all data. Figure from Telfair (1979).

heronries on coastal islands (98.4%), and somewhat less in woodlands (94.7%), wooded islands (93.3%), and swamps (90.0%) (Fig. 4). Fledging success for 18 heronries over the period of 1970 through 1974 averaged 93.6%.

Differences in hatching and fledging success among the 4 types of heronries could be related to the type of nest-site vegetation and the differential effects of weather. In woodland heronries, strong winds accompanying spring thunderstorms can dislodge eggs and chicks from their nests and chicks from their perches; or, eggs and chicks can be dislodged by falling dead limbs. In swamps, eggs and chicks in low, shrubby vegetation may be lost during floods associated with spring-summer thunderstorms and prolonged rains.

Despite these weather-related losses, breeding success of Texas Cattle Egrets is high relative to that of native herons and egrets. In part, this is because Cattle Egrets are particularly attentive toward their young. Indeed, one parent is in constant attendance of the young during the first 2 or 3 weeks after hatching of the first chick.

The incidence of 24 mixed clutches (1.4% of a sample of 1,707 clutches) and the resultant 3 mixed broods (0.2%) observed by Telfair (1979) does not indicate that the presence of Cattle Egrets has or will result in increasing nesting competition via usurped nests of native species. Interbreeding between Cattle Egrets and native species has not been observed.

POPULATION DYNAMICS

Breeding and winter censuses of Texas Cattle Egrets reveal an exponential growth pattern expected of a species expanding into an essentially "unlimited" environment. However, the estimated finite rate of population increase for breeding Cattle Egrets in Texas decreased from 1.86/year during 1959-1972, to 1.20/year during 1972-1976. These data suggest that Cattle Egrets may be approaching the carrying capacity of suitable habitats in Texas.

Mortality among breeding adult Cattle Egrets in Texas heronries was about 1.1%. Causes of death were pesticides, avian pedators, and shooting. Based upon band recoveries, mortality among juvenile Cattle Egrets occurred mainly in late fall and winter. The percent recovery of banded birds is greatest among juveniles banded late in the breeding season (71.0%).

Most recoveries of juvenile Texas Cattle Egrets have come from 4 Mexican states—Sinaloa (25.6%), Michoacan (11.6%), Tamaulipas (10.5%), and Jalisco (7.0%). Compared to juveniles, few yearlings and adults banded in Texas as chicks have been recovered (61.7% versus 38.3%).

During the fall, flocks of Cattle Egrets migrate southward along barrier islands off the Texas coast. At this time, they are subject to predation by Arctic Peregrine Falcons (*Falco peregrinus tundrius*) also migrating southward along these islands.

INTERACTIONS WITH NATIVE HERONS AND EGRETS

Nest establishment by Cattle Egrets in Texas is mostly noncompetitive with native species, and interspecific aggression is relatively low for the following reasons: Cattle Egrets (1) arrive at the heronries later in the spring than native species; (2) are less selective of nest sites and utilize unoccupied sites; (3) make use of abundant materials to build nests in an orderly manner, thus causing little disturbance to established nesters; and (4) reuse abandoned nests or take them apart for materials for their own nests. The latter behavior is also common among native species.

There is some evidence that the white-plumaged juvenile Little Blue Herons may associate with Cattle Egrets and thereby learn to feed in a similar manner, in close association with grazing cattle. However, at the present time, there is no evidence that typical feeding behavior of Little Blue Herons has been modified by imitative-learning from Cattle Egrets.

ASSOCIATION WITH CATTLE

Cattle Egrets do not associate with all cattle within a herd, nor with all herds within a specific area even in the vicinity of a large heronry, nor do they feed within the total area of a specific pasture or range. Between 1968-1976, within 44 counties in which or adjoining which Cattle Egrets nested, the ratio of grazing cattle/egret varied widely (6:1 — 122:1) with an average of 37:1. In herds accompanied by egrets, the ratio of associated egrets/bovine usually varied from 1:1 to 5:1 with an average of 3:1.

There is in Texas, at the present time, no correlation between distribution and density of grazing cattle and the breeding range and density of Cattle Egrets or location of heronries (cf. Figs. 2 and 5). Within the Cattle Egret's breeding range, there are counties containing large numbers of grazing cattle, but with no heronries in the vicinity containing Cattle Egrets; conversly, there are many counties (especially in coastal and coastal-prairie areas) containing small numbers of grazing cattle, but with 1 to 5 heronries containing large numbers of Cattle Egrets.

ECONOMIC IMPORTANCE AND HEALTH ASPECTS

Because of their feeding habits, diet, and population size, Cattle Egrets are economically among the most beneficial animals to Texas cattlemen and farmers. Consumption of grasshoppers by Cattle Egrets may indirectly benefit cattle since these herbivorous insects may be the primary food competitors of cattle.

Cattle benefit directly from Cattle Egrets feeding on flies. In Texas, these egrets consume large numbers of livestock-associated flies (4.3% of prey items). Fly-eating by Cattle Egrets benefits cattle because these insects are not only disease carriers, but also annoy livestock by inflicting painful bites and cause considerable loss of blood, weight, and meat and milk production. Some larval flies can cause extensive, fatal wounds.

Experimental data are lacking, but there is consensus among some veterinarians and cattlemen that the fly-eating ability of Cattle Egrets reduces the number of tabanid flies in herds and, thereby, the incidence of bovine anaplasmosis. If Cattle Egrets, via their fly-eating activities among cattle herds, can help control or at least lessen the effects of this important, costly disease, they are indeed of positive benefit to the cattle industry. Unlike other methods of fly control, predation by Cattle Egrets is without cost and occurs many hours daily among some herds during the summer to fall season when vectors are most numerous.

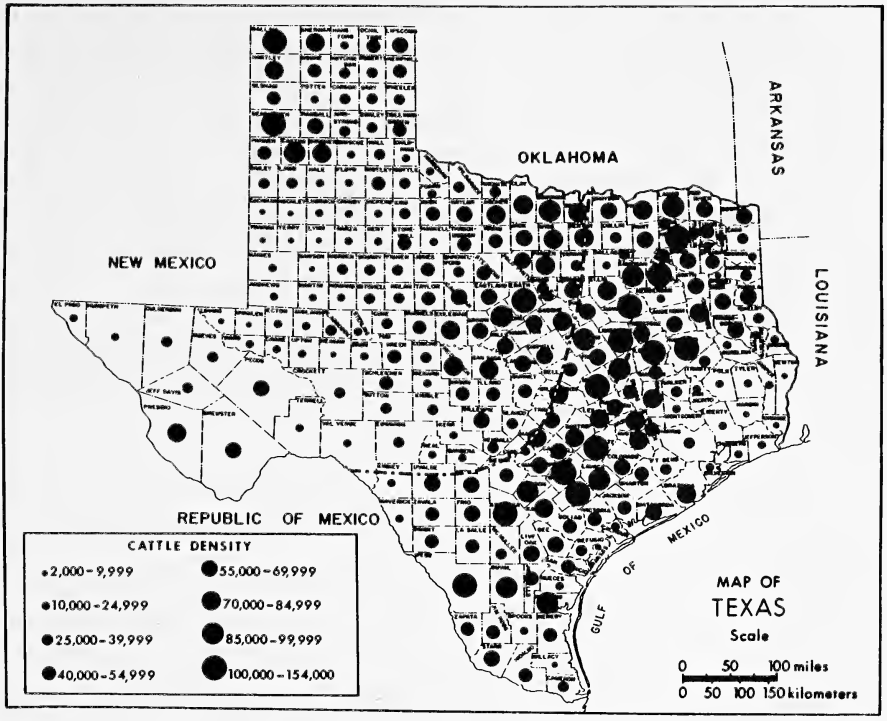

FIGURE 5. Distribution and density of cattle per county in Texas (black dots). The dot-dash line marks location of the Balcones Escarpment. Distribution and density of cattle populations are from the Texas Crop and Livestock Reporting Service (1979). Map updated from Telfair (1979).

The close association of Cattle Egrets with livestock, especially cattle, has caused veterinary entomologists and pathologists to speculate that these egrets may be involved as reservoirs in transmission of cattle diseases. In Texas and apparently elsewhere, little research has been conducted, implicative data and publications are lacking, and thus, the question of disease association with Cattle Egrets is moot. However, laboratory tests in Texas have shown that Cattle Egrets are not carriers of brucellosis. Furthermore, there is no evidence that Cattle Egrets pose a disease threat to humans (except those who enter heronries).

Materials dropped within heronries comprise large quantities of highly concentrated nutrients that eventually enter the soil, water impoundments, and river systems. These wastes may add substantially to the nutrient supply at the base of the soil and aquatic food webs. Although native herons, egrets, and ibises feed primarily in aquatic systems and thereby recycle nutrients and energy within those systems, Cattle Egrets transfer nutrients and energy from terrestrial to aquatic systems.

Heronries are not desirable when located adjacent to human habitation because of noise, odor, and concern about possible health hazards; but, no evidence exists that Texas heronries represent health hazards to adjacent human communities. Heronries may, however, produce detrimental effects upon nest and roost-site vegetation due primarily to the accumulation of excrement on the plants and in the substrate (soil and/or water). A direct relationship exists between materials deposited in heronries and increased levels of nitrogen and phosphorous in the waters beneath or in the vicinity of heronries. These heronries often stimulate production of thick mats of floating and submerged vegetation, particularly algae and duckweed. Presently available methods for preventing establishment or use of heronries are either undesirable, expensive, or illegal.

LITERATURE CITED

Frentress, C. D. 1975. "Pop" rivet fasteners for color markers. Inland Bird Banding News 47:3-9.

Mullins, L. M., G. W. Blacklock, D. R. Blankinship, A. H. Chaney, S. Kennedy, K. A. King, R. T. Paul, R. D. Slack, J. C. Smith, and R. C. Telfair II. 1982. An atlas and census of Texas waterbird colonies 1973-1980. (Compiled by the Texas Colonial Waterbird Soc.) Caesar Kleberg Wild. Instit., Texas A&I Univ., Kingsville, TX.

Oberholser, H. C. 1974. The bird life of Texas (E. B. Kincaid, Jr., ed.), vol. 1. Univ. Texas Press, Austin, TX.

Swepston, D. A., C. D. Frentress, and R. C. Telfair II. 1978. A method for banding and color-marking large numbers of wading birds, p. 219-225. *In* A. Sprunt IV, J. C. Ogden, and S. Winckler (eds.), Wading birds. National Audubon Society Research Report No. 7.

Telfair, R. C. II. 1979. The African Cattle Egret in Texas and its relation to the Little Blue Heron, Snowy Egret, and Louisiana Heron. Ph.D. dissertation, Texas A&M University, College Station, TX.

Telfair, R. C. II. 1981. Cattle Egrets, inland heronries, and the availability of crayfish. Southwest. Nat. 26:37-41.

Telfair, R. C. II. 1983. The Cattle Egret: a Texas focus and world view. Kleberg Studies in Natural Resources. The Caesar Kleberg Research Program in Wildlife Ecology and The Department of Wildlife and Fisheries Sciences, The Texas Agricultural Experiment Station, The Texas A&M University System, College Station, TX.

Texas Crop and Livestock Reporting Service. 1979. Texas county statistics. Texas Dept. Agr. and U.S. Dept. Agr., Austin, TX.

SWIM BLADDER STRESS SYNDROME IN LARGEMOUTH BASS

by GARY J. CARMICHAEL

National Fish Hatchery and Development Center
U.S. Fish and Wildlife Service
San Marcos, TX 78666

and J. R. TOMASSO

Aquatic Station, Department of Biology
Southwest Texas State University
San Marcos, TX 78666

ABSTRACT

Overinflated swim bladders were observed in largemouth bass (*Micropterus salmoides*) after handling and short-term transport. The affected fish swam near the surface with their backs exposed and, in some cases, became inverted and later died. Plasma corticosteroid concentrations of these fish were above normal levels while plasma chloride concentrations and plasma osmolality were below normal levels. Changes in these plasma characteristics are indicative of acute handling-induced types of stress in largemouth bass. It is suggested that some physiological response to physical disturbance may increase the deposition of gas from the blood into the swim bladder.

INTRODUCTION

Swim bladder stress syndrome (SBSS) is a condition in adult fish characterized by overinflation of the swim bladder causing the animal to swim at the surface of the water with the back exposed. It is distinguished from gas bubble disease in that it involves only the swim bladder and does not involve the formation of emphysema or emboli due to gas supersaturation (Bouck 1980). The initial description (Clary and Clary 1978) of the development of SBSS in salmonids in response to environmental stressors (other than gas supersaturation) was the only reference to the syndrome that we found in the literature.

During spring and summer 1982, at the San Marcos National Fish Hatchery and Development Center, SBSS developed on three occasions in groups of largemouth bass (*Micropterus salmoides*) immediately after they were handled and transported. Reported here are descriptions of SBSS in adult largemouth bass, the stressors applied immediately before the development of SBSS, and some hematological characteristics of the afflicted fish.

The Texas Journal of Science, Vol. XXXV, No. 4, January 1984

MATERIALS AND METHODS

Two groups of fish (50 in one group and 126 in the other) that later developed SBSS were moved from outdoor raceways to indoor tanks. These fish weighed approximately 400 g each. The 21-C water in both the raceways and tanks came from a common well. Both groups of fish were transported in large plastic cans containing water from the raceways. The water used to transport one group contained 50 mg/liter MS-222, a common fish anesthetic. A third group of fish that would later develop SBSS consisted of approximately 400 fish, each weighing about 100 g. They were seined from a culture pond and transported in pond water containing 50 mg/liter MS-222 to a raceway. When these fish were moved, the pond water temperature was 18 C and the raceway temperature was 21 C.

Blood samples were taken by syringe from the caudal peduncle of five fish that developed stage 3 SBSS (see Results and Discussion) in the first group. Blood from an additional six fish from the same group that did not develop SBSS was also sampled. Samples were taken 3 days after the initial handling disturbance (approximately 2 days after the first cases of SBSS were observed). Three stage 4 SBSS fish were dissected.

Total plasma corticosteroid concentrations were determined by the competitive protein binding method described by Murphy (1967) and modified by Fagerlund (1970). Glucose was determined by using Pierce auto-stat kits[1] (Pierce Chemical Company, Rockford, IL) based on the glucose oxidase Trinder-Emerson reaction. Chloride was determined by amperometric-coulometric titration with a chlorideometer. Osmolality was measured by freezing point depression with an osmometer.

RESULTS AND DISCUSSION

Clary and Clary (1978) described four distinct stages of SBSS in salmonids. Stage 1 consisted of the fish swimming in a head-down position near the surface of the water, frequently with the caudal fin protruding from the water. Stage 2 consisted of fish broaching the surface with their backs out of the water. Fish in stage 3 swam erratically on their sides, and stage 4 fish swam in an inverted position. Our largemouth bass also exhibited well defined SBSS stages, although they differed from those described by Clary and Clary in salmonids (Fig. 1). At stage 1 bass swam near the surface, normally oriented. Stage 2 was similar to stage 1 in salmonids, including the head-downward orientation and protruding caudal fin. Fish in stage 3 swam at the surface with their dorsal fin out of the water, and those in

[1]Use of trade names does not imply government endorsement of commercial products.

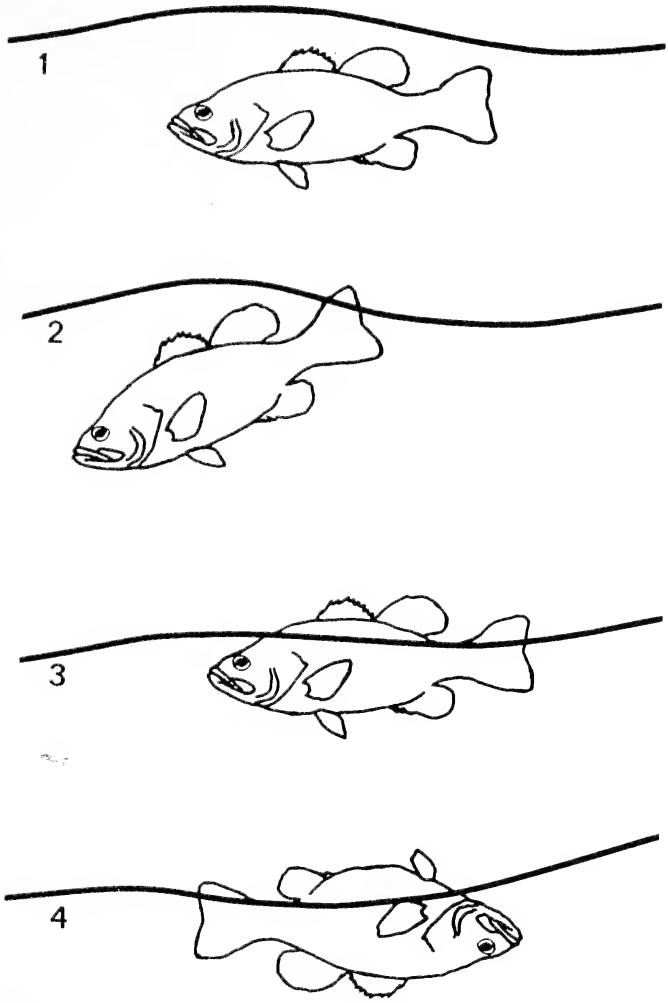

FIGURE 1. Developmental stages 1-4 of swim bladder stress syndrome in largemouth bass. See text for a description of each stage.

stage 4 swam inverted at the surface. The bass were never observed swimming on their sides as described for stage 3 salmonids.

Approximately one third of the first group of fish developed stage 3 SBSS within 48 h of transfer from raceways to tanks. Of these, most seemed to recover within a few days; however, since this was the first occurrence, accurate observation of SBSS development and recovery was not made. Of the second group, 22% developed stage 4 SBSS within 96 h of transfer. All of the stage 4 fish died. Ninety percent of the third group developed stage 1 or stage 2 SBSS within 48 h of transport. However, these fish appeared normal by 96 h after they were moved, and they fed on the fifth day after transport. These observa-

tions suggest that largemouth bass can recover from stages 1, 2, and 3 of SBSS but cannot recover from stage 4.

All of the fish dissected had overinflated swim bladders that tended to push the other organs in the body cavity toward the sides and bottom of the cavity. No gas bubbles were observed in the membranes or fins. Hemorrhage was not apparent and no fluid was observed in the swim bladder. No microscopic examination of the gills for emboli was conducted.

Slight physiological stress was indicated by plasma osmolality and concentrations of plasma chloride and corticosteroids in fish afflicted with SBSS, when compared to baseline information previously collected from healthy, undisturbed fish in our laboratory (Fig. 2). Fish that did not develop SBSS after transfer to the holding house (first group) had plasma osmolality, chloride and corticosteroid values that fell between baseline and SBSS-afflicted fish. The intermediate levels of these blood constituents in the normal-appearing fish indicated that, although these animals did not develop SBSS, they were stressed by the transfer from the raceways to the holding house. Declining plasma osmolality and chloride concentrations are characteristic of osmoregulatory dysfunction in freshwater fish and sometimes follow handling and hauling (Wedemeyer 1972; Tomasso et al. 1980). Elevated corticosteroid concentrations are indicative of acute stress such as that induced by handling and hauling (Wedemeyer 1972; Barton et al. 1980; Tomasso et al. 1980). The lack of a trend in the plasma-glucose levels we observed is surprising, given that plasma-glucose levels tend to increase with increasing corticosteroid concentrations in channel catfish, *Ictalurus punctatus* (Strange 1980), and in largemouth bass (unpublished data of senior author).

The physiological basis for SBSS is difficult to determine. An overinflated swim bladder may develop due to a rapid upward movement in the water column, causing a decrease in external pressure that occurs more rapidly than internal pressure can be reduced. Since the bass in this study were never in water more than 2 m deep, this explanation seems unlikely. An increase in temperature could also cause swim bladder inflation due to expansion of gas already in the swim bladder (Chamberlain et al. 1980). However, the small temptera-ture changes (0-3 C) to which our bass were exposed probably could not account for the large swim bladder volume changes observed.

Overinflation may also be due to dysfunction of the physiological mechanisms that transfer gases into and out of the swim bladder. Gas is deposited in the swim bladder either by the gas gland which secretes gases from the blood or, in physostomous fishes, through a pneumatic duct that connects the upper digestive tract to the swim bladder (see

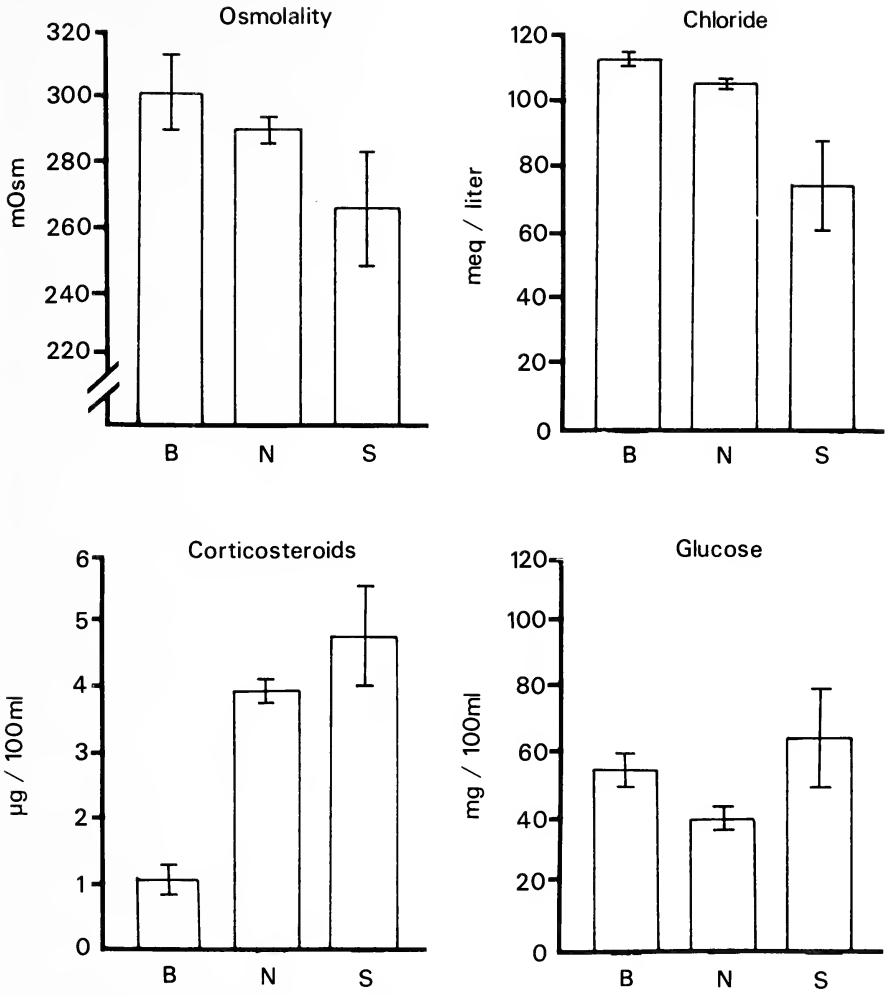

FIGURE 2. Plasma characteristics of baseline largemouth bass (B), apparently normal fish after transport stress (N), and fish with stage 3 swim bladder stress syndrome (S). Height of column and vertical bar represent mean ± standard error.

review by Steen 1970). Gas is removed from the swim bladder either through the pneumatic duct or through the oval gland, a special area of the bladder wall through which gases are reabsorbed into the blood. Overinflated swim bladders have been observed in Atlantic croakers (*Micropogon undulatus*) after exposure to water supersaturated with nitrogen and oxygen (Chamberlain et al. 1980). The authors hypothesized that supersaturated water caused an increase in dissolved blood gases to the point where the partial pressure of nitrogen and oxygen in the blood was higher than the partial pressure of these gases in the swim bladder. The gases then diffused from the blood into the swim

bladder by way of the oval gland. It is doubtful that this process was involved in producing overinflated swim bladders in largemouth bass. To our knowledge, the bass were not exposed to gas-supersaturated water in any of the ponds or holding facilities. The few dissolved oxygen readings available from routine monitoring all were below saturation levels and no other fish in our holding facilities exposed to the same water source demonstrated any symptoms of gas bubble disease.

Under conditions of normal gas saturation, secretion of gases into the swim bladder is a complex process that involves counter-current exchange of blood gases across the rete mirabile and drastic reduction in the hemoglobin's capacity to carry oxygen, caused by production of lactic acid in the gas gland. Perhaps the increased activity due to struggling during capture and transport in some way causes an increase in the secretion of gas into the swim bladder by way of the rete mirabile.

Unfortunately, we have been unable to identify a stressor that consistently induces SBSS. The three cases reported here that followed physical disturbance of the fish represent a very small percentage of the fish handled at our laboratory during the course of a year. The lack of a method to induce the syndrome has complicated attempts to understand its physiological basis.

LITERATURE CITED

Barton, B. A., R. E. Peter, and C. R. Paulencu. 1980. Plasma cortisol levels of fingerling rainbow trout (*Salmo gairdneri*) at rest and subjected to handling, confinement, transport and stocking. Canadian Journal of Fisheries and Aquatic Sciences 37:805-811.

Bouck, G. R. 1980. Etiology of gas bubble disease. Transactions of the American Fisheries Society 109:703-707.

Chamberlain, G. W., W. H. Neill, P. A. Romanowsky, and K. Strawn. 1980. Vertical responses of atlantic croaker to gas supersaturation and temperature change. Transactions of the American Fisheries Society 109:737-750.

Clary, J. R., and S. D. Clary. 1978. Swim bladder stress syndrome. Salmonid 1(6):8-9.

Fagerlund, U. H. M. 1970. Determination of cortisol and cortisone simultaneously in salmonid plasma by competitive protein binding. Journal of the Fisheries Research Board of Canada 27:596-601.

Murphy, B. E. P. 1967. Some studies of the protein binding of steroids and their application to the routine micro and ultramicro measurements of various steroids in body fluids by competitive protein-binding radio-assay. Journal of Clinical Endocrinology 27:973-990.

Steen, J. B. 1970. The swim bladder as a hydrostatic organ, p. 413-433. *In* W. S. Hoar and D. J. Randall (eds.), Fish physiology, Volume 4. Academic Press, New York, NY.

Strange, R. J. 1980. Acclimation temperature influences cortisol and glucose concentrations in stressed channel catfish. Transactions of the American Fisheries Society. 109:298-303.

Tomasso, J. R., K. B. Davis, and N. C. Parker. 1980. Plasma corticosteroid and electrolyte dynamics of hybrid striped bass (white bass x striped bass) during netting and hauling. Proceedings of the World Mariculture Society 11:303-310.

Wedemeyer, G. 1972. Some physiological consequences of handling stress in juvenile coho salmon (*Oncorhynchus kisutch*) and steelhead trout (*Salmo gairdneri*). Journal of the Fisheries Research Board of Canada 29:1780-1783.

DISTRIBUTIONAL RECORDS AND NOTES FOR NINE SPECIES OF MAMMALS IN EASTERN TEXAS

by **ARTHUR G. CLEVELAND**

Department of Biology
Texas Wesleyan College
Fort Worth, TX 76105

and **JOHN T. BACCUS**

Department of Biology
Southwest Texas State University
San Marcos, TX 78666

and **EARL G. ZIMMERMAN**

Department of Biology
North Texas State University
Denton, TX 76203

ABSTRACT

Localities for nine species of mammals in eastern Texas are reported. Also, notes on reproduction in *Reithrodontomys fulvescens, R. humulis,* and *Microtus pinetorum* are presented.

INTRODUCTION

The last review of east Texas mammals was over twenty years ago (McCarley 1959). Since that review, few additional records have been published. We have compiled records on several species that should be noted, extending ranges within and into east Texas. Specimens described are deposited in the museums of North Texas State University (NTSU), Southwest Texas State University (SWTS), and Texas Wesleyan College (TWC).

SPECIES ACCOUNTS

Tadarida brasiliensis (Saussure), Brazilian Free-tailed Bat

Specimens of the free-tailed bat have been reported from Anderson, Angelina, Brazos, Cherokee, Grimes, Harris, Nacogdoches, Sabine, and Shelby counties (Schmidly et al. 1977). A single male (SWTS) was secured from a building in Marshall, Harrison County. This record

extends the range of this species some 80 km north of its previously known Texas occurrence in Nacogdoches County (McCarley 1959).

Lepus californicus melanotis Mearns, Black-tailed Jack Rabbit

Packard (1963) reviewed the status of jack rabbit distribution in east Texas. Although he recorded specimens from several southeastern counties, the northeast was represented only by the report of Bailey (1905) from Bowie County and a single specimen from Wood County. We observed jack rabbits at five localities in sandy, upland savannah-grassland along the South Sulphur River in Delta County. A single specimen (TWC) was taken 1.6 km S Cooper. This record supports the contention of Packard (1963) that jack rabbits have been expanding their range eastward.

Spermophilus tridecemlineatus texensis Merriam, Thirteen-lined Ground Squirrel

Thirteen-lined ground squirrels have not been reported previously from east Texas (McCarley 1959). They were recorded by Davis (1974) from Grayson and Fort Bend counties. We observed this species at two localities in Delta County and one locality in Hopkins County. An adult male specimen (TWC) was taken 1.6 km N Klondike in Delta County. Three (TWC) were taken from Lamar County. These represent definite extensions into east Texas. Eastward expansions of thirteen-lined ground squirrels and other mammals appear to parallel the continued clearing of forested areas for agriculture.

Oryzomys palustris texensis Allen, Marsh Rice Rat

Although the distribution of the rice rat in coastal and eastern areas of Texas is well defined, there are few records for northeastern Texas. McCarley (1952 and 1959) reported specimen localities from Oklahoma and Arkansas.

Ten rice rats (SWTS) were collected in a grassy marsh adjacent to an old field near the Sabine River 11.2 km S Hallsville, Harrison County. Four additional Harrison County specimens (SWTS) were taken 8 km S Marshall. Two rice rats (SWTS) were trapped 3.2 km N Milam, Sabine County. Two (TWC) were collected along tributaries of the south Sulphur River (1.6 km S Liberty Grove; Klondike) in Delta County. A single rice rat (NTSU) was trapped in Paris, Lamar County. Two specimens each were reported by Parris (1974) from Hopkins and Hunt counties. These specimens extend the Texas range of this species (Davis 1974) 176 km north of Rusk County. Systematic trapping probably would reveal its presence in additional counties where it has not yet been collected, especially in the lowlands along the major rivers in east Texas.

Reithrodontomys humulis merriami (J. A. Allen), Eastern Harvest Mouse

Three of these diminutive mice (SWTS) were trapped in a grassy old field 3.2 km S and 3.2 km E Marshall, Harrison County. All specimens were secured from tangles of blackberry vines (*Rubus*) that were surrounded by heavy stands of grass. Prominent grasses were *Andropogon, Aristida, Panicum, Cenchrus* and *Sporobolus*. Other rodent associates were *Cryptotis parva, Reithrodontomys fulvescens* and *Microtus pinetorum*. A single specimen (SWTS) was taken from Lotta, Harrison County. These locality records extend the known range of the eastern harvest mouse in east Texas some 80 km north of its previously known occurrence in Nacogdoches County (McCarley 1959). Lowery (1974) recorded specimens from Caddo Parish in Louisiana.

McCarley (1959) and Davis (1974) reported no breeding information for this species in Texas. Two females (SWTS) obtained on 11 November contained three and four embryos, respectively. The average crown-rump lengths were 25 mm for the former and 3 mm for the latter. A male collected on the same day had scrotal testes. Thus, breeding probably extends well into autumn in east Texas.

Reithrodontomys fulvescens aurantius J. A. Allen, Deer Mouse

Hall (1981) failed to report any deer mice from east Texas. McCarley (1959) noted their presence in Brazos, Navarro, and Robertson Counties. Deer mice were recorded by Parris (1974) from Hopkins County although no specimens were available to confirm the report. As predicted by McCarley (1959), deer mice are now confirmed along the oak-hickory belt; we took specimens (TWC) from Delta, Hopkins, and Rains counties. William Caire took four specimens (NTSU) from Lamar County. These records substantiate deer mice from the oak-hickory belt of east Texas.

Peromyscus gossypinus megacephalus Rhoads, Cotton Mouse

McCarley (1959) reviewed the occurrence of the cotton mouse in east Texas. Davis (1974) recorded this rodent as far west as Red River County. A specimen (NTSU) was trapped 4.8 km E and 5.6 km S Telephone, Fannin County, in a mixed pine-oak woodland along the shoreline of Coffee Mill Lake. An additional specimen (SWTS) was taken 9.6 km N and 27.2 km E Tyler, Smith County.

Microtus pinetorum (Le Conte), Woodland Vole

Parmalee (1954) and McCarley (1959) included Bowie, Marion, Nacogdoches, Panola and Wood counties within the east Texas distribution of the woodland vole. Thirty-four voles (SWTS) were

collected 3.2 km S 3.2 km E Marshall; 1.6 km E Marshall and 11.2 km S Hallsville in Harrison County; and, 9.6 km N and 27.2 km E Tyler in Smith County. Trapping data indicate a habitat preference for transition areas at the interface of old field communities with pine stands. A single specimen (TWC) (adult female) was taken by the senior author 22.4 km W Hillsoboro in Hill County. This capture (200 km west of the Smith County specimens) provides the first intermediate locality between east Texas and central Texas reports (Gillespie and Kerr counties) of Davis (1974). Additional trapping in similar habitats should reveal the presence of woodland voles in other eastern and central Texas counties.

Davis (1974) reported a breeding season extending from February to October and suggested the possibility of a winter period. Specimens collected in November and January confirm the winter breeding hypothesis. Two females (SWTS) secured on 11 November contained two and three embryos respectively. The advanced state of embryonic development indicated a parturition date near the end of November. A juvenile female (SWTS) was trapped on 20 January. Based upon size measurements, we concluded a parturiation date in December. Males (SWTS) examined in December and January had scrotal testes.

LITERATURE CITED

Bailey, V. 1905. Biological survey of Texas. North American Fauna 25:1-222.

Davis, W. B. 1974. The mammals of Texas. Bull. Texas Parks and Wildlife Dept. 41:1-294.

Hall, E. R. 1981. The mammals of North America. John Wiley and Sons, New York, NY.

Lowery, Jr., G. G. 1974. The mammals of Louisiana and its adjacent waters. Louisiana State University Press. Printed by Kingsport Press, Kingsport, TN.

McCarley, W. H. 1952. The ecological relationships of the mammals of Bryan County, Oklahoma. Texas J. Sci. 4:102-112.

McCarley, W. H. 1959. The mammals of eastern Texas. Texas J. Sci. 11:385-426.

Packard, R. R. 1963. Distribution of the black-tailed jackrabbit in eastern Texas. Texas J. Sci. 15:107-110.

Parmalee, P. W. 1954. Food of the great horned owl and barn owl in east Texas. Auk 71:469-470.

Parris, S. D. 1974. Habitat distribution and taxonomy of mice in the upper Sulphur River watershed. M.S. thesis. East Texas State University, Commerce, TX.

Schmidly, D. J., K. T. Wilkins, R. L. Honeycutt, and B. C. Weynand. 1977. The bats of east Texas. Texas J. Sci. 28:127-143.

DEVELOPMENT OF TENSILE STRENGTH IN COMPATIBLE AUTOGRAFTS OF EGGPLANT (*SOLANUM PENNELLII*) *AND TOMATO* (*LYCOPERSICON ESCULENTUM*)

by MARY T. McGARRY *and* RANDY MOORE

Department of Biology
Baylor University
Waco, TX 76798

ABSTRACT

Three phases of cohesion between the stock and scion were observed during the development of compatible autografts in *Solanum pennellii* and *Lycopersicon esculentum* (Solanaceae). The first phase lasted 2 to 3 days after grafting and was characterized by an average increase in tensile strength of the graft union of approximately 2 g breaking weight (BW)/mm^2 graft area (GA)/day. Phase II lasted from days 3 to 15 and was characterized by a 20-fold increase in the tensile strength of the graft union. Phase III was characterized by a leveling off of the tensile strength of the graft union at a value approximating that of an intact (i.e., ungrafted) internode. The pattern of development of tensile strength reported here is similar to that observed for other compatible graft unions between herbaceous tissues.

INTRODUCTION

Recent renewal of interest in plant grafting has resulted in an increased understanding of the processes associated with graft formation. Studies of herbaceous grafts have included structural (Stoddard and McCully 1979; Moore and Walker 1981a, 1981b, in press; Moore 1982, in press a) as well as functional (Yeoman et al. 1978; Stoddard and McCully 1980; Moore and Walker 1981c) analyses of graft formation (see review by Moore 1981a). However, the only convincing mechanism to account for graft incompatibility has resulted from investigations using woody tissues of fruit trees. Graft incompatibility between (1) pear and quince (Gur et al. 1968; Gur et al. 1978) and (2) peach and almond (Gur and Blum 1973) appears to be due to the movement (and subsequent catabolism) of cyanogenic glycosides between tissues of the stock and scion. The diversity of incompatibility responses (Moore 1981b) makes it unlikely that this mechanism is applicable to all (or even many) incompatible grafts.

Several studies have quantified the development of tensile strength in compatible (Roberts and Brown 1961; Lindsay et al. 1974; Yeoman and Brown 1976; Moore 1982, in press b) and incompatible (Yeoman and Brown 1976; Moore in Press b) grafts. However, the tensile strength of

graft unions in most of these studies (Roberts and Brown 1961; Lindsay et al. 1974; Yeoman and Brown 1976) is reported only as g breaking weight (BW), rather than g BW/unit graft area (GA). Since (1) g BW would be expected to increase with increasing GA, and (2) GA is not given in these studies (Roberts and Brown 1961; Lindsay et al. 1974; Yeoman and Brown 1976), the results reported are not comparable with those reported for most other systems (see discussion in Moore 1982). More recent studies in which tensile strength was reported as g BW/unit GA (Moore 1982, in press b) have suggested that the development of compatible autografts, as measured by increases in tensile strength, may be similar in different grafting systems. It has also been suggested that the tensile strength of a compatible graft union may be used to determine the stage of graft development (Moore in press b).

In this study, we have quantified the development of tensile strength in compatible autografts of two members of the Solanaceae, eggplant (*Solanum pennellii*) and tomato (*Lycopersicon esculentum*), by measuring changes in the tensile strength of graft unions over time.

MATERIALS AND METHODS

Clonal populations of *Solanum pennellii* and *Lycopersicon esculentum* were used for this study. Grafts were made by horizontally cutting and then reuniting young expanding internodes. Grafts were monitored for 35 days. Measurements of the tensile strength of the graft union were made in a manner similar to that described by Lindsay et al. (1974). Measurements for each species and graft age were replicated at least 12 times. Diameters of the circular areas of cohesion between the stock and scion were measured with a vernier caliper in order to calculate GA. Values for the tensile strength of the graft union are expressed as the force required to separate the two graft partners (i.e., g BW) per unit of contact area (i.e., mm^2 GA). A more comprehensive discussion of plant growth conditions, grafting procedures, and techniques for determining the tensile strength of the graft union has been published previously (Moore 1982).

RESULTS AND DISCUSSION

Three phases of cohesion were observed during the development of compatible autografts in *L. esculentum* and *S. pennellii* (Fig. 1). Phase I cohesion lasted approximately 2 days after grafting and was characterized by an average increase in tensile strength of the graft union of approximately 2 g BW/mm^2 GA/day (Table 1). Phase I cohesion was positively correlated with the initial adhesion of the graft partners, and was presumably due to dictyosome-mediated deposition of cell wall materials in response to wounding (Moore and Walker 1981a, 1981b;

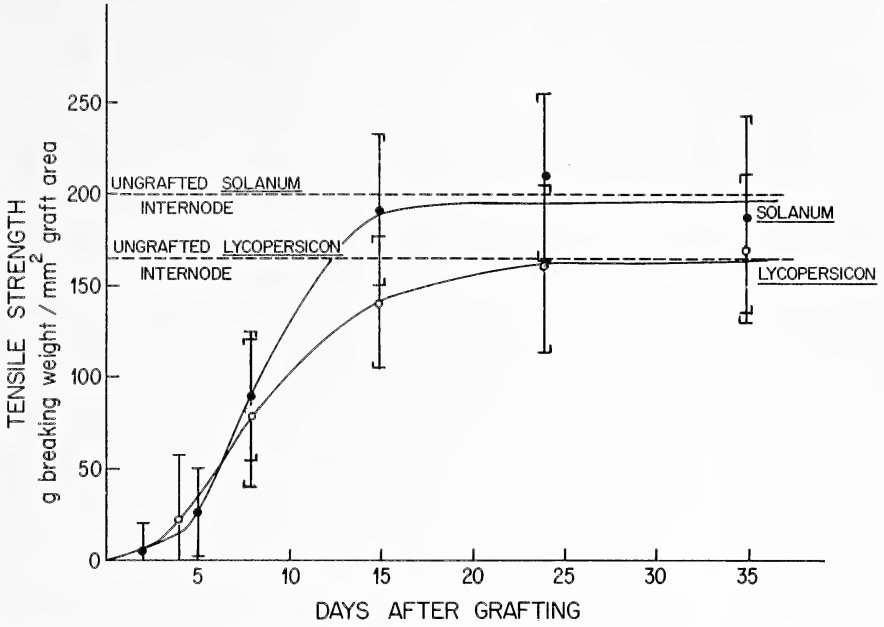

FIGURE 1. The development of tensile strength in compatible autografts of *Lycopersicon esculentum* and *Solanum pennellii*. Each data point represents the mean (± standard deviation) of at least 12 separate trials.

Moore 1982). The timing and extent of Phase I cohesion in compatible autografts of *L. esculentum* and *S. pennellii* were similar to those reported for autografts of *Sedum telephoides* (Moore in press b) and *Kalanchoe blossfeldiana* (Moore 1982).

Phase II cohesion lasted from days 3 to 15 after grafting and was characterized by an increase in the tensile strength of the graft union of approximately 15 g BW/mm² GA/day. At the end of Phase II cohesion, the tensile strength of the graft union was approximately 20 times greater than at the end of Phase I cohesion (Table 1), and approximated that of an ungrafted internode (Fig. 1). This rate of increase in tensile strength compared favorably with that reported previously for other compatible autografts (Moore 1982, in press b) and presumably was due to (1) the interdigitation of callus cells at the graft interface, (2) continued "normal" deposition of cell wall materials, and (3) redifferentiation of a lignified strand of xylem linking the stock and scion (Moore and Walker 1981a; Moore 1982, in press b).

The third phase of graft cohesion in compatible autografts of *L. esculentum* and *S. pennellii* occurred subsequent to day 15 in graft formation (Fig. 1). The tensile strength of the graft union leveled off at a value approximating that of an ungrafted internode. That is, grafts sampled during Phase III cohesion were characterized by a tensile

TABLE 1. Development of tensile strength in compatible autografts of *Lycopersicon esculentum* and *Solanum pennellii*.

Graft Phase	Compatible Autograft	
	Lycopersicon	*Solanum*
Phase I		
duration[a]	0-2 days	0-2 days
average change in tensile strength	2 g BW/mm²GA/day	2 g BW/mm² GA/day
Phase II		
duration[a]	3-15 days	3-15 days
average change in tensile strength	12 g BW/mm² GA/day	14 g BW/mm² GA/day
ratio of strength of graft union at end of Phase II cohesion: end of Phase I cohesion	19	22
Phase III		
duration[a]	subsequent to day 15	subsequent to day 15

[a]expressed in days after grafting

strength equal to that of an intact stem. As was true for Phases I and II cohesion, these observations were consistent with previous studies of other compatible autografts (Moore 1982, in press b).

The general pattern of graft development in compatible autografts of *L. esculentum* and *S. pennellii* was similar to that observed for other compatible autografts (Roberts and Brown 1961; Linday et al. 1974; Yeoman and Brown 1976; Moore 1981, in press b). In each system there was a "lag" phase (i.e., Phase I) during which the tensile strength of the graft union increased at a rate of 1 to 2 g BW/mm² GA/day. This was followed by a pronounced increase in the cohesive strength of the union (i.e., Phase II), after which it leveled off at a value similar to that of an ungrafted internode (i.e., Phase III). The similarity of graft development in these systems supports the previous suggestion that this general pattern of graft development is characteristic of compatible autografts. A more comprehensive discussion of how the development of tensile strength of compatible autografts correlates with (1) structural aspects of graft development, and (2) graft formation in general is presented elsewhere (Moore 1982, in press b).

ACKNOWLEDGEMENTS

This research was supported by a grant from the University Research Committee of Baylor University. This manuscript is submitted in partial fulfillment of the requirements for Biology 3V90 at Baylor University. The authors thank Ms. Barbara Wimpee for her excellent technical assistance in preparing Figure 1.

LITERATURE CITED

Gur, A., and A. Blum. 1973. The role of cyanogenic glycoside in incompatibility between peach scions and almond rootstocks. Hort. Res. 13:1-10.

Gur, A., R. M. Samish, and E. Lifschitz. 1968. The role of the cyanogenic glycoside of the quince in the incompatibility between pear cultivars and quince rootstocks. Hort. Res. 8:113-134.

Gur, A., D. Zamet, and E. Arad. 1978. A pear rootstock trial in Israel. Sci. Hort. 8:249-264.

Lindsay, D. W., M. M. Yeoman, and R. Brown. 1974. An analysis of the development of the graft union in *Lycopersicon esculentum*. Ann. Bot. 38:639-646.

Moore, R. 1981a. Graft compatibility-incompatibility in higher plants. What's New In Plant Physiol. 12:13-16.

Moore, R. 1981b. Graft compatibility and incompatibility in higher plants. Dev. Compar. Immunol. 5:377-389.

Moore, R. 1982. Graft development in *Kalanchoe blossfeldiana*. J. Exp. Bot. 33:533-540.

Moore, R. In Press a. Studies of vegetative compatibility-incompatibility in higher plants. V. A morphometric analysis of the development of a compatible and an incompatible graft. Can. J. Bot.

Moore, R. In Press b. Studies of vegetative compatibility in higher plants. IV. The development of tensile strength in a compatible and an incompatible graft. Amer. J. Bot.

Moore, R., and D. B. Walker. 1981a. Studies of vegetative compatibility-incompatibility in higher plants. I. A structural study of a compatible autograft in *Sedum telephoides* (Crassulaceae). Amer. J. Bot. 68:820-830.

Moore, R., and D. B. Walker. 1981b. Studies of vegetative compatibility-incompatibility in higher plants. II. A structural study of an incompatible heterograft between *Sedum telephoides* (Crassulaceae) and *Solanum pennellii* (Solanaceae). Amer. J. Bot. 68:831-842.

Moore, R., and D. B. Walker. 1981c. Studies of vegetative compatibility-incompatibility. III. The involvement of acid phosphatase in the lethal cell senescence associated with an incompatible heterograft. Protoplasma 109:317-334.

Moore, R., and D. B. Walker. In Press. Grafting *Sedum* and *Solanum* callus tissue in vitro. Protoplasma.

Roberts, J. R., and R. Brown. 1961. The development of the graft union. J. Exp. Bot. 12:294-302.

Stoddard, F. L., and M. E. McCully. 1979. Histology of the development of the graft union in pea roots. Can. J. Bot. 57:1486-1501.

Stoddard, F. L., and M. E. McCully. 1980. Effects of excision of stock and scion organs on the formation of the graft union in *Coleus:* a histological study. Bot. Gaz. 141:401-412.

Yeoman, M. M., and R. Brown. 1976. Implications of the formation of the graft union for the organization in the intact plant. Ann. Bot. 40:1265-1276.

Yeoman, M. M., D. C. Kilpatrick, M. B. Miedzybrodzka, and A. R. Gould. 1978. Cellular interactions during graft formation in plants, a recognition phenomenon? Soc. Exp. Biol. Symp. 32:139-160.

ABSTRACTS
OF THE
NINTH NORTH AMERICAN
PHYSARUM CONFERENCE

Southern Methodist University
Dallas, Texas
June 12-15, 1983

CONFERENCE COORDINATOR
Claude Nations
Department of Biology
Southern Methodist University
Dallas, TX 75275

CONFERENCE ORGANIZING COMMITTEE

Elaine King
Gil King
Nancy Nations
Harriet Schools
John Ubelaker

Sponsored by the Dedman College
and the Department of Biology
of Southern Methodist University

CELL-TYPE DEPENDENT EXPRESSION OF TUBULINS IN *PHYSARUM*. T. G. Burland, K. Gull*, T. Schedl, R. Boston, and W. F. Dove, *McArdle Laboratory, University of Wisconsin, Madison, WI 53706, and *The Biological Laboratories, University of Kent, Canterbury, UK.*

Using 2-dimensional gel electrophoresis, five species of tubulin have been resolved and identified in whole cell lysates of *Physarum* myxamoebae and plasmodia. The identities of these species have been established by 1)co-electrophoresis with myxamoebal $\alpha 1$ and $\beta 1$ tubulins purified by self-assembly into microtubules *in vitro*; 2)peptide mapping with Staphylococcus V8 protease and with chymotrypsin; 3)hybrid selection of specific mRNAs followed by translation *in vitro*; and, 4)immunoprecipitation with a monoclonal antibody specific for β-tubulin.

Differential expression of the *Physarum* tubulins has been observed: the $\alpha 1$ and $\beta 1$ electrophoretic species are found in both myxamoebae and plasmodia; the $\alpha 2$ and $\beta 2$ species are found only in plasmodia; and the $\alpha 3$ species is found only in the myxamoebal phase—it may be specific to the swarm cell.

Translation *in vitro* of myxamoebal and plasmodial RNAs has indicated that there are distinct mRNAs, and therefore probably distinct genes, for the $\alpha 1$, $\alpha 2$, $\beta 1$, and $\beta 2$ species. It is uncertain whether $\alpha 3$ is a product of a separate gene, or whether it arises by modification of $\alpha 1$. There is no detectable alteration in genome organization involving the tubulin DNA sequence family in concert with these changes in patterns of gene expression.

It remains possible that any of these tubulin species, no matter how electrophoretically pure, contains the products of more than one tubulin gene.

GENETIC ORGANIZATION OF THE TUBULIN DNA SEQUENCE FAMILIES. T. Schedl, T. G. Burland, and W. F. Dove, *McArdle Laboratory, University of Wisconsin, Madison, WI 53706.*

Physarum is highly polymorphic for restriction fragment length. Even within a single diploid isolate such as Wis 1, restriction fragments containing a particular DNA sequence are commonly dimorphic. This fact permits one to assign the genetic locus of any DNA sequence for which one has a cloned probe. In our laboratory, we have previously used this approach to analyze the organization of the actin DNA sequence family in *Physarum*. Cloned actin sequences from *Saccharomyces cerevisiae* and from *Drosophila melanogaster* showed concordant Southern blot against *Physarum* DNA (T. Schedl and W. F. Dove, J. Mol. Biol. 160:41-57, 1982).

A similar analysis has been possible for the DNA sequence families for α-tubulin and for β-tubulin. The α family contains 2 pairs of polymorphic Hind III bands and at least 2 bands that still remain monomorphic. The β family contains 2 pairs of polymorphic Hind III bands and at least 2 monomorphic bands. The segregation of the polymorphic bands for actin, α-tubulin, and β-tubulin has been followed in the progeny of a heterozygous plasmodium derived by the mating of mutants derived from CLd (Wis 1) crossed to MA275 (Wis 2). The only evidence for linkage yet found is at the complex actin locus, *ardA* (Schedl and Dove, loc cit.).

Southern blots have been compared between DNA from the myxamoeba and that from the plasmodium. Even though there is a shift in expression between these two phases for both the α- and β-tubulin families, there is no detectable change in Southern blot pattern aside from the segregation of polymorphisms. Thus, it seems that the change in gene expression in the tubulin family is not accompanied by major genome rearrangements.

GENETIC ANALYSIS OF MBC-RESISTANCE IN *PHYSARUM*. T. G. Burland, *University of Tromso, Norway, and McArdle Laboratory, University of Wisconsin, Madison, WI.* (Presented by W. F. Dove, *McArdle Laboratory.*)

Physarum myxamoebae are normally sensitive to methyl benzimidazole carbamate (MBC) at levels above 5μM. Mutants resistant to 5-100 μM have been isolated and analyzed genetically. Eight mutants have been analyzed to date; they lie in four separate genetic loci, *benA, benB, benC*, and *benD*.

It is known that benzimidazole-derived anti-mitotic agents bind to the tubulin subunit and promote the disassembly of microtubules. It is possible that MBC-resistance could involve alterations in β-tubulin, or indirect mechanisms, such as a decrease in permeability or an increase in detoxification. Do any of the *ben* loci control the structure of β-tubulin?

One allele of *benD*, 210, creates a new electrophoretic species in two-dimensional gels. This species has a peptide map of a β-tubulin and is immunoprecipitated by a monoclonal antibody for β-tubulin. The *benD* 210 mutation co-segregates with a β-tubulin DNA sequence. By this evidence, *benD* is a locus encoding a myxamoebal β-tubulin. Mutants at this locus are resistant to MBC in both the myxamoebal and the plasmodial phase of growth, and *benD* 210 shows the novel β-tubulin polypeptide in both growth phases. Quite surprisingly, however, the BEN210 mutant also displays a β-tubulin in the normal β1 position as a myxamoeba but not as a plasmodium. It seems then that a second locus acts in the myxamoeba to produce a β-tubulin identical in electrophoretic mobility to the product of the *benD* locus. This second locus seems not to be active in the plasmodial phase.

A second locus of MBC-resistance mutations that also seems to contain a structural gene for β-tubulin is *benA*. An allele of *benA* has been shown to co-segregate with a polymorphic β-tubulin DNA fragment in the progeny of the heterozygous plasmodium (BEN41 $\times$ MA275). However, mutations at *benA* appear to confer MBC resistance on plasmodia.

REGULATION OF TUBULIN SYNTHESIS IN THE *PHYSARUM* CELL CYCLE. T. Schedl, T. B. Burland, K. Gull*, and W. F. Dove, *McArdle Laboratory, University of Wisconsin, Madison, WI 53706, and *The Biological Laboratories, University of Kent, Canterbury, UK.*

Previous work has demonstrated that microtubular proteins are synthesized periodically in the plasmodial cell cycle; these microtubular proteins have been charcterized further and found to comprise two α and two β tubulin species. A simple mechanism to establish periodic synthesis is that of autoregulation, along lines suggested by Ben-Ze'ev et al. (Cell 17:319-325, 1979): the production of tubulin message would be inhibited by elevated concentrations of unpolymerized tubulin. As mitosis approaches, tubulin would polymerize and the rate of production of tubulin message would rise. To investigate this possibility, we have analyzed the timing of tubulin synthesis in the plasmodial cell cycle in relation to the appearance of microtubules. Tubulin synthesis was estimated by pulse-labeling 7 mm discs of a single large parent plasmodium for 15 min with ^{35}S-methionine, followed by lysis and resolution of tubulins on two-dimensional gels analyzed by fluorography. The appearance of microtubules was followed by electron microscopy of samples fixed at the mid-point of each methionine pulse. Twenty-two samples were taken, at 15 min intervals from 210 min before metaphase to 105 min after. Tubulin synthesis begins ca. 165 min before metaphase, reaches a peak in early prophase, and falls precipitously after telophase. Significant synthesis occurs during mitosis. By contrast, microtubules are present only from a time just prior to early prophase—ca. 120 min after the onset on tubulin synthesis—until just after telophase, when the rate of tubulin synthesis is falling precipitously.

These observations are contrary to simple expectations for an auto-regulatory mechanism switching tubulin expression ON; they do not rule out such a mechanism acting to switch expression OFF after mitosis.

PHYSARUM HISTONES. Harry R. Matthews, Jaap H. Waterborg, Liane M. Mende and Reinhold D. Mueller, *Department of Biological Chemistry, School of Medicine, University of California, Davis, CA 95616.*

Our recently published procedure (M. Mende, J. H. Waterburg, R. D. Mueller and H. R. Matthews, Biochem. 22:38-51, 1983) for isolating *Physarum* plasmodial histones will be reviewed. In subsequent work with *Physarum* histone H4, we have separated the fragments produced by acetic acid digestion and determined the complete sequence of two of them. By analogy with calf H4, these peptides are at the C-terminus and give the sequence from residue 69 to the C-terminus (residue 102). In the 34-residue sequence, there are two minor differences from calf H4; arg-77 is lys in calf; and lys-79 is partially methylated in *Physarum*. Agr-77 also occurs in pea H4 but the methylated lysine at position 79 has not been reported in other H4s. In the N-terminal region, amino acid compositions of chymotryptic and tryptic peptides strongly imply that *Physarum* H4 has the same sequence as calf H4 from residue 1 to 37. To determine the acetylation sites, *Physarum* H4 was labelled with ^{3}H-acetate, digested under conditions where only arginine-X bonds were cleaved and subjected to Edman degradation. This digestion yields only two labelled peptides, 1-3 and 4-17. Peptide 1-3 is not susceptible to Edman degradation. The pattern of release of label during consecutive cycles of Edman degradation shows that acetylation occurs at positions 5, 8, 12 and 16 of the whole molecule, as in calf H4.

ANALYSIS OF HISTONE ACETYLATION IN THE *PHYSARUM* CELL CYCLE. Harry R. Matthews and Jaap H. Waterborg, *Department of Biological Chemistry, School of Medicine, University of California, Davis, CA 95616.*

There are three patterns of histone acetylation in the *Physarum* cell cycle correlated with S phase (acetate incorporation into 4 core histones) or G2 phase (incorporation into H3 and H4 only) or metaphase (no incorporation). The pattern observed in G2 is not affected by cycloheximide (10 μg/ml) or hydroxyurea (50 mM) but is reduced by cordycepin (200 μg/ml). This strengthens the correlation of the G2 phase pattern of histone acetylation with transcription. In S phase, newly synthesized histone H4 occurs in a form different from pre-existing H4. This form is converted to the bulk form between the end of S phase and mid-G2 phase, possibly by methylation. In S phase, cycloheximide inhibits both protein and DNA synthesis, in *Physarum*, and converts the histone acetylation pattern to a G2 phase-like pattern. The difference between the normal S phase histone acetylation and the G2 phase histone acetylation is termed "S phase specific" acetylation. S phase specific acetylation of H4 occurs only on newly synthesized H4 and is sensitive to fluorodeoxyuridine or hydroxyurea. S phase specific acetylation of histones H2A, H2B and H3 is not sensitive to these inhibitors although it is sensitive to cycloheximide. The data fit a model of chromosome replication in which S phase specific acetylation of H4 is linked with nucleosome assembly and maturation while the other core histones are acetylated after their synthesis but independently of nucleosome assembly.

HISTONE GENE EXPRESSION IN *PHYSARUM POLYCEPHALUM*: HISTONE SYNTHESIS DURING THE CELL CYCLE AND CONFORMATIONAL CHANGES OF THE H4 HISTONE GENE. M. L. Wilhelm, F. X. Whihelm, B. Toublan and R. Jalouzot, *Institut de Biologie Moléculaire et Cellulaire, 15 rue René Descartes, 67084 Strasbourg cé*dex, France.

Synchronous cultures of *Physarum polycephalum* were used to detect conformational changes of the histone genes during the cell cycle and to follow the synthesis of total and nuclear proteins at various times after mitosis. To monitor the rate of protein synthesis the cultures were labeled with a mixture of ^{14}C-lysine and ^{14}C-arginine. In the nuclei the incorporation of radioactive precursors increases rapidly, is maintained at a high level during most of the S phase and decreases at its end. Thus the rate of nuclear protein synthesis measured in isolated nuclei follows closely the rate of DNA synthesis. By gel electrophoresis and fluorography of the gel it was shown that newly synthesized histones are present in S-phase nuclei but not in G2 or during mitosis. Histone synthesis is therefore restricted to S-phase. To correlate chromatin structure and gene activity DNase I was used as a probe to detect conformational changes of the histone genes during the cell cycle. The degradation of histone was followed by gel electrophoresis and hybridization with a probe for the H4 histone gene. It was found that even during mitosis when chromatin is condensed into chromosomes, the histone genes are preferentially degraded by DNase I. The histone genes retain a characteristic structure which is recognized by DNase I during all stages of the cell cycle and thus independently of the biosynthesis of histones. Experiments are now in progress to determine whether the histone genes can be shut off when *Physarum* is induced to differentiate into dormant cells (spores or spherules).

ANALYSIS OF POLY A$^+$ AND ACTIN mRNAS DURING SPHERULATION IN *PHYSARUM POLYCEPHALUM*. Gerald Lemieux and Vern L. Seligy, *Molecular Genetic Section, National Research Council of Canada, Ottawa, Ont., K1AOR6.*

Total RNA was extracted from microplasmodia at different times during starvation-induced spherulation in *P. polycephalum*. The poly A$^+$ fraction was prepared by chromatography on oligo-dT cellulose and translated in a rabbit reticulocyte lysate. The proteins were separated by two dimensional gel electrophoresis and detected by fluorography. Results showed that the mRNA population was relatively stable during the first 24 hours of differentiation. After 32 hours, the protein pattern revealed the diminution of some major spots and the appearance of new ones. By 48 hours, a time at which spherulation is essentially complete, the variations detected earlier were more pronounced. One of the major spots whose intensity was greatly reduced in spherules had a molecular weight of 43,000. The use of DNase-Sepharose chromatography enabled us to identify this protein as actin. At least two other minor spots, one slightly more acidic and the other slightly more basic than actin, were also detected by affinity chromatography on DNase-Sepharose. Since *P. polycephalum* contains at least four actin genes, these satellite spots may reflect the expression of more than one actin gene. These results definitely show that the synthesis of specific mRNA is involved in the differentiation of microplasmodia into spherules.

REPLICATION-TRANSCRIPTION-COUPLING IN *PHYSARUM*. Gerald Pierron and Helmut W. Sauer, *Department of Biology, Texas A&M University, College Station, TX 77843.*

EM spreads of chromatin at 15 minutes post metaphase reveal activated transcription units in newly replicated chromatin. In most cases both replicated DNA strands are symmetrically transcribed and putative replication origins reside inside the transcription

unit. Hence, in *Physarum* a set of genes is activated in synchrony in 10^8 nuclei, a situation conducive to the isolation of such genes and identification of their products. Other evidence suggests that, following mitosis, initiation of transcription by RNA polymerase B as well as elongation require newly replicated chromatin devoid of nucleosomes.

Since the classical density-shift experiments suggest a temporal sequence of DNA replication, it follows that in *Physarum* genes may become activated in a fixed order. Replication-transcription-coupling potentially comprises a novel mechanism of gene-expression control, if not the basic program of gene regulation in the cell cycle, and allows for a new look at quantal cell cycles and cellular determination.

In preliminary experiments we have 1) devised a reproducible method to separate, on a preparative scale, newly replicated from non-replicated DNA, 2) hybridized restricted total DNA of *Physarum* after electrophoresis and Southern blotting with nick translated probes of distinct genes (actin, histones, which cross-react with *Physarum* DNA) and 3) constructed a genomic library in a lambda based vector. In current experiments we ask when these marker genes are replicated during S phase and whether the order of replication is invariant in different strains and/or changing during the life cycle of *Physarum*.

CHANGES IN THE ABUNDANCE OF mRNA SPECIES DURING THE MITOTIC CYCLE OF *PHYSARUM POLYCEPHALUM*. Robert A. Cox and Nadia J. Smulian, *National Institute for Medical Research, Mill Hill, London NW7 1AA, UK.*

A partial clone bank was used to measure changes in the abundance of mRNA species at intervals during the mitotic cycle of *Physarum*. The bank comprised approx. 900 colonies of *Escherichia coli* made tetracycline sensitive by the insertion of a *Physarum* genomic DNA between the Hind III site and *Bam*H1 site of the plasmid pAC184. The bank was screened with radioactive cDNA probes copied from (1) RNA of microplasmodia; (2) RNA isolated from a macroplasmodium harvested in S-phase, and (3) RNA isolated from a macroplasmodium harvested in late G-2 phase. Fifty-four colonies hybridized equally strongly with all three probes, suggesting that the complementary RNA species were equally abundant throughout the mitotic cycle. Five colonies hybridized most strongly with the cDNA probe copied from S-phase RNA, suggesting that the designated RNA species were more abundant in S-phase. One colony hybridized most strongly with the late G2-phase probe, as might be expected for an RNA that is more abundant in G2-phase. One colony, p5.13, was used to select its complementary RNA which was then found to direct the synthesis of a protein of approximately 25,000 daltons. This mRNA species was shown to be polyadenylated and was found to increase three-fold in abundance during late S-phase, as measured by a novel isotope-dilution technique.

ASSAY OF A(5′) pppp(5′)A AND A(5′)pppp(5′)G IN *PHYSARUM POLYCEPHALUM* AND OTHER EUKARYOTES: AN ISOCRATIC HIGH PERFORMANCE LIQUID CHROMATOGRAPHY METHOD. Preston N. Garrison and Larry D. Barnes, *Department of Biochemistry, University of Texas Health Science Center, San Antonio, TX 78284.*

A(5′)pppp(5′)A has been proposed to serve as a molecular signal that triggers DNA replication. In preliminary studies, synthesis of A(5′)pppp(5′)A was detected in the slime mold *Physarum polycephalum* by labeling cells with [2-^{3}H] adenosine and analyzing by TLC and HPLC a fraction which copurified with standard A(5′)pppp(5′)A. When published methods proved inadequate for the assay of unlabeled cellular A(5′)pppp(5′)A by HPLC, a set of purification procedures was developed which allowed assay of as little as 2 pmol of A(5′)pppp(5′)A. A(5′)pppp(5′)A was purified from cellular extract by

covalent boronate chromatography, treated with alkaline phosphatase to hydrolyze residual mononucleotides and analyzed by isocratic ion-exchange HPLC. The analysis was facilitated by a pre-column switching procedure which allowed early eluting species to be diverted from the analytical column.

Using this procedure A(5′)pppp(5′)A has been detected in *Physarum polycephalum* (1.4 pmol/mg protein), *Saccharomyces cerevisiae* (3.6 pmol/mg protein), and rat liver (3.3 pmol/mg protein). In each case a minor peak was also seen, which was identified as A(5′)pppp(5′)G. The identity of both peaks was confirmed by coelution with standards on isocratic and gradient HPLC and treatment with enzymes, including a dinucleoside polyphosphate pyrophosphohydrolase from *Physarum polycephalum.*

MOLECULAR STRUCTURE OF THE EXTRACHROMOSOMAL NUCLEOLUS OF *PHYSARUM POLYCEPHALUM.* Chen-Chen Kan and Robert Marsh, *Biology Programs, The University of Texas at Dallas, Richardson, TX 75080.*

Nucleoli relatively free of polysaccharide granules and containing less than 1% intact nuclei were purified from synchronous *Physarum polycephalum* macroplasmodia late in G_2 phase. A histone-depleted rDNA-containing nucleolar complex with a standardized sedimentation coefficient around 165,000 S was obtained after treating the nucleoli with 2 N NaCl or a combination of heparin and dextran sulfate, followed by sedimenting them in a neutral sucrose gradient. The S-value of the residual nucleolar complex was not affected by RNase A digestion, but the complex was dissociated by a divalent cation chelating agent such as EDTA. Within the residual complex, 6 proteins predominated. None of these proteins appeared to any appreciable extent among the extracted proteins. Visualization of the ethidium bromide-stained residual nucleolar complex by fluorescence microscopy revealed a halo of fluorescence surrounding the central spherical structure. Electron microscopic examination showed the halo to be composed of the 60 kb rDNA molecules, which are present at 600-800 copies per late G_2 nucleolus and encode the ribosomal RNA. It appears that the linear rDNA molecules are attached to the scaffold at internal sites on the rDNA molecules, with ends of the rDNA molecules being free.

CLONING *PHYSARUM* DNA IN CHARON 4A AND CHARACTERIZATION OF SOME CLONES. Cheryl Knox, Mary Jo Maher, and Robert Marsh, *The University of Texas at Dallas, Richardson, TX 75080.*

An *Eco*Rl partial genomic library of *Physarum polycephalum* M3 has been constructed with bacteriophage Charon 4A as vector. Theoretically, there is a 70% chance of any sequence being present. Attempts to expand this library or to construct a library using cosmid pHC79 have been unsuccessful.

The *Physarum* M3 genome has been probed for actin, α and β tubulin, and amylase sequences in gel blots of *Eco*Rl restriction fragments hybridized with isolated DNA inserts from plasmids pDmAct (*Drosophila* actin), pDTA4 (*Drosophila* α tubulin), pDTB4 (*Drosophila* β tubulin), pAmy21 and pAmy104 (mouse amylases). Actin sequences were found in 8 *Eco*Rl fragments in agreement with Schedl and Dove (J. Mol. Biol. 160:41-57, 1982) for Wis 1 sublines, tubulin sequences were detected in 2 fragments (2.25 and 3.2 kb), and amylase sequences in 2 other fragments (1.4 and 0.45 kb). When our partial genomic library was screened with total DNA from these plasmids, several phages exhibiting homology were isolated. However, the homology has been demonstrated to be to the pBR322 vector DNA. Since no actin, tubulin or amylase genes have been isolated from the library, one of the clones showing homology to pBR322 is being characterized and mapped for study of DNA replication in its vicinity.

THE EFFECTS OF GROWTH CONDITIONS ON PROTEIN KINASE ACTIVITY AND cAMP BINDING ACTIVITY IN *PHYSARUM POLYCEPHALUM*. Joan H. McCune, Christina L. Shoemaker and Ronald W. McCune, *Department of Microbiology and Biochemistry, Idaho State University, Pocatello, ID 83209-0009.*

Previous studies in this laboratory on arginine metabolism in *Physarum polycephalum* have indicated that arginase is an inducible enzyme in this organism. Thus, under conditions of high arginine concentration, this enzyme will be present and active. The products of arginase action are urea and ornithine. One of the enzymes which can act on ornithine is ornithine decarboxylase, the first enzyme in the biosynthesis of polyamines. Other laboratories have shown ornithine decarboxylase to be present in *Physarum*. Ornithine decarboxylase in *Physarum* is phosphorylated by protein kinase which converts ornithine decarboxylase to an inactive form. The protein kinase in turn is apparently regulated by the level of polyamines in *Physarum*. In some eucaryotic systems, protein kinase is stimulated by cAMP. It was therefore of interest to examine the effects of various growth conditions, especially conditions where arginase is and is not induced, on the activity of protein kinase and cAMP binding activity. The organism was grown on semi-defined medium and OV-40 medium with either valine or arginine. Protein kinase activity and cAMP binding activity were examined.

PURIFICATION OF CALMODULIN FROM *PHYSARUM FLAVICOMUM* AND CORRELATIVE STUDIES ON CYCLIC AMP PHOSPHODIESTERASE. Thomas J. Lynch and Mary E. Farrell, *Department of Biology, University of Arkansas at Little Rock, Little Rock, AR 72204.*

Calmodulin, an important cellular regulatory protein, has been identified in the haploid and diploid stage of *P. flavicomum*. Calmodulin was purified by affinity chromatography using fluphenazine or CAPP as the binding ligand. Calmodulin binds to the ligand in the presence of calcium and is preferentially released upon the addition of the calcium chelator EGTA. Myxomycete calmodulin appears to be similar to calmodulin isolated from higher organisms. These similarities include molecular weight as determined by polyacrylamide gel electrophoresis, requirement of calcium for activity and lack of species specificity. Phosphodiesterase from both stages of the life cycle exhibited two apparent km values and showed greatest activity in the presence of Mg^{++} and Ca^{++}. The enzyme from both stages was inhibited by phenothiazines, suggesting the involvement of calmodulin regulation of the enzyme. To test this hypothesis, calmodulin free phosphodiesterase was prepared by passage of a crude supernatant through DEAE-sephacel. This calmodulin free enzyme was assayed in the presence and absence of exogenous calmodulin. Repeated experiments failed to show any regulation of myxomycete phosphodiesterase by calmodulin.

LOCALIZATION, PURIFICATION, AND CHARACTERIZATION OF A PROTEINASE INVOLVED IN ENCYSTMENT OF *PHYSARUM FLAVICOMUM*. Hiltrud U. White and Henry R. Henney, Jr., *University of Houston, Houston, TX 77004.*

An intracellular proteinase involved in the differentiation of *Physarum flavicomum* haploid cells to microcysts was localized in lysosomes, purified and characterized. The total intracellular proteinase activity, as well as specific activity, increased during encystment. Lysosomes were isolated by sucrose density gradient centrifugation. The lysosomal nature of the isolated fraction was confirmed ultrastructurally with electron microscopy and functionally with assays for typical lysosomal marker enzymes. The lysosomal proteinase was further purified by affinity chromatography followed by gel filtration chromatography. Its molecular weight was estimated to be 32,000 and it exhibited no quarternary structure. Mercaptoethanol or dithiothreitol were essential for enzyme stability. The enzyme was most stable at pH 2 to 3 and its pH optimum for

azocasein hydrolysis was pH 3. The enzyme was relatively stable up to 45 C and its maximal rate of activity occurred at 55 C. It was sensitive to an acid proteinase inhibitor, as well as inhibitors which react with thiol proteinases. The enzyme is classified as an acid (carboxyl) proteinase with essential thiol groups.

A TANNIC ACID-METHYLAMINE TUNGSTATE CONTAINING FIXATIVE FOR MYXOMYCETE PLASMODIA. M.H. Chestnut, *Department of Botany, Washington State University, Pullman, WA 99164.*

Macroplasmodia of *Badhamia utricularis* were fixed for transmission electron microscopy by several methods, including (a) glutaraldehyde-osmium tetroxide, (b) osmium tetroxide-glutaraldehyde-osmium tetroxide, (c) osmium tetroxide-glutaraldehyde + tannic acid-osmium tetroxide, and (d) osmium tetroxide-glutaraldehyde + tannic acidmethylamine tungstate. Sclerotia were germinated on moistened filter paper circles, and the resulting starving plasmodia were processed using one of the above fixative combinations. All fixative solutions were buffered with PIPES to pH 7.0 at 300 ± 20 m0sm. Segments of fixed plasmodial strands were dehydrated in a graded ethanol series, and embedded in either L. R. White acrylic resin or Medcast (Epon substitute). Silver-gray sections were cut with a diamond knife on a Sorvall MT-2B ultramicrotome, collected on formvar-coated 100 mesh grids, stained with lead citrate and/or uranyl acetate, and examined in an Hitachi 300 electron microscope at 75Kv. Results showed that method A gave good organelle preservation, but overall strand morphology was unacceptable. Addition of a 2 minute osmium tetroxide pre-treatment in methods B, C, and D preserved strand morphology. Method B produced low contrast and some indication of cytoplasmic extraction. Methods C and D produced high contrast and good preservation, method D being preferred for detail of membranes and 50-70A filaments. High contrast was dependent on lead staining. The osmium tetroxide-glutaraldehyde + tannic acid-methylamine tungstate procedure produced the best results overall, and eliminated some of the common problems encountered in fixing myxomycete plasmodia for electron microscopy. The high contrast obtained with this method allowed routine use of silver-gray sections, thereby potentially increasing resolution. (An extended version of this presentation has been submitted for publication in the Journal of Microscopy).

HOW SYNCHRONOUS IS *PHYSARUM*? Gerard Pierron[1] and Mannfed Kubbies[2], [1]*Department of Biology, Texas A&M University, College Station, TX 77843, and* [2]*Human Genetik, University of Wurzburg, 8700 FRG.*

Flow-cytometric analysis of Hoechst-strained isolated nuclei provided convincing confirmation of natural synchrony in *Physarum*. About 99% of 10^8 nuclei divided in less than 5 minutes as evidenced by a shift of DNA fluorescence from 4c to 2c. Futhermore, this high degree of synchrony is maintained throughout S phase. It was shown that 1) all nuclei initiate DNA replication in synchrony, 2) DNA replication occurs at a constant rate ($4 \cdot 10^9$d/min) for 80 minutes until 75% are replicated, 3) the remaining DNA is replicated in synchrony, albeit at a slower rate ($1 \cdot 10^9$d/min), and 4) the DNA content in G_2 phase is stable.

Of the nuclei derived from liquid cultures, 27% are in S phase whereas 72% are G_2+ mitosis. Less than 1% of the nuclei have a DNA fluorescence compatible to a G_1 DNA content.

In addition, flow-cytometry of nuclei from different strains have revealed the following facts: 1) DNA content (4c values) is variable, due to the amount of late replicating, presumably A-T rich DNA sequences, 2) one strain (derived from M_3C_{IV}) was found to contain two stable populations of nuclei (4c=1.05 and 0.87 pg.DNA). Both kinds divide and replicate DNA in synchrony in the mixoploid plasmodium. It is concluded that early replicating DNA provides sufficient information for the synchronous cell-cycle.

THE USE OF *PHYSARUM* IN TOXICITY TESTING. J. Mohberg and M. M. Kelly, *Division of Science, Governors State University, Park Forest South, IL 60466.*

Toxicity of several fuels—hydrazine, straight chain hydrocarbons and ethanol—has been investigated in growing microplasmodia and sporulating plasmodia of two strains of *Physarum*, a derivative of M_3b and an $mt_1 \times mt_2$ cross, LU647 × 5001d. Effect on microplasmodial growth was determined according to Becker, Daniel and Rusch (Cancer Res. 23:1910, 1963), except that cultures were grown in conical flasks in Brewer's medium (Biochim. biophys. Acta 402:363, 1975). Plasmodia were induced to fruit by transferring plasmodia (8-cm diameter) to niacin-salts medium (Daniel and Rusch, J. Bacteriol. 83:234, 1962), starving them for three days and illuminating for 4 h. Cultures were exposed to drugs for 2 to 6 h before melanization. Effects were assessed by microscopic examination and by counting spores per sporangium. Results are tabulated below:

	Test Substance		
Test System	Hydrazine 2 HCl	Hydrocarbons (1%v/v)	Ethanol
Microplasmodial growth	ED_{50},*ca*	C^6, C^8, C^{10}, no growth	ED_{50}, *ca*
	40μg/ml	C^{12}, C^{14}, C^{16}, growth normal	1.5%
Sporangial formation	Cleavage & melanization blocked by 400 μg/ml	Not studied	Stalk formation & cleavage inhibited with 1.5%

Utilization of ethanol and the C^{12}-C^{16} hydrocarbons has yet to be demonstrated directly, but all show a sparing effect on glucose.

(Supported in part by Air Force Contract F33615-82-K-0514.)

PRELIMINARY ANALYSIS OF AN EXTRACELLULAR INDUCER OF THE AMOEBAL-PLASMODIAL TRANSITION FROM THE MYXOMYCETE *DIDYMIUM IRIDIS*. W. Nader and G. L. Shipley, *Department of Biology, Texas A&M University, College Station, TX 77843.*

The differentiation of myxamoebae to plasmodia is an inducible process mediated by an extracellular pheromone, the "inducer". Cell-free culture supernatants from *Didymium iridis* suspension cultures have proven to be a ready source of inducer activity. Concentrated supernatants (see below) were capable of accelerating differentiation (selfing) of the Colonia strain of *Physarum polycephalum* as well as mating in *Physarum* and *Didymium*, suggesting the inducer pheromones of these two species are structurally similar. Inducer activity in *Didymium* cultures reached a maximum at the end of log-phase growth. Activity was measured in a semi-quantitative bioassay based on the induction of zygote formation in suspensions of mating compatible *Didymium* amoebae. Culture supernatants concentrated 15-50 fold were prepared by lyophilization and ammonium sulfate precipitation followed by desalting over Biogel P-2 prior to further characterization. Activity was stable at -20 C for months, at 37 C for at least 5 h, but was destroyed at 100 C in 5 min. No significant losses in activity were observed when preparations were incubated with trypsin, proteinase K, RNAse A or DNAse. Treatment with periodate (20mM, 3 h) eliminates the activity. The activity bound to a boronate-

conjugated agarose column and was removed by 2 M sorbitol. The later findings suggest the presence of carbohydrate groups in the pheromone. The activity was totally excluded from Biogel P-10 (20,000 d exclusion). A Biogel P-150 column resulted in a major peak of activity of 120,000 d and a minor peak at 26-30,000 d. The relationship of these two peaks is not clear at this time. The activity will bind to DEAE-cellulose in 10 mM Imidazole, pH 7 at 24 C or in 2 mM Imidozole, PH 7 at 4 C. Elution of activity can be accomplished in 100 mM KCl. Futher attempts to purify and characterize the pheromone are in progress.

REPRODUCTIVE SYSTEMS AND SPECIATION IN *DIDYMIUM IRIDIS*: AN EVOLUTIONARY MODEL. O'Neil Ray Collins, *Department of Botany, University of California, Berkeley, CA 94720.*

Over the last 23 years, a considerable amount of genetical information on the myxomycete life cycle has been generated and this constitutes a firm foundation for evolutionary studies. The fact that true slime molds are primitive holotrophic eukaryotes, displaying a prominent amoeboflagellate stage, adds a special dimension of evolutionary interest. It is conceivable, for example, that Myxomycetes are direct descendants of the earliest sexual amoeboflagellates, which might have been the originators of isogamous eukaryotic sex. A multiple allelic mating system is the ideal one for such organisms, so its existence in present-day myxomycete amoeboflagellates is easy to explain. In *Didymium iridis*, this system is combined with efficient asexual (apomictic) and vegetative reproductive modes, permitting a remarkable amount of adaptability and opportunities for evolutionary studies.

Here, I present data on the spontaneous conversion of apomixis to heterothallism in an isolate of *D. iridis* and examine the behavior of the new heterothallic convertant in intra- and interisolate crosses. Data are interpreted in the context of speciation and evolutionary relationships between the apomictic and heterothallic reproductive modes.

LIFESPANS AND SENESCENCE IN THE SLIME MOLDS. J. Clark, *School of Biological Sciences, University of Kentucky, Lexington, KY 40506.*

The diploid plasmodia of heterothallic isolates of the slime molds *Physarum polycephalum* and *Didymium iridis*, when grown as non-axenic surface cultures, have a determinate lifespan controlled by their genotypes. This study extends the report of senescence to a third heterothallic species, *Physarum cinereum*, and to three non-heterothallic species—*Physarum pussilum, Physarum compressum* and *Stemonitis flavogenita*. Also five non-heterothallic isolates of *Didymium iridis* were found to display senescence. However, two isolates, one of *Stemonitis flavogenita* and one of *Physarum gyrosum*, did not undergo a recognizable senescence during this study. The apparent lack of a definite lifespan during axenic culture of *Physarum polycephalum* was also investigated. While axenic cultures have remained vigorous during more than three years of continuous growth, subcultures taken from these isolates have displayed progressively shorter lifespans when transferred to non-axenic surface cultures (i.e., older axenic cultures yield short lived non-axenic cultures).

A STEREOLOGICAL ANALYSIS OF CYTOLOGICAL CHANGE DURING SPORE MATURATION IN *DIDYMIUM IRIDIS*. W. R. Fagerberg and C. W. Mims, *Department of Biology, Southern Methodist University, Dallas, TX 75275, and Department of Biology, Stephen F. Austin State University, Nacogdoches, TX 75962.*

Young and mature spores of *Didymium iridis* were studied using stereological analytical techniques. Changes in the V_v ratios of the nuclear, autophagic vacuole, mitochondrial, microbody, lipid and cell wall compartments, as well as actual volume

changes in these compartments were evaluated during maturation (24 h period). V_v values which describe how spore volume is apportioned to each organelle compartment show that during maturation spores change from cells where nearly all organelle compartments occupy equal cell volume to cells where the volume is dominated by the cell wall and autophagic vacuole compartments. The rest of the spore volume is unequally divided amongst the other organelles. A major event during spore maturation is a 50% decrease in spore volume. Our data support the hypothesis that this is a multi-step process. The first step involves a rapid decrease in spore size, probably due to water loss. An outer spore wall is then laid down, terminating a further decrease in spore size. Additional cell wall material is then laid down with a concomitant loss in protoplast volume. The loss in protoplast volume is the result of a decrease in the volumes of the organelle compartments as a result, presumably, of metabolic activity and/or water loss. Cytological changes during spore maturation show mature spores to be highly differentiated from earlier stages. The factors controlling changes in the organelle compartments remain to be discovered.

PLASMA MEMBRANES FROM *PHYSARUM POLYCEPHALUM* AMOEBAE AND PLASMODIA. Dominick Pallotta, Anne Barden, Francois Bernier, Josee Kirouac Brunet and Gerald Lemieux, *Departments of Biology and Biochemistry, Université Laval, Québec, P. Q., Canada G1K 7P4.*

Amoebae and plasmodia growing in liquid shaken cultures were used as starting material for plasma membrane preparations. Amoebae were collected, swollen in hypotonic buffer and then broken in a Thomas tissue grinder. The plasma membranes were collected by differential centrifugation and purifed by centrifugation in a continuous 30-50% sucrose gradient. The membranes sedimented in a single band having a density of 1.16 g/cm^3. They were found by enzymatic assay and by electron microscopy to be free of lysosomes, mitochondria and nuclei and minimally contaminated by endoplasmic reticulum. Plasmodia were collected, washed and homogenized in a Waring blender. Plasmodial plasma membranes were prepared by differential and sucrose gradient centrifugation and also by the dextran polyethelene glycol 2-phase system. Enzyme assay and electron microscopy showed that these membranes were essentially free of contaminating organelles. Amoebal and plasmodial plasma membrane proteins were characterized by SDS-acrylamide gel electrophoresis. In both cases fewer than 10 major bands were seen on Commassie blue stained gels. Differences in some of these major bands were seen when amoebal and plasmodial plasma membrane proteins were compared.

PLASMA MEMBRANE PROTEINS FROM GENETICALLY DIFFERENT AMOEBAL STRAINS OF *PHYSARUM POLYCEPHALUM*. Remi Martel, Anne Barden, Gerald Lemieux and Dominick Pallotta, *Departments of Biochemistry and Biology, Université Laval, Québec, P. Q., Canada G1K 7P4.*

The *MatB* locus controls amoebal cell fusion in *Physarum polycephalum*. In an attempt to study the molecular basis of cell fusion the plasma membrane proteins of amoebae carrying different *matB* alleles were analysed. For this work the method of Barden et al. (B.B.A. in press) was used to prepare plasma membranes from strains carrying the *matB1, matB2* or *matB3* alleles. The membrane proteins for each strain were separated by SDS gel electrophoresis. When the gels were colored with Commassie blue, about 10 major and 20 minor bands were seen. More bands were revealed with the silver staining method. With both staining techniques the electrophoretic profiles were similar for all strains studied. A more detailed analysis of membrane proteins was carried out by 2-dimensional gel electrophoresis as described by O'Farrell (J.B.C. 250:4007, 1975). For amoebae growing on agar with live bacteria, minor differences were seen among strains

carrying different *matB* alleles. The most striking differences appeared between strains growing axenically in liquid medium and those growing on agar plates. Two major plasma membrain proteins found in all agar-grown amoebae were absent from liquid-grown amoebae.

EVIDENCE FOR A FACTOR THAT ALTERS THE SURFACE PROPERTIES OF COMPATIBLE MYXAMOEBAE. E. M. Goodman, P. Tipnis and G. Hanks, *Biomedical Research Institute, University of Wisconsin-Parkside, Kenosha, WI 53141.*

It is a well recognized phenomenon in *Physarum* that mixing compatible mating types will induce amoebae to differentiate after a certain as yet undefined lag period. Futher, several experiments suggest that a soluble mating factor(s) may be involved in this process. We decided to study the surface properties of myxamoebae under various conditions where compatible amoebae were in contact with the growth medium of the opposite mating type but not in direct physical contact.

The basic experiments involved the use of parabiotic chambers where compatible mating types were separated by a 0.45 μ millipore membrane, and growing myxamoebae in media that previously supported the opposite mating type. An aqueous, two-phase polymer system of dextran and polyethylene glycol was used to assess alterations in cell-surface properties. Data showed that the growth medium from one mating type can alter the surface properties of the compatible mating type.

SURFACE DIFFERENCES BETWEEN SEXUALLY COMPATIBLE MYXAMOEBAE OF *PHYSARUM POLYCEPHALUM*. Henry C. Aldrich and Julia B. Reiskind, *Department of Microbiology and Cell Science, University of Florida, Gainesville, FL 32611.*

Myxamoebae of strains RSD4 and MA185 were grown axenically on the same semidefined liquid medium in shake culture. Plasma membranes were isolated from both strains using Jacobson's technique of binding the cells to Affi-Gel 731 beads, vortexing to lyse the cells, and eluting plasma membraines with SDS/EDTA/phosphate buffer at pH 8.2. The solubilized membranes were electrophoresed on polyacrylamide slab gels and the polypeptide profiles compared after both Commassie Blue and Con A-peroxidase staining. We also observed that an alcohol-precipitable, soluble fraction was recoverable from the supernate when RSD4 cells were washed with cold 40 mM KCl/50 mM potassium phosphate buffer at pH 6.2. This evidently represents a soluble component of cell coat, and it is not recoverable from MA185 cells. Binding of Con A and wheat germ agglutinins was followed using fluorescein and ferritin labels. This table illustrates the differences found between the two mating types:

	Native memb.: lectins bound	Buffer washed: lectins bound	Sol. coat present?	SDS-PAGE results	Agglut. sheep RBC?
RSD4	None	Con A, WGA	Yes	1 unique polypep.	No
MA185	Con A	Con A, WGA	No	5 unique polypeps.	Yes

Both strains contain polypeptides which bind Con A, but none of these is common to both strains. These results demonstrate clear differences between the cell surfaces of myxamoebae of the two mating types, differences which are distinct enough to function in sexual recognition.

PHYSARUM STRAINS TEMPERATURE SENSITIVE IN VEGETATIVE GROWTH. Thomas E. Evans and Helen H. Evans, *Division of Radiation Biology, School of Medicine, Case Western Reserve University, Cleveland, Ohio 44106.*

Populations of exponentially growing LU-648 amoebae were mutagenized with either nitrosoguanidine or ethyl methanesulfonate. After outgrowth, survivors were cloned, replica-plated and screened for temperature sensitivity by growth at 22 and 30.8 C. Retesting of putative mutants was done by cloning at the two temperatures; strains that produced colonies of about 50 or fewer cells at 30.8 C by the time wild-type control colonies contained approximately 10^5 cells were kept for further study.

Mutant strains were crossed with CW-202 (mt_1, $fusA_1$), and resulting fusion group III plasmodia ($fusA_1/fusA_2$) were starved for the induction of sporulation. Spores were germinated clonally and clones tested for temperature sensitivity (segregation patterns obtained thus far are all 1:1). Temperature sensitive clones were plated pair-wise on mating plates, and fusion group III plasmodia were then used for analysis of the temperature sensitive allele as a homozygous diploid.

Growth curves of four such strains show that the markers are expressed in both haploid amoebae and diploid plasmodia. Biochemical testing as well as heterokaryon analysis indicated that each of the strains was functionally and genetically distinct.

Of particular interest was amoebal strain CW-435. A feulgen analysis of amoebae showed that the population became partially binucleate after incubation for various times at the restrictive temperature; the degree of binucleation increased to about 30% after four days. The nuclei of both the uninucleate and binucleate cells were determined to be 2*C* in DNA content (i.e., were apprarently arrested in G_2). A branched pathway model involving a single transition point is consistent with these observations.

TS MUTANT ISOLATION IN *PHYSARUM* AXENIC MYXAMOEBAE. Thomas G. Laffler and John Carrino, *Department of Microbiology-Immunology, Northwestern University Medical School, Chicago, IL 60611.*

The analysis of cell-cycle regulation in *Physarum* would be greatly facilitated if an ample supply of cell-cycle mutants was available. Attempts at isolating these mutants by non-selective methods have not generated significant numbers of mutants, and bromodeoxyuridine (BrdUrd) suicide selections with monoxenic cultures of myxamoebae yield mainly BrdUrd-resistant thymidine-kinase-defective (tk^-) mutants.

We have found that thymidylate synthesis in axenic cultures of myxamoebae is inhibited by methotrexate, and growth can be restored by adding thymidine to the medium. This provides a selection for tk^+ that can be used to eliminate the tk^- background in BrdUrd-suicide selections. Presently, we are developing the methodology for BrdUrd suicide selections with myxamoebae of strain 301.5 (matA3, AxE).

SOME GROWTH CHARACTERISTICS OF WHITE *PHYSARUM* MICROPLASMODIA. Claude Nations, Ivan Pinon, and John L. McCarthy, *Department of Biology, Southern Methodist University, Dallas, TX 75275.*

White microplasmodia of *Physarum polycephalum*, LU887xLU897, enter a wet-weight stationary phase of growth six days following the transfer of quiescent cultures to fresh nutrient medium. When growth is determined on the basis of dry weight or protein content the microplasmodia complete logarithmic growth within four days and the percent of wet weight that is protein begins to decline after three days. When microplasmodia are subcultured from log-phase cultures, wet growth plateaus within five days; dry weight and protein content peak after four days of culture and the magnitude of the growth obtained exceeds that of reanimated quiescent cultures by more than 40%, over the same period. The highest continuing growth rate was maintained

with a three-day subculture schedule when growth was measured either as dry weight or on the basis of protein.

No accumulation of lactic acid was detected over a five day period of growth. Unlike yellow microplasmodia that lower the pH of their media from 4.6 to 4.0 or lower (John Daniel, 6th International Cell Cycle Conference) the white microplasmodia were observed to increase medium pH from 4.6 to 5.2 within four days of growth.

INDEX TO VOLUME XXXV (1983), THE TEXAS JOURNAL OF SCIENCE

by CHARLOTTE A. NEILL

Medical Sciences Library
Texas A&M University
College Station, TX 77843

and L. JOSEPH FOLSE

Department of Wildlife and Fisheries Sciences
Texas A&M University
College Station, TX 77843

PREFACE

This index has separate subject and author sections.

The subject index is patterned after that currently used in the Proceedings of the National Academy of Sciences: The key word or phrase is followed by the complete title and initial page of each relevant article and abstract. However, when the key word(s) comprises the name of a biological or chemical taxon mentioned strictly in the context of a survey, the relevant article or abstract is identified only by initial page number. In the latter case, biological species are indexed only to the generic level, except that common names of species are used in cases where corresponding scientific names did not appear in the article or abstract.

Index terms were chosen both from titles and texts. Key words supplied by authors also were used. Index terms were alphabetized by a computer program that disregarded conformational prefixes, numerals, and hyphenated Greek letters.

The author index includes the names of all authors, both of articles and abstracts. Each name is followed by the number of the first page of that author's article or abstract.

C.A.N. did the indexing; L.J.F. developed the microcomputer programs (in Pascal) that assimilated the key-word information and produced the index.

SUBJECT INDEX

AUTHOR INDEX

REVIEWERS

The persons listed below have reviewed manuscripts for the Texas Journal of Science within the past two years. The Academy is very grateful for their help.

Aldrich, D.V.
Amoss, M.S.
Arnold, K.A.
Baccus, J.T.
Baker, R.
Behal, F.T.
Bickham, J.W.
Bilyeu, R.G.
Binderim, G.E.
Bragg, L.H.
Bratton, G.
Brown, P.K.
Brown, R.F.
Bullin, J.
Burch, R.
Buzan, D.
Cameron, G.N.
Campbell, J.M.
Casto, S.D.
Chamberlain, G.C.
Chapman, B.R.
Choate, J.R.
Clark, D.R.
Clark, K.A.
Clark, W.J.
Coburn, D.
Cole, C.J.
Cox, R.A.
Crick, R.E.
Cunningham, J.
Dalquest, W.M.
Davies, F.
Dial, B.E.
Dillin, D.R.
Ditton, R.B.
Dockweiler, C.J.
Doctor, V.M.
Dolbeer, R.A.
Ebrey, T.
Etheridge, R.
Ezell, A.W.
Fares, Y.
Finlay, B.
Fleharty, E.D.
Flowers, A.I.
Folse, L.J.
Foster, B.G.
Foster, D.M.
Frentress, C.
Fullington, R.W.
Gary, H.E., Jr.
Giovanella, B.C.
Gorsline, D.S.
Gray, J.
Greenbaum, I.F.
Guthery, F.S.
Harrel, R.C.
Harry, H.W.
Hartley, C.J.
Hatch, S.L.
Huffman, D.G.
Jee, R.
Johnson, J.D.
Judd, F.W.
Kelsch, S.W.
Kimber, C.
Koenig, H.J.
Kofron, C.P.
Kroh, G.C.
Kyba, E.P.
Landry, A.M., Jr.
Leeper, P.W.
Leonard, J.E.
Lestrade, J.P.
Lieb, C.S.
Lind, O.T.
Linder, L.E.
Longley, G.
Longnecker, M.
Lovell, R.T.
Lueking, D.R.
Lundelius, E.L.
Marcum, J.P.
Martin, S.F.
Martyn, R.D.
McCarley, H.
McCullough, J.D.
McCune, E.D.
McIntosh, W.A.
McKinley, C.R.
McLemore, E.W.
McWilliams, E.
Meyers, D.G.
Morrison, D.G.
Moyer, R.C.
Namkoong, G.
Naugle, N.W.
Neal, J.
Nix, J.F.
Nixon, E.S.
Norton, S.J.
Odell, P.L.
Owen, J.G.
Pace, C.N.
Pearson, B.J.
Pearson, W.D.
Phinney, H.K.
Poole, C.F.
Potempa, T.
Powell, E.
Powell, G.L.
Pulich, W.M., Jr.
Rezak, R.
Richardson, A.
Rutledge, J.T.
Sauer, H.W.
Schmidly, D.J.
Scudday, J.F.
Sealander, J.A.
Siehr, D.J.
Silvy, N.J.
Smeins, F.E.
Srinivasan, V.K.
Stewart, K.W.
Stipanovic, R.D.
Strange, R.J.
Stubbs, G.G.
Thompson, G.A., Jr.
Thompson, P.B.
Thummel, R.P.
Tizard, I.
Turner, C.
Van Horn, D.E.
Vincent, J.
Waldrop, J.E.
Warner, I.M.
Watkins, J.
Weller, M.W.
Wellman, P.J.
Whiteside, B.G.
Whitmore, D.H.
Wicksten, M.K.
Wilkins, K.W.
Williges, G.G.
Wilson, F.
Wilson, L.D.
Wilson, R.P.
Winfree, B.
Winston, A.J.
Wormuth, J.H.
Yancey, T.E.
Yates, S.
Yuen, T.S.

THE TEXAS ACADEMY OF SCIENCE, 1983-84

OFFICERS

President:	Bernard T. Young, Angelo State University
President-Elect:	Michael J. Carlo, Angelo State University
Vice-President:	William J. Clark, Texas A&M University
Immediate Past President:	Elray S. Nixon, Stephen F. Austin State University
Secretary-Treasurer:	Everett D. Wilson, Sam Houston State University
Editor:	William H. Neill, Texas A&M University
AAAS Council Representative:	Arthur E. Hughes, Sam Houston State University

DIRECTORS

1981	Richard L. Noble, Texas A&M University
	Bob F. Perkins, University of Texas, Arlington
1982	Billy J. Franklin, Texas A&I University
	Ethel W. McLemore, Dallas
1983	D. Lane Hartsock, Austin
	Katherine Mays, Bay City

SECTIONAL CHAIRPERSONS

I—*Mathematical Sciences*: Barbara Schreur, Texas A&I University
II—*Physical Sciences*: Virginia L. Rawlins, North Texas State University
III—*Earth Sciences*: James C. Grenda, Angelo State University
IV—*Biological Sciences*: Edward Schenider, Southwest Texas State University
V—*Social Sciences*: James O. Standley, Stephen F. Austin State University
VI—*Environmental Sciences*: Robert D. Larsen, Southwest Texas State University
VII—*Chemistry*: John T. Moore, Stephen F. Austin State University
VIII—*Science Education*: Fred L. Fifer, University of Texas, Dallas
IX—*Computer Sciences*: H. P. Haiduk, Amarillo College
X—*Aquatic Sciences*: Fred L. Rainwater, Stephen F. Austin State University

COUNSELORS

Collegiate Academy: Shirley Handler, East Texas Baptist College
Helen Oujesky, University of Texas, San Antonio
Junior Academy: Ruth Spear, San Marcos
Peggy Carnahan, San Antonio

COVER PHOTO

Ovals of Cassini

by Amir-Moez and Fredricks, pp. 277-282

2nd CLASS POSTAGE
PAID AT HUNTSVILLE
TEXAS 77341
AND AT ADDITIONAL
MAILING OFFICE
AT LUBBOCK
TEXAS 79401

ISSN 0040-4403

SMITHSONIAN INSTITUTION LIBRARIES

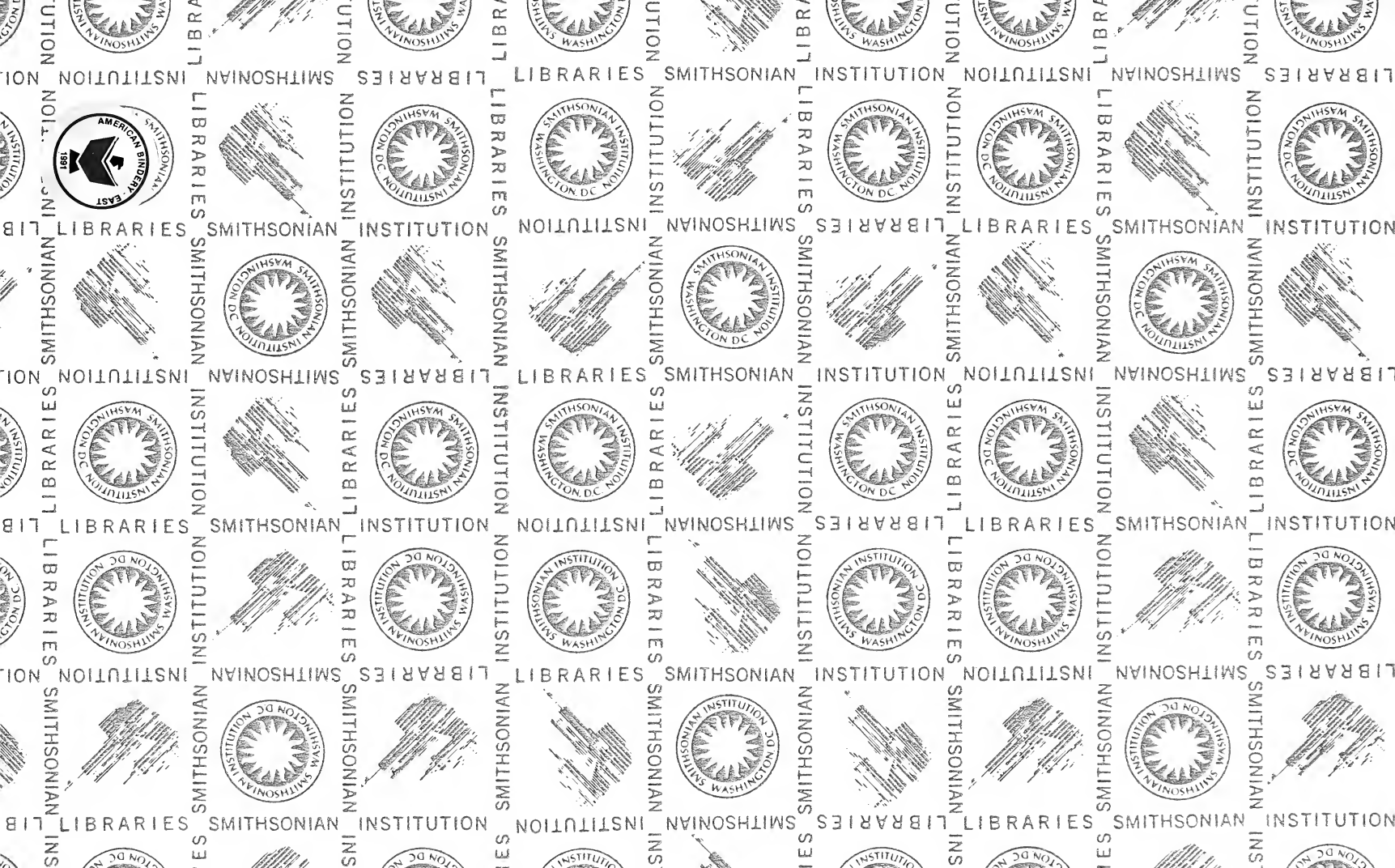
SMITHSONIAN INSTITUTION LIBRARIES
AMERICAN BINDERY EAST 1991